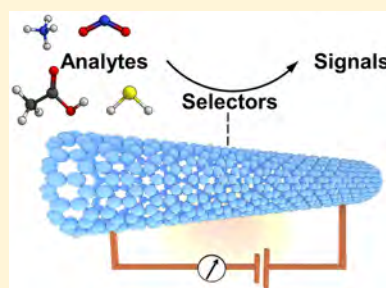


Carbon Nanotube Chemical Sensors

Vera Schroeder,¹ Suchol Savagatrup, Maggie He, Sibo Lin,¹ and Timothy M. Swager^{*1,2}

Department of Chemistry and Institute for Soldier Nanotechnologies, Massachusetts Institute of Technology, 77 Massachusetts Avenue, Cambridge Massachusetts 02139, United States

ABSTRACT: Carbon nanotubes (CNTs) promise to advance a number of real-world technologies. Of these applications, they are particularly attractive for uses in chemical sensors for environmental and health monitoring. However, chemical sensors based on CNTs are often lacking in selectivity, and the elucidation of their sensing mechanisms remains challenging. This review is a comprehensive description of the parameters that give rise to the sensing capabilities of CNT-based sensors and the application of CNT-based devices in chemical sensing. This review begins with the discussion of the sensing mechanisms in CNT-based devices, the chemical methods of CNT functionalization, architectures of sensors, performance parameters, and theoretical models used to describe CNT sensors. It then discusses the expansive applications of CNT-based sensors to multiple areas including environmental monitoring, food and agriculture applications, biological sensors, and national security. The discussion of each analyte focuses on the strategies used to impart selectivity and the molecular interactions between the selector and the analyte. Finally, the review concludes with a brief outlook over future developments in the field of chemical sensors and their prospects for commercialization.



CONTENTS

1. Introduction and Scope	600	2.1.4. Hydrogen Sulfide (H_2S) and Sulfur Dioxide (SO_2)	620
1.1. Chemical Sensing Mechanisms	601	2.1.5. Benzene, Toluene, and Xylene (BTX)	621
1.1.1. Intra-CNT	601	2.2. Aqueous Environmental Sensing	622
1.1.2. Inter-CNT	603	2.2.1. CNT-Based pH Sensors	622
1.1.3. Schottky Barrier (SB) Modulation	603	2.2.2. CNT-Based Metal Ion Sensing	622
1.2. Functionalization of CNTs	604	3. CNT-Based Sensors for Food and Agriculture	624
1.2.1. Noncovalent Functionalization of CNTs with Small Molecule Units	604	Applications	624
1.2.2. Wrapping of CNTs with Polymers	605	3.1. Food Quality	625
1.2.3. CNTs Decorated with Metal Nanoparticles	605	3.1.1. Fruit Ripeness	625
1.2.4. Covalent Functionalization	605	3.1.2. Taste and Smell	625
1.3. Device Architecture and Fabrication	607	3.2. Food Safety	626
1.3.1. Single CNTs vs CNT Networks	608	3.2.1. Food Spoilage	627
1.3.2. Device Architectures	609	3.2.2. Integrity of Packaging and Oxygen Sensors (O_2)	627
1.3.3. Fabrication	610	3.2.3. Pesticide Contamination	629
1.4. Performance Parameters	611	3.2.4. Foodborne Pathogens	630
1.4.1. Parameters of Performance and Figures of Merit: What They Are and How to Measure Them?	611	4. CNT-Based Biological Sensors	631
1.4.2. Specific Challenges on the Performance of CNT-Based Chemical Sensors	612	4.1. Breath Analysis	631
1.5. Theoretical Models	612	4.1.1. Volatile Organic Compounds (VOCs)	631
2. CNT-Based Sensors for Environmental Monitoring	614	4.1.2. Inorganic Gases	633
2.1. Gas/Vapor Sensors for Environmental Applications	614	4.2. Health Monitoring and Detection of Biomolecules	634
2.1.1. Ammonia (NH_3) and Nitrogen Dioxide (NO_2)	614	4.2.1. Glucose Detection	634
2.1.2. Hydrogen (H_2) and Methane (CH_4)	617	4.2.2. DNA Sensors	636
2.1.3. Carbon Monoxide (CO)	618	5. CNT-Based Sensors for National Security	639
		5.1. Chemical Warfare Agents	639
		5.1.1. Nerve Agents and Vesicant Agents	639
		5.1.2. Pulmonary Agents	642

Special Issue: Chemical Sensors

Received: May 27, 2018

Published: September 18, 2018

5.1.3. Blood Agents	643
5.2. Explosives	643
6. Summary and Concluding Remarks	645
Author Information	646
Corresponding Author	646
ORCID	646
Notes	646
Biographies	646
Acknowledgments	646
References	646

1. INTRODUCTION AND SCOPE

Carbon nanotubes (CNTs) have been a subject of research for more than 20 years. Mirroring this academic endeavor is the worldwide commercial interest, leading to the production capacity of several thousand tons of CNTs per year.¹ These developments have paved ways to the wide array of emerging applications^{2,3} in microelectronics,^{4,5} computing,⁶ medicinal therapy,⁷ electrochemical biosensors,⁸ and chemical sensors.^{9,10} However, the field is far from mature, and our understanding of the chemical and physical properties of these materials continues to grow. At the outset, it is fair to state that the chemistry of CNTs remains dubious and often imprecise.¹¹ Although advances in the production have allowed preferential synthesis of single-walled carbon nanotubes (SWCNTs) with metallic or semiconducting properties with selectivity of 90–95%,^{12,13} production of pure semiconducting tubes remains cost prohibitive. Commercial supplies of SWCNTs, despite improvements in consistency, are still polydisperse in length, diameter, and chirality. Separation methods by density-gradient centrifugation with selective surfactants,¹⁴ conjugated polymer wrappings,^{15,16} or gel chromatography^{17,18} are not readily scaled. Bottom-up syntheses have seen heroic efforts¹⁹ but remain far from full realization. Similarly, multiwalled carbon nanotubes (MWCNTs) can be produced in high volume through large-scale chemical vapor deposition (CVD); however, they suffer from structural deviations and contaminations that often require costly treatment for removal.

One may ask why CNTs continue to garner such attention given the complexity and what some chemists may even refer to as impurities. Clearly, scientific curiosity is one answer. The other motivation driving CNT research is their unusual optical, electrical, mechanical, and chemical properties. CNTs are unique organic electronic wires with shape persistence. These π -electron wires possess quantized electronic states with coherence lengths that are longer than what is possible for conducting polymers, making them ideal building blocks for nanoelectronic devices. Furthermore, CNTs can be organized in nanowire networks and with the addition of recognition elements are ideal for sensing applications. Indeed, it was understood from the early 1990s that molecular and nanowire architectures could produce sensors with superior sensitivity, benefiting from the restricted transport along percolative paths and the large surface area-to-volume ratio.²⁰ Hence, these principles were translated quickly to create the first example of SWCNT chemical sensors by Dai and co-workers.²¹ The authors strived to realize the concept of a nanowire in its purest form by connecting electrodes with an individual SWCNT to observe the change in its conductivity when exposed to oxidative p-doping (NO_2) and reductive undoping (NH_3) gases. This study is certainly historic in the field of SWCNTs. However, similar to the onset of every area, much

more progress was required to usher CNT platforms into versatile and useful sensors.

It is indisputable that selectivity underpins the utility of any chemical sensor. Of course, sensitivity and stability must be given the appropriate weight as discussed in the later sections of this review. The advancements in system integrations and electrical interfaces have lowered the stringent requirements of these latter parameters. For example, electrical signals can be isolated and amplified, and trace analytes can be captured and released using preconcentrators. However, without selectivity, the sensors are often rendered ineffective as a result of confounding effects in real-world environments such as interfering species, varying humidity, and fluctuation in temperature. Specificity, or perfect selectivity, is often not needed, and robust sensors can be created from arrays of sensing elements, with each sensor having limited discriminating ability.²² Array-based sensors, such as a CNT-based chemical nose/tongue, are applicable to most types of chemical sensing and continue to progress toward the idea of a “universal sensor”. Inspired by the biological olfactory system, each individual channel in the sensor array needs not be perfectly orthogonal to every other channel. On the contrary, a unique “fingerprint” corresponding to each analyte or group of analytes can arise when each channel of an array responds to several analytes in varying degrees. Nevertheless, it is seldom a disadvantage to incorporate sensors that are inherently selective to the target analytes. Indeed, a combinatorial approach of several highly selective and cross-selective sensing channels might lead to an optimized performance of the sensor array. SWCNTs are natural sensing materials as their transport properties are extremely responsive to their environment. They have suffered from limitation in selectivity at the inception of this field. This limitation contributed to the relatively few commercial CNT-based sensors in spite of a massive worldwide research effort.

As a result, this review will place significant emphasis on the ways in which chemical science and engineering can be applied to create CNT-based sensors exhibiting selective responses to target analytes. Such approaches predominantly include functionalization with selectors (e.g., polymer-wrapping and sidewall attachments). Quite often the sensing performance of CNTs depends not only on the molecular recognition but also on the response of the collective system, which can be affected by nonspecific chemical, thermal, and mechanical interactions. As will be discussed, the mechanism of chemical sensing may likely be intra-CNT and inter-CNT in nature; however, the other interfaces (CNT–electrodes and CNT–dielectric) must also be considered. In functionalization of SWCNTs, it was proposed initially that noncovalent attachments were preferred as a result of the simplicity of the technique and the small perturbation on the base transport properties of the SWCNTs. Early applications of these methods to immobilized proteins appeared to give excellent performing biosensors.²³ However, detailed follow-up studies by the same researchers later revealed that the interfaces between the metal electrodes and the CNTs were non-innocent, and the interactions at these locations constituted the major responses for these sensors.²⁴ Hence, if the primary response occurs at locations other than sites comprising receptors/selectors, the sensor will lack predictably selective responses. In surveying the literature on chemical sensors, it is imperative to be properly skeptical regarding the advertised selectivity. Indeed, we will call out

some of the results presented in this review when there is no apparent chemical rationale for the anticipated selectivity.

Although the nanocarbon area presents considerable diversity for chemical sensors, this review will strictly focus on electrical transduction using CNTs. The majority of nanocarbon sensors are based upon SWCNTs. Semiconducting CNTs are highly sensitive to carrier pinning and populations (i.e., doping levels). These are finite conductive pathways through the nanowire networks, and perturbing such pathways increases the tortuosity for charge transport from one electrode to the other (i.e., resistivity). In addition to electrical transport, semiconducting SWCNTs are emissive. Similar to the concepts developed around semiconducting molecular wires,²⁵ transport of excitons in SWCNTs can provide signal gain and emissions at long wavelengths for *in vivo* applications.²⁶ This area is promising, and we direct interested readers to a review by Strano and co-workers.²⁷ Although there is ongoing interest in graphene-based sensors,^{28,29} the metallic state of these 2D materials is more difficult to quench or enhance, allowing carrier migration around perturbed regions. MWCNTs provide the wire architecture; however, the inner tubes in these structures are prevented from interacting with the surrounding chemical environment. As a result, the intra-CNT mechanisms are not operative because the carriers can migrate through the unperturbed pathways of the inner core. Nevertheless, with suitable modulation of the inter-MWCNT transport, these materials can constitute effective sensors.

It is our intent to provide the reader a comprehensive perspective on the field of electrically read CNT-based sensors. However, there have been previous reviews that have covered aspects of this field that may complement some of our descriptions.^{2,9,10,30–35} This review is conceptually self-contained and intended to serve as an informational resource to both newcomers and experienced researchers in the area of CNT-based sensors. As a result, we will cover some contributions that were highlighted in previous reviews. For researchers working in the sensor area, it is natural to think about real-world applications. It is also our perspective that these materials will become a significant commercial sensor platform in the near future. Thus, after introducing the concepts, we have organized the coverage of the literature by the respective application areas as shown in Figure 1. This approach is also intended to assist researchers with interest in the use of sensors who are not sensor developers themselves.

1.1. Chemical Sensing Mechanisms

The discussion on the exact mechanisms that cause the response of carbon nanotube-based sensors is very much alive.

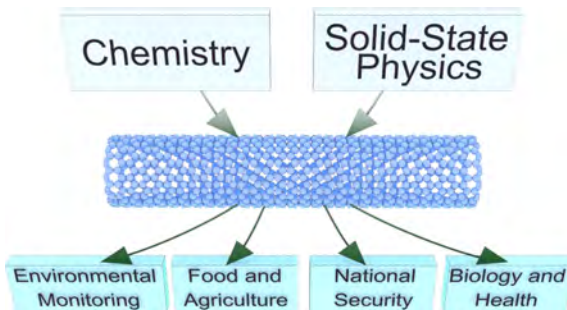


Figure 1. Schematic highlighting the application fields of the CNT-based chemical sensors covered in this review.

In contrast to conducting polymers, whose behavior can be described via molecular mechanisms, the properties of CNTs need to be described beyond local molecular structures, as is done in solid-state physics. As a result of their extended π system, the frontier orbitals of CNTs are best described through band structures rather than discrete molecular orbitals. Accordingly, chemical intuition is often not sufficient when trying to predict or describe CNT-based sensing mechanisms. In this section, we will discuss several mechanisms that give rise to signals in CNT-based chemical sensors of different architectures and functionalization techniques. Responses of CNT-based sensors are attributed to effects arising within the tubes (intra-CNT), effects arising at contact points between tubes (inter-CNT), or effects due to the contact between the tubes and the electrodes (Schottky barrier modulations) (Figure 2). The strength of these different mechanisms can

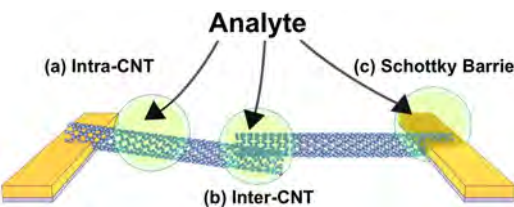


Figure 2. Schematic of sensing mechanisms in CNT-based sensors: (a) at the sidewall or the length of the CNT (intra-CNT), (b) at the CNT–CNT interface (inter-CNT), and (c) at the interface between the metallic electrode and the CNT (Schottky barrier).

depend strongly on the analyte, the defect concentrations in the CNTs, and the device architecture. For a historical discussion of the first investigation of CNT–sensor behavior and mechanistic investigations, we refer the interested reader to the reviews on CNT gas sensing mechanisms.^{36,37}

1.1.1. Intra-CNT. Intra-CNT sensing mechanisms are modes of interaction between analyte and individual nanotubes or nanotube bundles. They include changes in the number or mobility of charge carriers and generation of defects on the walls of the tubes.

Charge transfer induced directly or indirectly by analyte interactions will modulate the conductance of the CNT by changing (decreasing or increasing) the concentration of the majority charge carriers. Under ambient conditions, CNTs are p-doped as a result of physisorption of oxygen molecules on their surfaces. Thus, exposure to further p-dopants will increase the hole conduction and cause a decrease in the resistance, while n-type dopants will induce the reverse effect.^{21,38–41} Direct charge transfer between the analyte and CNTs has been identified as a major sensing mechanism for polar analytes.^{21,41–43} In some cases, this mechanism has a more localized nature. For example, interactions of a Lewis-basic localized pair of electrons can create a local pinning force for cationic carriers as opposed to the fractional transfer of electron density to delocalized CNT states. For individual SWCNTs,^{21,39,44} charge transfer between analyte and tube can be observed experimentally through the current–voltage (I – V) characteristics, photoemission spectroscopy (PES), and Raman spectroscopy.

Investigation of I – V characteristics through field-effect transistor (FET) experiments is a powerful tool for probing the sensing mechanism of CNT-based devices. When plotting the current through the CNT material as a function of the

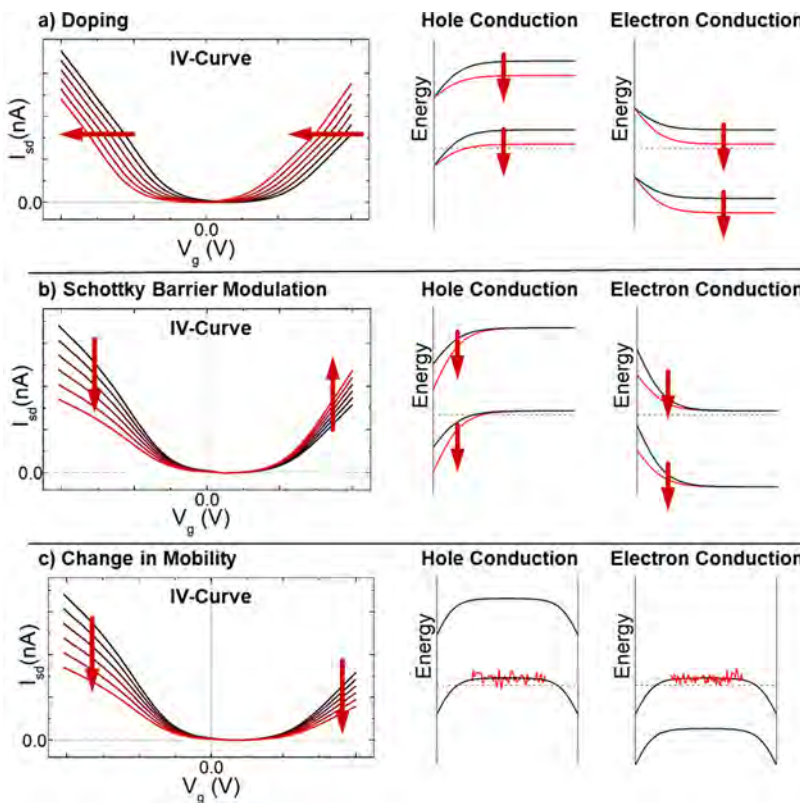


Figure 3. Intra-CNT (semiconducting) sensing mechanism through changes in charge carrier concentration or mobility. Hypothetical transfer (I – V_g) curves and band diagrams before (black) and after (red) exposure to the analyte for three different sensing mechanisms. Dotted line in the band diagram corresponds to the metal work function of the electrode, and diagrams are given for both p- and n-type semiconductors interfaces with a metal. (a) n-Doping of the CNT induces a shift of the I – V curve to more negative voltages. (b) Schottky barrier modulation corresponds to a change of the barrier height between the work function of the metal electrode and CNT and asymmetric change in conductance for electron and hole transport. (c) Change in mobility can be induced by the addition of resistive elements or carrier scattering which reduces the conductivity in both p- and n-type materials. Inspired by ref 53.

applied gate voltage (transfer curve), different sensing mechanisms induce characteristic changes. Adsorption of electron-donating species (charge transfer to the tube from the analyte) induces negative charge in the CNT, thus n-doping the CNT and shifting the threshold voltage toward a more negative gate voltage and vice versa (Figure 3a).²¹ Modulation of the metal/CNT junction induces asymmetric conductance change, as electron and hole conductions are affected differently (Figure 3b). Lastly, a reduction of the charge carrier mobility through charge carrier trapping or scattering sites induces a reduction in conductance (Figure 3c).^{45,46} Any perturbation of the ideal SWCNT structure introduces charge scattering sites, which reduce the mobility of the charge carriers and thus the conductance. Using I – V curves, changes in charge carrier mobility have been observed for scattering through adsorption of charged or polar species^{47–51} or via deformation of the tube.⁵²

The effect of charge transfer on the doping levels of CNTs can also be estimated from shifts in the Raman spectrum.^{54–58} A shift of the G-band—stretching of the sp^2 C–C bond in graphitic materials—toward higher wavenumbers is indicative of an electron-accepting analyte and a shift toward lower frequencies is indicative of an electron-donating analyte (Figure 4). This shift can have a magnitude of $\pm 30\text{ cm}^{-1}$ for strong dopants and has been observed for inorganic⁵⁴ and organic dopants.^{59,60}

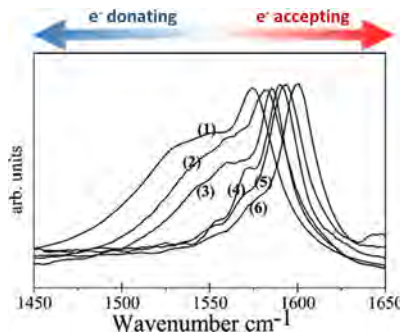


Figure 4. G-bands in the Raman spectra of SWCNTs when interacting with electron-donating and -accepting molecules: (1) tetrathiafulvalene, (2) aniline, (3) pristine SWCNT, (4) nitrobenzene, (5) tetracyanoquinodimethane, and (6) tetracyanoethylene. Reproduced with permission from ref 59. Copyright 2008, American Chemical Society.

In addition to charge-transfer effects, analytes can also promote the degradation of the CNT sidewalls. In particular, the chemisorption of NO_2 via formation of nitro and nitrite groups has been identified as a plausible sensing mechanism.^{61–63} Soylemez et al.⁶⁴ reported a chemiresistive glucose sensor based on poly(4-vinylpyridine) (P4VP)-wrapped SWCNTs functionalized with glucose oxidase. Upon exposure to glucose, hydrogen peroxide is formed which oxidizes the SWCNT sidewall. The degradation of the conjugated sp^2

network of pristine CNTs increases the number of defect sites of the SWCNT, also observable as an increased D/G peak intensity ratio of the Raman spectrum. Strong localized interactions associated with carrier pinning can manifest increases in the D/G peak ratios.

1.1.2. Inter-CNT. For devices consisting of a network of CNTs, mechanisms at the interface between tubes can have a significant influence on the electronic properties of the overall network. Small changes in the distance between two CNTs dramatically influence the contact resistance as the probability of charge tunneling decreases exponentially with distance.^{65,66} The intertube conduction pathways can be modulated either by partitioning of analytes into interstitial spaces between tubes or by swelling of the supporting matrix/wrapper. Alternatively, an analyte can trigger the disassembly of a molecular/polymer wrapping of the CNTs, Figure 5.

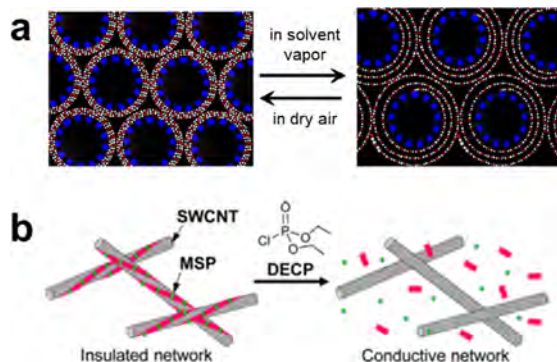


Figure 5. CNT-based chemical sensors based on inter-CNT mechanisms. (a) Illustration of polymer swelling upon exposure of a CNT/polymer composite to solvent vapors. Reproduced with permission from ref 70. Copyright 2007, Elsevier. (b) Schematic illustration of a chemiresistive sensor comprising SWCNTs and metallosupramolecular polymer (MSP) showing the polymer degradation upon exposure to chemical warfare agent mimic diethyl chlorophosphate (DECP). Reproduced with permission from ref 73. Copyright 2017, American Chemical Society.

Swelling of a matrix material causes a decrease in the bulk conductance of CNT networks by increasing the width of tunneling gaps (Figure 5a). For example, Ponnamma et al.⁶⁷ reported the influence of swelling on the electronic properties of a MWCNT–natural rubber composite. The swelling index was determined by quantifying the equilibrium uptake of a given solvent for all tested composites. They reported that the swelling index correlates with the magnitude of the decrease in conductance for all tested samples. A similar sensing behavior has been observed for porphyrins⁶⁸ and covalently^{69,70} and noncovalently^{71,72} attached polymers toward VOCs.

Alternatively, sensing systems that detect the increase in conductivity from new conducting pathways are similarly promising. Ishihara et al. reported the design of a sensor based on the dewrapping of SWCNTs, which provided an increase of conductance by 5 orders of magnitude.⁷³ In this case, the SWCNTs were wrapped with a metallosupramolecular polymer designed to depolymerize upon contact with an electrophilic analyte (chemical warfare agent mimic, diethyl chlorophosphate); the depolymerization caused the formerly isolated SWCNTs to come into electronic contact (Figure 5b). Similarly, Lobeck et al.⁷⁴ and Zeininger et al.⁷⁵ used CNTs wrapped by poly(olefin sulfone) (POS) polymers to detect

ionizing radiation. Upon exposure to radiation, the metastable POS spontaneously depolymerizes with fragmentation resulting in an increase in the interconnections between CNTs and the overall CNT network conductivity.

1.1.3. Schottky Barrier (SB) Modulation. In certain cases, the device performance is influenced not only by intra- and inter-CNT effects but also by modulation of the junction of the metal electrode and CNT (Schottky barrier). To differentiate between the previous mechanisms and effects at the electrode/CNT interface, several groups have observed the sensing behavior with and without passivation of the CNT/electrode contacts. In these experiments, passivating layers are deposited selectively over the whole device, over the areas where CNTs are in contact with the electrode, or over the length of the CNTs that is not in contact with the electrodes, Figure 6.

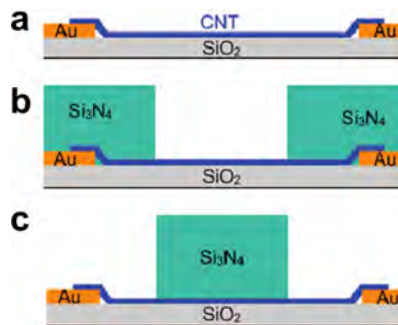


Figure 6. Three sensor architectures used to probe Schottky vs intratube sensing mechanisms. Schematic for (a) device with bare CNTs, (b) device with passivated CNT–electrode contacts, and (c) device with passivated length of CNTs that are not in contact with the metal electrode. Reproduced with permission from ref 76. Copyright 2009, American Chemical Society.

Bradley et al. contact passivated different areas of a pristine CNT device with SiO₂ and tested the response of the resulting sensors toward NH₃.⁷⁷ They found that complete coverage with SiO₂ drastically attenuated the response to NH₃ exposure, proving SiO₂ a suitable passivating material. Coverage of the electrode/CNT contact areas resulted in a sensor with comparable responsiveness and faster reversibility than the nonpassivated sensor. From this result, they concluded that the NH₃ sensing mechanism is the result of processes occurring over the length of the CNT and not at the CNT/electrode interfaces. Liu et al. used poly(methyl methacrylate) (PMMA) to passivate the channel of the electrode contact areas of a CNT–FET and detect NO₂ and NH₃.⁷⁸ In contrast to Bradley et al., they observed changes in the transfer characteristics for both channel- and electrode-passivated devices, suggesting that the effects on both the metal/CNT junction and the length of the CNT have significant contributions to the sensor signal. Zhang et al. also employed PMMA to passivate the contact of a CNT device used to detect NO₂; however, they found that the sensing response is mainly due to the interface between the electrode and the CNT.⁷⁹ Similarly, Peng et al. used devices partially passivated by Si₃N₄ and found that the sensing response toward NH₃ mainly results from the metal–CNT junction.⁷⁶ Considering the inconsistencies between these reports, it is understandable that the debate on the sensing mechanism persists.

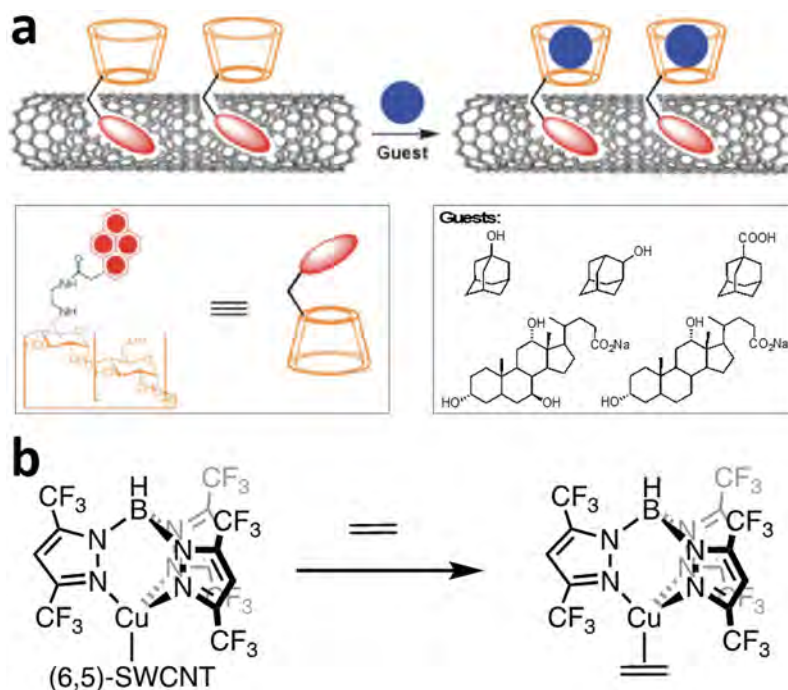


Figure 7. Noncovalent functionalization of CNTs with small molecules. (a) SWCNTs noncovalently functionalized with pyrenylcyclodextrins, which in a chemiresistor can detect closely related analogues of adamantane and sodium cholate. Reproduced with permission from ref 87. Copyright 2008, Wiley-VCH Verlag GmbH & Co. (b) Chemiresistive sensor using a composite of SWCNTs functionalized by coordination of a fluorinated tris(pyrazolyl)borate copper(I) complex to the π -sidewalls to provide selectivity to ethylene gas.

To clarify the contradictory findings just discussed, Salehi-Khojin et al. investigated the sensing behaviors of CNTs with different defect levels.⁸⁰ They reported that the dominating sensing mechanism is strongly dependent on the bottlenecks in the conduction pathways. For highly conductive CNTs, the sensing behavior is dominated by mechanisms influencing the electrode–tube junctions, while the response of devices with less conductive, defect-rich CNTs is dominated by intratube effects. Generalization remains difficult there can be different types of defects in CNTs and other components in the sensor material can influence intratube and metal–tube electron transport.

Apart from the nature of the CNTs, the choice of metal for the electrode also influences the behavior of the CNT/electrode junction. Kim et al. reported increased sensing responses from CNT devices containing Pd instead of Au electrodes.⁸¹ This result was attributed to the stronger interactions between the Pd surface and CNTs and the resulting barrier-free electronic transport across the junction, which agreed well with several theoretical studies.^{82,83} Zhang et al. demonstrated that targeted disruption of this Pd/CNT junction is a useful approach to fabricate H_2 sensors using CNTs without any further functionalization.⁸⁴ A further discussion on the H_2 sensing capability of Pd/CNT junctions can be found in section 2.1.2, Hydrogen (H_2) and Methane (CH_4).

1.2. Functionalization of CNTs

As mentioned previously, pristine CNTs have very limited selectivity when interacting with analytes. In this context, CNT functionalization is needed to tailor sensitivity and selectivity toward target analytes. Functionalization is also critical to improving the solution processability, enabling processing of these otherwise insoluble nanomaterials. Various approaches exist for the functionalization of CNTs, and they can be

grouped as noncovalent and covalent modifications. Anchored chemical groups, macromolecules, or biomolecules that serve a function to recognize, interact, or react with a target analyte selectively are referred to as selectors. Noncovalent functionalization involves the adsorption of small molecules (often surfactants) to the surface of CNTs or wrapping of polymers and biomolecules around the tubes. Covalent functionalizations utilize reactions to attach chemical groups covalently to the conjugated surfaces or termini of CNTs. Covalent functionalization has the advantage that it can produce strong and stable anchors of functional groups to CNT; however, the rehybridization of the carbon atoms from sp^2 carbons to more sp^3 character on the surface of CNT at the attachment sites lowers the electronic delocalization, thereby perturbing their intrinsic optical and electronic properties. Therefore, careful control of the degree of functionalization is important to achieve an optimal balance between covalent anchoring of selectors and perturbation of the π surface. Noncovalent approaches are generally less perturbative to the intrinsic properties of CNTs. However, physisorbed selector molecules or coatings have limited stability and can display changes in their configuration around the CNT, undergo phase segregation, and can even desorb in solution-based applications. Covalently functionalized carbon nanotubes are in general more robust for applications in environmentally challenging conditions. Several approaches to the functionalization of CNTs to impart sensor selectivity are described here. Comprehensive reviews of other functionalization methods that have not been applied in sensors are available elsewhere.^{11,85}

1.2.1. Noncovalent Functionalization of CNTs with Small Molecule Units. CNTs can be functionalized noncovalently by physisorption of small aromatic molecules and surfactants through π – π and hydrophobic interactions. Dai

and co-workers reported a simple and general method of immobilizing proteins onto CNTs using a bifunctional molecule containing a pyrene moiety for CNT adsorption and a succinimidyl ester for attachment of proteins by nucleophilic substitution reaction with the proteins' surface amine functional groups. The immobilized proteins can be observed with atomic force microscopy (AFM) and transmission electron microscopy (TEM). This method is highly specific and efficient for immobilization of biomolecules, and the authors demonstrated the attachment of biotinyl-3,6-dioxaoctanediamine and two proteins, ferritin and streptavidin.²³ Other functionalities anchored by pyrene units include amino groups,⁸⁶ cyclodextrin (Figure 7a),⁸⁷ and boronic acid,⁸⁸ which were used for the detection of trinitrotoluene (TNT), organic guest molecules, and glucose, respectively. Bis(trifluoromethyl) aryl groups are also suitable for non-covalent functionalization.⁸⁹

Simple physical mixtures of CNTs and a small molecule or macromolecule selectors can impart selectivity in gas sensing. Composites made of CNTs dispersed with small aromatic units can however produce inhomogeneous compositions with variable performance. Successful gas detection has been realized with physical mixtures of CNTs with selectors that can interact with desired analytes through various supramolecular interactions such as hydrogen-bonding,⁹⁰ halogen-bonding,⁹¹ $\pi-\pi$,⁹² metal-ligand (Figure 7b),^{93–96} and host-guest interactions.⁹⁷

1.2.2. Wrapping of CNTs with Polymers. Polymer wrapping represents a noncovalent approach of solubilizing and functionalizing CNTs, wherein the collective contacts can provide for a stable composition. CNTs can be efficiently dispersed in water with sonication in the presence of single-stranded DNA (ssDNA) as a result of multiple favorable $\pi-\pi$ interactions.⁹⁸ Hydrophobic interactions with polymers having surfactant characteristics can drive solubility in water, and saccharides and polysaccharides are capable of solubilizing and functionalizing CNTs. Although CNTs are not soluble in an aqueous starch solution, they are soluble in starch-iodine complex. Stoddart and co-workers attributed these observations as a result of preorganization of amylose in starch into a helical conformation by iodine. Displacement of iodine inside the helix by CNTs by a “pea-shooting” mechanism leads to amylose-wrapped CNTs. The water-soluble starch-wrapped CNTs dispersions can undergo triggered disassembly by enzymatic hydrolysis with amyloglucosidase.⁹⁹ Addition of this enzyme to starch-wrapped CNTs results in quantitative precipitation within 10 min.¹⁰⁰ A variety of saccharides and polysaccharides^{101,102} have been used for the noncovalent functionalization of CNTs.¹⁰³ Conjugated polymers are a natural class of CNT wrappers and have drawn much attention. Conjugated polymer-wrapped CNTs can be obtained by polymerizing an appropriate monomer in the presence of CNTs¹⁰⁴ or by two-component mixing.¹⁰⁵ Swager and co-workers showed that conjugated polymers attached to selector side chains can provide selectivity for the detection of specific analytes and even resolve very similar structural isomers.^{47,73,97,106,107} CNTs can also be functionalized with polymeric surfactants containing long alkyl chains that interact via hydrophobic interactions.^{108,109} Dai and co-workers demonstrated the adsorption of Tween 20 conjugates containing biotin, staphylococcal protein A (SpA), or human autoantigen UIA to CNTs. Poly(ethylene oxide) chains of

Tween 20 block the surface of CNTs and are crucial to suppress nonspecific binding of proteins.¹⁰⁸

1.2.3. CNTs Decorated with Metal Nanoparticles.

Although many examples of sensors based on unfunctionalized “pristine” CNTs have been reported, it is important to note that residual metal catalysts or particles left from the CNT production process have been accredited for the sensitivity of unpurified CNTs to certain analytes.² As a result, intentional incorporation of metal nanoparticles represents a productive approach for producing specific or stronger responses. Unfunctionalized CNTs are insensitive to H₂ gas, but electron beam evaporation of 5 Å of palladium (Pd) onto CVD-grown single CNT or CNT networks provides sensitivity to H₂ gas at a 4–400 ppm level in air at room temperature. The high sensitivity is understood to stem from the dissociation of H₂ to atomic hydrogen on Pd. This process lowers the work function of Pd and subsequently causes electron transfer from Pd to CNT, decreasing the carrier density and conductivity of p-type CNTs.¹¹⁰ Using a “dry transfer printing” process, Sun et al. showed that CNT chemiresistive devices functionalized with Pd nanoparticles could be fabricated on flexible poly(ethylene terephthalate) (PET) substrate that can withstand 1000 cycles of bending and relaxing without significant sensing performance degradation.¹¹¹ Deshusses and co-workers electrochemically deposited gold nanoparticles from commercially available ready-to-use gold electroplating solutions onto spray-printed carboxylated-SWCNT films on gold electrodes. The resulting chemiresistive sensors can detect H₂S in air at room temperature with a limit of detection of 3 ppb.¹¹² Similar to H₂, unfunctionalized CNTs are also insensitive to carbon monoxide. The functionalization of CNTs with SnO₂ nanocrystals can overcome the inherent insensitivity of MWCNTs to H₂ and CO gases as well as enhancing sensitivity to NO₂. Chen and co-workers showed that MWCNTs decorated with SnO₂ nanocrystals can detect ppm levels of NO₂, H₂, and CO gases at room temperature, an improvement over existing SnO₂ sensors which operate typically at temperatures over 200 °C. Uniform decoration of ~2–3 nm sized SnO₂ nanocrystals was achieved by deposition of aerosol SnO₂ onto MWCNTs on gold interdigitated electrodes by electrostatic-force-directed assembly (ESFDA).¹¹³

1.2.4. Covalent Functionalization. Although noncovalent functionalization appears attractive toward tailoring the selectivity of CNT sensors, long-term stability, robustness, and leaching of noncovalent coatings remain a concern.^{114,115} Covalent functionalization offers strong and stable anchoring of functional groups which allows the robust applications of functionalized CNTs in harsh environmentally challenging conditions and for in vivo studies.^{116,117} Using covalent modification, selectors can be precisely attached to CNTs via their termini or sidewalls for long-term stability and reproducibility with well-defined chemical composition.

The capability of the CNT sidewalls to undergo chemical reactions has led to the development of an extensive collection of covalent functionalization methods.^{11,85} Zhang et al. developed a highly efficient modular functionalization method capable of attaching a variety of chemical groups to the sidewall of CNTs. The reaction involves the addition of zwitterionic intermediates formed in situ from 4-dimethylaminopyridine (DMAP) and disubstituted acetylenedicarboxylates to the surface of CNTs.^{118,119} Versatile, functional handles including terminal alkynes and allyl groups can be grafted, which can allow postfunctionalization procedures such as 1,3-

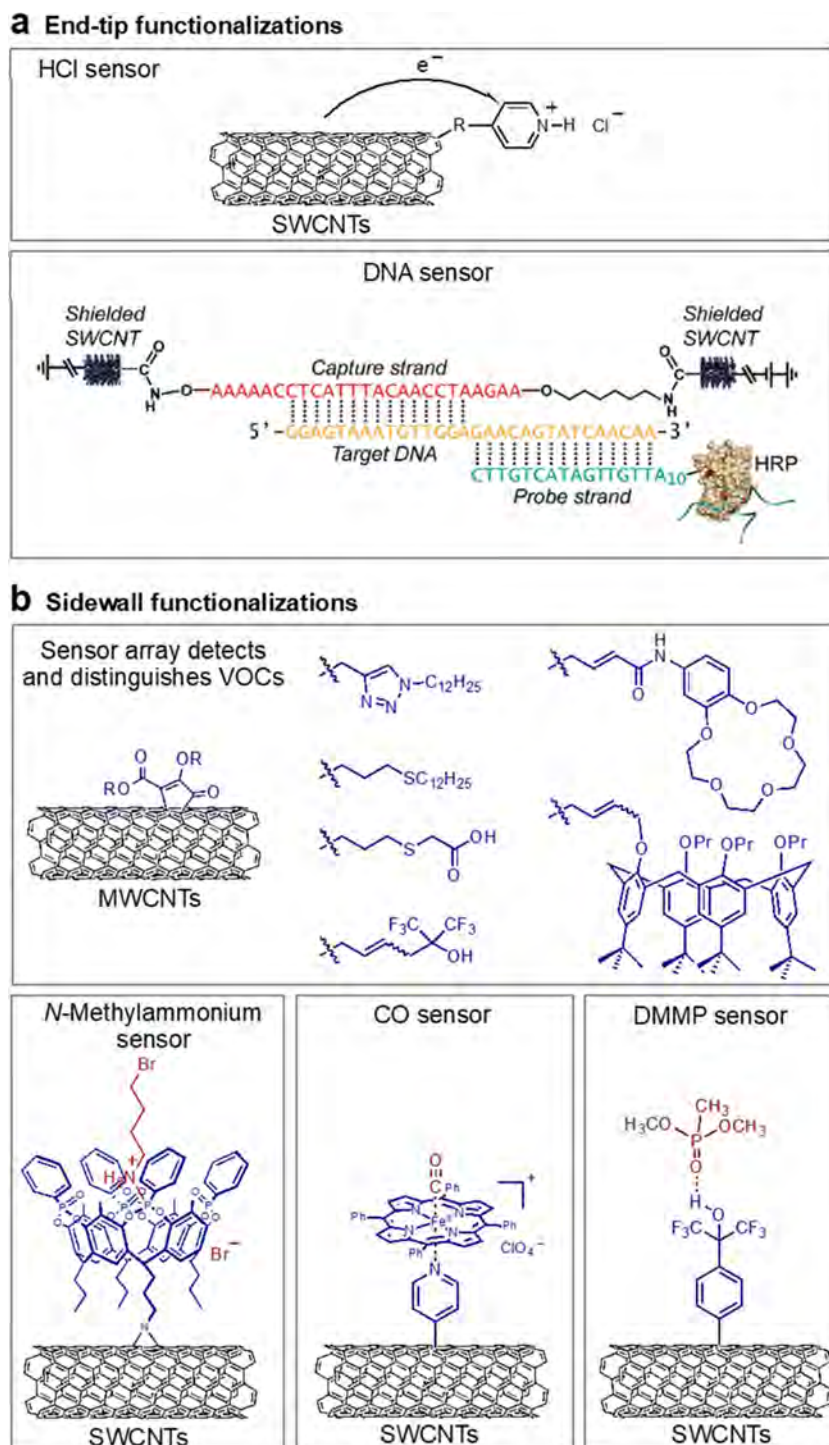


Figure 8. Examples of covalent functionalization of CNTs: (a) End-tip and (b) Sidewall functionalization. DNA sensor scheme is adapted with permission from ref 120. Copyright 2011, American Chemical Society.

dipolar cycloaddition, thiol–ene addition, and olefin cross-metathesis reactions for further diversification. Using this method, sidewall-functionalized MWCNTs consisting of allyl, propargyl, alkyl triazole, thioalkyl chain, carboxylic, HFIP, calix[4]arene, and crown ether groups were synthesized and fabricated into chemiresistive sensors that were able to selectively identify a diverse array of volatile organic compounds, Figure 8.

Thermal aziridination using organic azides provides access to covalently functionalized CNTs that has been theoretically

suggested to provide minimal perturbation to the transport properties.^{121–123} Early recognition of this advantage by Schnorr et al. resulted in a focused study on a variety of SWCNTs containing hydrogen-bonding groups such as thiourea, urea, and squaramide via thermal aziridination of 3-azidopropan-1-amine followed by another step to attach the selectors. The resulting SWCNT chemiresistive sensor array consisting of different hydrogen-bonding groups was able to detect ppm levels of cyclohexanone and nitromethane, vapor signatures of explosives. These sensors are highly reproducible

between measurements and exhibit long-term stability, critical parameters to consider regarding practical applications.¹²² Thermal aziridination was also employed in the covalent functionalization of SWCNTs with a tetraphosphonate cavitand for *N*-methylammonium detection in aqueous conditions. Sarcosine, a potential biomarker for prostate cancer, and its ethyl ester hydrochloride derivative can be selectively detected in water at a concentration of 0.02 mM (Figure 8b).¹²⁴ More recently, SWCNTs covalently functionalized with methyl pentafluorobenzoate and pentafluorobenzoic acid via aziridination enabled the detection of low ppm levels of ammonia and trimethylamine at room temperature. The sensors show no interference from volatile organic compounds and are operational in air and under high humidity.¹²⁵

He and Swager used a reductive approach and functionalized CNTs with different aryl groups and *N*-heterocycles. CNTs were first reduced with sodium naphthalide in THF in situ followed by addition of aryl iodonium salts.¹²⁶ CNT attachment of pyridyl groups at the 4 position is particularly useful for the anchoring of transition metal complexes. The potential of this pyridyl anchor was exemplified by the localization and electronic coupling of iron porphyrins ($\text{Fe}(\text{tpp})\text{ClO}_4$) to CNTs functionalized with pyridyl groups in the development of heme-inspired carbon monoxide sensors (Figure 8b).¹²⁷ Although covalent functionalization is critical to achieve higher sensor selectivity, excessive functionalization can disrupt the π surface of CNTs, increasing the base resistivity and lowering sensitivity. Therefore, optimal sensor response to a targeted analyte requires a well-controlled degree of covalent functionalization.

Covalent functionalization by reactions with diazonium ions is widely used on carbon nanomaterials. Liu and co-workers functionalized SWCNTs with pendant hexafluoroisopropanol (HFIP) groups with a degree of functionalization of 1 HFIP per 75 carbons for DMMP detection. The HFIP attachment was conducted by in situ generation of an aryl diazonium ion through reaction of 2-(4-aminophenyl)-1,1,1,3,3-hexafluoropropan-2-ol with isoamyl nitrite at 70 °C.⁶²¹ Johnson and co-workers covalently attached antibodies to SWCNTs functionalized with aryl groups containing sulfo-*N*-hydroxysuccinamide (NHS) esters.^{128,129} Considering the invasive characteristics of covalent functionalization, Wang and co-workers heavily functionalize the outer wall of double-walled CNTs (DWCNTs) with 4-benzoic acid moieties using diazonium chemistry. Since the inner tube is sealed and protected by the functional outer tube, the interaction between functional groups on the outer wall can induce an electrical change to the inner wall.¹¹⁶

Various metal oxides can be covalently attached to CNTs using sol–gel processes.^{130,131} The synthesis of CNT–metal oxide using a sol–gel process involves the oxidation of CNTs to generate carboxyl and hydroxyl groups on the graphitic surface. These groups can react with a colloidal solution (sol) of metal alkoxide or metal halide precursors. Subsequent hydrolysis and condensation reactions provide an integrated network (gel) of metal oxide on CNTs. Resulting CNT–metal oxides commonly give one-dimensional core–shell structures. Liang et al. provided an early example of MWCNTs coated with tin oxide nanocrystal via the sol–gel method from tin(II) chloride that can detect ppm levels of NO , NO_2 , ethanol, and acetylene gas at 300 °C.¹³² Additionally, the thickness of the tin oxide shell can influence the sensing properties.¹³³ Other

examples include MWCNTs functionalized with silica network and gold nanoparticles for the electrochemical detection of dopamine and ascorbic acid^{134,135} and SWCNT– TiO_2 core–shell hybrids synthesized using titanium isopropoxide as a precursor that possess a unique photoinduced acetone sensitivity.¹³⁶ Moreover, SWCNT–indium oxide hybrids can be prepared from oxidized SWCNTs and indium chloride in ammonium hydroxide. The crystallinity of indium oxide, as controlled by the temperature of calcination, was reported to be important to the sensor's response to acetone and ethanol.¹³⁷ Similar to the synthesis of other metal oxides, SWCNT– CuO hybrids were prepared from copper(II) chloride in ammonium hydroxide and found to be sensitive to ethanol vapors and humidity at room temperature.¹³⁸

Attachment of chemical groups or macromolecules to the ends of CNTs is generally achieved via amidation or esterification reactions with the carboxylic groups on oxidized CNTs that have been shortened by controlled acidic oxidation.^{139–141} Although these strong acid oxidative treatments can damage and shorten CNTs, subsequent end-tip functionalization does not perturb the π surface of CNTs. Haddon detected hydrogen chloride by introducing basic sites at the SWCNT ends through covalent attachment of pyridines (Figure 8a). The protonation of pyridine groups by hydrogen chloride induces the electron transfer from semiconducting SWCNTs. The sensor responded with decreasing resistivity because holes are introduced to the valence band of semiconducting SWCNTs.¹⁴²

Biomolecules can be precisely positioned at the ends of single CNTs and CNT networks for sensing applications. Nuckolls and co-workers elegantly cut individual SWCNT positioned between two gold electrodes using electron-beam lithography and oxygen plasma ion etching to open a nanometer-scale gap.¹⁴³ The gap was covalently bridged via amide coupling with amine-functionalized single-stranded DNA. Well-matched duplex DNA was shown to mediate charge transfer between the two SWCNT ends. The single CNT–DNA device was able to detect a single base pair mismatch in a 15-mer DNA with an increase in resistance relative to a well-matched oligomer.¹⁴⁴ Schemes for the regiospecific covalent functionalization of CNT ends with biomolecules suffer several limitations, including nonspecific surface adsorption, the introduction of defect sites on the sidewall during the oxidation process, and aggregation of tubes. Weizmann et al. exquisitely utilized a surface protection strategy to achieve regiospecific terminally linked DNA–CNT nanowires that addresses the limitations in bulk. In this strategy, strong-acid-oxidized SWCNTs were surface protected through surfactant and polymer wrapping with Triton X-100/PEG ($M_n = 10\,000$), followed by amide coupling with amine-functionalized DNA at the termini to form DNA–CNT nanowires.¹⁴⁵ The specificity of this process was also confirmed by the selective attachment of gold nanoparticles to the CNT termini.¹⁴⁶

1.3. Device Architecture and Fabrication

CNTs can be integrated in a straightforward manner into a variety of electronic device architectures with a variety of fabrication approaches. The design choices for devices utilizing CNTs as an *electrical* component of a sensor will be discussed in this section. Fluorescent sensors or other sensors that take advantage of the *optical* properties of CNTs have been reviewed elsewhere.^{26,27} This review will also not discuss the

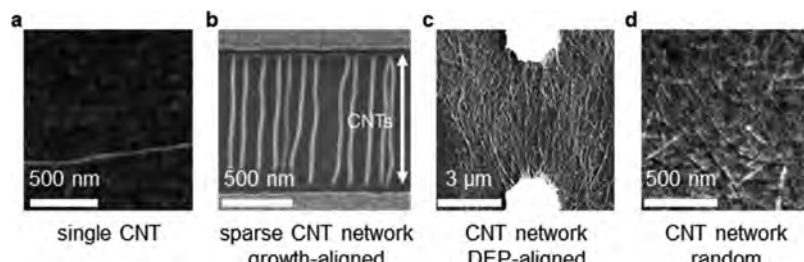


Figure 9. AFM/SEM images of (a) single CNT,²¹ (b) sparse, growth-aligned CNT network,¹⁶² (c) dielectrophoresis (DEP)-aligned CNT network,¹⁶⁸ and (d) random CNT network.¹⁶⁹ Images adapted with permission from refs 162, 21, 168, and 169. Copyright 2017, 2000, 2010, and 2011, Nature Publishing Group, American Association for the Advancement of Science, Springer, and American Chemical Society, respectively.

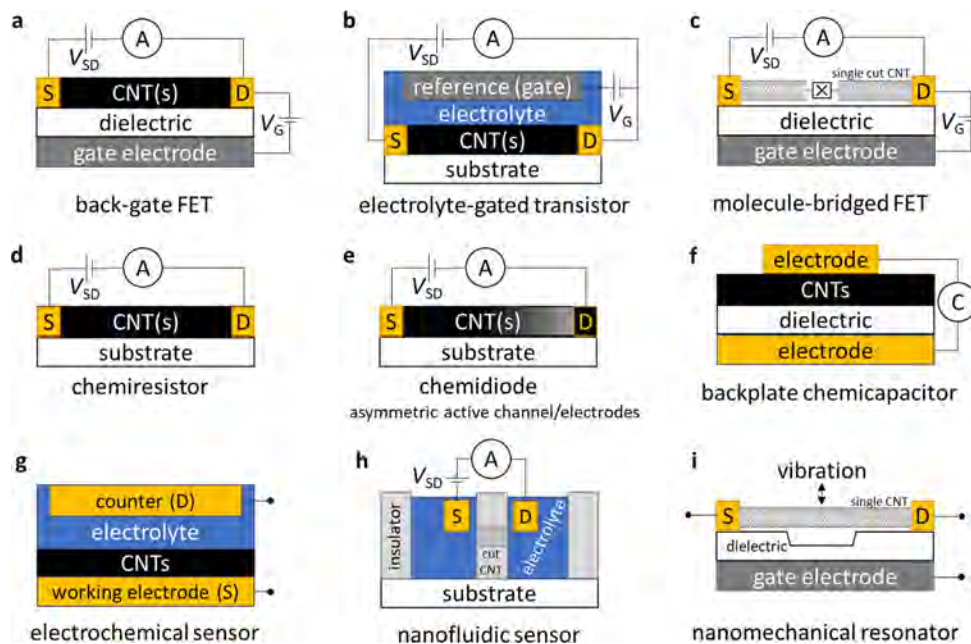


Figure 10. Illustrative CNT sensor architectures: (a) back-gate FET, (b) electrolyte-gated transistor, (c) molecule-bridged FET, (d) chemiresistor, (e) chemidiode, (f) back-plate chemicapacitor, (g) electrochemical sensor, (h) nanofluidic sensor, and (i) nanomechanical resonator. S = source, D = drain, \oplus = ammeter, V = voltage, \odot = capacitance meter, \boxplus = molecular bridge.

use of CNTs as tip augmentations of scanning probe microscopies.^{147,148}

1.3.1. Single CNTs vs CNT Networks. While the chemistry of pristine and functionalized CNTs is the primary parameter to tune sensor selectivity and sensitivity, the choice of CNT quantity and morphology also plays a large role in determining sensor characteristics.^{5,149} Devices using individual CNTs (Figure 9a), wherein a single chemical event can interrupt all of the transport,²⁰ can have higher sensitivity and a lower limit-of-detection than devices using multiple CNTs. Single-molecule sensors have been claimed using single-CNT architectures.^{144,150–157} From a purely scientific standpoint, single-CNT devices offer the ability to eliminate complexity from inter-CNT interactions, thereby simplifying the chemical sensing mechanisms (see section 1.1) and precluding sensor drift/degradation that results from long-term movement/settling of CNT networks (see section 1.4). However, single-CNT devices are more time-consuming to fabricate and characterize than CNT network devices, and their lower signaling electrical currents also require more expensive measuring equipment. Furthermore, CNT-to-CNT variation and device-to-device reproducibility remain a challenge.

Sensors using CNT networks (Figure 9d) can be quickly and inexpensively fabricated with a variety of methods (vide infra). The response of a CNT network offers higher device-to-device reproducibility than single-CNT devices, but metallic CNTs in the network are less sensitive to analytes than semiconducting CNTs, and overall sensor response can be attenuated.⁵¹ For optimal intra-CNT sensing responses, the CNTs should be debundled, so that charge carriers remain accessible to analyte interactions and/or coupled to selector/receptor groups.^{51,158} For sensors in which inter-CNT effects are proposed to determine electrical response, analogous single-CNT devices would exhibit no response. The nanotube density is also an important consideration, as lower density films with higher surface-to-volume ratios have been shown to offer higher sensitivity and lower limit of detection.¹⁵⁹

As an intermediate between single CNTs and random CNT networks, aligned CNTs can be used (Figure 9b and 9c). When compared to single-CNT devices, the baseline noise of aligned CNT sensors can be much lower¹⁶⁰ and device yield/reproducibility is higher. Relative to random CNT networks, aligned CNTs, if sparse enough, can limit inter-CNT effects and exhibit higher sensitivity.⁵¹ Highly aligned, sparse CNT networks have been made with a variety of techniques

including growth along a surface template,^{161,162} spin coating,⁵¹ deposition in lithographically patterned trenches,¹⁶³ and alignment along solution interfaces.^{164,165} Aligned CNT networks in which neighboring CNTs are intertwined and in electrical contact with each other (Figure 9c) exhibit anisotropic electrical properties that can be measured either along or perpendicular to their alignment axis.¹⁶⁶ For a detailed review on the comparison of random CNT networks and aligned CNTs in different electronic devices, we refer the reader to review articles out of the Rogers' group.^{4,167}

1.3.2. Device Architectures. *1.3.2.1. Transistors.* The field-effect transistor architecture utilizing CNT(s) as the active channel (CNT–FET) is a versatile sensor platform (Figure 10a). Early CNT-based chemical sensors, reported by Kong and Dai, were chemically responsive transistors (*chemitransistors*), obtained by chemical vapor deposition growth of an individual SWCNT across patterned Pd catalyst islands on SiO_2/Si layered substrate.^{21,170} In chemitransistors, the channel current (I_{SD}) across a range of gate voltages (V_G) is compared before and after analyte exposure. Thus, one I_{SD} – V_G curve offers many features, and seemingly subtle changes can be accurately correlated with analyte exposure using linear discriminant analysis.¹⁷¹ To optimize sensitivity, the CNT active channel should be semiconducting and not metallic, which is an issue considering currently as-produced SWCNTs are mixtures of chiralities. In addition to the back-gate architecture, chemitransistors can utilize a top-gate architecture, in which a dielectric and metal gate electrode are deposited on top of the CNT(s). The top dielectric layer partially passivates the CNT against degradation but also limits direct CNT–analyte interactions, which can lower sensor response.^{161,172}

The dielectric and gate electrode layers of a conventional solid-state FET can be replaced with liquid electrolyte and an electrochemical gate electrode. This electrolyte-gated transistor (EGT) architecture (Figure 10b), originally developed for the study of conjugated organic polymers and referred to as electrochemical transistors,¹⁷³ is also referred to in the CNT literature as an electric double-layer transistor.^{174–176} The CNT–EGT architecture targets solution-phase analytes and can be incorporated into microfluidic sensors.¹⁷⁷ CNT–EGTs exhibit higher on–off ratios with lower switching potentials than CNT–FETs operated via a conventional back-gate.^{178,179} These advantages translate to CNT–EGT sensors, as small changes (<500 mV) in V_G can result in markedly improved analyte sensitivity.¹⁷⁹

In addition to serving as the active channel, CNTs can serve as the electrodes for molecule-bridged transistors (Figure 10c). Single CNTs are precisely cut by electrical breakdown or lithographically patterned etching, and the resulting nanometer-scale gap can be bridged by a variety of conductive (redox-active) molecules.^{143,157,180} The chemical responsiveness of the bridging unit has been leveraged to detect pH, metal ions, proteins, and DNA.^{143,144,157} When the CNT gap is bridged by single-stranded DNA, conductivity increases upon formation of a DNA duplex with the complementary strand. However, if the complementary strand contains one base-pair mismatch, conductivity decreases nearly 300-fold.¹⁴⁴ Fabrication of these CNT–molecule–CNT junction chemitransistors is not trivial, but the sensing response of proposed molecular linkers can be evaluated *in silico* prior to fabrication.¹⁸¹

1.3.2.2. Two-Electrode Solid-State Sensors. While the three-electrode transistor architecture offers much more data

for sensing analysis, architectures using only two electrodes offer operational simplicity that would be suited for distributed, low-cost sensors. In the absence of applied gate voltage, CNTs can exhibit changes in conductivity on exposure to analytes. These chemically responsive resistors (*chemiresistors*, Figure 10d) constitute a very simple sensor design with minimal power and instrumentation requirements. In liquid-phase electrochemical systems, these sensors have been referred to as chemiresistive,^{182,183} conductometric,¹⁸⁴ or amperometric.¹⁸⁵ In this review, we reserve the term *amperometric sensing* for electrochemical sensors in which electrolyte solution plays an integral role in the conduction pathway. Chemiresistors benefit from low cost and ease of fabrication, which allows for rapid screening of a diverse array of selectors.^{68,93,117,186,187} Their low operational power requirements can enable wireless sensor networks, where the CNT chemiresistor is incorporated into passively powered RFID tags (Figure 11).^{90,107,188,189}

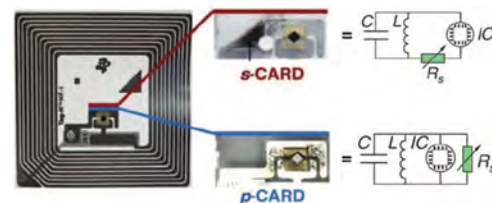


Figure 11. Two methods to integrate CNT chemiresistors into commercial RFID tags (left) and their equivalent circuit diagrams (right). Reproduced with permission from ref 90. Copyright 2016, Wiley-VCH Verlag GmbH & Co. KGaA.

Most chemiresistors are characterized using a single small bias voltage (V_{SD}). At higher bias voltages, the I_{SD} – V_{SD} curve for CNTs deviates from Ohm's law linearity for an ideal resistor.¹⁹⁰ Analysis of the nonlinear voltage regime could allow extraction of more data from chemiresistive sensors. This approach has been used for Pd–CNT–Pd devices to sense H_2 via Schottky barrier modification.⁸⁴

A nonlinear, rectifying I_{SD} – V_{SD} curve is expected if the chemiresistor architecture is sufficiently electronically desymmetrized. Such a *chemidiode* (Figure 10e) changes its I_{SD} – V_{SD} curve upon exposure to analyte. If the source and drain electrodes are materials with different work functions then a Schottky diode is formed. A Pd–CNT–Si Schottky diode has been used to sense H_2 .¹⁹¹ Symmetric metal–CNT–metal devices can detect asymmetric deposition of a second metal at one of the electrodes via the resulting rectified I_{SD} – V_{SD} curve.^{192,193} Alternatively, the *p*-type CNT active channel can be asymmetrically functionalized with molecular,¹⁶⁹ polymeric,¹⁹⁴ or metallic *n*-dopants to form *p*–*n* rectifying diodes.¹⁹⁵ Current reports of chemidiodes have focused primarily on the observation of increased rectifying behavior upon exposure to a single high concentration of analyte. Calibration of chemidiodes against a range of analyte concentrations is a promising approach for future research to consider.

CNTs can also be used as the active element in a conductor/dielectric/conductor capacitor architecture. Although the capacitance between an individual CNT and a gate electrode has been studied,¹⁹⁶ capacitive sensing studies have primarily utilized CNT networks/films (*chemicapacitors*, Figure 10f), often in a FET-type architecture with separate source and drain top electrodes. Using a parallel-plate capacitor model or an *RC*

transmission line model, gate capacitive measurements of CNT films on back-gate FET devices have been used to estimate CNT coverage density.^{197,198} The capacitance of the film changes upon exposure to analyte as a result of the polarization of analyte molecules near the CNT surfaces. Snow and co-workers reported that CNT-based sensors exhibit larger responses with faster recovery kinetics in capacitance rather than in resistance mode.^{199,200} However, a study by Esen and co-workers using an *RC* transmission line model attributed the bulk of the chemicapacitive response of a CNT film to changes in its resistance.²⁰¹ An alternative measure of chemicapacitance is to connect a two-terminal chemiresistor-like device to an AC voltage source and impedance analyzer and to model the source–drain capacitance and resistance of the equivalent circuit. Using this method, ammonia vapors exhibit a faster and larger capacitance than conductivity response²⁰² and CO₂ was found to exhibit a capacitive response but not a resistive response.²⁰³

1.3.2.3. Electrochemical Sensors. CNT films can function as electrodes for solution-phase electrochemical sensors (Figure 10g).^{8,204} When used with biological selectors/analytes, these are also referred to as biosensors. Their high specific surface area allows wide dynamic sensor range, resistance to fouling, and high loadings of electrocatalysts or selectors. CNT films have been functionalized with a variety of enzymes to amperometrically detect biological analytes. Potentiometry has been used for CNT-based pH sensors.^{185,205–207} Potential differences generated in solution can be amplified by using the CNT electrode as an extended gate electrode for a metal oxide semiconductor FET (MOSFET) chip.²⁰⁸ Voltammetry measurements, requiring a potentiostat, assist in analyzing complex mixtures by separating electroactive species by their redox potentials.^{209,210} This is particularly useful for distinguishing and quantifying different dissolved metal ions.^{211,212}

A single CNT with open ends from oxidative cutting can function as a well-defined, size-selective pore to separate the cathode and anode, forming a nanofluidic sensor (Figure 10h). Amperometric measurements show a change in electroosmotic current as analytes pass through CNT pores. On the basis of the magnitude and duration of the current change, similar analytes can be distinguished from one another; this has been applied to discrimination of different alkali metal ions,¹⁵⁵ oligonucleotides of varying length,¹⁵⁶ or differently charged dye molecules.²¹³ In a more advanced architecture, a top-gate electrode can be fabricated for the CNT pores, resulting in a nanofluidic FET which provides more data for distinguishing various analytes.²¹⁴

1.3.2.4. Miscellaneous. Electronic analytical methods based on resonant frequencies have been augmented by incorporation of CNT(s), such as circular disk resonators^{215,216} and quartz crystal microbalance²¹⁷ (QCM). The details of these analytical methods are beyond the scope of this reference. However, it should be noted that a suspended individual CNT in a modified FET-type device can be driven into resonant vibration modes by applying offset sinusoidal potentials from the gate electrode (Figure 10i). Such *nanomechanical resonators* have been used to detect minute mass changes on the CNT.²¹⁸ A side-gate device has been used to detect adsorption of naphthalene molecules or xenon atoms to the CNT with impressive yuctogram-scale resolution (1 yg = 10⁻²⁴ g).¹⁵⁴ Thus far, these studies have only been conducted on unfunctionalized CNTs.

1.3.2.5. Sensor Arrays. To better identify or quantify analytes from complex sample mixtures, multiple sensing elements can be integrated onto the same device, often using shared counter/drain/gate electrodes. Ishihara and co-workers elegantly used a minimal array consisting of two chemiresistors to make a formaldehyde sensor.²¹⁹ One element, functionalized with hydroxylamine hydrochloride, becomes more conductive upon exposure to formaldehyde vapors, while the other element is unresponsive to formaldehyde but serves as a reference to account for conductivity changes arising from humidity and temperature variations. More elaborate multi-channel arrays can be formed from a variety of cross-reactive sensing elements, in which a variety of analytes can be determined simultaneously, in a process reminiscent of olfaction/taste.²² Electronic noses/tongues comprising CNT electrical elements have been used to discriminate between a variety of analytes such as volatile organic compounds^{68,117,122} or malignant vs healthy cells.¹⁷¹ By giving a sensor array a training set of samples, fingerprint responses can be determined with mathematical techniques such as principal component analysis (PCA) and linear discriminant analysis (LDA).²²⁰

1.3.3. Fabrication. To incorporate CNTs into electric devices, there are two general fabrication strategies: fabrication using as-grown CNT films or the deposition of purified CNTs. The former approach, usually performed via high-temperature chemical vapor deposition onto prepatterned electrodes, produces robust electrode/CNT contacts, and with sparse CNT deposition bundling and inter-CNT effects can be avoided. However, for as-grown single-CNT devices, it is difficult to control the angle of CNT growth between electrodes and device yield is low, especially for larger channel lengths.^{21,170} Additionally, for as-grown CNT devices, a distribution of CNT diameters and chiralities are formed and limited on-device purification steps are available. Metallic CNTs can be preferentially disrupted using electrical breakdown,^{162,221,222} plasma etching,²²³ thermal oxidation,²²⁴ or irradiation,²²⁵ resulting in higher on–off ratios for CNT transistors. CNTs aligned during growth can be alternatively transferred to different substrates with lift-off techniques.^{6,226}

In contrast, device fabrication strategies that rely on deposition of preformed CNTs can take advantage of solution-based functionalization schemes (section 1.2) and purification strategies, which can enrich specific diameters or chiralities.^{227,228} The purified CNTs can be further purified/treated after deposition to enhance transistor on/off ratio, chemitransistor sensitivity, and response time.²²⁹ CNTs can be deposited onto prepatterned electrodes or vice versa; electrodes can be deposited onto CNTs. The former method is convenient for laboratory research, as prepatterned electrodes can be produced in bulk. However, in these cases, the CNTs are only held onto the electrode weakly, and device performance may drift as a result of a high and variable contact resistance at the CNT–electrode interface.²³⁰ In contrast, postdeposition of metal electrodes onto CNTs fixes them in place with greater contact areas and lower contact resistances.²³¹

Deposition of CNTs from a suspension by inkjet printing, spray coating, spin coating, drop casting, or doctor blading can fix CNTs in place by rapid removal of solvent. Alternatively, CNTs can be deposited using external forces to make more robust sensing materials. Such techniques include layer-by-layer assembly²¹⁰ and alternating current dielectrophoresis

(DEP).²⁰² Variation of AC waveform, electrode geometry, and substrate all play a role in DEP, and individual CNTs can be repeatedly deposited. The resulting aligned CNT devices exhibit higher on/off ratios than random network devices.⁴

Solvent-free deposition methods for purified CNTs have also been explored. Mirica and co-workers pioneered *abrasive deposition* using compressed pellets of CNTs ball milled with selectors.^{91,187,232} Abrasive deposition is a simple, low-cost, and rapid fabrication method suitable for teaching laboratories and rapid prototyping.²³³ Limitations of this method include the need for a rough substrate, the use of relatively large amounts of CNTs (~25–150 mg) to fabricate one compressed pellet, and the limited mechanical integrity of pellets, which is particularly acute with poorly adhering selectors (e.g., TiO₂ nanoparticles). *Adhesive deposition* of “bucky gels”—viscous, nonvolatile, CNT-containing mixtures—has been explored with ionic liquids and deep eutectic liquids,^{234,235} and related methods are used in the production of some commercial chemiresistive sensors.²³⁶

1.4. Performance Parameters

The promise of practical chemical sensors has motivated the constantly expanding research on CNTs. All analytical methods must possess the capability to provide quantitative or, in some cases, qualitative measurements. Chemical sensors, by definition, are devices with the capability to recognize and transduce the chemical information on the samples. In the simplest cases, the chemical information is the analyte concentration and the read out is a change in a readily measured signal. Ideally, a sensor is sensitive, selective, and stable. Achieving these figures of merit continues to be a challenge for the development of all sensors. Furthermore, chemical sensors are an alternative to large equipment in analytical labs, and it is implicit that they are inexpensive, physically small (ideally portable), and robust under field conditions. CNT-based sensors are viewed as being well suited for these requirements. Additionally, qualities such as reproducibility, rapid response times, and low drift are demanded for practical sensors. We detail the requirements for practical sensors and its challenges from the chemical perspective. Central to our discussion are the interactions between functionalized (selector/receptor modified) CNTs and the analyte. This section will introduce and provide brief descriptions of the relevant figures of merit and how they are measured. This section will conclude with a discussion of challenges arising from the properties of CNTs.

1.4.1. Parameters of Performance and Figures of Merit: What They Are and How to Measure Them? The sensing response curve describes how the devices respond to the exposure of the analyte as a function of time. Figure 12a illustrates a hypothetical curve when the device is exposed to increasing concentration of the analyte. The choice of the architecture of the sensing device will govern the type of signal measured by the sensor. The sensing traces are often reported as the relative changes in measured resistance (R), current (I), conductance ($G = I/V$; the symbol is not to be confused with Gibbs free energy), capacitance (C), power gain, and resonant frequency (f_0) of the device vs time. Different conventions have been adopted for plotting these measurements—most popularly normalized differences $\Delta X/X_0$, X/X_0 , or simply ΔX (where $X = R$, I , G , C , or gain). For example, the change in conductivity ($-\Delta G/G_0$) is calculated by observing the

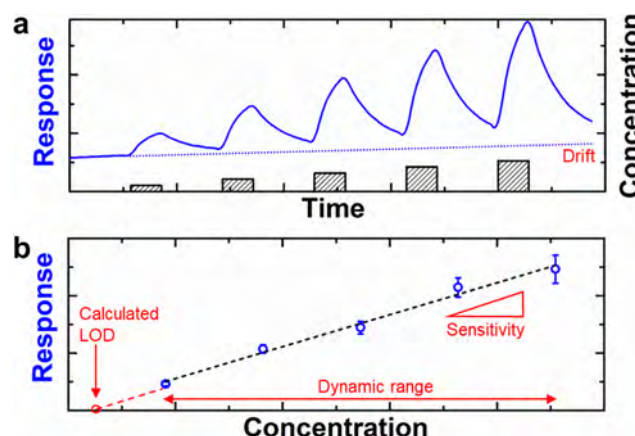


Figure 12. Hypothetical sensing response curve (a) and calibration curve (b) of a sensor exposed to increasing concentration of the analyte. Adapted with permission from ref 35. Copyright 2016, Wiley-VCH Verlag GmbH & Co. KGaA.

normalized difference in the current before (I_0) and after (I) exposure to the analyte using eq 1

$$-\frac{\Delta G}{G_0}(\%) = \left[\frac{I_0 - I}{I_0} \right] \times 100 \quad (1)$$

The calibration curve (Figure 12b) shows the relationship between the response of the sensor and the concentration of the standard solution.²³⁷ The standard solutions for the analyte should be carefully chosen to cover the relevant concentration range. Sensitivity is defined as the capability to discriminate small differences in concentration or mass of the analyte. In other words, sensitivity of the sensor is the slope of the calibration curve. The range of the concentration of the standard solution measured for the calibration curve constitutes the dynamic range, the range of which the signal is linearly proportional to the concentration is the linear range.²³⁸

Limit of detection (LOD) is the lowest amount of an analyte in a sample which can be detected with reasonable certainty. The theoretical or calculated LOD, as established in the literature,^{239–241} is determined as the concentration that corresponds to the signal at three standard deviations of noise above the baseline using the calibration curve. Briefly, the root-mean-square noise ($\text{rms}_{\text{noise}}$) of the sensors is first calculated as the deviation of the sensing response curve from the appropriate polynomial fit. The LOD is then calculated using eq 2

$$\text{LOD} = 3 \times \frac{\text{rms}_{\text{noise}}}{\text{slope}} \quad (2)$$

The slope in eq 2 is the linear regression fit of the sensor response vs concentration curve (slope of the calibration curve). The drive for achieving lower LOD is often governed by application-dependent requirements. These values for environmental safety are published by regulatory agencies. The ability to detect a low concentration of the analyte is often coupled with dynamic range of the sensors which describes the range of concentration the sensor can be calibrated to. Sensors with low LOD often deviate from linearity at high concentrations as a result of saturation.

Selectivity of a single sensor is defined as the ability to discriminate the analyte of interest from other species within

the sample.²⁴² Specificity is also used to express selectivity: in a literal interpretation, a specific sensor recognizes only the target analyte and no other compounds. Such ideal sensors are rare as a result of similarity between analytes and lack of perfect molecular recognition. Cross signaling, also known as cross reactivity, between sensors and analytes leads to a compounding of the signals and loss of selectivity. Selectivity is measured from the signals arising from the analyte and the possible interfering compounds separately, with the assumption that there are no synergistic cooperative effects of multiple analytes and the sensor. The calibration curves (signal vs concentration) of each are then compared. The ratio of the signals of the analyte to those of the interfering compounds defines the selectivity of the sensor. This method is operationally simple and generally adequately quantifies the desirable signal relative to possible cross signaling. However, it may overlook the competing effects between different compounds and the analyte. The second method comprises replicating the matrix (simple or complex) of the real-world samples in which the analyte is mixed with expected interfering compounds. In such case, the selectivity of the sensor can then be determined by the differences in signal of the analyte with and without the interfering agents.

Stability is defined as the capability of the sensors to produce repeatable outputs for an identical environment over time. To measure the stability of the sensors, repeated measurements should be taken over time or over many cycles of exposure to the analyte. More methodically, full calibration curves are obtained for multiple devices over time. During the operational timeline of a sensor, issues regarding stability may arise from several sources, such as drift, hysteresis, and irreversibility. These issues are particularly prevalent in the development of sensors for highly reactive analytes. Drift is defined as the change in signal over time independent of stimuli. It remains one of the challenges to be solved for CNT-based sensors. The common sources of drift can be identified as either the physical changes occurring to the selectors/receptors and the context of their interactions with the CNTs, very small changes in the positions of nanotubes that effect CNT–CNT junctions, or parasitic electrical effects including the electromotility of ions under small applied potentials. The perturbation of the sensing layer caused by gas flow, pressure differentials, and thermal rearrangements can lead to signal drift.³³ Hysteresis is the difference between the output of the sensors when an analyte concentration is approached from an increasing and decreasing range. It is also influenced by the degree of irreversibility of the sensor, which is the background signal of the sensor before and after exposure to the analyte.

Lastly, the response and recovery times are important key factors when evaluating the performance of chemical sensors. The response time is defined as the time for the sensor to reach 90% of its steady state or maximum value upon an exposure to a given concentration of the analyte, while the recovery time is measured as the time required for the sensor to recover to 10% of its peak value. Reversibility is coupled with recovery time as the extent to which the output can be restored after an exposure.

1.4.2. Specific Challenges on the Performance of CNT-Based Chemical Sensors. The last subsection provided definitions for evaluating the chemical sensor performance; we now introduce specific performance challenges for CNT-based chemical sensors. Significant effort has been applied to the development of practical CNT-based chemical sensors.

However, many challenges still need to be addressed to realize many sensing applications.

1.4.2.1. Quality Controls and Reproducibility. The quality and the purity of the CNTs often led to differences in the sensing performance as reported by different research groups. For example, the differences in the performance can stem from the source/growth of CNTs,^{243,244} defect levels in the CNTs,^{245–249} or sensor fabrication.^{250,251} Obtaining high purity and specific size/helicity of the CNTs is a formidable task. Separation methods that produce high-purity CNTs are currently inefficient, not readily scaled, and thereby increase sensor costs. Establishing standardized baselines requires extensive characterization of the CNTs.

1.4.2.2. Operating Temperature. Room-temperature operation is one clear advantage of CNT-based sensors over conventional sensors based on metal oxide semiconductors. Although operating at room temperature enables lower power consumption, it can lead to competing nonspecific interactions. In this context, water sensitivity is an important parameter to be tested for practical CNT-based sensors. In addition, thermal stability of the selector/receptor–CNT composite should be tested for applications that would expose the sensors to elevated or fluctuating temperature.

1.4.2.3. Reversibility. Strong interactions designed for ultratrace analyte LOD can lead to slow off rates and prevent the sensor recovery in an analyte-free environment. Slow desorption of gas molecules can often be alleviated using thermal treatments or photoirradiation. These treatments, however, increase the complexity (in both design and operation) and cost of the overall systems. Thus, intrinsic reversibility endowed from the interaction between the well-designed selectors and the analyte is generally preferred.

1.5. Theoretical Models

Theoretical models have been used extensively to understand and predict CNT behavior and properties. Specifically, computations on CNTs have been used to probe their electronic properties in pristine²⁵² and deformed forms,²⁵³ thermal conductivity,²⁵⁴ elasticity,^{255–257} and flexibility.^{258–260} We direct interested readers to in-depth reviews on the thermal and mechanical properties of carbon nanotubes^{261–264} and details of the computational methods.^{265–268} This section highlights theoretical models for analyte–carbon nanotube interactions. These studies are used to understand the experimental data generated in sensing experiments or to computationally design novel sensors.

The possibility of probing the sensing mechanism of carbon nanotube-based sensors with computational models has been demonstrated by Cho and co-workers.²⁶⁹ In this early work, the interactions between CNT and adsorbed gas molecules were investigated using density functional theory (DFT) calculations. The carbon nanotube was represented as a carbon nanohoop with one-dimensional periodic boundary conditions along the tube axis. To investigate the adsorption-induced nanotube doping, the electronic and energy states of a tube with and without adsorbed molecules of NO₂, NH₃, CO, O₂, and H₂O were compared. Electron donation from the tube to the analyte was observed for NO₂ and O₂, while electron donation from analyte to the tube was observed for NH₃. These findings were in agreement with published experimental results.^{21,270} Since this study, a large number of studies on adsorption of small gaseous molecules on CNT systems have been reported. The binding energies determined through

different computational methods range widely (e.g., for adsorption of NO_2 on (10,0)-SWCNT, binding energies from 0.92 to 18.6 kcal/mol); however, the proposed sensing mechanisms are qualitatively consistent with the major sensing mechanism (e.g., adsorption of NO_2 induces p-doping on the CNTs).^{21,38,63,269,271,272} Other sensing mechanisms that have been proposed for NO_2 include chemisorption via formation of nitro and nitrite groups,^{61–63} changes in the density of states (DOS) of the CNT,²⁷⁰ electron localization effects,⁴⁶ or changes in the dipole moment of NO_2 .²⁷³

The wide variety of results for the seemingly simple system of NO_2 adsorbed on CNTs reveals the complexity of treating CNTs computationally. Challenges associated with their modeling include: (a) their large and conjugated π system contains highly strained bonds, which are inherently difficult to represent computationally;⁶² (b) the individual interaction energies between analyte and carbon nanotube are often very small and the resulting physisorbed states cannot be determined with great accuracy by DFT; and (c) the chirality of the CNT has a strong influence on its electronic properties, which often complicates comparisons between computational studies or computational and experimental findings.^{274,275} Consequently, the choice of the computational method²⁷⁶ and length of the investigated CNT model²⁷⁷ can have large influences on the outcome of the theoretical study.

To create computationally tractable systems, studies have used periodic boundary conditions to model the quasi one-dimensional CNTs—a typical ratio of diameter to length is about 1:1000—which limits the selection of approximate exchange-correlation functionals and analysis methods. When truncated CNTs—with end states saturated with hydrogen atoms—are used, one risks using CNTs that are too small and cannot reflect the delocalized nature of the CNT electronic states accurately.^{277,278} It has become apparent that not only CNT length but also the shape of the “cut” determines computational outcomes of truncated CNT studies. Specifically, the theoretical description of truncated CNTs can be improved by taking the Clar sextet rule into account. The Clar valence bond theory, as postulated in 1964, describes polyaromatic hydrocarbons with both conventional two-electron π bonds and aromatic sextets (benzene). Clar demonstrated that the valence bond structure with the most aromatic sextets best models the reactivity of polyaromatic hydrocarbons and that structures possessing only aromatic sextets are especially stable, Figure 13.²⁷⁹ It has been shown that structures with the maximum amount of aromatic sextets for a given chirality and number of carbon atoms best describe the reactivity and geometry of CNTs and CNT–reactant studies.^{280–284} Accordingly, computational investigations employing “straight cut” CNT samples might misrepresent the reactivity of the studied model, which might be the source of some inconsistencies in published results on CNT–analyte interactions. For detailed discussions on the Clar sextet rule in CNTs, we refer the interested reader to key studies by Matsuo et al.,²⁸¹ Baldoni et al.,^{278,283} and Ormsby et al.^{282,284}

Keeping the stated challenges in mind, we highlight several applications where computational studies have successfully predicted or explained the experimental behavior of CNT-based chemical sensors. Intrinsic doping of nanotubes with heteroatoms can be used to increase the sensitivity and selectivity of the CNTs toward electron-accepting or -donating analytes. Accordingly, n-type dopants like nitrogen,^{286–289} phosphorus,²⁹⁰ and sulfur²⁹¹ deliver higher binding energies

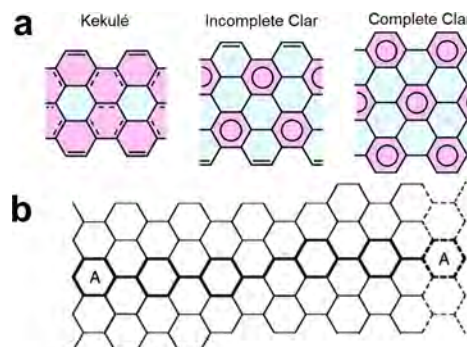


Figure 13. (a) Schematic representations of Kekulé, incomplete Clar, and complete Clar networks. Kekulé structure infers a 1,3,5-cyclohexatriene-type cyclic conjugated system, and the Clar structure represents a benzene structure with equivalent C–C bond lengths. Nucleus-independent chemical shift coding: red, aromatic < -4.5 ; blue, nonaromatic > -4.5 . Reproduced with permission from ref 281. Copyright 2003, American Chemical Society. (b) Planar representation of a chiral (6,5) CNT. Dashed lines represent replication of hexagons when the structure is rolled up to give the nanotube. Clar unit cell is highlighted with thick lines. For (6,5) CNTs the Clar unit cell contains five aromatic sextets and one double bond. Reproduced with permission from ref 285. Copyright 2009, The Royal Society of Chemistry.

and stronger charge transfer between electron-accepting analytes like NO_2 and the CNT. Similarly, p-type dopants like boron^{286,288,292–296} and aluminum^{287,289,290,297,298} show strong binding with electron-donating analytes like NH_3 , formaldehyde, cyanides, or hydrogen halides.

Tubes decorated with a single metal atom or a metal cluster have been studied extensively using computational methods. A number of groups reported computational studies that probed the adsorption mechanism and reactive behavior of gaseous analytes on metal-decorated CNTs^{298–304} or CNTs decorated with metal nanoparticles (NPs).^{45,46,137,305–309} Metal–analyte combinations with higher binding energies, stronger charge transfer, or stronger perturbations in the density-of-states are believed to lead to stronger signals in sensing studies. On the basis of these computational findings, well-informed matching between selectors and CNTs is possible.

Several studies have been conducted in which experimental sensing data is supplemented by computational studies.^{45,127,137,286,305,310,311} Ellis et al. fabricated CNT sensors decorated with indium oxide with sensitivity for ethanol and acetone.¹³⁷ The authors noted that the sensitivity toward ethanol and acetone for materials prepared by low-temperature sintering was comparable; however, the sensitivity of ethanol could be improved significantly by sintering the indium oxide at 400 °C, forming a crystalline In_2O_3 phase. The authors performed DFT calculations to elucidate the trends in the sensing behavior. Adsorption for both ethanol and acetone on the surface of indium oxide (In_2O_3)₈-decorated-SWCNTs leads to comparable charge transfer to the CNT and changes in the DOS around the Fermi level. However, computational adsorption studies on the surface of crystalline In_2O_3 showed a different picture. Acetone is adsorbed physically on the surface; ethanol, however, undergoes dissociative adsorption via transfer of H atom to the surface with formation of an ethoxy species. The observed vibrational frequencies, from infrared spectroscopy, corresponded well with the calculated frequencies for the adsorbed ethoxy species supporting this model.

In short, computational models have proven useful to suggest or supplement sensing mechanisms and help in the design of novel CNT-based sensors. These theoretical models, however, must be chosen carefully. The CNTs can be represented using periodic boundary conditions or truncated CNTs long enough to capture the extended and delocalized nature of their electronic states. The insights gained from computational studies are certain to help elucidate the sensing behavior and guide future designs of CNT sensors.

2. CNT-BASED SENSORS FOR ENVIRONMENTAL MONITORING

The promise of cost-effective, low-powered sensors has propelled the research of CNT-based sensors toward many applications, including passive environmental sensing. Detection of chemicals that are potentially harmful to human and environmental health in both gas and liquid media poses continued challenges in terms of sensor selectivity and sensitivity. Pristine CNTs have been shown to interact with many gaseous analytes, and there are continuing efforts in the functionalization of CNTs to expand the analyte scope and performance. Liquid-phase sensing places additional shear forces on a stationary CNT film and thereby highlights additional stability challenges. This section details sensors for environmentally relevant analytes in both gas and liquid media. The nature of the interactions between the analytes and the CNTs is particularly important, and new functional synthetic selectors integrated with CNTs are highlighted.

2.1. Gas/Vapor Sensors for Environmental Applications

Since the pioneering work by Dai and co-workers,²¹ many studies on CNT-based sensors for gases and vapors have been reported. The focus studies have ranged from the various detectable gases, the uses of different types of CNTs (single-walled, multiwalled, semiconducting, or metallic), functionalization methods, transduction mechanisms, and different measurable quantities. Gas sensing has been thoughtfully covered by Kauffmann and Star¹⁰ in 2008 and multiple other recent reviews.^{9,32,312} The purpose of this section is to focus on important analytes and how their interactions with the CNT systems can be used in sensing applications. We provide overviews of each analyte including earlier and the most recent developments. In particular, CNT sensors of interest are designed to detect ammonia (NH_3), nitrogen dioxide (NO_2), hydrogen (H_2), methane (CH_4), carbon monoxide (CO), hydrogen sulfide (H_2S), sulfur dioxide (SO_2), benzene, toluene, and xylene (BTX). The detection of oxygen (O_2) is covered in section 3.2 on food safety, and carbon dioxide (CO_2) is discussed in section 4.1 on breath analysis.

2.1.1. Ammonia (NH_3) and Nitrogen Dioxide (NO_2)

High concentrations of ammonia (NH_3) threaten human health as immediate severe irritation of the nose and throat can occur with exposures of 500 ppm, and 1000 ppm vapors can cause pulmonary edema.³¹³ However, even at lower concentrations, ammonia can lead to irritation to the eyes, skin, and respiratory system.³¹⁴ The main source of NH_3 emissions comes from agricultural processes, including animal husbandry and fertilizer applications.^{313,315} The Occupational Safety and Health Administration (OSHA) has designated the total weight-average (TWA) permissible NH_3 exposure limit (PEL) over 8 h to be between 25 and 50 ppm.³¹⁶ Furthermore, the Environmental Protection Agency (EPA) has warned on the toxicity of aqueous ammonia (both NH_4^+ and NH_3) to

aquatic animals and ecosystems.³¹⁷ Similarly, nitrogen dioxide (NO_2) has detrimental impacts on human health and the environment. NO_2 in the atmosphere acts as a pollutant that causes acid rain and photochemical smog. The combustion processes from chemical plants and motor vehicles contribute significantly to the atmospheric level of both NH_3 and NO_2 .^{313,315} At high concentrations, NO_2 can cause irritation in the human respiratory system. Long exposures also contribute to the development of asthma and respiratory symptoms. Accordingly, the NO_2 OSHA exposure limit is 5 ppm TWA over 8 h.³¹⁶

The approaches in the development of CNT-based sensors for NH_3 and NO_2 bear heavy resemblances to each other. This section first discusses the responsiveness of pristine CNTs and progresses to CNTs functionalized with metal and metal oxide nanoparticles (NPs), polymers, and small molecules. The adsorption of NH_3 and NO_2 gas onto pristine CNTs without any chemical functionalization has been shown to produce sensing responses by many groups.^{77,241,243–246,250,251,318–323} In accord with our earlier discussions, the performances of the sensors vary depending on the technique of fabrication and the quality of the CNTs. To avoid repetition, interested readers are referred to the discussions of chemical sensing mechanisms (section 1.1), functionalization of CNTs (section 1.2), and theoretical models of chemical sensing (section 1.5).

Rigoni et al. recently demonstrated chemiresistive sensors comprising pristine SWCNTs with 20 ppb sensitivity to NH_3 and a LOD of 3 ppb, Figure 14.²⁵⁰ Their impressive performance was attributed to the careful preparation of SWCNT layers through sonication and dielectrophoresis to minimize film thickness and to remove loosely bound agglomerates.²⁵⁰ Multiple groups have explored fabrication methods focusing on scalability and/or operational simplicity. For example, Huh and co-workers screen-printed SWCNTs that can detect 5 ppm of NH_3 .²⁵¹ Mirica et al. demonstrated a solvent-free method to deposit pristine SWCNTs by mechanical abrasion of compressed powders onto the surface of various papers.²⁴¹ The devices fabricated on weighing papers with low surface roughness detected NH_3 over a large dynamic range (0.5–5000 ppm).²⁴¹ Moreover, several studies concluded that defects along the wall of the SWCNTs enhance the response to NH_3 gas.^{245,246} These earlier results agreed with a recent mechanistic study by Salehi-Khojin et al. that revealed a dependency of sensing response on the defect levels.³²⁴ Interestingly, Penza et al. concluded that the sensitivity of the MWCNT films to NH_3 (and NO_2) also depends on the catalyst used for their growth, with the Co-grown outperforming the Fe-grown MWCNTs.²⁴³ In addition, Wang et al. prepared MWCNTs using microwave plasma-enhanced chemical vapor deposition (CVD) with Ni catalyst, which detected NH_3 with a linear dynamic range from 5 to 200 ppm.²⁴⁴ The enhanced sensing capabilities in these two cases were attributed to structural defects on the MWCNTs.

Analogously, multiple research groups have shown pristine individual CNTs and networks to be responsive to low NO_2 concentrations. Li et al. fabricated sensors by simple casting of SWCNT dispersions onto interdigitated electrodes to produce a linear response between 6 and 100 ppm and a calculated LOD of 44 ppb.²⁴⁰ The authors noted that the recovery after each exposure could be accelerated from 10 h to 10 min by illumination with UV light.²⁴⁰ Cantalini et al. deposited thin films of MWCNTs by plasma-enhanced CVD onto Pt electrodes that were sensitive to 10–100 ppb of NO_2 in dry

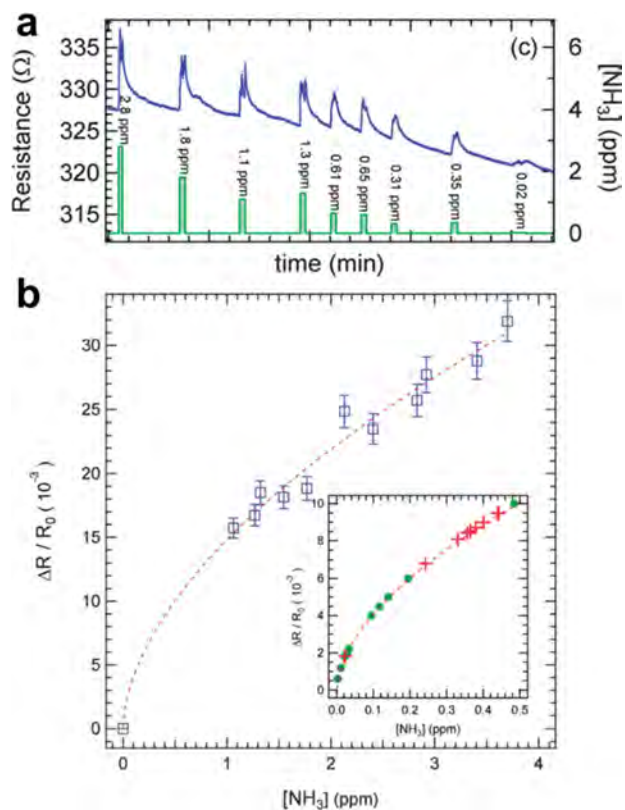


Figure 14. Responses to NH₃ (a) and calibration curve (b) of pristine SWCNT-based sensor using high-quality SWCNTs prepared through careful sonication and electrophoresis. Sensors exhibit good sensitivity to 20 ppb with a limit of detection of 3 ppb concentration of NH₃. Reproduced with permission from ref 250. Copyright 2013, the Royal Society of Chemistry.

air.³²⁵ The sensors were operational at room temperature, but the optimal performance in terms of sensitivity and recovery time was achieved at 165 °C.³²⁵ Although thermal treatment or photoirradiation is often required to recover to the original baseline after the exposure of NO₂, Ammu et al. reported that inkjet-printed films of CNTs on acid-free paper display full spontaneous reversibility, Figure 15.²³⁹ These sensors were effective for NO₂ detection at concentrations as low as 125 ppb in ambient air.²³⁹ The authors reasoned that full recovery upon removal of NO₂ is consistent with the initial formation of a weak charge-transfer complex between NO₂ and the CNTs rather than the formation of covalent bonds.²³⁹

One common method to improve the selectivity and sensitivity of the NH₃ detector is to create composites of metallic NPs and CNTs. One of the first examples was reported by Star et al., in which isolated networks of SWCNTs were decorated with different metallic NPs to create a sensor array for the detection of NH₃ as well as other gases.⁴⁹ Penza et al. improved the sensor performance of Fe-grown MWCNTs by sputter deposition of Au and Pt NPs.³²⁶ The authors ascribed the increase in sensitivity to the catalytic spillover effect at the surface of the NPs.^{326,327} Targeting wearable sensors, Lee et al. reported a flexible and transparent sensor that can detect 255 ppb NH₃ using spray-deposited SWCNTs with Au NPs.³²⁸ Similarly, Ag and Co NPs were added to MWCNTs by Cui et al.³²⁹ and Nguyen et al.,³³⁰ respectively, to increase the sensor sensitivity and recovery rates. Ag NPs were added to a composite of poly(4-vinylpyridine) (P4VP)-

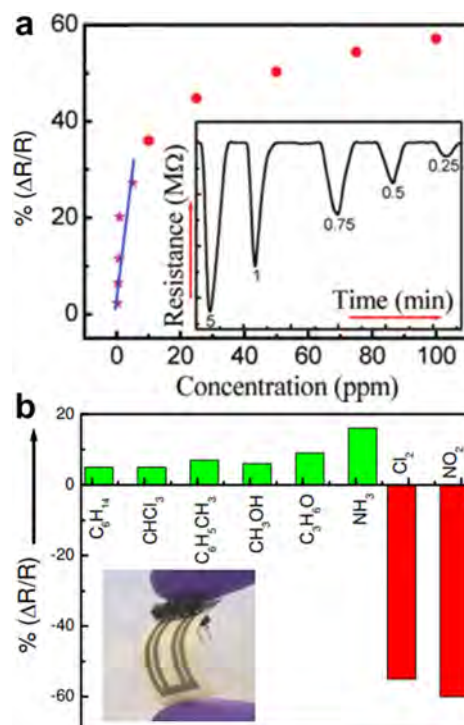


Figure 15. Flexible NO₂ sensors fabricated from inkjet-printed films of CNTs on 100% acid-free papers. (a) Plot of relative change in resistance vs the concentration of NO₂ of CNT/paper films. Inset shows plots of resistance vs time at low concentration in ppm. (b) Plot of selectivity for a CNT/paper film showing increases in resistance for common organic vapors and decreases in resistance to NO₂ and Cl₂. Inset shows an optical image of the sensor printed on paper. Reproduced with permission from ref 239. Copyright 2012, American Chemical Society.

wrapped SWCNTs for enhanced NH₃ detection at 20 ppm.³³¹ Under aerobic conditions, metallic Ag NPs are oxidized to silver oxide in the SWCNT composite. These oxygen ions lead to electron depletion regions that promote the adsorption of electron-rich ammonia, resulting to the additional improvement in sensitivity of the sensors.^{329,331}

Although metal oxide gas sensors are commercially available, many require high operating temperature and thus consume a large amount of power and have very limited selectivity.¹⁰ Composites of CNTs with various metal oxides have led to sensors that are operational at room temperature. For example, Hoa et al. fabricated SWCNT–tin oxide (SnO₂) hybrid sensory materials by simple heat treatment and oxidation of a Sn thin film with SWCNTs produced by arc-discharge methods and created sensors with a 10 ppm LOD for NH₃.³³² A hybrid sensor of SnO₂ prepared by sol–gel synthesis and SWCNTs was shown by Ghaddab et al. to detect 1 ppm of NH₃ (and 20 ppb of O₃).³³³ However, the authors noted that the sensitivity of the sensor depended heavily on the source of SWCNTs.³³³ SnO₂-coated CNTs have also proved successful as NO₂ sensors.^{113,334,335} In another example by Rigoni et al., physical mixing of SWCNTs with indium–tin oxide (ITO) NPs resulted in a 3-fold increase in sensitivity (compared to pristine SWCNTs) to NH₃ with a limit of detection of 13 ppb.³³⁶ Interestingly, the response of the composite was p-type at low concentrations of NH₃ with low humidity and switched to n-type at higher humidity levels, which was attributed to hole compensation by water.³³⁶ We

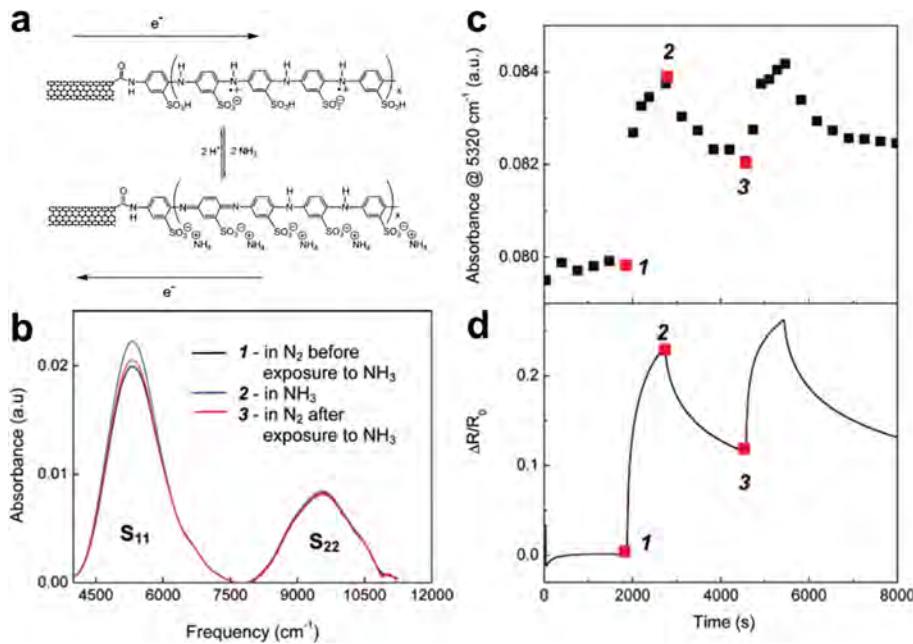


Figure 16. NH₃ sensors based on films of poly(*m*-aminobenzenesulfonic acid)-functionalized SWCNTs (SWCNT-PABS). (a) Mechanism of the interaction between SWCNT-PABS with NH₃ with the arrows indicating the charge-transfer direction between SWCNTs and PABS. (b) NIR spectra after baseline correction of SWCNT-PABS recorded before (black, 1), during (blue, 2), and after (red, 3) the exposure to 20 ppm of NH₃. (c) Change in the absorbance at 5320 cm⁻¹ (S₁₁ transition) correlates well with the change in resistance (d). Reproduced with permission from ref 339. Copyright 2007, American Chemical Society.

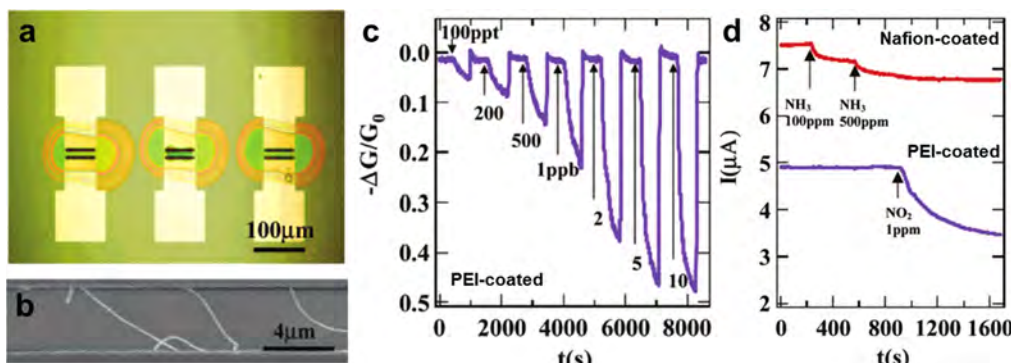


Figure 17. Detection of NO₂ using polymer-coated SWCNTs. (a) Optical image of devices after coatings of polymer solutions. (b) SEM micrograph of SWCNTs bridging the electrodes. (c) Relative change in conductance of a polyethylenimine- (PEI) coated SWCNT sensor when exposed to various concentration of NO₂. Recovery of the sensors was facilitated by UV illumination. (d) Comparison between Nafion- and PEI-coated SWCNTs. Nafion-coated devices (top, red) responded to NH₃ but not to NO₂, while PEI-coated devices only responded to NO₂. Reproduced with permission from ref 345. Copyright 2003, American Chemical Society.

speculate that hydroxide ion from NH₄OH formation may be involved. Finally, CNTs have also been used as a template for layer-by-layer assembly of porous indium oxide (In₂O₃) nanotubes that also demonstrated room-temperature sensing capability.³³⁷ Despite the wide range of the choice of metal/metal oxide NPs, the techniques of fabrication, and architectures of the sensors, the enhancement in the sensitivity toward NH₃ and NO₂ was attributed to the catalytic function of the NPs and good electronic communication between CNTs and NPs.^{49,326,338} Although the sensitivity to reducing (NH₃) and oxidizing (NO₂) gases are enhanced by metal oxides, the analyte interactions can be largely characterized as nonspecific acid–base interactions; hence, other elements are likely needed to produce sensors with high selectivity.

Composites of polymers and CNTs have also been demonstrated as effective sensors as a result of strong

interactions between NH₃ and the selected polymers. Bekyarova et al. covalently grafted poly(*m*-aminobenzenesulfonic acid) (PABS), a sulfonated poly(aniline), onto SWCNTs to create chemiresistors capable of detecting 20 ppm of NH₃, Figure 16.³³⁹ The authors proposed that the increase in the measured electrical resistance was the result of deprotonation of the PABS side chains, which, in addition to lowering the electronic transport within the PABS, enhances the electron transfer from the PABS oligomers to the SWCNTs (Figure 16a). Specifically, the NH₃-induced changes in the near-infrared (NIR) spectrum of the first semiconducting interband transition of the SWCNTs (S₁₁) correlated well with the change in the resistance of the sensors (Figure 16b–d).³³⁹ The sensitivity of this system of SWCNT-PABS can achieve a NH₃ LOD of 100 ppb (20 ppb for NO₂) by adjusting the initial resistance of the sensor.¹⁴¹ In addition, composites of

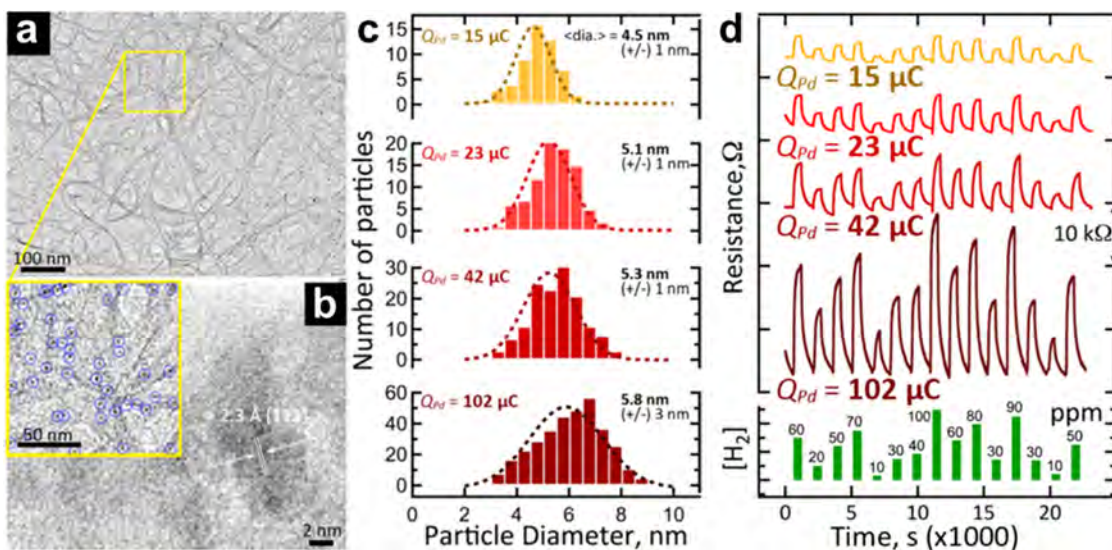


Figure 18. Palladium NP-decorated CNT ropes as H_2 chemiresistors. (a) TEM image of a CNT rope after deposition of Pd NPs. (b) (Inset) Pd NPs are highlighted by blue circles, and a high resolution TEM image of a NP is shown in the main picture. (c) Histogram of the size of the Pd NPs for electrodepositions of various quantities of Pd in terms of the Coulombic loading (Q_{pd}). (d) Sensing responses to ppm levels of H_2 for the different Coulombic loading of Pd nanoparticles. Reproduced with permission from ref 362. Copyright 2017, American Chemical Society.

poly(aniline) (PANI) and CNTs, prepared by electropolymerization on SWCNT electrodes³⁴⁰ or by in situ polymerization of aniline in SWCNT suspension,^{341,342} showed low limits of detection to NH_3 (50 ppb Zhang et al.³⁴⁰) and fast recovery times. Interestingly, Li et al. reported that poly(methyl methacrylate) (PMMA) when combined with MWCNTs produced n-type gas sensing characteristics with a decrease in resistivity when exposed to NH_3 .³⁴³ The authors proposed that the uncommon n-type behaviors may have been related to the modification of the semiconducting properties of MWCNTs upon the pretreatment with hydroxylamine hydrochloride.³⁴³ Lastly, Datta et al. noncovalently functionalized SWCNTs with poly(*N*-methyl pyrrole) (P[NMP]) that exhibited excellent linear response from 10 ppb to 1 ppm of NH_3 .³⁴⁴ When evaluating sensors that have no clear transduction designs, it is likely that a major component of sensitivity enhancements is coupled to organization effects. The selectivity in many of the experimental compositions discussed here reflects the relatively high intrinsic sensitivity of the CNTs to NH_3 and NO_2 .

Noncovalent functionalization of SWCNTs with polymers also proved effective in detecting NO_2 . Qi et al. showed that a coating of polyethylenimine (PEI) or Nafion onto SWCNTs resulted in gas sensors with selectivity for NO_2 or NH_3 , respectively, Figure 17.³⁴⁵ The presence of PEI transformed the SWCNTs from p-type to n-type semiconductors, and the sensors were sensitive to 100 ppt of NO_2 while being insensitive to NH_3 . This selectivity arises because the effect of NH_3 adsorption is outcompeted by the polymeric amine. Remarkably, the authors reported that coating with Nafion, instead of PEI, allowed the sensors to detect NH_3 without interference from NO_2 . Polymer–CNTs composites prepared by in situ polymerization also offers promising sensing results and simple fabrication. For example, An et al. polymerized uniform coatings of poly(pyrrole) (PPy) on SWCNTs.³⁴⁶ Sensors derived from this material behaved as an n-type semiconductor and displayed improved sensitivity over pure SWCNTs or PPy toward NO_2 .³⁴⁶

Another method of imparting selectivity toward ammonia and other amines is through functionalization with organometallics, in particular those with extended π systems capable of strong π -stacking interactions (see section 3.2.1). Liang et al. reported metal–phthalocyanine/MWCNT-containing chemiresistive devices with high sensitivity toward NH_3 for Co- and Zn-containing metal complexes and smaller interactions with other metal centers (Cu, Pb, Pd, and Ni).³⁴⁷ The trend in the calculated values of the binding energy between the metal centers and NH_3 from DFT agreed qualitatively with the enhancement in sensitivity.³⁴⁷ Kaya et al. developed Cu and Co metallophthalocyanines for enhanced π interactions with one pyrene and six polyoxyethylene substituents.³⁴⁸ The authors observed higher responses to NH_3 for samples containing Cu than Co. The discrepancies with earlier reports regarding the sensitivity with Cu metal centers were attributed to the substituents in the macrocycle, the number of active sites, and the thickness and morphology of the thin films.³⁴⁸ In a study that involved first-row metals from Cr through Zn, Liu et al. developed chemiresistive sensors containing porphyrin complexes for the detection of food spoilage (section 3.2 on food safety).⁶⁸ In these devices, the interaction between the metal centers and the analyte as well as the redox potential of the complex were highlighted as essential to determine the selectivity and sensitivity.^{93,347,348}

2.1.2. Hydrogen (H_2) and Methane (CH_4). Hydrogen (H_2) and methane (CH_4) pose a threat as they can explode even at low concentrations in air.³⁴⁹ Additionally, methane is a potent greenhouse gas, and it is important to detect sources of its release into the atmosphere. Thus, the detection of H_2 and CH_4 becomes paramount to prevent explosions for distribution systems/centers, mines, and petroleum fractional distillation plants. Similarly, an expanded natural gas production will require the detection of methane leakage to prevent environmental pollution and loss of revenue. The promising potential of H_2 as a clean energy carrier has propelled research efforts in areas such as fuel cells, automobile engines, and various chemical and industrial processing.^{34,349} Such developments also place the need for hydrogen sensors in household

environments and mobile transportation systems.³⁴⁹ Hydrogen gas and methane have no appreciable interactions with pristine CNTs, and research efforts primarily focus on exploiting the composite of CNTs and metallic NPs. While theoretical³⁵⁰ and experimental^{49,351} reports have shown Pt-decorated CNTs to be sensitive to H₂, the majority of CNT-based H₂ sensors in the literature focused on the use of Pd metal.³⁵² These sensors can be grouped into two main categories depending on whether Pd metal is deposited on the CNTs (Pd decorated) or used as the electrodes (Schottky contact based).

Kong et al. reported one of the first examples of Pd-decorated SWCNTs that functioned as H₂ sensor.¹¹⁰ In their report, a thin coating of Pd was deposited by electron beam evaporation on an individual SWCNT, and upon exposure to ppm levels of H₂, the measured conductance decreased.¹¹⁰ Pd undergoes a reversible reaction with hydrogen to produce a low electron affinity palladium hydride, which promotes electron donation to compensate for hole carriers in SWCNTs and leads to higher resistance. A number of subsequent publications endeavored to improve the ease of fabrication and the performance of this type of sensor.^{49,111,353–361} For example, Sayago et al. fabricated sensors by spray coating of SWCNTs and then functionalizing with Pd NPs,^{354,355} and Sun and Wang created Pd–SWCNTs sensors on flexible substrates.^{111,358} In addition, Sippel-Oakley et al. observed that thermally evaporated Pd exhibited faster responses and recoveries than sensors prepared by sputter coating Pd on SWCNT thin films, suggesting that sputtering damages the π sidewalls.³⁵⁶ Similar to the detection of NH₃ and NO₂, differences in the performance of H₂ sensors may depend directly or indirectly on CNT sidewall defects. Khalap et al. compared the sensing responses between sensors comprising individual Pd-decorated SWCNTs with and without sidewall defects.³⁵⁹ Their results demonstrated that a positive relationship between the defect sites and Pd NPs led to the 1000-fold increases in hydrogen response (resistance), and only 2-fold increases were observed in defect-free samples. More recently, Penner and co-workers reported the effects of the size of Pd NPs electrodeposited on CNT ropes, Figure 18.³⁶² From their results, modest changes in the diameter of the Pd NPs greatly affected the amplitude and the time of the responses.

Schottky contact-based H₂ sensors rely on the modulation of the contact electronic barrier height between the electrons and the CNTs upon exposure to hydrogen gas. The work function of Pd is sensitive to H₂, and hydride formation reduces the work function. Javey et al. demonstrated this mechanism in a Pd-contacted SWCNTs field-effect transistor.³⁶³ The contacts between metallic Pd and semiconducting SWCNTs exhibited ohmic behavior before H₂ and Schottky diode behavior after H₂.³⁶³ Their results suggested that the lower work function of Pd led to the formation of higher Schottky barriers, and electron tunneling through these structures decreases exponentially with length for dramatic reductions in current. To exploit this phenomenon for H₂ sensing, Wong et al. fabricated a microelectronic diode with the structure of the thin layer of Pd deposited on top of MWCNTs on doped silicon and detailed response with 100% H₂.¹⁹¹ Myung and co-workers later improved on this configuration to achieve sensors with high sensitivity, large dynamic range (from 25 to 2000 ppm), and fast response/recovery times, Figure 19.⁸⁴ The authors aligned SWCNTs across prefabricated Pd microelectrodes by AC dielectrophoresis and stressed the importance of using semiconducting SWCNTs.⁸⁴ Carriers are more likely to flow

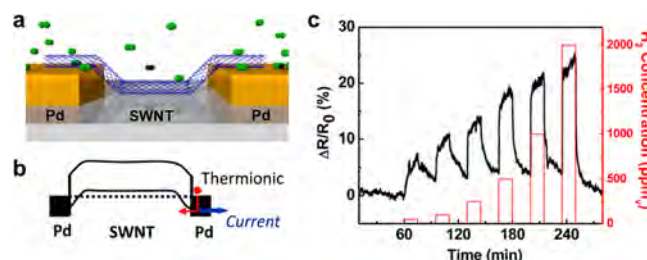


Figure 19. Schottky contact-based H₂ gas sensor. (a) Schematic representation of the sensor comprising aligned SWCNTs bridged across the Pd microelectrode. (b) Band diagram of the sensor when exposed to H₂, which decreased the work function of Pd and created a Schottky barrier. (c) Sensing response to various concentrations of H₂. Reproduced with permission from ref 84. Copyright 2014, American Chemical Society.

through metallic SWCNTs, which do not produce Schottky barriers at the electrode interfaces, leading to the attenuation of the signal and sensitivity. Choi et al. demonstrated an alternative solution by using preseparated semiconducting SWCNTs to fabricate networks between Pd electrodes.³⁶⁴ The results highlighted the importance of minimizing the amount of metallic CNTs and optimizing the density of the SWCNT networks for the performance of the sensors.

CNT-based sensors for methane are not as common as H₂ sensors as a result of the difficulty of obtaining selectivity toward CH₄. For metal-decorated SWCNTs, Star et al. reported that CH₄ showed no significant response at room temperature.⁴⁹ In an earlier example, Lu et al. reported the fabrication of CH₄ sensors comprising Pd-decorated SWCNTs that showed increases in conductance when exposed to 6–100 ppm of methane.³⁶⁵ Subsequent exposure to UV light facilitated the desorption of the gas molecules and recovered the sensing baseline.³⁶⁵ More recently, Paprotny and co-workers demonstrated CH₄ sensors using MWCNTs functionalized with metal oxide NPs (either SnO₂ or ZnO) through atomic layer deposition (ALD).^{366,367} Both chemiresistors functioned at room temperature and were sensitive to ppm levels of methane in dry air.^{366,367} The proposed mechanism involved the adsorption of CH₄ molecules on the metal oxide NPs, leading to the increase in the sensor's relative resistance. However, cross reactivity to other gases will remain a challenge for CH₄ sensors based on metal-decorated CNTs. In cases where reactivity of the constituent metal oxides or NPs have not been established under the reported conditions in the absence of the CNTs, it is proper to be suspect of results, which could be coupled to changes in the gas (oxygen levels) or humidity rather than methane. Hence, we consider the development of chemiresistive CH₄ sensors to be at an early stage and encourage the readers to consider new approaches to detect this challenging analyte.

2.1.3. Carbon Monoxide (CO). Carbon monoxide (CO) is the colorless, tasteless, and odorless toxic gas that is responsible for the majority of fatal poisoning worldwide.³⁶⁸ CO is produced from the incomplete combustion of carbon fuels, and emissions from vehicles and industrial processes are major sources. OSHA has designated the PEL of 35 ppm time-weighted average (TWA over 8 h) and 200 ppm ceiling (5 min exposure).³⁶⁹ The higher affinity of CO over O₂ toward the iron porphyrin complexes found in hemoglobin and myoglobin leads to CO poisoning.^{370,371} Although detectors for CO are available with metal oxide semiconductors (MOS) and solid

electrolyte (SE),¹⁰ CNT-based sensors could fill the need for massively distributed or even wearable sensors to prevent poisoning in domestic and industrial environments.³⁷²

Although CO does not engage in strong binding or charge-transfer interactions with pristine CNTs,^{127,248,270,311} successful examples of sensors comprising pristine CNTs exist in the literature. Varghese et al. demonstrated the capacitive sensing of CO with pristine CNTs, albeit only at concentrations of 100%.²⁰³ Pristine CNTs have also been used in the resonance frequency-based detection of CO; in these sensors, the adsorption of CO was detected as a change in the resonance frequency of the active layer.^{215,216} Increased interaction between the CNTs and CO have been observed theoretically for deformed,³⁷³ boron-doped, nitrogen-doped CNTs,³⁷⁴ and aluminum-doped CNTs.³⁷⁵ Sensors capable of ~1 ppm detection have been demonstrated using CNTs with carboxylic acid ($C_{(CNT)}-COOH$) sidewall defects^{248,376} and sulfonated SWCNTs,³⁷⁷ which are assumed to have covalent $C_{(CNT)}-SO_3H$ or $C_{(CNT)}-OSO_3H$ groups. In an alternative chemical modification, Zhao et al. used oxygen plasma to create disordered structures and eliminate metallic CNTs to produce a CO sensor capable of detecting 5 ppm of CO.²⁴⁹ The authors, however, noted that the presence of water molecules led to complications, suggesting that the oxygenated defects can give rise to unwanted side reactivity.²⁴⁹

CNTs functionalized with NPs of metals and metal oxides have been reported as effective CO sensors. Changes in the transfer of electron density from the metal NPs to the CNTs upon the adsorption of CO molecules is reported to give rise to the sensing response.³⁷⁸ Star et al. reported the sensing properties of 18 chemiresistive SWCNT channels functionalized with different metals.⁴⁹ In particular, the Pt-decorated SWCNTs showed sensitivity toward 2500 ppm of CO.⁴⁹ SWCNTs modified with Au,^{378,379} Pd³⁸⁰ (ab initio study), and tin oxide (SnO_2)^{381,382} were also reported as room-temperature CO detectors. In addition, composites of polymers and CNTs have been shown by several groups to detect CO molecules. For example, Wanna et al.³⁸³ showed reproducible responses to CO exposure from 100 to 500 ppm with a composite of CNTs and maleic acid-doped PANI, while Lin et al.³⁸⁴ fabricated a CO (and NH_3) sensor using a composite of $Co_3O_4/PEI-CNTs$. In the metal-free PANI-modified material, the basis of sensitivity to CO is not clear.

The translation of known reactivity or bonding of analytes to sensors optimally leverages chemical knowledge. In this context, recently efforts toward noncovalent modification of CNTs with organometallic complexes have proved promising. The composites of these two materials improve the selectivity of the CNTs and overcome the inherently low conductivity of the organometallic compounds. Liu et al. employed a metal complex with a well-defined, experimentally supported molecular sensing mechanism.³¹¹ The organocobalt complex contains a pendant amino ligand internally bound to the central metal atom, which can be trapped in the open form with a free amine upon binding of CO. The large geometrical differences between the cobalt complexes required a solution phase to display an efficient equilibrium. Hence, in this case, a network of unfunctionalized SWCNTs was coated with an inert fluorocarbon oil containing the selector complex. The CO favors the free amine form of the complex, which subsequently engages in charge transfer (electron donation) to p-doped SWCNTs and produces a decrease in conductance, Figure 20a and 20b.³¹¹ The sensor was shown to be stable in

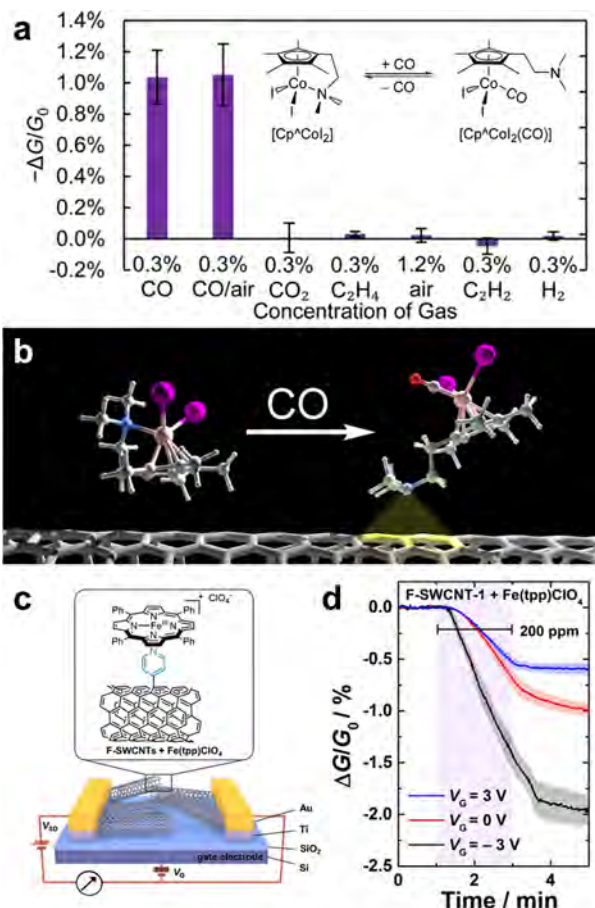


Figure 20. SWCNT-based CO sensors. (a, b) Sensing scheme of the binding event of CO by cobalt complex showing the freeing of amine ligand upon binding of CO. Averaged change in conductance of cobalt complex/SWCNT chemiresistor in response to several gases and gas mixtures. Reproduced with permission from ref 311. Copyright 2016, American Chemical Society. (c) Schematic depiction of CO sensor comprising pyridyl-functionalized SWCNTs and iron porphyrin ($Fe(tpp)ClO_4$). Covalent pyridyl ligands facilitate the in situ reduction of iron porphyrin to modulate the sensitivity of the sensor. (d) Sensing responses of iron porphyrin/pyridyl-functionalized SWCNTs toward 200 ppm of CO with applied gate voltage of -3, 0, and +3 V. Reproduced with permission from ref 127. Copyright 2017, Wiley-VCH Verlag GmbH & Co. KGaA.

air and with near perfect selectivity to CO over CO_2 , C_2H_2 , C_2H_4 , and H_2 . Biological-based recognition mechanisms also provide important opportunities, and heme-inspired materials have been reported both experimentally^{127,385} and computationally^{181,386} to detect CO. He et al. computationally investigated the electronic transport properties of a system comprising two SWCNTs covalently linked via an iron(II) porphyrin when exposed to CO.^{181,386} They found that the binding of the CO molecule to the Fe center of the porphyrin hinders the electron transport between the two SWCNTs.^{181,386} Savagatrup et al.¹²⁷ demonstrated the use of the inactive iron(III) porphyrin anchored to pyridyl-functionalized SWCNTs that was reduced in situ to active iron(II) structure via the application of a moderate gate voltage. Upon the fractional in situ reduction to the nominally air-sensitive iron(II) state, sensing responses to CO increased significantly, Figure 20c and 20d.¹²⁷ This method is consistent with solution

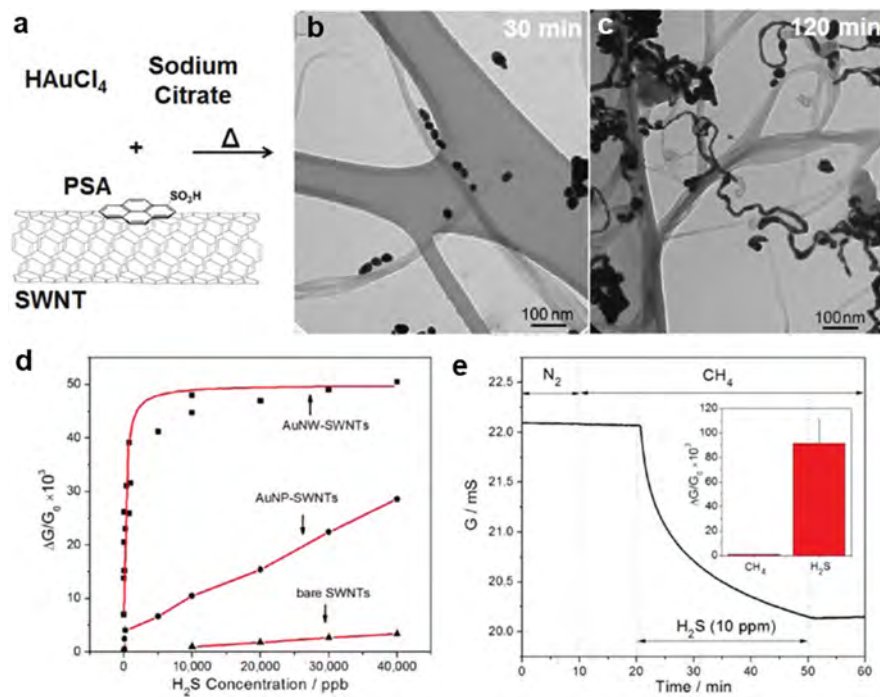


Figure 21. Hydrogen sulfide (H_2S) detection using gold nanowires–SWCNTs hybrid network (Au NW–SWCNTs). (a) 1-Pyrenesulfonic acid (PSA)-functionalized SWCNTs suspended in aqueous solution were used as the template for citrate reduction of HAuCl_4 to generate AuNPs; subsequent heating produced Au NWs. (b) TEM images of Au NPs and (c) Au NWs on SWCNTs. (d) Relative change in conductivity of Au NW–SWCNTs network to 5 min exposures of various concentration of H_2S gas. (e) Detection of H_2S in methane (CH_4); inset shows the sensor response to 100% CH_4 and 10 ppm of H_2S in methane. Reproduced with permission from ref 394. Copyright 2017, American Chemical Society.

studies, wherein iron(III) porphyrins do not interact with CO but the iron(II) porphyrins bind CO strongly.

2.1.4. Hydrogen Sulfide (H_2S) and Sulfur Dioxide (SO_2). Both hydrogen sulfide (H_2S) and sulfur dioxide (SO_2) are common waste gases and atmospheric pollutants. H_2S is a colorless, foul smelling, and poisonous gas that is generated/released in large amounts from coal, natural gas, and petroleum refineries as well as bacterial decomposition of animal and human waste.³⁸⁷ H_2S acts as neurotoxin at low concentration and causes severe eye, nose, and throat irritation at moderate concentration.³⁸⁸ Prolonged exposure to levels above 100 ppm can cause death, and individuals can become desensitized to the smell of H_2S , thereby compromising their ability to detect this danger.³⁸⁸ SO_2 is highly corrosive and readily oxidized in air to create sulfuric acid. Both gases pose significant threats to the environment and human health.³⁸⁹ The 8 h TWA PELs are set at 10 ppm for H_2S and 5 ppm for SO_2 .³¹⁶ Thus, accurate measurement of the two sulfur-containing vapors is of crucial interest.

Although most reports of CNT-based detection of H_2S rely on NP-decorated CNTs, there are examples suggesting that pristine and defective CNTs can provide responses. For example, inkjet-printed SWCNTs have been used to create both chemiresistive³⁹⁰ and chemFET sensors.³⁹¹ In addition, plasma treatment of MWCNTs to introduce carboxyl- and nitrogen-containing groups has been shown to increase the selectivity toward H_2S over SO_2 .³⁹² Such sensors are likely to be less selective, but could find utility in applications wherein other interferants are not present.

CNTs decorated with metal or metal oxide NPs have proved to be most promising for the detection of H_2S . Guided by DFT calculations, Zhang et al. suggested the potential of Au- and Pt-decorated CNTs for sensing of both H_2S and SO_2 .^{299,393}

in these system, SO_2 accepts electrons from the metal–SWCNT networks, while the opposite occurs with H_2S .^{299,393} Experimentally, several examples of composites of Au nanostructures and SWCNTs have been demonstrated.^{112,327,394,395} Deshusses and co-workers decorated SWCNTs with Au NPs using a electrodeposition method and reported a 3 ppb H_2S LOD at room temperature.¹¹² The sensing mechanism was reported as H_2S modulation of the electron exchange between the Au NPs and the defects on the SWCNTs. Similarly, Ding et al. reported a synthesis of gold nanowires (Au NWs) using SWCNTs as templates, Figure 21.³⁹⁴ Citrate-stabilized Au NPs were self-assembled on 1-pyrenesulfonic acid (PSA)-decorated SWCNTs template and fused to create Au NWs after heating. The hybrid network of Au NW–SWCNTs showed improved sensitivity to H_2S when compared to pristine SWCNTs and Au NP–SWCNTs and can detect ppb concentrations of H_2S without cross-sensitivity to CH_4 , CO_2 , and O_2 .³⁹⁴

A major challenge of sensors composed of Au–SWCNTs (and Ag–SWCNTs³⁹⁶) is the strong affinity of metallic NPs to sulfur-containing molecules, thereby leading to irreversible responses. Thus, most H_2S sensors rely on mild heating in ambient conditions for recovery.^{112,394} Similarly, UV irradiation can accelerate desorption of H_2S in sensors containing organometallics.³⁹⁷ Several groups have made efforts toward the development of H_2S sensors with fast self-recovery by replacing gold with other metal or metal oxide NPs. For example, SnO_2 has proved to be an attractive alternative.^{398–400} The combination of SnO_2 and CNTs allows for room-temperature operations, which is unobtainable for a system with SnO_2 alone.¹¹³ Mendoza et al. reported a sensor based on SnO_2 –CNT composite films fabricated by CVD with recovery times of 1 min at room temperature.³⁹⁸ In addition,

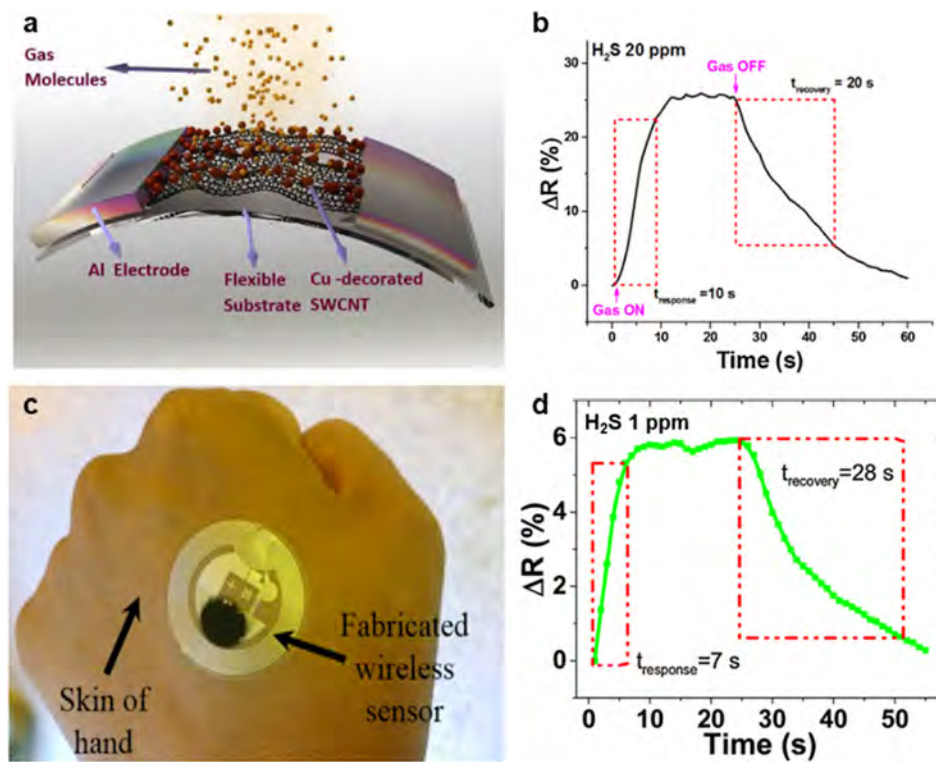


Figure 22. H_2S sensors based on SWCNTs decorated with Cu or CuO NPs. (a) Schematic of flexible sensors comprising Cu-decorated SWCNTs as the conduction channel between Al electrodes on polyethylene terephthalate (PET) substrates. (b) Response to the exposure of 20 ppm of H_2S . Reproduced with permission from ref 401. Copyright 2015, Elsevier. (c) Wireless sensor fabricated using a commercial 13.56 MHz RFID tag with CuO-SWCNT as the sensing material. (d) Response and recovery times of the sensor when exposed to 1 ppm of H_2S . Reproduced with permission from ref 402. Copyright 2016, Elsevier.

Asad et al. demonstrated that copper and copper oxide NPs enhance the sensitivity and selectivity of SWCNTs for H_2S , Figure 22.^{401,402} The authors fabricated flexible chemiresistive sensors and RFID-based wireless sensors that detect ppm levels of H_2S at room temperature with rapid self-recovery.^{401,402}

Examples of CNT-based SO_2 sensors are limited; however, nonfunctionalized SWCNTs and MWCNTs have been shown to respond to SO_2 experimentally.^{403,404} In addition, Li et al. predicted computationally that Ni-doped CNTs should be more sensitive to SO_2 than pristine CNTs.⁴⁰⁵ Goldoni et al. used spectroscopic analysis to reveal that interactions between SO_2 and SWCNTs are similar to those between NO_2 and SWCNTs.³²³ Correspondingly, poor selectivity between SO_2 and NO_2 limits further development of commercialized sensors. Interestingly, Yao et al. achieved selective discrimination between the two gases using chemiresistive random networks of SWCNTs.³⁸⁹ The authors reported a differentiation of SO_2 and NO_2 at various humidity levels. At high humidity level (92%), the resistance of the device decreased in response to NO_2 but the resistance increased with SO_2 .³⁸⁹ Their experimental results were consistent with DFT calculations that indicated electron donation should occur between the $\text{SO}_2/\text{H}_2\text{O}$ complex and the p-type CNTs.³⁸⁹ Complicating the development of sensors for SO_2 and NO_2 is the fact that both species are sufficiently reactive that they chemically evolve in ambient atmospheres. Hence, the actual responses from measurements under realistic conditions with moisture and humidity may arise from a daughter product of these gases.

2.1.5. Benzene, Toluene, and Xylene (BTX). Nonpolar compounds and aromatic hydrocarbons, namely, benzene, toluene, (ethylbenzene), and xylene (BTX or BTEX), are considered highly hazardous volatile pollutants. Benzene, in particular, is classified as both an acute and a chronic health hazard.^{406–408} The PEL concentrations given by OSHA are 1, 200, and 100 ppm for benzene, toluene, and xylene, respectively.⁴⁰⁹ These compounds are present in the vicinity of natural gas and petroleum deposits and are produced from incomplete combustion of fossil fuels and automobile exhausts. In addition, BTX are used widely as components for petrochemical products, gasoline thinner, and solvents for chemical reactions. BTX in consumer products have also been reported.⁴⁰⁸ In addition to gas chromatography (GC) coupled with mass spectrometer (MS) or flame ionization detection (FID), several methods for the detection of BTX have been reported including the use of quartz crystal microbalance (QCM)-based sensors^{410,411} and spectroscopy.⁴¹² CNT-based devices have also been used as selective sensors^{92,97,413} or as part of an array.^{117,414}

For example, Rushi et al. reported chemFET devices comprising SWCNTs functionalized noncovalently with iron tetrphenylporphyrin (FeTPP) or cobalt tetrphenylporphyrin (CoTPP) that responded to BTX at concentrations well below those given by the PEL.⁴¹³ The authors found that FeTPP-functionalized devices performed significantly better than the CoTPP counterparts, suggesting that the choice of the central metal ion is important for device optimization. An alternative method using chemiresistors integrated with polymer concentrator was reported by Im et al., Figure 23.⁹² The authors synthesized cellulose acetates functionalized with 2,3,4,5,6-

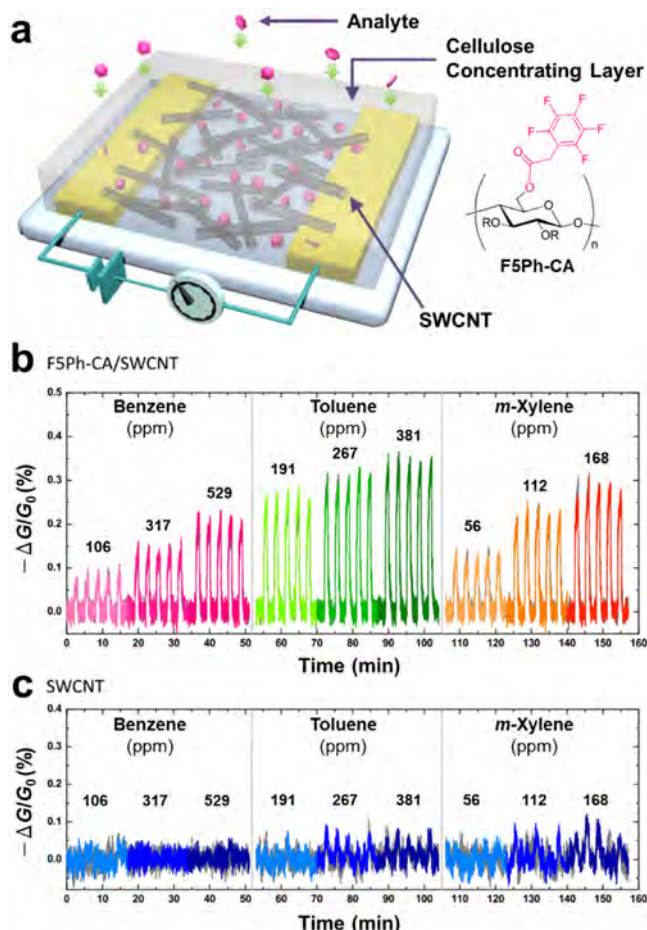


Figure 23. BTX gas sensing system of SWCNTs and cellulose polymer concentrator. (a) Schematic diagram of chemiresistor with SWCNTs and cellulose concentrating layer. (b) Change in conductance of the sensors in response to BTX gases at various concentration. (c) Responses of controlled devices without the cellulose concentrating layer. Reproduced with permission from ref 92. Copyright 2016, MDPI.

pentafluorophenylacetyl (F5Ph) and deposited the concentrating layer on top of SWCNTs. The integrated sensors performed significantly better than devices with pristine SWCNTs at detecting BTX; however, interference from ethanol, commonly found in petrochemicals, was reported. While the sensitivity and recovery are promising in both examples, selectivity among BTX or from interfering compounds remains challenging. Distinguishing among BTX or among the different isomers of xylene often requires sensing arrays.^{97,117,414} Further discussions on CNT-based sensing arrays in the context of sensors for BTX and other volatile organic compounds (VOCs) can be found in section 4.1.1.

2.2. Aqueous Environmental Sensing

Detecting trace analytes in the liquid phase is important for environmental monitoring, assessment of water quality, and health diagnostics.^{51,415} The large surface area and excellent chemical stability of CNTs make them promising aqueous chemical sensors.⁵¹ In this section, we will detail CNT-based sensors developed for aqueous environmental monitoring. Discussions on the following specialized aqueous sensors will be addressed in the later sections: detection of pesticides

(section 3.2.3), health diagnostics and biorelated applications (section 4.2), and detection of warfare agents (section 5).

2.2.1. CNT-Based pH Sensors. Fluctuations in pH can have significant effects on chemical processes; thus, measuring and controlling pH are important in environmental, industrial, and biological applications. Monitoring the pH values in real time can provide high temporal resolution and requires sensitive and stable sensors. CNT-based pH sensors provide a simple alternative to conventional sensors that could be costly, large, and incompatible with integrated circuits.⁴¹⁶ Specifically, CNT-based chemiresistors relinquish the need for a reference electrode, glass membrane, and significant power supply.

Several groups have reported that nonfunctionalized CNTs respond to changes in the pH of aqueous solutions. Takeda et al. fabricated FET devices using acid-treated SWCNTs that showed a reliable response and stability in liquid environments.⁴¹⁷ Similarly, Li et al. introduced carboxyl groups on the surface and termini of the SWCNTs before alignment on microelectrodes using dielectrophoresis.⁴¹⁶ The resulting sensors demonstrated changes in the resistance over the pH range of 5–9.⁴¹⁶ The sensors were stable in buffer solution over the 10-day experimental period.⁴¹⁶ Despite these successful examples, concerns regarding the selectivity persist. Without functionalization, it is likely that CNTs will have limited selectivity between hydronium ions and metal cations.

Similar to the gas-phase sensors, composites of conductive polymers and CNTs proved to be an attractive platform for pH sensing. The electrical properties of poly(aniline) (PANI) depend significantly on the degree of protonation, leading to rapid response to changes in solution pH. Liao et al. demonstrated that PANI/SWCNTs composite possessed tunable conductivity over a wide pH range in water.⁴¹⁸ In addition, Roth and co-workers reported a simple process for the fabrication of PANI/CNTs and PPy/CNTs on transparent and flexible electrodes.^{207,419} Although conductive polymers provide the necessary selectivity, long-term stability is potentially problematic. To improve the stability of the sensors, Gou et al. functionalized oxidized SWCNTs by electropolymerization of poly(1-amino anthracene) (PAA), Figure 24, which was designed to have stronger interactions as a result of the polymer's extended π system.²⁰⁶ PAA/SWCNT displayed high electroconductivity and thermal stability compared to the other systems (PPy/SWCNT and PANI/SWCNTs) and retained sensitivity to pH 2–12 over 120 days.²⁰⁶ The authors also demonstrated selectivity to hydrogen ion over potential interferants (Ca^{2+} and Na^+).²⁰⁶

2.2.2. CNT-Based Metal Ion Sensing. Toxic metal ions in water represent serious personal and environmental health concerns. Some species, such as iron, cobalt, zinc, copper, and manganese, are required for metabolic and signaling processes in living organisms at low concentrations, but can be toxic at higher concentrations.⁴²⁰ Other metals/elements (cadmium, lead, arsenic, chromium, and mercury) are highly toxic even at trace levels.⁴²⁰ The World Health Organization (WHO) and the US Environmental Protection Agency (EPA) issued the permissible exposure limit of these toxic metal ions in water. For example, the limits for iron, zinc, and copper are on the order of 1–10 ppm, while the limits are more stringent for cadmium, lead, arsenic, chromium, and mercury at the range of 1–10 ppb.^{420,421} The mechanisms of the toxicity of each species on the living cells are beyond the scope of this review; interested parties will benefit from reading recent reviews on

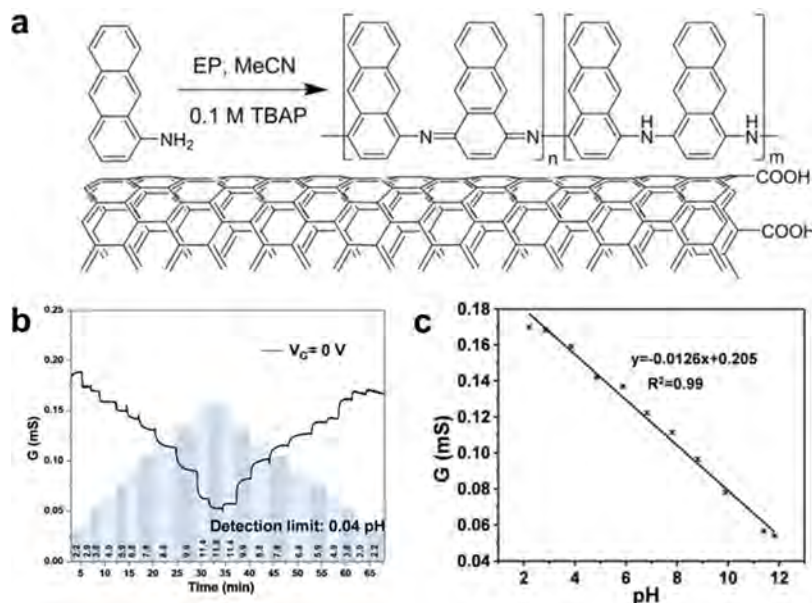


Figure 24. Chemiresistive pH sensor based on oxidized SWCNTs functionalized with conductive polymer poly(1-amino anthracene) (PAA). (a) Electropolymerization of PAA from 1-amino anthracene onto oxidized SWCNTs. (b) Sensing responses of the pH sensors to various pH solutions. Vertical bars represent the pH values. (c) Calibration curve of conductivity vs pH values. Reproduced with permission from ref 206. Copyright 2015, Nature Publishing Group.

the topic.⁴²⁰ For the detection of toxic metal ions, CNTs are most often used as an electrode material because of their large surface area, small size, ease of functionalization, and excellent electrical conductivity. In addition, CNTs have been shown to be an excellent sorbent for metal ions.⁴²² Considering the large amount of work reported in this field, we can only present representative examples. We direct interested readers to specialized reviews.^{211,420,422,423}

Electrochemical sensors using CNT-covered electrodes proved promising for the detection of multiple toxic metal ions. The main technique is anodic stripping voltammetry (ASV), which involves the electrochemical deposition of metals (analyte) at a constant potential and subsequent stripping of the deposited analyte from the electrodes. While the inherent selectivity toward toxic metals arises from a specific redox potential, the addition of molecular recognition by functionalization is often needed to selectively accumulate the analyte at the electrode interface. For example, Wanekaya and co-workers demonstrated the trace detection of Pb^{2+} and Cu^{2+} using cysteine-modified MWCNTs with a LOD of 1 and 15 ppb, respectively.⁴²⁴ Cysteine, an amino acid with high affinity toward the target metals, was covalently functionalized onto MWCNTs, which were casted onto the electrode surface for ASV analysis.⁴²⁴ The authors reported no interference for the Cu^{2+} peak from common anions (Cl^- , SO_4^{2-} , or CO_3^{2-}) and cations (Cd^{2+} and Ni^{2+}); however, excessive Cu^{2+} , Cd^{2+} , and Ni^{2+} reduced the peak current associated with Pb^{2+} .⁴²⁴ Calixarene-functionalized CNTs have proved promising for molecular recognition.⁴²⁵ To selectively detect Pb^{2+} , Wang et al. covalently attached thiocalixarene onto MWCNTs, Figure 25.²¹² Due to the highly selective recognition of thiocalixarene to Pb^{2+} , the authors reported that the sensing of Pb^{2+} was not affected by 100-fold excess amounts of Zn^{2+} , Ni^{2+} , or Cd^{2+} .²¹²

In addition to electrochemical analysis, chemiresistive and FET-based sensors have been used for the detection of toxic metals. FET sensors provide the advantage of real-time detection without the accumulation step necessary for ASV

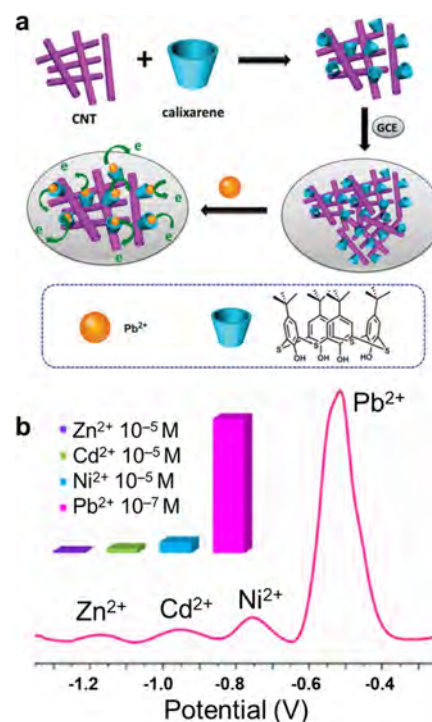


Figure 25. Determination of Pb^{2+} using thiocalixarene-functionalized MWCNTs for anodic stripping voltammetry (ASV). (a) Schematic representation of the fabrication thiocalixarene/MWCNTs-functionalized glassy carbon electrode (GCE) and the detection of Pb^{2+} . (b) Response signals after 15 min accumulation of 10^{-7} M Pb^{2+} with 100-fold excess amounts of Zn^{2+} , Cd^{2+} , and Ni^{2+} . Reproduced with permission from refs 212 and 425. Copyright 2016 and 2012, the Royal Society of Chemistry and American Chemical Society, respectively.

detection. Kim et al. reported the detection of mercury ions using pristine SWCNTs, Figure 26.⁴²⁶ The selectivity toward Hg^{2+} over other metal cations was attributed to the favorable

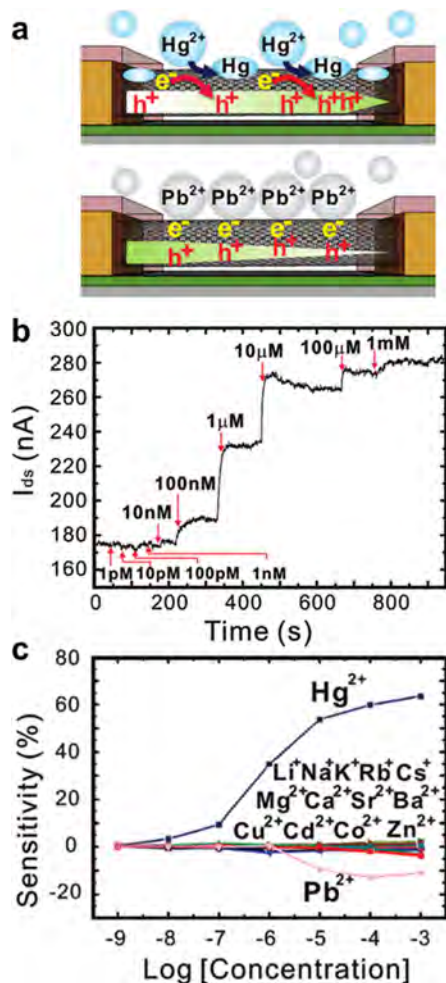


Figure 26. SWCNT-FET sensor for the detection of Hg²⁺. (a) Schematic of the proposed mechanism for the selectivity toward Hg²⁺. (b) Real-time measurement of the change in current after exposure to various concentrations of Hg²⁺. (c) Sensitivity vs concentration of various metal cations. Reproduced with permission from ref 426. Copyright 2009, American Chemical Society.

and irreversible reduction from Hg²⁺ to Hg⁰ by SWCNTs at less negative reduction potentials than needed for other

ions.⁴²⁶ Star and co-workers also reported the detection of Co²⁺ using a combined optical spectroscopic and chemiresistive measurement on SWCNTs noncovalently functionalized with polyazomethine (PAM).⁴²⁷ The large conformational change of PAM upon complexation with Co²⁺ gave rise to the selectivity of the sensors.⁴²⁷ In another example, Forzani et al. introduced coatings of polymers functionalized with different peptide sequences and lengths in SWCNT-based FET sensors.⁴²⁸ The authors demonstrated a selective platform by leveraging the well-known selectivity of His₆ for Ni²⁺ and Gly-Gly-His for Cu²⁺ ions.⁴²⁶

3. CNT-BASED SENSORS FOR FOOD AND AGRICULTURE APPLICATIONS

Food (along with water) is the most important consumable. Several processes in food management and agriculture production can be monitored and improved through chemical sensing. Specifically, these processes include monitoring of food ripeness, prevention of food spoilage, ensuring the quality of food storage, and detection of pesticides and pathogens. Worldwide, one-third of the food produced for human consumption—approximately 1.3 billion tons—are wasted or lost, due partially to the lack of accurate and real-time measurements of the condition of perishable goods along the supply chain, Figure 27.^{429,430} Economically viable sensing systems can inform both the suppliers and the consumers, improve coordination of harvest and transportation, monitor storage in both industrial and consumer settings, and identify pesticide-contaminated food.

CNT-based sensors offer several advantages that are required in food applications. Their small size, low power consumption, and simplicity combined with their capability to detect complex analytes allow the production of economically viable sensors that are ideal for product tracking and supply chain management. For example, CNT-based sensors have been incorporated into circuitry that allows for real-time information on the state of food using smartphones or other connected devices for use in smart packaging,¹⁸⁹ detection of fruit ripening,⁹⁶ food spoilage,⁹³ and pesticide detection.⁴³¹ Apart from improving food safety and minimizing food loss, CNT-based gas sensors can be used for characterizing the

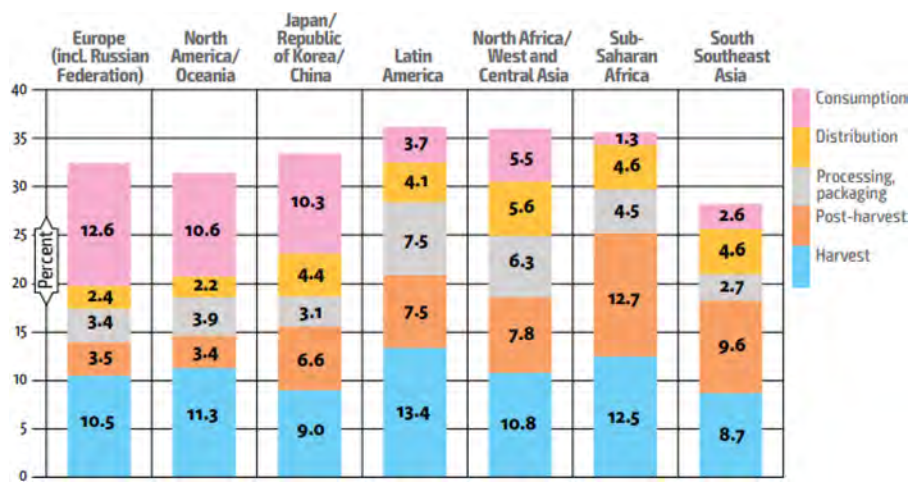


Figure 27. Distribution of food losses and waste along the supply chain by region and by stage (consumption, distribution, processing/packaging, postharvest, and harvest). Reproduced with permission from ref 429. Copyright 2017, Food and Agriculture Organization of the United Nations.

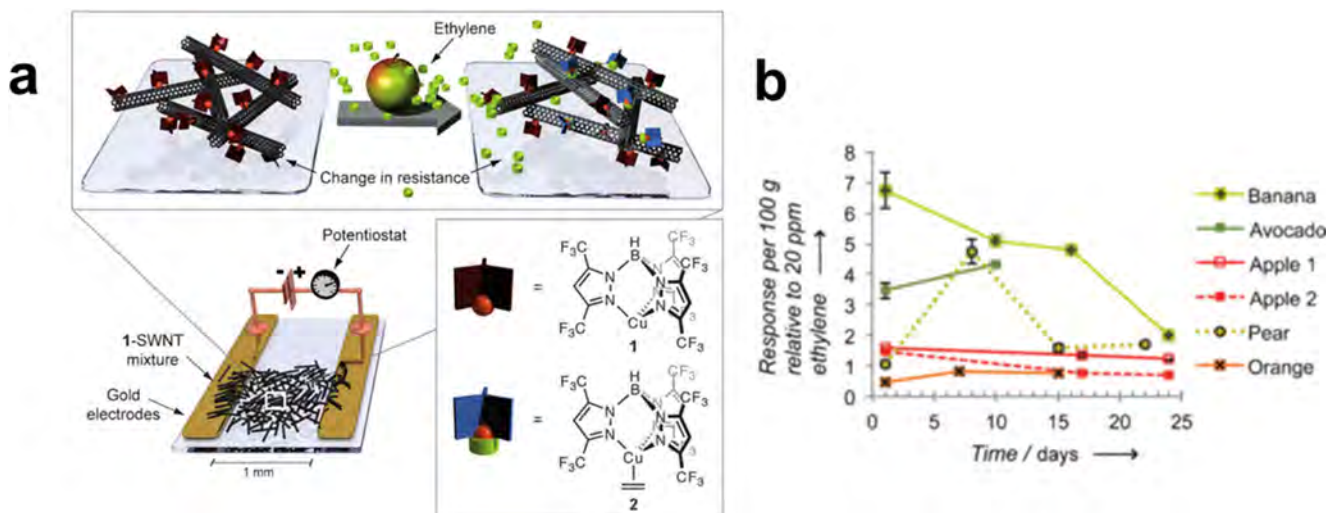


Figure 28. Detection of ethylene in real fruit samples. (a) Chemiresistive sensor using SWCNTs and a fluorinated tris(pyrazolyl)borate copper(I) complex, **1**, that can be bound directly to SWCNTs to detect ethylene gas. This complex is known to bind ethylene as shown, **2**. (b) Ethylene response of SWCNT-based sensor to banana, avocado, apple, pear, and orange samples over 25 days. Reproduced with permission from ref 96. Copyright 2014, Wiley-VCH Verlag GmbH & Co. KGaA.

flavor (taste) and odor (smell) of products to authenticate and control the quality of food products.

3.1. Food Quality

3.1.1. Fruit Ripeness. Climacteric fruits (e.g., apples and bananas) produce the fruit-ripening hormone ethylene at the onset of ripening. Ethylene is one of the smallest molecules with biological activity, and this volatile signaling molecule controls changes in color, aroma, texture, and flavor of fruit, regardless of whether it is produced naturally in the fruit or applied artificially to induce ripening.^{432,433} Thus, the processes of ripening and senescing of these fruits can be controlled through the concentration of ethylene in the atmosphere.⁴³⁴ Monitoring/managing ethylene concentration is useful for both determination of the optimal harvesting time and preservation of freshness in storage and transportation.

The detection of ethylene using CNT-based sensors was investigated both experimentally^{96,435,436} and computationally.⁴³⁷ Pristine CNTs show no sensitivity toward ethylene gas at room temperature,⁹⁶ and the addition of selector moieties is required. To this end, Leghrif et al. reported the detection of ethylene at room temperature using MWCNTs decorated with tin oxide (SnO_2) nanoparticles.⁴³⁵ Although the chemiresistors responded to as low as 3 ppm of ethylene, interference from NO_2 was reported. Esser et al.⁹⁶ developed an ethylene selective sensor by coordinating a fluorinated tris(pyrazolyl)-borate copper(I) complex to SWCNTs that was capable of forming air-stable complexes with ethylene, Figure 28a. The authors demonstrated the sensor's selectivity and utility by conducting studies on a range of fruit samples. The climacteric fruits (banana, avocado, apple, and pear) showed a decrease of ethylene production over time after they reached peak ripeness, while the nonclimacteric fruit (orange) showed an overall low production of ethylene, Figure 28b. Interestingly, the detector could differentiate between an apple stored at room temperature ("Apple 1") and an apple stored in the refrigerator ("Apple 2"), demonstrating the ability to monitor the state of the fruit simply by sampling the headspace. Additionally, Zhang et al. used the composite of MOF-199 containing copper metal centers and MWCNT to adsorb

ethylene from the headspace of durian husk, wampee, blueberry, and grapes for gas chromatography. This method showed an exceptionally low LOD of 13 ppb.⁴³⁶

3.1.2. Taste and Smell. In addition to monitoring fruit ripeness, CNT sensors are also used to effectively determine the taste and smell of various food. Sensors for this application are often referred to as electronic tongues and noses (e-tongues and e-noses). We refer interested readers to reviews of metal oxide- and polymer-based electronic noses,⁴³⁸ bioelectronic noses,^{439–442} electronic noses for food^{443,444} and medical applications,⁴⁴⁵ and computational analysis of electronic noses.⁴⁴⁶ The goal is to imitate the senses of taste and smell through a sensor readout. Humans have around 400 different olfactory receptors that collaboratively give rise to the sense of smell.⁴⁴⁷ Once in your olfactory system, the binding of an odorant (a molecule with a smell) to a receptor triggers a neural signal.⁴⁴⁸ To imitate such processes in sensors, researchers have incorporated olfactory receptors in CNT-based sensors to discriminate between different odorants differing by a single carbon center.

CNT sensors have been developed using olfactory receptors from humans,^{415,449–458} rodents,^{459–462} insects,⁴⁶³ and canines.⁴⁶⁴ Park and co-workers first demonstrated the use of human olfactory proteins for the detection of odorants in 2009.^{451,458} In early generations of these devices, lipid membranes containing human olfactory receptors were coated on SWCNT networks.⁴⁵¹ Upon binding of the odorant, the olfactory receptor shifts from the inactive, neutral state to the active, negatively charged state, which reduces the mobile charge-carrier density in the SWCNT network. This sensor was able to differentiate between butyrate molecules that only differ by a few carbon atoms (amyl butyrate, butyl butyrate, propyl butyrate, and pentyl valerate, Figure 29b) and to detect the amyl butyrate at picomolar concentrations.⁴⁵¹ A follow-up study by the same group further improved on the sensitivity of the sensors by mimicking cell signaling pathways in natural olfactory systems more closely.⁴⁴⁹ Here, nanovesicles decorated with olfactory receptors trigger an influx of Ca^{2+} ions into the nanovesicles upon exposure to odorants, Figure 29. The accumulation of positive charges in the nanovesicles induces a

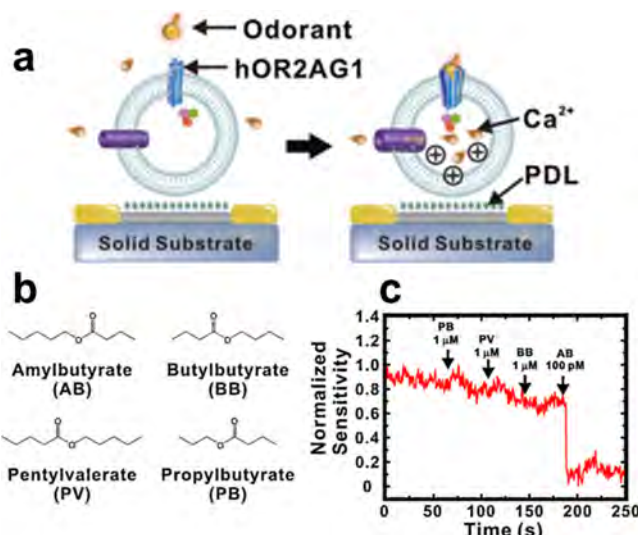


Figure 29. Detection of taste and smell. (a) Schematic of the response of nanovesicle toward exposure to an odorant molecule. Odorant molecule activates the olfactory receptor (blue) which triggers the uptake of Ca^{2+} ions through the calcium ion channels (purple), inducing a field-effect gating on the poly D-lysine (PDL) and CNT active channel. (b) Structures of different odorant molecules that can be differentiated using human olfactory receptor hOR2AG1. (c) Change in conductance upon exposure of sensing device to different odorant molecules. Reproduced with permission from ref 449. Copyright 2012, Elsevier.

field effect on the SWCNT, reducing their conductance. Devices of this architecture were able to detect amyl butyrate at concentrations as low as 100 pM, Figure 29c. Additionally, CNT-based sensors employing olfactory receptors have been used to quantify sour,⁴⁶² sweet,⁴⁵² salty,⁴⁶⁰ bitter,^{453,455,461} and umami tastes.⁴⁶³

Beyond quantifying human taste or smell using receptor proteins, several research groups have developed CNT-based sensors for the differentiation between high-quality products. These sensors can authenticate the product by quantifying the differences between similar products based on taste or smell. Wei et al. developed CNT- and graphene-based electrochemical sensors using Ni and Cu foams as the selectors to differentiate Chinese rice wines by age and manufacturer.⁴⁶⁵ Similarly, Tang and co-workers developed a MWCNT/polymer composite sensor array comprising eight different sensing channels to differentiate between several complex alcohol vapors (sake, sorghum liquor, medical liquor, and whiskey), Figure 30.^{466,467} The signals here were attributed to differential swelling behaviors of the composites. Interestingly, Kachoosangi et al. reported electrochemical CNT sensors that quantified the “heat” in several hot sauces by measuring the concentration of capsaicin.⁴⁶⁸

3.2. Food Safety

Ensuring food safety is of great societal concern. Food-related illness was estimated to have a large economic cost due to premature death, medical care, loss of productivity, and litigation.^{469,470} To address the increasing need for quality

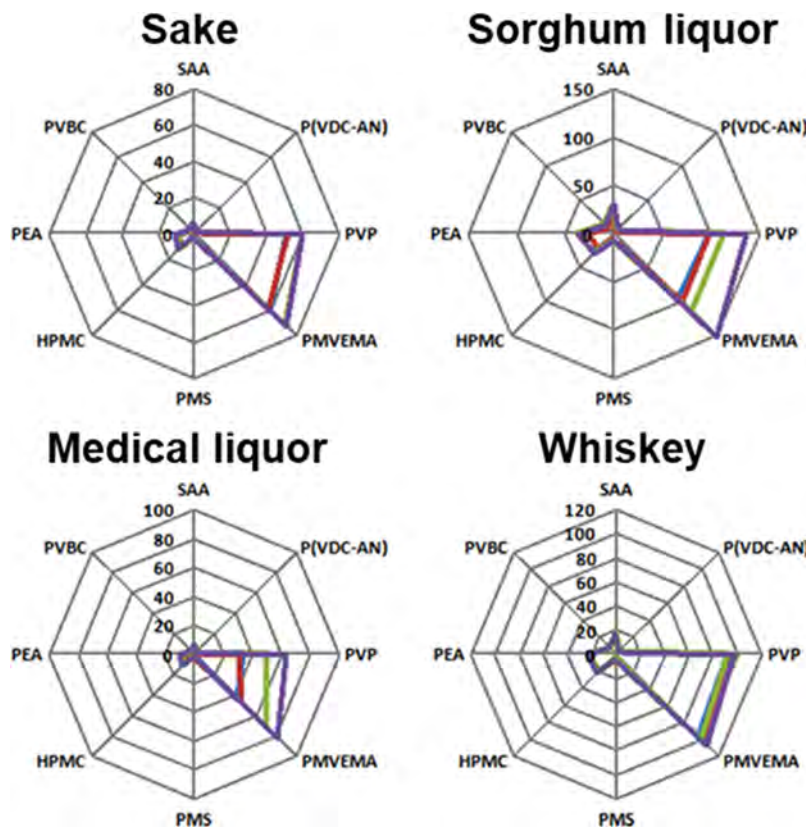


Figure 30. Detection of taste and smell. Differentiation between four different complex alcohol vapors using MWCNT/polymer composites: styrene/allyl alcohol copolymer (SAA), poly(vinylidene chloride-*co*-acrylonitrile) (P(VDC-AN)), polyvinylpyrrolidone (PVP), poly(methyl vinyl ether-*alt*-maleic acid) (PMVEMA), poly(α -methylstyrene) (PMS), hydroxypropyl methyl cellulose (HPMC), poly(ethylene adipate) (PEA), and poly(vinyl benzyl chloride) (PVBC).⁴⁶⁶ Reproduced with permission from ref 466. Copyright 2011, Elsevier.

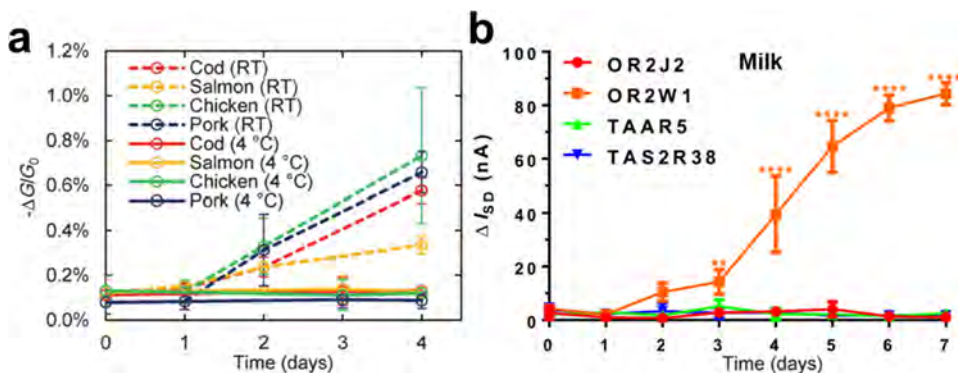


Figure 31. Detection of food spoilage. (a) Response of chemiresistive sensor using cobalt *meso*-aryl-porphyrins as the selector toward meat and seafood samples stored at RT and in the refrigerator over 4 days. Reproduced with permissions from ref 93. Copyright 2015, Wiley-VCH Verlag GmbH & Co. KGaA. (b) Response of CNT-based sensor functionalized with four different human olfactory receptors (OR2J2 for octanol, OR2W1 for hexanal, TAAR5 for trimethylamine, TASR38 for goitrin) while monitoring spoiling of milk over 1 week. Reproduced with permissions from ref 454. Copyright 2017, Elsevier.

control, comprehensive sensing technologies for monitoring the quality of food along the entire supply line are needed. CNT-based sensors have been developed to detect food spoilage through biomarkers associated with food spoilage directly or by confirming the integrity of the packaging. In addition, we will discuss the detection of residual pesticides and foodborne pathogens.

3.2.1. Food Spoilage. Monitoring food spoilage in real time can help prevent the consummation of potentially harmful products as well as the unnecessary disposal of food that is still fit for human consumption. To inform a consumer about the state of the packaged consumable, inexpensive and disposable sensors can be incorporated on the inside of the packaging.⁴⁷¹ Several CNT-based sensors have been developed to fill this specific need. These sensors detect volatile biomarkers indicative of food spoilage. For example, biomarkers include biogenic amines and ammonia for spoilage in meat and fish products,^{472,473} hexanal for spoiled milk,⁴⁷⁴ and 1-octen-3-ol for fungal infections of grain.⁴⁷⁵ A large number of sensors for ammonia have been developed, which we detailed in section 2.1.1. In this section, we will strictly discuss devices that have been tested on food samples.

Liu et al. developed a chemiresistive sensor containing a series of cobalt *meso*-aryl-porphyrin complexes for the selective detection of ammonia and biogenic amines.⁹³ By investigating porphyrins with different substitution patterns and counterions, the authors found that the sensor response correlated with the electron deficiency of the metal center and that the highest response to biogenic amines was achieved with the electron-poor [Co(tetrakis(pentafluorophenyl)porphyrinato)][ClO₄]. This sensor was used to monitor the spoilage of meat and seafood samples over several days, showing clear differentiation between samples stored at room temperature and samples stored at 4 °C in the refrigerator, Figure 31a. Similar results were obtained from chemiresistive CNT-based sensors containing human olfactory receptors to detect spoilage of meat,⁴⁵⁴ oysters,^{476,477} and a wide variety of seafood.^{454,478} The detection of more complex biomarkers of spoilage is less explored; however, great progress has been made by using olfactory receptors to detect specific small organic molecules. For example, increases in geosmin and 2-methylisoborneol, metabolites of bacteria, are indicative of bacterial contamination of water.⁴¹⁵ Using SWCNTs functionalized with human olfactory proteins, both molecules can be

detected chemiresistively at nanomolar concentrations.⁴¹⁵ Human olfactory protein/CNT devices have also been developed for the detection of spoiled milk. The spoiling of milk correlates with the amount of hexanal in the headspace over the liquid.⁴⁷⁴ This analyte can be detected using olfactory receptors that bind hexanal at concentrations of 1 μM as demonstrated by Son et al.⁴⁷⁴ The authors used their olfactory receptor/CNT sensor to monitor the spoiling of milk over a week and recorded a steady increase in hexanal concentration, Figure 31b.⁴⁵⁴

3.2.2. Integrity of Packaging and Oxygen Sensors (O₂). While sensing biogenic decomposition products is a viable method to detect food spoilage, monitoring the integrity of food packaging can provide a general indicator of the quality of the content. Food and pharmaceuticals can be protected from oxidative degeneration via packaging in inert atmosphere,^{479,480} and the detection of oxygen inside of the packaging is a vital method to monitor the intactness of this barrier.⁴⁸¹ Apart from monitoring food packaging, detection of oxygen has many important applications including environmental monitoring and biological and medical applications. For example, the control of automobile exhaust emissions and optimization of industrial processes are made possible by oxygen sensors.^{482,483} Furthermore, the measurement of biochemical oxygen demand (BOD) can be used to characterize the amount of organic waste contained in water.⁴⁸⁴ Measuring the dissolved oxygen partial pressure in arterial blood provides an evaluation of a patient's condition.⁴⁸⁵ Several review articles cover the luminescence-based and colorimetric detection of oxygen using optically active organic or inorganic materials sensors.^{486,487} Both pristine and functionalized CNTs show responsiveness toward O₂ adsorption and are promising materials for the development of oxygen sensing devices.

The consensus on the exact description of the interaction between O₂ molecules and CNTs has not been reached; however, physisorbed O₂ seems to induce p-doping of CNTs. Zettl and co-workers originally reported that the physical properties of CNTs, including local densities of electrical states and electrical resistance, are extremely sensitive to the presence of oxygen.^{39,488} The doping effect of O₂ on the electronic structure of CNTs has been reported for both experimental investigations and computational results.^{40,489–493} However, Derycke et al. concluded that the adsorption of O₂ mainly

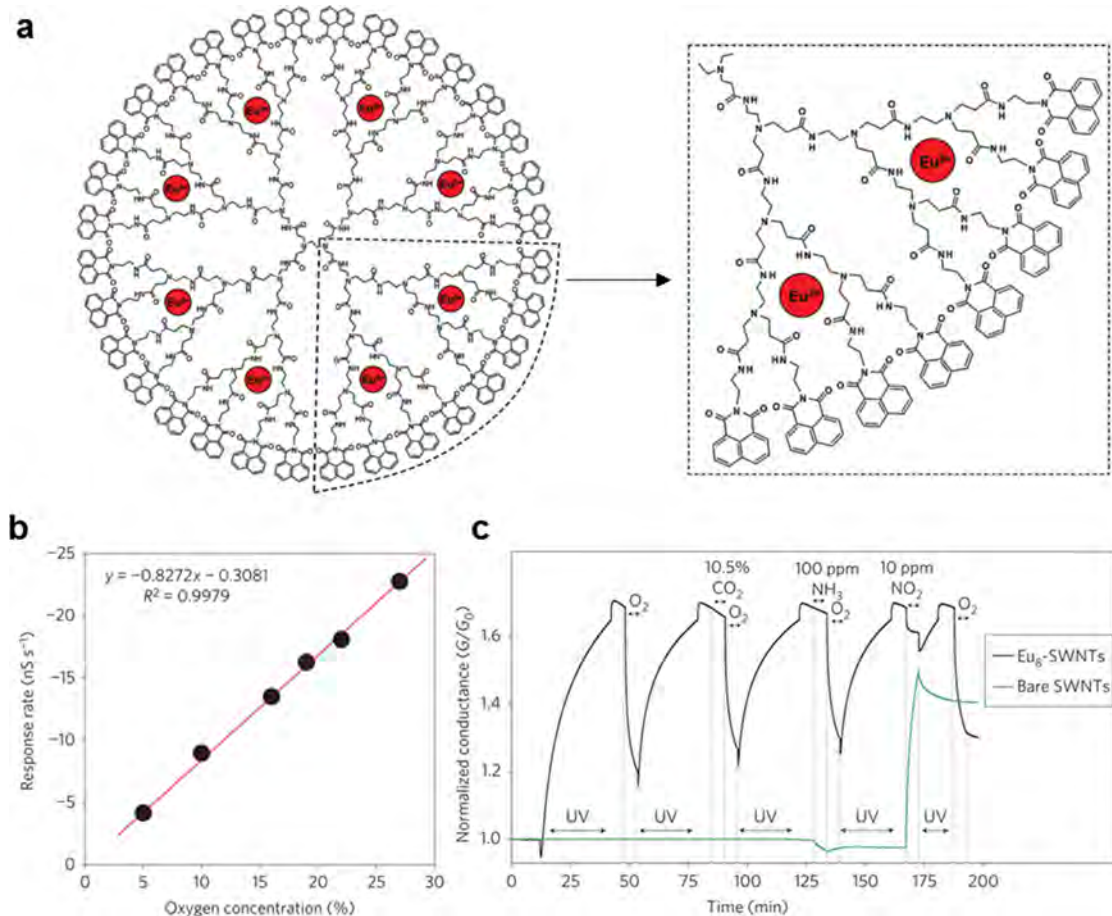


Figure 32. Chemiresistors based on SWCNT networks decorated with an oxygen-sensitive Eu³⁺-containing dendrimer complex. (a) Chemical structure of the europium-containing dendrimer complex (Eu₈) containing eight Eu³⁺ cations coordinated within a 1,8-naphthalimide-terminated, G3-PAMAM dendrimer core. (b) Electrical response rate of the Eu₈-SWCNT chemiresistor to increasing oxygen concentration. (c) Comparison of the normalized conductance between Eu₈-SWCNTs (black curve) and pristine SWCNTs (green curve) when exposed to illumination with 365 nm ultraviolet light in flowing N₂, pure O₂, 10.5% CO₂, 100 ppm of NH₃, and 10 ppm of NO₂. Reproduced with permission from ref 495. Copyright 2009, Nature Publishing Group.

modifies the Schottky barriers of the CNT–metal contacts rather than doping of the CNTs themselves.⁴⁹⁴ These conflicting experimental reports may originate from the differences in the quality of the CNTs. For example, Goldoni et al. demonstrated that the removal of contaminants (Na and Ni) and defect sites renders the electronic spectra of CNTs insensitive to O₂, CO, H₂O, and N₂.³²³

An additional limitation toward the development of CNT-based oxygen detectors arises from the slow desorption rate of O₂ from the nanotubes at room temperature. In earlier reports, reversible sensitivity of oxygen relied on the application of high vacuum.^{39,488,494} To develop a lower power and portable platform, Kauffman et al. reported a chemiresistive device that can be refreshed to the original conductance using ultraviolet illumination (UV, 365 nm) after exposure to O₂, Figure 32.⁴⁹⁵ The device comprised SWCNTs decorated with an oxygen-sensitive Eu³⁺ dendrimer complex (Eu₈). The authors found that the initial rate of change in the conductance scaled linearly with the concentration of oxygen in the range of 5–27%.⁴⁹⁵ Furthermore, the sensors showed good selectivity to O₂ compared to CO₂, NH₃, and NO₂.⁴⁹⁵

For applications wherein the presence of oxygen leads to detrimental effects, such as in modified atmosphere packaging (MAP) for oxygen-sensitive food and drugs, irreversible

responses to oxygen could prove useful as they will report on the cumulative level of oxygen.¹⁸⁹ To this end, Zhu et al. described the development of a wireless oxygen dosimeter using Fe^{II}–poly(4-vinylpyridine)–SWCNT composites with passive radiofrequency identification (RFID) tags, Figure 33.¹⁸⁹ Poly(4-vinylpyridine) (P4VP) was used to disperse the SWCNTs³³¹ and to bind Fe^{II} species through the pyridyl ligands. Fe^{II} is reducing and transfers electron density to the carbon nanotubes, thereby eliminating the hole carriers and increasing the resistivity. Oxygen exposure of varying concentrations (2–21%) led to irreversible responses that can be detected by a smartphone through passive RFID tags, which allowed the wireless detection of oxygen inside of food packaging.¹⁸⁹ To limit the effects of humidity and prevent contact with food, the device was covered with a thin layer of polydimethylsiloxane (PDMS), which functioned as an oxygen-permeable moisture barrier. Exposure to oxygen irreversibly oxidizes the selector (Fe^{II} to Fe^{III}) and induces oxidation of the SWCNTs, increasing the number of hole charge carriers and the conductance. For the *in vivo* detection of oxygen in water, Xiang et al. developed an electrochemical sensor comprising microsized Pt NP-covered CNT-based electrodes. Although the authors demonstrated the detection of oxygen in the brains of anesthetized rats, a similar device could be used

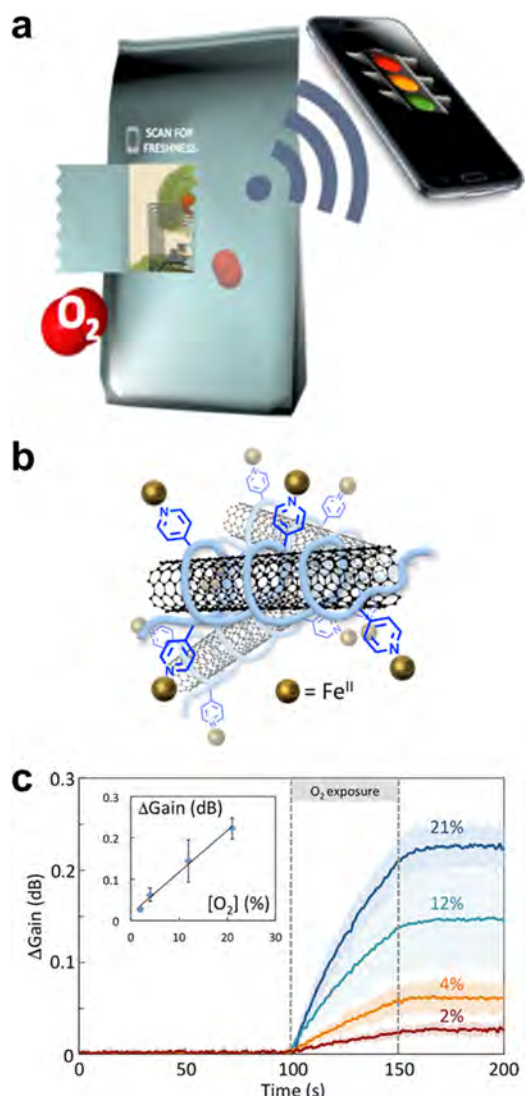


Figure 33. Wireless oxygen sensors enabled by near-field communication (NFC) tag. (a) Schematic drawing of a smart packaging that measures oxygen exposure from the inside. Radio-frequency readers, in this case, a smartphone, can remotely read the sensor's state and access the quality of the package contents without a line of sight. (b) Schematic of poly(4-vinylpyridine)-dispersed SWCNTs and coordinating Fe^{II} ions as the sensing element. (c) Sensing responses to various O₂ concentrations (diluted in N₂). Inset shows the calibration curve of the sensor. Reproduced with permission from ref 189. Copyright 2017, American Chemical Society.

to detect oxygen on the inside of air-sensitive liquid food packaging.

3.2.3. Pesticide Contamination. Overuse of pesticides and contamination of food poses a risk for human health and biodiversity.⁴⁹⁶ Millions of tons per year of pesticides are used to protect crops from insects to improve agricultural production.⁴⁹⁶ Nevertheless, the use of pesticides has been linked to the collapse of honeybee colonies,⁴⁹⁷ an increase in amphibian mortality,⁴⁹⁸ and a decrease of biodiversity in aquatic ecosystems.⁴⁹⁶ Additionally, residual pesticides in agricultural products can threaten human health. These exposures have been linked to the development of several types of cancer (breast, pancreatic, non-Hodgkin lymphoma, leukemia, brain, prostate, and kidney),⁴⁹⁹ neurotoxicity,⁵⁰⁰

genotoxicity,⁵⁰⁰ birth defects,⁵⁰⁰ fetal death,⁵⁰⁰ and decreased neurodevelopment.⁵⁰¹ Additionally, pesticides have been used as chemical nerve agents in chemical attacks as will be described in section 5.1 on Chemical Warfare Agents.⁵⁰² Overall, the use of pesticides causes an estimated \$10 billion in environmental and societal damage annually in the United States alone.⁵⁰³ Monitoring the concentration of pesticides can prevent overuse and help protect the environment and human health.

Several CNT-based sensors have been developed that can quantify pesticide concentration in complex matrixes of food samples. The examples include soybean sprout, potato, tomato, pear, apple, cabbage, onion, carrot, and celery samples, orange juice, strawberry juice, beer, and milk.^{431,504–507} A large number of these sensors rely on the selective oxidation or reduction of the pesticide on a functionalized CNT-based electrode.^{431,504–510} Possible selectors for the detection of organophosphorous pesticides (OPs) are the enzymes that are effected by the OPs. The biocatalytic activity of the enzyme acetylcholinesterase (AChE) is the removal of the neurotransmitter acetylcholine (ACh) through hydrolysis. Poisoning with OPs inhibits AChE, which leads to a buildup of ACh at the nerve synapses, causing rapid twitching of voluntary muscles and paralysis. This same reaction cascade was used in CNT-based sensors to detect OPs in many reports.^{431,505,507,509–511} For example, Yu et al. observed that addition of ACh to AChE-functionalized CNT electrodes generated a concentration-dependent amperometric current increase, Figure 34.⁵⁰⁵ Addition of the OP paraxon reduced the

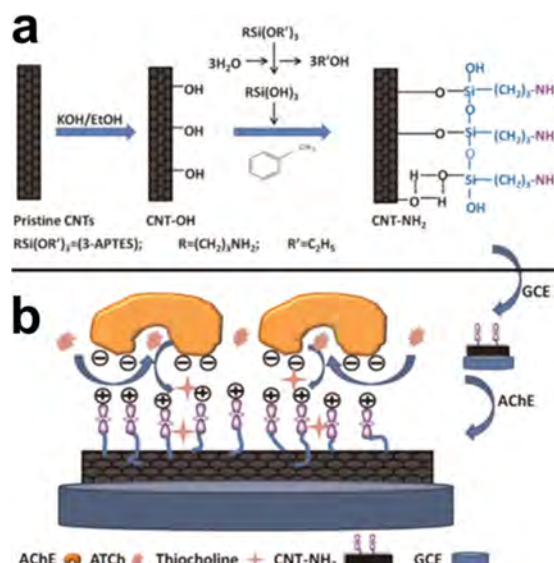


Figure 34. Detection of pesticides. (a) Schematic representation of the amination process of CNT (3-APTES, 3-aminopropyltriethoxysilane). (b) Schematic of acetylcholinesterase (AChE) immobilization onto the NH₂-functionalized CNTs (acetylthiocholine chloride ATCh). Reproduced with permission from ref 505. Copyright 2015, Elsevier.

current increase as a result of the inhibition of the enzymatic hydrolysis of ACh. Alternative to these enzymatic transduction schemes, sensors with nonenzymatic selector moieties have been identified for the electrochemical sensing of pesticides on CNT-enhanced electrodes. These systems include iron

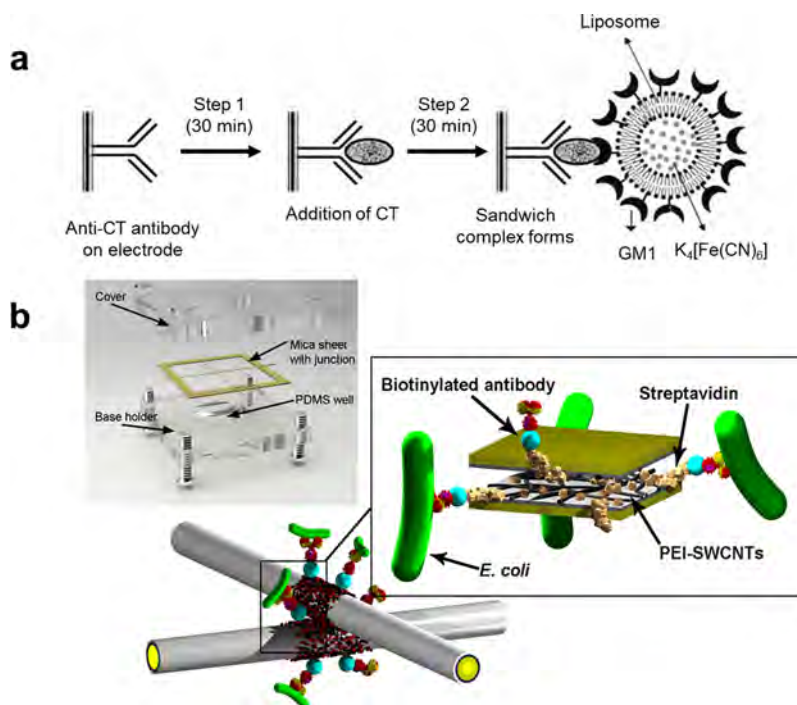


Figure 35. CNT-based pathogen detection. (a) Schematic representation of electrochemical sensor for cholera toxin (CT). In the first step, CT is bound by an antibody-containing MWCNT electrode. In the second step a potassium ferrocyanide-containing liposome is bound to amplify the binding event of CT.⁵²⁴ (b) Chemiresistive detection of *E. coli* using a CNT-coated nanojunction functionalized with antibodies.⁵²⁵ Reproduced with permission from refs 524 and 525. Copyright 2006 and 2014, American Chemical Society and Public Library of Science, respectively.

porphyrin,^{508,512} ruthenium phthalocyanine,⁵⁰⁶ patterned polymers,^{504,513,514} and metal nanoparticles.⁵¹⁵

3.2.4. Foodborne Pathogens. Apart from detection of biomarkers for the spoilage of food or the monitoring of food packaging, foodborne pathogens can be detected directly. Infections with pathogenic microorganisms, such as *Campylobacter*, *Salmonella*, *Listeria monocytogenes*, and *Escherichia coli* (*E. coli*),⁵¹⁶ can cause diarrheal diseases, which remain a leading cause of preventable death of children in developing countries.^{517,518} According to the World Health Organization (WHO), even in the United States 76 million cases of foodborne diseases occur annually, out of which 325 000 require hospitalization and 5000 lead to death.⁵¹⁸ Infection can occur through ingestion of contaminated foods or water, person-to-person transmission, or contact with infected animals.⁵¹⁹ To minimize the risk of infection, rapid and real-time identification of infected food items poses a pressing need.⁵¹⁹ Current methods for the detection of foodborne pathogens include optical-based biosensors, mass-sensitive biosensors, electrochemical biosensors, culture and colony counting, immunology-based methods, and polymerase chain reaction. These methods are detailed in several excellent review articles focused on the detection of foodborne pathogens.^{516,520} A review of nanomaterial-based pathogen detection was also presented by Inbaraj et al.⁵²¹ In this section we discuss the CNT-based detection of pathogens in water or biological media.

To detect pathogenic microorganisms in complex media, several groups have functionalized CNTs with antibodies with specific interactions with the target bacteria or toxin. Bhardwaj et al. developed a paper-based electrochemical sensor using antibodies (Ab) as the selector unit to detect *Staphylococcus aureus* (*S. aureus*).⁵²² The antibodies were covalently attached to the sidewalls of the CNTs using 1-ethyl-3-(3-

(dimethylamino)propyl)carbodiimide hydrochloride (EDC) and *N*-hydroxysuccinimide (EDC/NHS) coupling. After functionalization, a dispersion of the Ab-CNTs was deposited on the working electrode of the electrochemical device where the binding of *S. aureus* can be observed as an increase of the peak current. The response time of sensors was shown to be 30 min, and the sensor was operational in milk. Similarly, Zhao et al. investigated an electrochemical sensor for *Shigella flexneri* based on an Ab-functionalized MWCNT/sodium alginate composite (MWCNT/SA).⁵²³ Sodium alginate acts as a dispersing agent for the MWCNTs and as a biocompatible scaffold to facilitate binding of horseradish peroxidase labeled antibodies to *S. flexneri*. Binding of *S. flexneri* inhibits the activity of the horseradish peroxidase, which can be seen as a decrease in the peak current in the electrochemical signature of the device. Viswanathan et al. investigated the electrochemical detection of cholera toxin (CT), a bacterial protein toxin secreted by the bacterium *Vibrio cholerae*.⁵²⁴ The device is operated in a two-step process: the first step consists of the binding of CT through a poly(3,4-ethylenedioxythiophene)/antibody (PEDOT/Ab) composite on a MWCNT electrode, and the second step consists of the binding of a $K_4[Fe(CN)_6]$ -containing liposome, Figure 35a. The binding of the potassium ferritin-containing liposome is proportional to the CT concentration and enhances the peak current of the electrochemical feature of the sensing device. Using this two-step process, the authors were able to determine the concentration of CT in tap water and in kitchen wastewater with a detection time of 60 min.

The rapid detection of foodborne pathogens using functionalized nanojunctions has been reported by Jun and co-workers.^{525,526} PEI/SWCNT-coated microwires are assembled into crossbar junctions (Figure 35b) with a 10 μ m gap between the wires. The wire junction is functionalized by self-assembly

of streptavidin and biotinylated antibodies to *E. coli*, which binds strongly to the streptavidin binding pocket, Figure 35b. The current through the nanojunction decreases upon each subsequent addition of biomolecule (streptavidin, biotinylated antibodies, *E. coli*), possibly via a deformation of the CNT sidewall or electrostatic disturbance of the CNT network by the biomolecules. Using a single junction, the authors were able to detect *E. coli* in water with a detection time of 5 min.⁵²⁵ Using a 4-wire design, arranged in a 2×2 grid, the authors were able to detect *E. coli* and *S. aureus* simultaneously.⁵²⁶ Two adjacent junctions were functionalized using antibodies to *E. coli* while the remaining two junctions were functionalized using antibodies to *S. aureus*. When exposed to a mixture of bacteria, the multijunction device can determine the concentration of both strains of bacteria independently. Expanding on this 2×2 array might allow the detection of all major foodborne pathogenic bacteria in a rapid fashion (detection time 5 min).

4. CNT-BASED BIOLOGICAL SENSORS

Health monitoring and the detection of biomolecules are crucial for many areas of healthcare ranging from the diagnosis of diseases to real-time monitoring the conditions of patients. These applications can assist in a global reduction of mortality and medical costs. For example, early discrimination of different infections can facilitate appropriate treatment and preventative measures. The present medical testing protocols require expensive equipment and/or dedicated laboratories with a long turnaround time. Hence, CNT-based sensors offer the attractive features of portability and cost effectiveness for point-of-care diagnostics. This section describes CNT-based sensors addressing biological applications. We aim to highlight examples of sensors that derive selectivity from the choice of functionalization and/or the use of sensor arrays for two main topics: breath analysis and the detection of biomolecules. Interested readers may benefit from full reviews on this topic.^{7,31,33,527}

4.1. Breath Analysis

The analysis of exhaled breath provides a noninvasive and potentially portable method for the detection of diseases and monitoring a person's physical condition.^{528–531} Volatile molecules from human breath have been linked to various diseases including breast, lung, gastric, colon, and prostate cancers,^{532–536} Alzheimer's and Parkinson's diseases,⁵³⁷ multiple sclerosis,⁵³⁸ diabetes,⁵³⁹ and hyperglycemia.⁵³⁹ Extensive clinical trials are often required to establish the link between the presence of biomarkers in human breath with the indication and state of a disease. These efforts are best initially quantified by precision analytical assessments using standardized chromatographic techniques, such as gas chromatography mass spectrometry (GC-MS).⁵⁴⁰ We highlight that a large volume of work on breath analysis has been accomplished by the group of Haick^{42,541,542} and Owlstone Medical.⁵⁴³ Nanomaterials, including CNTs, are ideal for breath analysis due to their chemical versatility and ease of incorporation into sensing platforms.⁵³⁰ We will focus on two main categories of analytes: volatile organic compounds (VOCs) and inorganic gases.

4.1.1. Volatile Organic Compounds (VOCs). VOCs in a biological context are the products or byproducts of cellular metabolism or oxidative stress caused by reactive oxidative species (ROS).^{536,544,545} These compounds are often separated

into different categories based on their functional groups: hydrocarbons, alcohols, aldehydes, ketones, esters, nitriles, and aromatic compounds.⁵³⁶ The concentration of these compounds in bodily excreted fluids and breath is affected by changes in diet, environmental exposures, and disease states of the patient.^{546–548} The typical VOCs originated from cellular activity in humans include hydrocarbons, aldehydes, and ketones.³³ For example, peroxidation of lipids by ROSs can produce ethane, pentane, and aldehydes; high-level fat metabolism produces detectable levels of acetone; and halitosis can lead to a high concentration of hydrogen sulfide, methyl mercaptan, and dimethyl sulfide.³³

As a result of the large number of VOCs present in typical breath samples, it is natural to construct arrays of sensors to discriminate the different chemical species. As described in section 1.3 on device architectures sensing arrays provide "finger prints" for a given compound or class of compounds, which can then be analyzed by computational methods (linear discriminant analysis, LDA, and principal component analysis, PCA). Some of the first examples of CNT-based detection of VOCs via a sensing array was demonstrated by Haick and co-workers with the goal to discriminate healthy subjects from those suffering from lung cancer and chronic renal failure.^{42,541} The authors constructed arrays from semiconducting SWCNTs coated with 10 different nonpolymeric organic materials and tested their performance in the differentiation between simulated breath of healthy and diseased subjects, Figure 36.⁵⁴¹ PCA of the obtained signal revealed that the discrimination between cancerous and healthy breath was confounded by the effects from humidity, and reduction of the relative humidity from 80% to below 10% led to excellent discrimination.⁵⁴¹ In their follow-up study, FET devices were used instead of chemiresistors with less debilitating effects from humidity.⁴² Recently, the same group has reported the use of functionalized SWCNTs arrays in combination with molecularly modified gold nanoparticles to diagnose 17 different disease conditions from 1404 subjects with 86% accuracy.⁵⁴²

Several groups have developed CNT-based sensor arrays that can differentiate between different VOCs. For example, Liu et al. used noncovalently functionalized SWCNTs with a series of metalloporphyrin complexes with a diversity of different metal centers.⁶⁸ The authors constructed PCA plots from signals obtained from chemiresistors comprising SWCNTs and eight metalloporphyrins to distinguish five classes of VOCs (amines, hydrocarbons, aromatic, ketones, and alcohols).⁶⁸ They reported a large separation of the amines from other VOCs as a result of their charge-transfer capabilities and sufficient discrimination between the remaining four classes based on their intermolecular interaction or swelling effects.⁶⁸ Hybrids of SWCNTs and metalloporphyrins have also been reported by Shirsat et al. to distinguish acetone, ethanol, methanol, and methyl ethyl ketone.⁵⁴⁹ Common surfactants have also been incorporated with CNTs to create VOC sensing arrays. Chatterjee et al. prepared aqueous solutions of MWCNTs dispersed in common surfactants—sodium deoxycholate (DOC), sodium dodecylbenzenesulfonate (SDBS), 1-hexadecyl trimethylammonium bromide (CTAB), benzalkonium chloride (BnzlkCl), and triton x-405 (TX405)—and spray-coated CNT films onto interdigitated electrodes using the layer-by-layer technique.⁵⁵⁰ The authors reported that the sensing responses of the array depended on the interactions between the surfactants and the analytes as

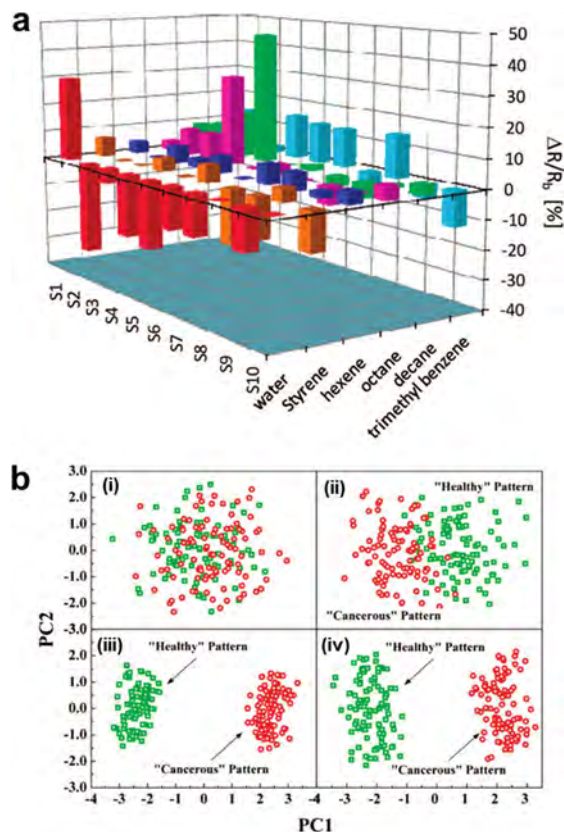


Figure 36. Detection of simulated patterns of lung cancer biomarkers using arrays of SWCNTs coated noncovalently with thin films of organic materials. (a) Patterns of responses of chemiresistive networks of SWCNTs coated with 10 different organic materials (S1–S10) when exposed to the representative VOCs for 10 min. (b) PCA score plots of the 10 sensing arrays upon exposure to “healthy” and “cancerous” mixtures of VOCs at (i) 80% RH, (ii) 10% RH, (iii) 1% RH, and (iv) 80% RH with preconcentration of VOCs of 50 times. Reproduced with permission from ref 541. Copyright 2008, American Chemical Society.

well as their supramolecular assembly with MWCNTs.⁵⁵⁰ Individually, each sensor provided limited discrimination; however, PCA demonstrated separation between methanol, ethanol, water, acetone, chloroform, and toluene.⁵⁵⁰

Although noncovalent functionalization has been successful at producing selective sensing arrays, they often do not produce sensors with sufficient robustness toward the harsh conditions. With the goal of creating robust CNT-based chemiresistive arrays, Sarkar et al. covalently anchored poly(tetraphenylporphyrin) on SWCNTs to detect acetone, and the resulting sensors showed good stability over a period of 180 days.⁵⁵¹ Wang and Swager synthesized a series of covalently functionalized MWCNTs with cross-sensitive recognition groups via a two-step synthetic protocol, Figure 37.¹¹⁷ The authors chose each selector to maximize the differential interactions with the range of targeted analytes. Propargyl- and allyl-MWCNTs (**1** and **2**) are both polar and hydrogen-bond accepting and were expected to interact strongly with vapors with large dipoles. Selectors with long alkyl chains (**3** and **4**) favor dispersion interactions that were aimed to detect aliphatic hydrocarbons. Hydrogen-bond-accepting vapors (e.g., ethers and ketones) were targeted by the carboxylic acid group and hexafluoroisopropanol (**5** and **6**). Calix[4]arenes (**7**) favor the adsorption of aromatic and

chlorinated hydrocarbons due to their highly polarizable pocket; and last, crown ether (**8**) provided hydrogen-bonding basicity to interact with acids and alcohols. As a result, the sensor array successfully discriminated the 20 tested VOCs into five different classes without interfering effects from humidity. Moreover, the distinct pattern of responses when subjected to the linear discriminant analysis (LDA) accurately identified all 20 VOCs. The carefully chosen selectors in this array further discriminated chemical space in an intuitively meaningful way. For example, in the PCA plot, Figure 37, the analytes at the boundaries between functional classes have characteristics of both classes. Within the ethers and ketones, the analytes proximate to the hydrocarbons are dihexylether and 2-decanone, which have hydrocarbon character. Similarly, for alcohols, 1-octanol is closest to the hydrocarbons. Also, for the aromatics, 1,3,5-trimethylbenzene wherein the aromatic structure is masked by the methyl groups is also closest to the hydrocarbons. Hence, this study clearly illustrated that careful chemical designs, rather than random collections of selectors, are best at selectively characterizing complex VOCs.

An advantage of array-based sensors comprising multiple units with limited selectivity is that the library of the “finger prints” can be easily updated to detect a new class of analyte. In applications where one specific biomarker has been identified as sufficient proof that a disease is present, the detection of a single analyte can be a powerful diagnostic tool.²² Thus, array-based sensors will benefit when used in parallel with sensors capable of detecting a single analyte. For example, Wang et al. fabricated vertically aligned-CNTs with a conductive polymer coating to detect *n*-pentane with a projected LOD of 50 ppm with good selectivity over methanol and toluene.⁵⁵² Vertically aligned CNTs were coated with poly(3,4-ethylenedioxothiophene) (PEDOT) via oxidative chemical vapor deposition, followed by a coating of non-conducting polystyrene (PS). Adsorption of pentane on the surface of PEDOT disrupts the conductive pathway, and added selectivity is achieved by the layer of PS that excludes polar VOCs.⁵⁵² As discussed above, calix[4]arenes have the tendency to interact with aromatic hydrocarbons. Wang et al. demonstrated that chemiresistors of SWCNTs wrapped with calix[4]arenes-substituted polythiophene could distinguish between different isomers of xylene, Figure 38.⁹⁷ Using quartz crystal microbalance (QCM) studies and NMR binding studies, the authors verified that the selectivity arose from the preferential binding of *p*-xylene within the calixarene cavity over the other two isomers.⁹⁷ Selectivity based on structural isomers that do not have large differences in dipoles is rare for chemical sensors, and this study is another demonstration of merits of integrating selective recognition elements into CNT sensors.

In addition to composites of polymers and CNTs, metal and metal oxide nanoparticles have also been demonstrated as selectors for CNT sensor VOC arrays. Ding et al. fabricated chemFET sensors with the composite of SWCNTs and TiO₂ that exhibited responses to acetone vapor at 400 ppb.¹³⁶ In this study, oxidized SWCNTs with defect sites on the sidewall directed covalent nucleation and growth of titanium oxide layers. The proposed sensing mechanism relies on the UV photoinduced generation of electron/hole pairs in the TiO₂ layer and the adsorption of acetone that prevents recombination to cause a detectable drop in conductance.¹³⁶ This sensor showed high selectivity toward acetone over NH₃, H₂, CO, and NO and was able to detect 20 ppm of acetone in both air and

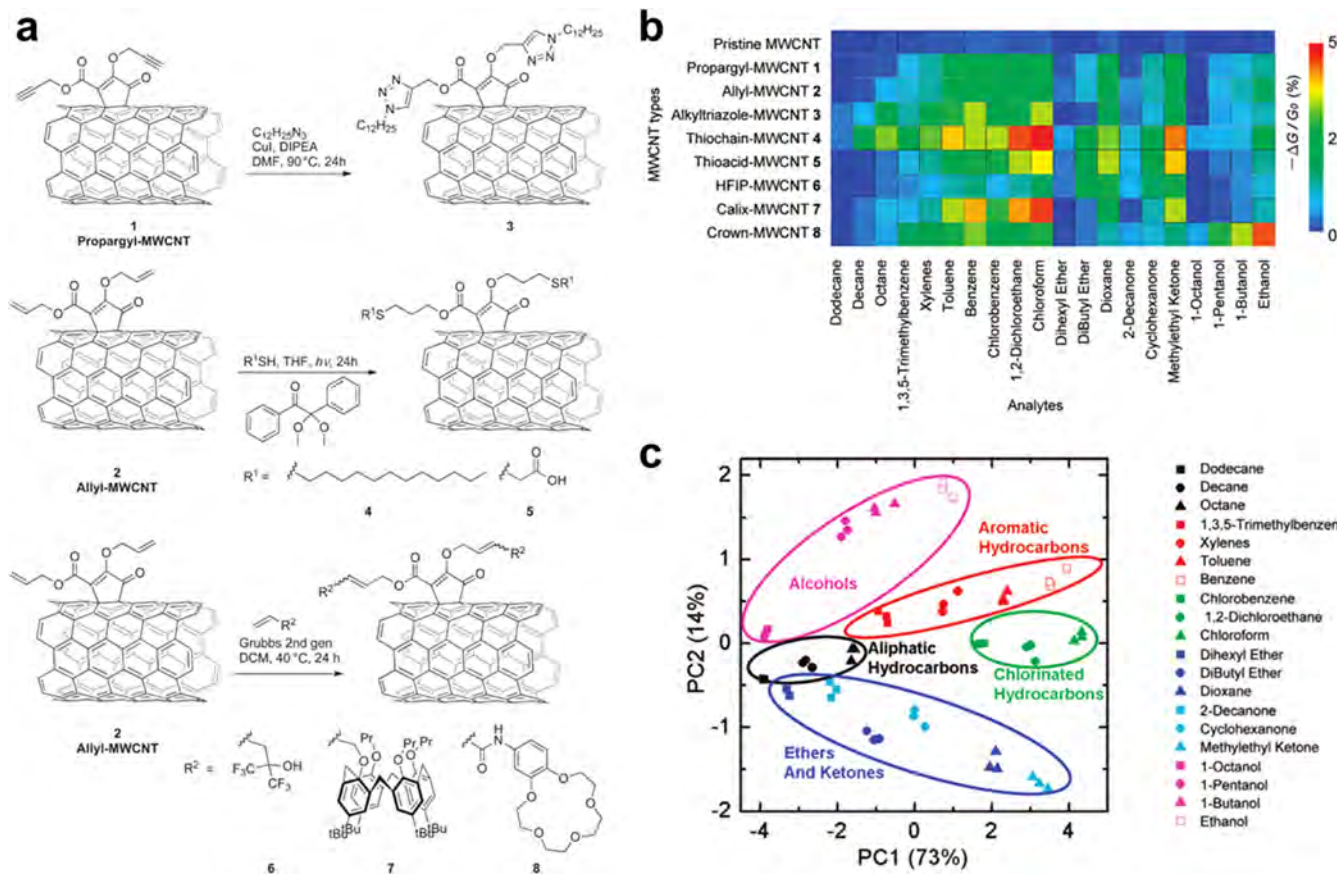


Figure 37. Sensing arrays of pristine and covalently functionalized MWCNTs for discrimination of 20 representative VOCs. (a) Chemical structures and synthetic routes for the covalently functionalized MWCNTs. (b) Patterns of changes in the conductance of pristine MWCNT and eight functionalized MWCNTs to VOCs at 1% of their saturated vapor pressure. (c) Principal component score plots of an array of pristine MWCNTs and eight functionalized MWCNTs to the 20 VOCs. Reproduced with permission from ref 117. Copyright 2011, American Chemical Society.

high humidity despite interferences from O₂ and water vapor.¹³⁶ Yoon et al. have also shown the incorporation of soft Lewis acid Pd²⁺ cations in a polymer wrapped around SWCNTs. In this case, PdCl₂ is coordinated to P4VP-wrapped SWCNTs (described previously in the section on functionalization) to produce a highly selective sensor toward vapors of thioethers.³³¹ Specifically, the PdCl₂ salt imparted a large dosimetric response to methyl *n*-propyl sulfide diluted in air, a breath biomarker for diseases such as malaria.³³¹

4.1.2. Inorganic Gases. In addition to VOCs, inorganic gases are important biomarkers for medical monitoring. The primary gases of interest are carbon dioxide (CO₂), nitric oxide (NO), ammonia (NH₃), and hydrogen sulfide (H₂S). Monitoring the concentration or the partial pressure of CO₂ in the respiratory gases, called capnography, is commonly used during medical procedures such as during anesthesia and intensive care. Using capnography, it is possible to monitor the patients' metabolic status and infer any alterations to obstructive conditions such as cardiac arrest, bronchitis, asthma, and anesthesia.^{553,554} NO is involved in many physiological processes including immune response, regulation of blood pressure, and neural communication.⁵⁵⁵ However, direct measurement of NO is difficult due to its extremely short physiological half-life in aerobic environments. Increased level of NH₃ in exhaled breath can also be used as the biomarker of patients with renal failure or disease (ppm levels compared to ppb range for healthy individuals).^{33,556,557}

Various types of NH₃ sensors are discussed in section 2.1.1 on environmental application. In addition, H₂S (discussed previously in section 2.1.4 on environmental monitoring) can serve as a breath marker for some diseases such as diabetes and halitosis.

Although earlier reports of CNT-based sensors exhibiting sensitivity to CO₂ exist, selective sensors have predominantly relied on polymer-wrapped CNTs as the sensing materials. Varghese et al.²⁰³ and Ong et al.⁴⁹² demonstrated the sensing capability of MWCNT-SiO₂ composite toward CO₂; however, cross sensitivity with other gases and humidity were also reported. Star et al. incorporated CNTs functionalized with poly(ethylenimine) (PEI) and starch polymers in FET devices to show excellent sensitivity to CO₂, the dynamic operating range was shown to be from 500 ppm to 10% of CO₂ in air.⁴⁸ The authors attributed the sensing behaviors to the reduction of electron-donating character of PEI and structural rearrangement of the starch polymer upon exposure to CO₂. Li et al. reported chemiresistive sensors comprising poly(ionic liquid)-wrapped SWCNTs, Figure 39.⁵⁵⁸ Dispersions of poly[1-(4-vinylbenzyl)-3-methylimidazolium tetrafluoroborate (PIL) and SWCNTs were deposited onto interdigitated microelectrodes and displayed a dynamic range of CO₂ responses between 500 ppt to 10 ppm. The interactions between the [BF₄⁻] anion and CO₂ were attributed as the sensing mechanism that gave rise to the selectivity to CO₂ over CO, H₂, CH₄, ethanol, O₂, and water vapor. Lastly, Olney et al.

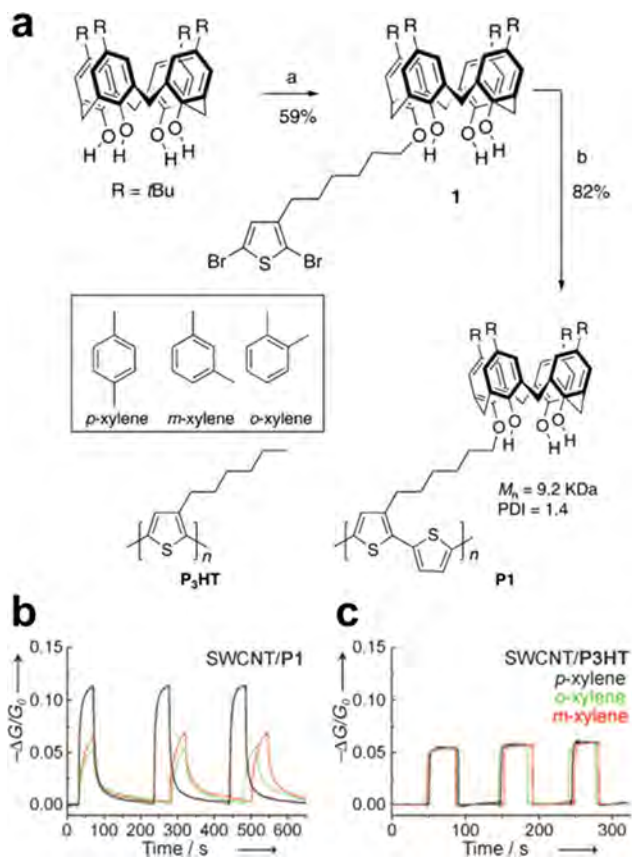


Figure 38. Molecular recognition of SWCNT/polythiophene chemiresistor toward xylene isomers. (a) Chemical structures of xylene isomers and poly(3-hexylthiophene) (P3HT), and synthesis scheme of *p*-*tert*-butylcalix[4]arene-substituted polythiophene (P1). Conductance change of the chemiresistor of (b) SWCNTs and P1 and (c) SWCNT and P3HT to *p*-xylene, *o*-xylene, and *m*-xylene at 400 ppm. Reproduced with permission from ref 97. Copyright 2008, Wiley-VCH Verlag GmbH & Co.

prepared a composite of PEDOT:PSS and SWCNTs that showed sensitivity to CO_2 down to 10 ppm.⁵⁵⁹ The observed increase in conductivity upon the adsorption of CO_2 was suggested to be caused by conformational change and phase separation of the PEDOT:PSS. Although cross-sensitivity with methane was noted, in this case the conductivity decreases, which provides a means to distinguish between the two gases. The robustness of this rather indirect and seemingly chemically nonspecific mechanism remains to be determined.

Few examples of NO sensors based on CNTs are reported. Star and co-workers extended the use of their FET devices with PEI-coated CNTs to detect NO in simulated breath.⁵⁶⁰ The composite of PEI and CNTs is moderately sensitive to NO; thus, the authors incorporated a CrO_3 converter to oxidize NO to NO_2 prior to the sensors. They noted that the addition of an ascarite scrubber was required to remove the interfering signal from CO_2 .

4.2. Health Monitoring and Detection of Biomolecules

This section focuses on designs of CNT-based biosensors and their uses for the detection of biomolecules. CNTs can serve as both the electrodes for electrochemical methods and the transducer in a chemiresistor or chemFET.⁵²⁷ For practical sensors, the dynamic range of the sensors must correspond with the physiological concentrations of the targeted

biomarker. For example, the difference in the concentration of glucose in blood of a person with diabetes can be as low as 1 mM, with the average values ranging between 4 and 9 mM.⁵²⁷ Significant work has been done over the past two decades to incorporate CNTs as biosensors. This section highlights selected reports, mainly focusing on the detections of glucose and DNA. Not surprisingly, CNT-based sensors have been developed for the detection of many other biomolecules. Enzymatic biosensors are relatively simple to incorporate into CNT electrodes for electrochemical analysis, leading to analyte-specific recognition. The common analytes found in the literature include proteins,⁵² cholesterol,^{561–563} dopamine,^{564–568} serotonin,^{567–569} nicotinamide adenine dinucleotide (NAD),^{570–572} and cytochrome *c*.^{573,574} We direct interested readers to recent full reviews that cover these other analytes.^{8,31,527,575–577}

4.2.1. Glucose Detection. One of the most frequently performed medical tests is the detection of blood glucose level. Monitoring this concentration is used to diagnose and manage diabetes, resulting in a high demand for glucose sensors. Both electrochemical and chemFET sensors have been reported with glucose oxidase (GOx) as the selector. The dramatic reduction in the overpotential for the generation of hydrogen peroxide (H_2O_2) and the direct electron transfer from GOx to the CNT electrodes proved extremely useful for electrochemical sensors using GOx/CNT composites.⁸ However, the immobilization of the enzymes onto CNT electrodes via simple adsorption faces several problems, namely, the lowering of the enzyme activity (denaturation) and leaching of adsorbed enzymes.⁵²⁷ One solution to overcome these problems was the use of metal and metal oxide NPs to anchor GOx on CNTs. To this end, Tang et al. reported an electrochemical sensor based on the adsorption of GOx onto Pt nanoparticle-decorated CNT electrodes. The authors attributed the excellent electrocatalytic activity to the large surface area obtained by the addition of both CNTs and Pt nanoparticles, resulting in the large linear range (0.1–13.5 mM) and high sensitivity of 14 $\mu\text{A}/\text{mM}$.⁵⁷⁸ The sensor showed moderate stability, retaining 73.5% of the initial activity after 22 days of testing.⁵⁷⁸ Successful examples were also reported for MWCNTs decorated with ZnO nanoparticles by Wang et al.⁵⁷⁹ and with Pt–Pd bimetallic nanoparticles by Chen et al.⁵⁸⁰ In these examples, a layer of polymeric film was used to eliminate common interferents, such as uric acid, ascorbic acid, and fructose, and improve stability. Wang et al. showed only 10% decrease in detection current after 160 days, and Chen et al. reported 15% loss of sensitivity after 28 days.

In addition to the adsorption of GOx onto CNTs electrodes decorated with NPs, multiple groups have reported immobilization of GOx using electropolymerization of conductive polymers on CNTs. In this method, GOx is mixed with the monomer which is then electropolymerized at a CNT electrode. Gao et al. electropolymerized polypyrrole (PPy) on aligned MWCNTs decorated with Fe particles in the presence of GOx.⁵⁸¹ They observed a large linear range (2.5–20 mM) and concluded that both the alignment of the MWCNTs and the Fe particles were critical to lower the oxidation potential of H_2O_2 , thereby preventing the over-oxidation of PPy.⁵⁸¹ Similarly, Wang and Musameh prepared sensors using a PPy/GOx composite that demonstrated a LOD of 0.2 nM and a linear range from 0 to 50 mM.⁵⁸² Pilan and Raicpol reported a composite of PANI/functionalized SWCNT/Prussian Blue for the electrochemical detection of

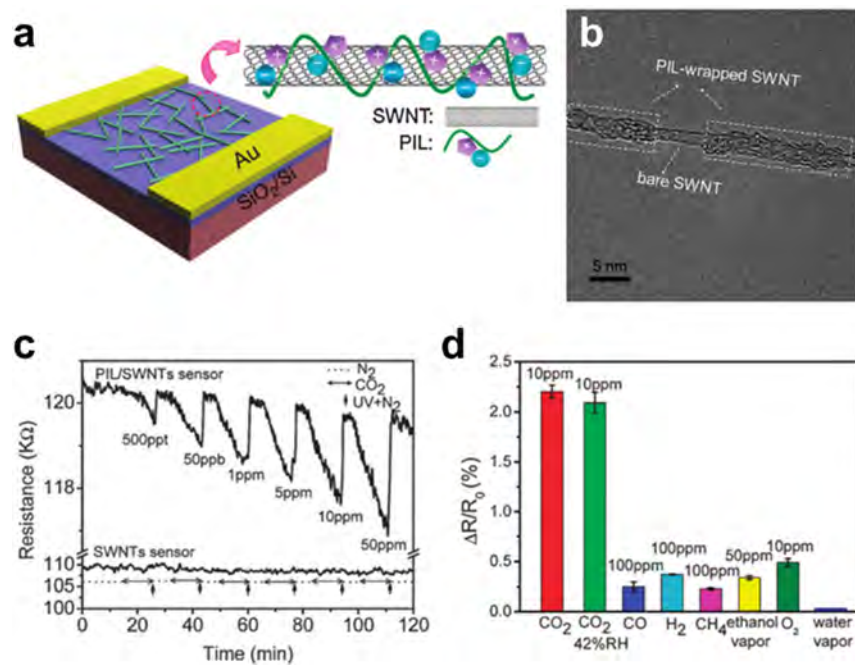


Figure 39. Poly(ionic liquid)-wrapped SWCNTs for detection of CO₂. (a) Schematic of the sensors comprising poly[1-(4-vinylbenzyl)-3-methylimidazolium tetrafluoroborate (PIL) and SWCNTs. (b) TEM image of an individual SWCNTs partially wrapped by PIL. (c) Change in the resistance of the PIL/SWCNTs sensors when exposed to increasing concentration of CO₂. Exposure to UV light in N₂ was used to recover the sensors to the baseline. (d) Sensitivity toward interfering gases and the effects of humidity. Reproduced with permission from ref 558. Copyright 2012, The Royal Society of Chemistry.

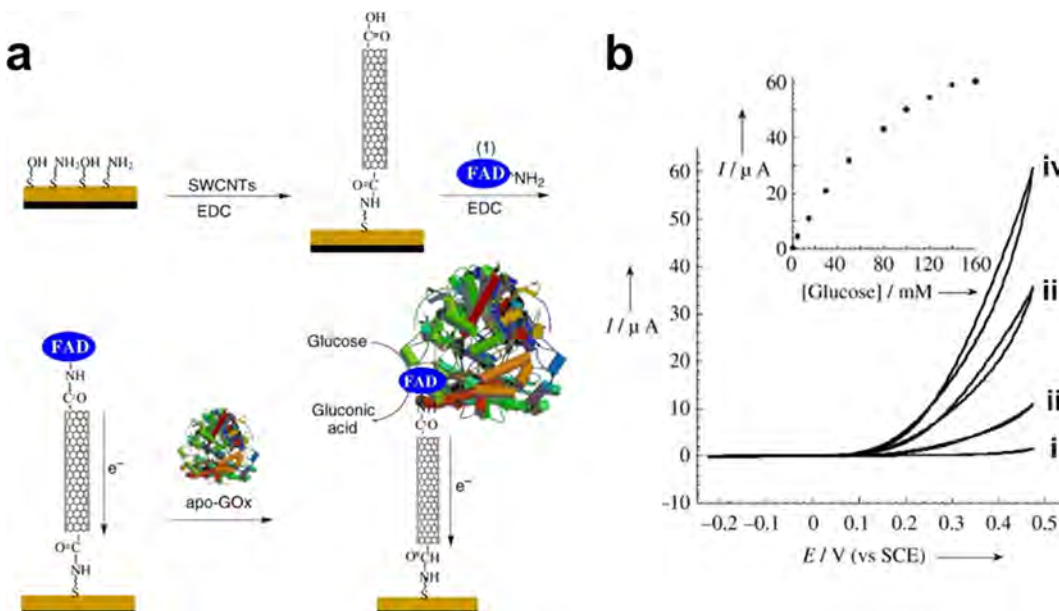


Figure 40. Covalent immobilization of GOx onto the edge of SWCNTs for amperometric sensing of glucose. (a) Assembly of a SWCNT-based GOx electrode. (b) Cyclic voltammograms of the electrocatalyzed oxidation of different concentrations of glucose by the GOx at (i) 0, (ii) 20, (iii) 60, and (iv) 160 mM glucose. Inset shows the calibration curve of the amperometric responses as a function of the concentration of glucose. Reproduced with permission from ref 584. Copyright 2004, Wiley-VCH Verlag GmbH & Co.

glucose.⁵⁸³ They demonstrated selectivity to glucose over the common interfering species of acetaminophen, uric acid, lactate, and ascorbic acid.⁵⁸³ Alternatively, Patolsky et al. demonstrated a covalent attachment of a reconstituted GOx onto the edge of SWCNTs that are linked to an electrode surface, Figure 40.⁵⁸⁴ SWCNTs were first coupled to the surface of Au electrodes with a mixed monolayer of thioethanol and cystamine in the presence of 1-ethyl-3-(3-

(dimethylamino)propyl) carbodiimide hydrochloride (EDC). The amino derivative of the flavin adenine dinucleotide (FAD) cofactor was then coupled to the carboxyl group at the end of the SWCNTs; subsequently, apo-glucose oxidase (apo-GOx) was reconstituted on the FAD units. Cyclic voltammograms of the bioelectrocatalytic oxidation of glucose provided the calibration curve of amperometric current as a function of the glucose concentration and revealed that the SWCNTs

behaved as electrical contacts between the active site of the GOx and the electrode.

Alternatively, nonenzymatic CNT-based sensors for glucose have been reported.⁵⁸⁵ These sensors rely on the catalytic properties of metallic nanoparticles decorated on the CNTs to generate an electrochemical response of glucose. Lin et al. used nickel and copper NP-decorated MWCNTs as the electrodes that showed activity toward glucose oxidation,⁵⁸⁶ while Gougis et al. used pulsed laser deposition of gold NPs onto CNT electrodes.⁵⁸⁷ Recently, Baghayeri et al. demonstrated selective glucose electrochemical sensors using Ag NPs electrodeposited onto MWCNTs functionalized with metformin, Figure 41.⁵⁸⁸ The reported sensor showed a low LOD at 0.3 nM with the linear range from 1 nM to 350 μ M without interference from common molecules found in human blood serum and urine samples.

CNTs also enable chemiresistor and chemFET approaches to glucose sensors. Besteman et al. reported one of the earliest examples of SWCNT-based glucose sensors.⁵⁸⁹ GOx was attached to the sidewall of individual SWCNTs; upon addition of glucose, a modest increase in conductance was observed.⁵⁸⁹ Soylemez et al. reported the functionalization of a poly(4-vinylpyridine) (P4VP)-wrapped surface-anchored array of SWCNTs with alkylation of the pyridyl groups electrostatically assembled GOx.⁶⁴ The P4VP-SWCNT scaffold provided prolonged stability, retaining 83.3% of its initial response, and excellent electrical communication between the GOx and the SWCNTs, enabling real-time chemiresistive sensing of glucose. The authors reported the dosimetric responses with the linear range from 0.08 to 2.2 mM and validated their method using commercial beverages. In another example, Lee and Cui developed flexible sensors via layer-by-layer self-assembly of SWCNTs, poly(diallyldimethylammonium chloride) (PDDA), polystyrenesulfonate (PSS), and GOx on polyethylene terephthalate (PET).⁵⁹⁰ The sensors were capable of detecting glucose down to 0.5 mM with a linear range from 0.5 to 25 mM. Using molecular-based recognition principles, Lerner et al. reported the detection of glucose using the complexation by boronic acid moieties, Figure 42.⁸⁸ The reduction in source-drain current occurred due to the increased carrier scattering upon the formation of boronate anion complex. As a control, exposure to lactose showed negligible response as a result of its lower binding affinity to the pyrene boronic acid moieties. Lastly, Cella et al. employed a displacement sensing scheme on a SWCNT-based chemiresistive platform.¹⁰¹ In this study, SWCNTs were initially functionalized with hydrophobic dextran derivative (DexP) that subsequently formed complexes with concanavalin A (ConA). The lower affinity of ConA to DexP when compared to glucose resulted in the release of ConA from the SWCNTs upon the addition of glucose, leading to detectable changes in the resistance.

4.2.2. DNA Sensors. Detection of DNA is particularly important for the diagnosis and treatment of genetic disorders, prevention against biowarfare agents, detection of infectious agents and pathogens, and drug discovery.⁵⁹¹ Selective predictable base-pairing interactions between and within DNA strands have led to the development of sensors employing optical, piezoelectric, and electrochemical transductions.⁵⁹² CNT-based electrochemical DNA sensors were originally pursued as a result of their high sensitivity, selectivity, and reproducibility. These early sensors relied on the immobilization of single-stranded DNA (ssDNA) on the electrode and changes in electrical current triggered by

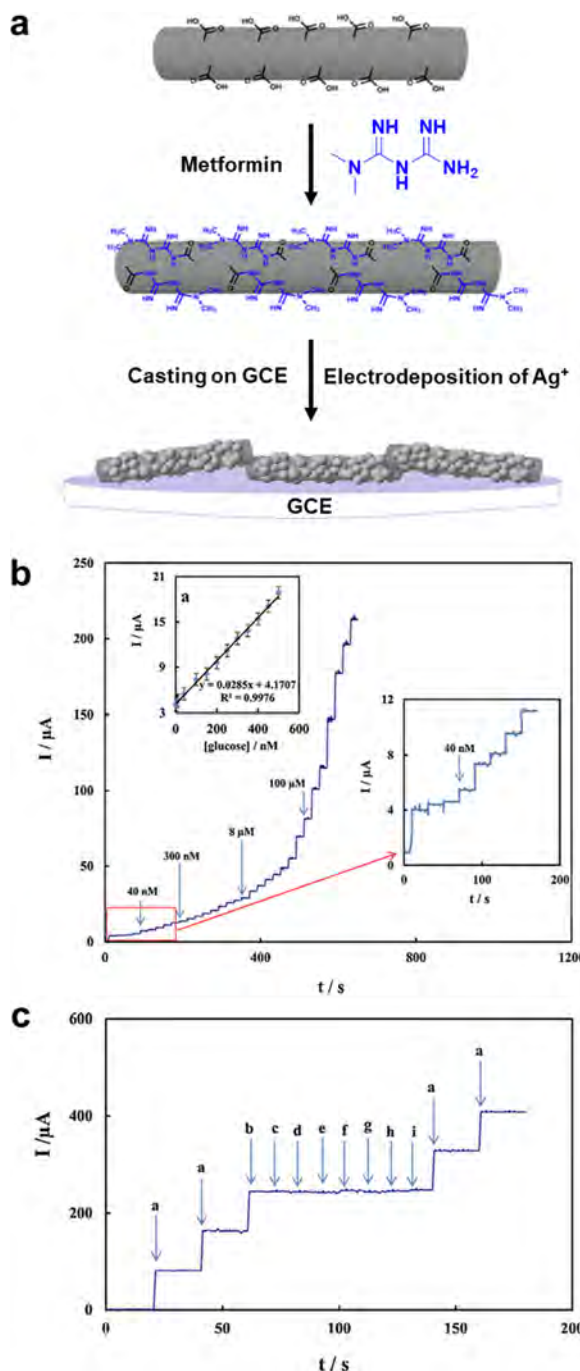


Figure 41. Nonenzymatic glucose sensor based on Ag nanoparticles (NPs) on functionalized CNTs. (a) Scheme for the preparation of Ag NPs on metformin-functionalized MWCNTs. (b) Amperometric response of the sensor to successive addition of different concentration of glucose in 0.1 M NaOH at a working potential of 0.70 V. Inset shows the plot of electrocatalytic peak current vs concentration of glucose from 1.0 to 500 nM. (c) Amperometric response to (a) 100 μ M glucose and 400 μ M (b) acetic acid, (c) ethanol, (d) ascorbic acid, (e) uric acid, (f) dopamine, (g) L-Dopa, (h) epinephrine, and (i) L-tyrosine. Reproduced with permission from ref 588. Copyright 2016, Elsevier.

hybridization of the complementary sequence.⁵²⁷ For example, Wang et al. used CNTs for amplification of enzyme-based electrical sensing of proteins and DNA.⁵⁹¹ In this study, CNTs were loaded with alkaline phosphatase (ALP) enzyme tracers, which carried the enzyme tags and preconcentrated the analyte

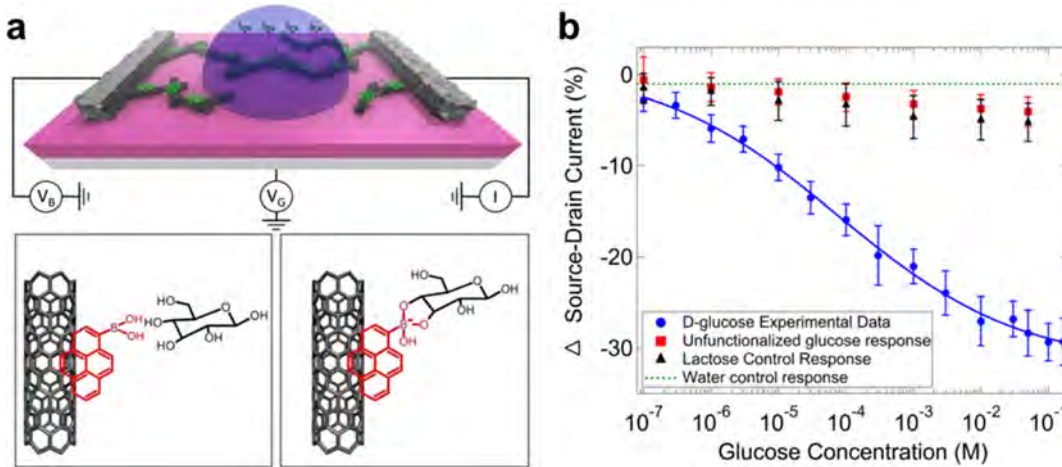


Figure 42. Boronic acid-functionalized CNT-based FET sensor for the detection of glucose. (a) Schematic of the FET sensors and illustration of binding of glucose to a CNT functionalized with pyrene-1-boronic acid. Bound glucose forms a boronate anion complex. (b) Sensing response as a function of the concentration of glucose (blue circles). Control experiments included responses from unfunctionalized devices to glucose (red squares), responses from functionalized devices to lactose (black triangles), and null response of functionalized devices to DI water. Reproduced with permission from ref 88. Copyright 2013, AIP Publishing LLC.

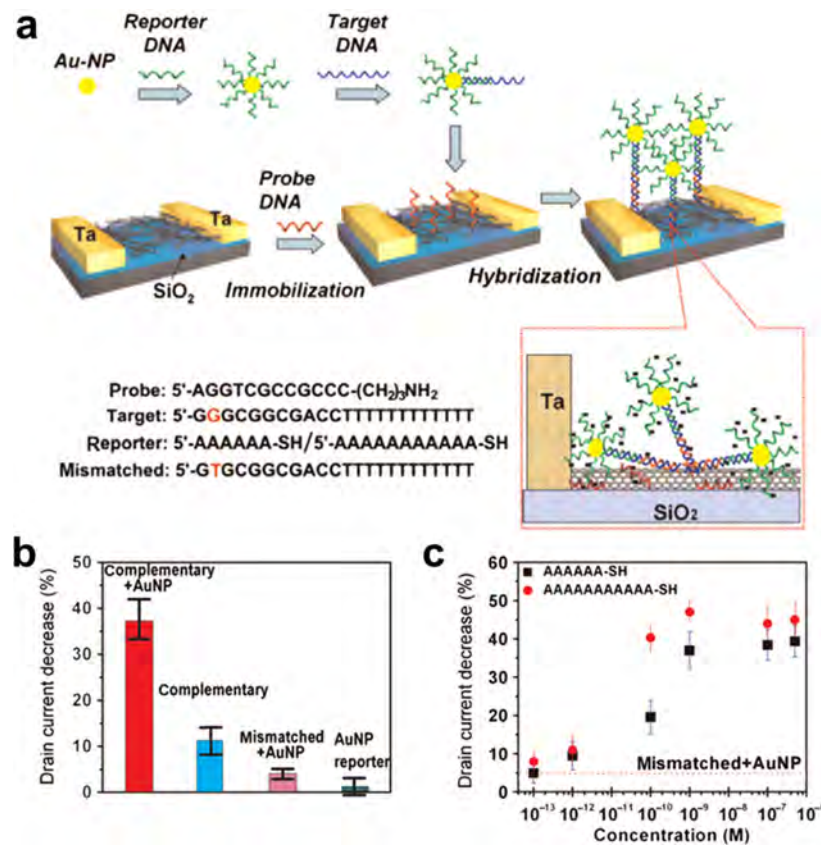


Figure 43. Detection of femtomolar DNA using Au NPs to enhance SWCNT-based FET sensors. (a) Schematic illustration of the enhancement of DNA detection using reporter DNA-functionalized Au NPs. (Right) Proposed molecular binding on the FET sensors. (b) Relative decrease in source-drain current for four sensing experiments. Reporter DNA used in this graph is 6A DNA. (c) Comparison of the relative decrease in current versus the concentration of the target DNA enhanced by 6A and 11A reporter DNA–AuNPs. Reproduced with permission from ref 596. Copyright 2008, Wiley-VCH Verlag GmbH & Co.

to yield enhanced sensitivity. This scheme generated a low LOD of the target DNA of 1 fg mL^{-1} (54 aM, 820 copies or 1.3 zmol in the $25 \mu\text{L}$ sample).⁵⁹¹ Similarly, He and Dai reported the covalent functionalization of ssDNA chains onto aligned CNT electrodes to detect complementary DNA and target sequences of DNA.⁵⁹³ The authors used an acetic acid-

plasma treatment on aligned CNTs to generate carboxyl groups on the tips and walls of CNTs. They then grafted ssDNA chains through the 1-ethyl-3-(3-(dimethylamino)propyl)carbodiimide (EDC)-based amide coupling and demonstrated reversible electrochemical responses.

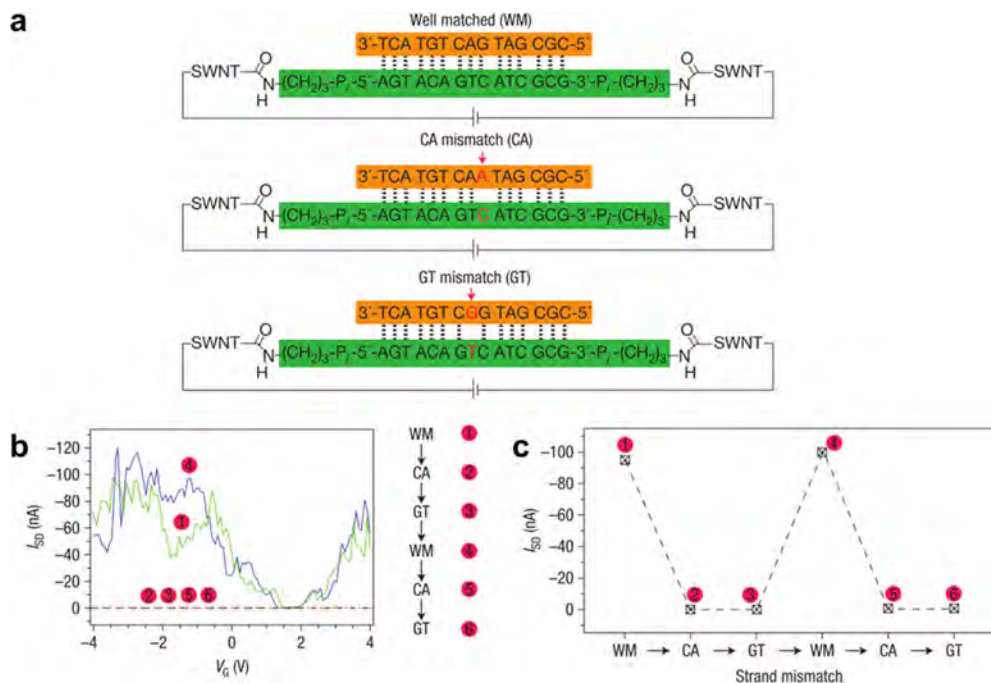


Figure 44. Conductivity of a single DNA duplex bridged between SWCNT. (a) Schematic of the covalent functionalization of SWCNT and DNA strands. Replacing the well-matched (WM) duplexes with DNA CA and GT mismatches resulted in a large effect on the conductance. (b) Transfer characteristics of a SWCNT device taken through the sequence 1–6 at a source-drain voltage of 50 mV. Current levels for mismatch points (2, 3, 5, and 6) are ~ 300 times lower than the well-matched points (1 and 4). (c) Current at a constant gate voltage (V_G) of -3 V and source-drain voltage of 50 mV through sequence 1–6. Reproduced with permission from ref 144. Copyright 2008, Nature Publishing Group.

Multiple groups have reported the use of chemFETs to detect the change in resistance of an individual CNT or networks of CNTs in the presence of DNA. Star et al. reported SWCNT-based FET devices that selectively detect the immobilization and hybridization of DNA.⁵⁹⁴ By monitoring the FET transfer characteristics of the networks of pristine SWCNTs during the addition of ssDNA oligonucleotides, the authors observed a shift of the threshold voltage toward more negative gate voltages upon the initial noncovalent adsorption of ssDNA molecules. Subsequent DNA hybridization with complementary target DNA resulted in a reduction of the measured conductance at a given gate voltage. This detection scheme proved successful in differentiation between mutant and wild-type alleles of the *HFE* gene that is responsible for hereditary hemochromatosis. To improve the sensitivity of FET-based devices in detecting complementary strands of DNA, Gui et al. introduced a naphthalene-based DNA intercalator that binds selectively to double-stranded DNA.⁵⁹⁵ After the addition of the intercalator, the sensors hybridized with complementary DNA showed significant reduction in conductivity compared to samples with mismatched DNA. Building on the previous study, Dong et al. also reported the use of DNA-functionalized Au NPs to enhance SWCNT-based FET sensors with a 100 fM LOD, Figure 43.⁵⁹⁶ In this study, each target DNA binds to the DNA-functionalized Au NPs and the probe DNA immobilized on the SWCNT. The close proximity of the Au NPs to the electrode–SWCNT contacts significantly enhance the change in conductivity upon binding of the target DNA as measured by transfer characteristics. Interestingly, the authors reported that devices with Ta electrodes exhibited larger enhancement than devices with Au electrodes.⁵⁹⁶ In the detailed mechanistic study by the same group, they reported that the change in

metal–SWCNT junctions, rather than the channel conductance, dominates the sensing of DNA.⁵⁹⁷ This result highlights the different electrical features of CNT devices described in the introduction and that there are multiple mechanisms that require consideration in developing CNT sensors.

The selectivity endowed by the composites of DNA–CNT sensors is highlighted by the ability to detect base pair mismatches. Because charge transport can occur over significant distances through the stacked aromatic base pairs of DNA, it is found to be extremely sensitive to the integrity of base pairing. Single-base mismatches can attenuate the charge transport through the DNA strand.⁵⁹⁸ Nuckolls and co-workers described the first measurements of the conductivity of a single DNA duplex wired between an individual SWCNT through covalent bonds, Figure 44a.¹⁴⁴ The authors fabricated the devices by cutting individual SWCNTs with an electron beam and then used oxygen plasma to ensure the presence of the carboxylic acid functionalities on both sides of the gap. The gaps were then bridged by ssDNA anchored at both sides by robust amide linkages. Through this device, the difference in conductivity between well-matched and mismatched duplex was clearly observed. Figure 44b shows that a single mismatch (both CA and GT) attenuated the current through the DNA strand. In addition to the use of individual SWCNTs, Weizmann et al. reported networks of ssDNA-bridged CNTs for the chemiresistive detection of complementary DNA, Figure 45.¹²⁰ This approach made use of formation of oligomeric (SWCNT–ssDNA)_n sequences between electrodes. The ssDNA gaps rendered the materials insulating. Selective binding of the ssDNA analyte resulted in the formation of double-stranded DNA assemblies; however, the transport through extended sequences of DNA did not introduce sufficient conductivity for detection. To produce robust

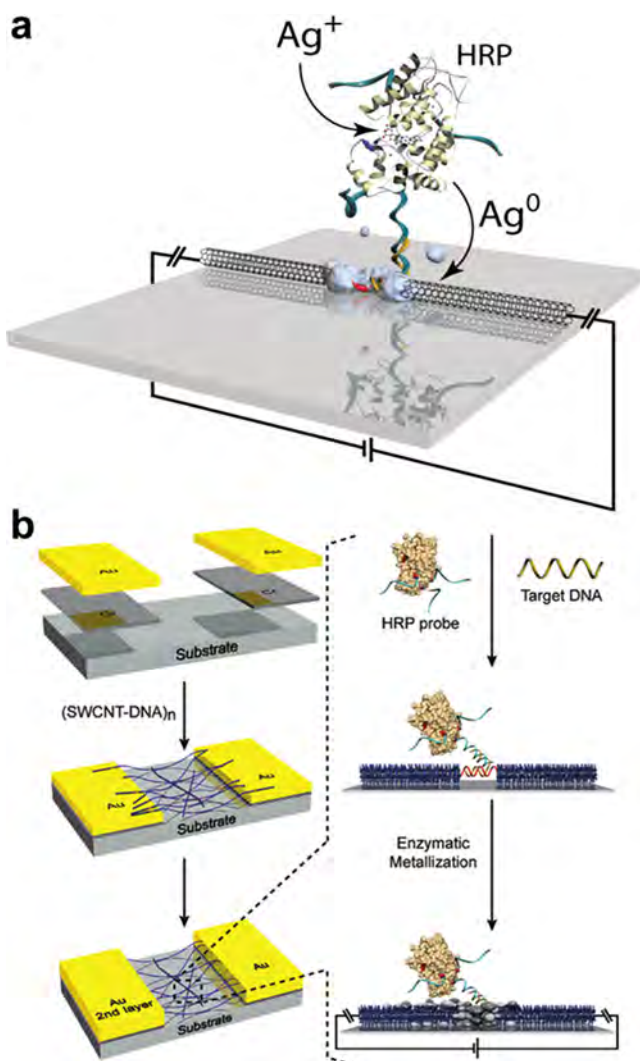


Figure 45. CNT-network-based DNA detection scheme. (a) Schematic representation of a single junction of a ssDNA/SWCNT construction. (b) Schematic of device architecture and sensing scheme. Hybridization with the target DNA strand results in the spatial localization of horse radish peroxidase (HRP) that can be used to deposit Ag metal to create a conductive bridge. Reproduced with permission from ref 120. Copyright 2011, American Chemical Society.

detection events, horseradish peroxidase (HRP) enzyme functionalized to complement the target DNA was used. The target DNA with HRP would recognize and localize at the gaps between the SWCNTs, and HRP could then be used to deposit silver metal. The net result, shown schematically in Figure 45, was a conductive network wherein the gaps between SWCNTs were connected by conductive silver. Simple measurements of conductivity demonstrated a LOD of 10 fM with the ability to discriminate single, double, and triple base-pair mismatches.¹²⁰

5. CNT-BASED SENSORS FOR NATIONAL SECURITY

The use of chemical warfare agents and explosives is unfortunately an ongoing menace to society that is unlikely to cease in the near future. Considering the continued threat of domestic and international terrorism, early detection of these agents can minimize casualties and injuries to military

personnel and civilians alike.⁵⁹⁹ In this part of the review we will cover the detection of chemical weapons and explosives.

5.1. Chemical Warfare Agents

Chemical warfare agents (CWAs) have been used as weapons of mass destruction in military conflicts since World War I, and the use of mustard gas, phosgene, and chlorine caused 1.3 million casualties.⁶⁰⁰ In recent years, chemical weapons in the hands of terrorists and rogue nations also pose a threat even in peaceful times.⁶⁰¹ In this section, we will discuss CNT-based sensors for the detection of CWAs categorized by their biochemical interaction with the victim: nerve agents, vesicating agents, respiratory agents, and blood agents. For a more general review including the historical context, toxicology, and destruction of chemical warfare agents, we refer the interested reader to a review article by Jang et al.⁶⁰³ For a review on the biomonitoring of exposure for diagnostics and verification of CWA usage, we refer to Noort et al.⁶⁰⁰

Current methods for the detection of CWAs include ion mobility spectroscopy,⁶⁰⁴ mass spectrometry,⁶⁰⁴ surface acoustic wave (SAW),⁶⁰⁵ electrochemical sensors,⁶⁰⁶ infrared spectroscopy,⁶⁰⁷ fluorescence,^{608–610} and colorimetric sensors.^{611,612} Although all of these techniques offer excellent sensitivity and specificity, there are limitations inherent to the different approaches. Analytical techniques like mass and infrared spectroscopies require bulky, sensitive, and/or power-intensive instrumentation that is unsuitable for field work. Colorimetric detectors have excellent portability; however, they cannot be used to monitor real-time data and are not readily incorporated into more sophisticated circuitry.³⁷² CNTs offer the opportunity to produce portable sensing methods that naturally couple into electrical devices—based on chemiresistive, electrochemical, or SAW elements—capable of continuous monitoring of the environment.

5.1.1. Nerve Agents and Vesicant Agents. Nerve agents are compounds that disrupt the nervous system by irreversibly inhibiting the activity of acetylcholinesterase (AChE)—an enzyme responsible for breaking down the neurotransmitter acetylcholine (ACh).^{602,613} The inhibition of AChE leads to accumulation of ACh in the nerve, which leads to overstimulation. Early symptoms include agitation and muscle weakness, severe poisoning and respiratory failure, unconsciousness, confusion, convulsions, and death.^{602,613} Lethal concentrations for typical organophosphorous nerve agents are in concentrations as low as 10–100 ppb.⁶¹⁴ As a result of the severe consequences of exposures to these nerve agents, sensors are usually developed by testing on chemically similar but less harmful nerve agent mimics.⁶⁰³ Figure 46 shows the chemical structures of a select number of nerve agents, nerve agent mimics, and decomposition products that were used in the studies covered in this review.

Vesicant agents, such as sulfur mustard and nitrogen mustard, Figure 47, cause skin blisters, eye injuries, and respiratory disorders, and were first used in World War I. Although the cellular and biochemical consequences of exposures are not fully understood, it is known that mustard gas acts as a bifunctional alkylating agent able to react with nucleophiles under physiological conditions.⁶⁰⁰

As a result of the high reactivity of nerve agent mimics, even pristine SWCNTs display nonspecific sensing responses. Novak et al. first reported the sensitivity of CNT films to ppb levels of the simulant DMMP in air.⁴¹ In addition to a decrease in conductance of the p-doped CNTs, the authors

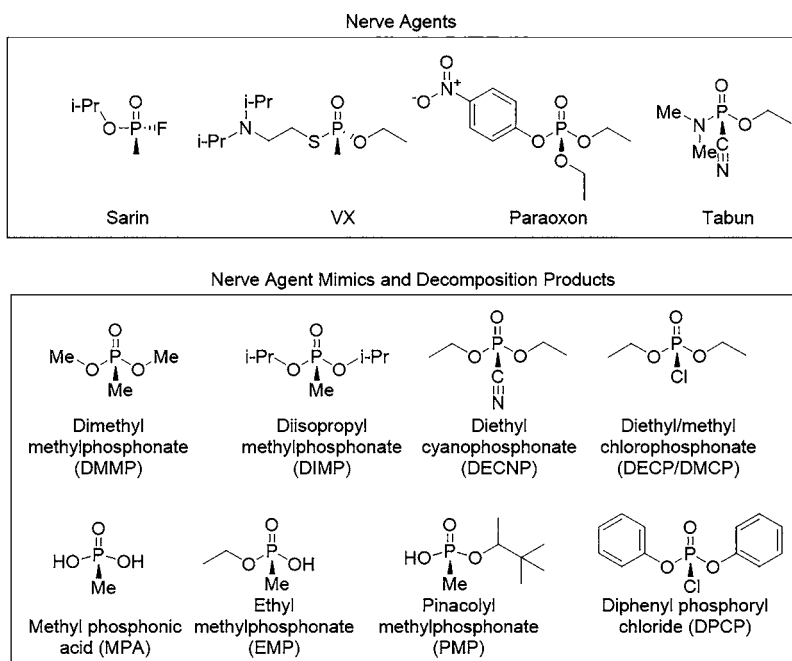


Figure 46. Chemical structures of selected nerve agents, nerve agent mimics, and decomposition products.

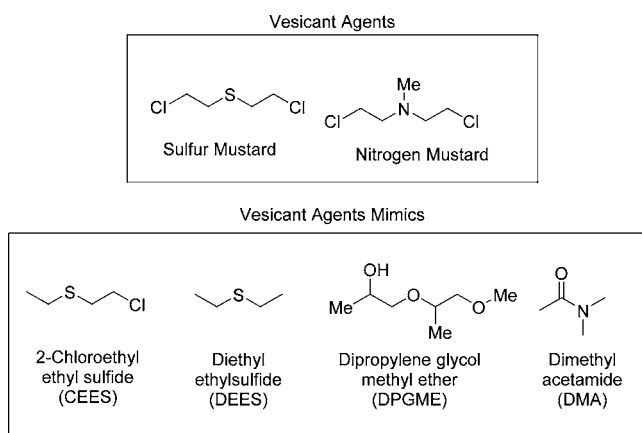


Figure 47. Chemical structures of selected vesicant agents and vesicant agent mimics.

observed a shift in the FET threshold voltage by -2 V, which indicates electron charge donation from the adsorbent to the CNT network. These findings are consistent with the strong electron-donating properties of DMMP through the terminal phosphonate oxygen. The decrease in conductance of pristine CNT sensors was also demonstrated with single-tube devices⁸¹ and pristine-CNT sensors assembled on flexible substrates.⁶¹⁵ In addition to gas-phase sensors, Roberts et al. reported liquid-phase detectors to determine the concentration of DMMP.⁵¹ The DMMP used in the water-based sensors may be partially hydrolyzed, which complicates the evaluation of liquid-phase sensors of DMMP. Lastly, pristine CNTs were also used in chemocapacitors to detect DMMP at ppb levels.⁶¹⁶

Several groups have explored sensors based on CNTs functionalized with polymeric materials. Lee et al. applied polypyrrole/CNT composites to increase the chemiresistive response of pristine CNT sensors 3-fold.⁶¹⁷ Complementary, Cattanach et al. used a passivating layer made of polyisobutylene to selectively block interfering vapors (water, hexane, and xylene) and fabricate a chemiresistive sensor.⁶¹⁸

Chuang et al.⁶¹⁹ developed a sensor array consisting of 30 channels with 15 different polymer/CNT composites to differentiate between several chemical warfare agents and organic solvents. Although none of the channels show exceptional sensitivity toward DMMP or mustard gas, the array successfully generates unique fingerprints for all tested compounds.

Alternatively, hydrogen-bonding acidic selectors have yielded highly selective and sensitive sensors. A popular molecular moiety is hexafluoroisopropanol (HFIP), first introduced by Snow et al.¹⁹⁹ The authors observed a 100-fold increase of the LOD for devices covered in a HFIP-terminated monolayer. Our group has demonstrated the wrapping of SWCNTs with HFIP-substituted polythiophene⁴⁷ and poly(3,4-ethylenedioxythiophene)¹⁰⁶ to increase their sensitivity toward DMMP in chemiresistive sensors (3-fold increase over unsubstituted polymer, Figure 48).⁴⁷ Sensors containing the HFIP-substituted polymer showed high sensitivity toward DMMP over potential interfering VOC gases and water.^{47,106} Investigations of the sensing mechanism showed a shift of the threshold voltage in FET measurements to a more negative voltage, suggesting charge donation or trapping of holes by the interaction of the analyte and the SWCNTs.⁴⁷ Changes in the Schottky barrier between SWCNTs and electrodes were eliminated from consideration by comparing the response of devices with poly(methyl methacrylate) (PMMA) passivation of the electrodes, active SWCNT channel, or both. The completely passivated devices showed no response toward DMMP, demonstrating the effectiveness of PMMA to block the diffusion of DMMP, and devices with passivated electrodes showed the same response as sensors containing no PMMA. In addition to HFIP, Kumar et al. reported that the noncovalent functionalization of CNTs with *p*-hexafluoroisopropanol aniline via drop casting resulted in a 3.7-fold increase of the chemiresistive sensing of DMMP.⁶²⁰ Covalent attachment of the same molecule by Kong et al. through diazonium chemistry leads to a 13-fold increase in response toward DMMP.⁶²¹

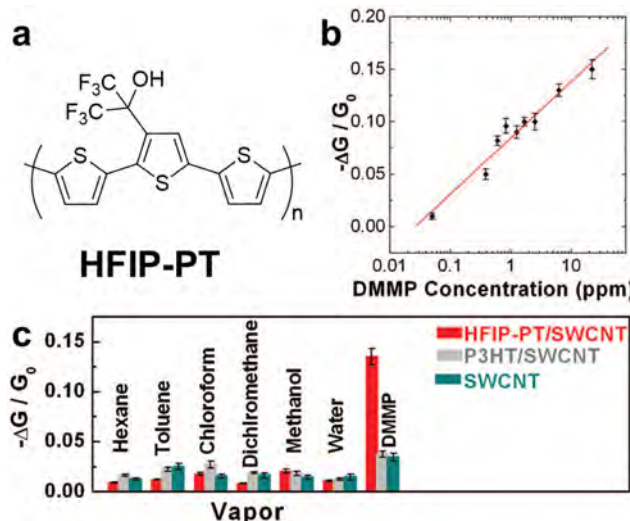


Figure 48. CNT-based sensing of nerve agents. (a) Chemical structure of HFIP-substituted polythiophene, HFIP-PT, (b) change in conductance of the sensor at DMMP concentration of 0.05–25 ppm, and (c) comparison of response toward DMMP and common VOCs. Reproduced with permission from ref 47. Copyright 2008, American Chemical Society.

Investigation of the transfer characteristics confirmed charge transfer as a significant sensing mechanism. Another hydrogen-bonding molecule used in the sensing of DMMP is tetrafluorohydroquinone (TFQ). Wei et al.⁶²² demonstrated the chemiresistive detection of 20 ppt DMMP using SWCNTs noncovalently with TFQ and identified heavy hole doping as the cause of increased conductance upon exposure to DMMP.

Kraatz and co-workers reported several electrochemical sensors for nerve agents and mustard gas mimics based on noncovalent⁶²³ and covalent modification of SWCNTs.^{624,625} As the nerve agents themselves are electrochemically inactive, the authors employed a redox-active selector. Specifically, the authors employed ferrocene–amino acid conjugates that were either blended with MWCNTs or attached covalently. Electrochemical- or impedance-based sensing allows detection of CWA mimics in water at concentrations in the picomolar range.

Single-strand DNA (ssDNA) can be used to create stable SWCNT dispersions to create CNT-based sensors. Practitioners of this method make use of the ability of specific DNA dispersants (a) to interact with specific analytes and (b) to effectively isolate individual SWCNTs making use of π – π stacking between DNA bases and nanotube sidewalls.^{98,626}

Johnson and co-workers reported the sensing of DMMP using devices containing individual p-type semiconducting nanotubes that were noncovalently functionalized with different DNA base sequences.⁶²⁷ Although the DNA-DMMP recognition mechanism was not investigated in detail, ssDNA functionalization increased the sensitivity toward DMMP by a factor of 2.5 compared to the pristine device. In a second study, the group developed a CNT-based gravimetric sensor functionalized with the same two ssDNA sequences.⁶²⁸ In the gravimetric device, the CNTs improved the device performance by increasing the surface area and providing the sensor with a large number of mass adsorption sites. However, both base sequences showed the same sensitivity toward DMMP, a 3-fold increase over pristine CNT sensors. Most recently Johnson and co-workers expanded their work on ssDNA-

functionalized CNT sensors to a wider scope of analytes (enantiomers of limonene, pinene, and homologous carboxylic acids).^{629,630} Using different ssDNA sequences the authors were able to differentiate between different isomers and enantiomers. The authors hypothesized that the assembly of DNA on the surface of CNTs generates sequence-specific sets of binding pockets near the CNT sidewall and that binding of analytes in these pockets results in a sequence-specific response for different ssDNA–CNT devices. The authors suggest that ssDNA-functionalized sensors make promising candidates for the fabrication of electrical noses. Lee et al. used ssDNA- and SDS-wrapped aligned CNTs to detect DMMP where DNA was used as a dispersing agent without investigation of the DNA–analyte interaction.⁴³ Liu et al. developed a chemiresistive sensor in which the CNTs were functionalized with ssDNA after deposition of the tubes on the device.⁶³¹

Several groups have developed sensors comprising selectors designed to react with chemical warfare agent molecules. Liu et al. used acetylcholinesterase, the enzyme interacting with nerve agents in the body, to selectively react with organophosphates in the electrochemical detection of paraoxon in water.⁶³² Delalande et al. reported the design of a DPCP sensor based on the modulation of the Schottky barrier between CNTs and gold electrodes.⁶³³ The gold electrodes were functionalized with an organophosphorous-sensitive self-assembled monolayer such that exposure to DPCP leads to intramolecular cyclization under formation of a quaternary ammonium salt, Figure 49. For exposures of just 1 ppm DPCP, this reaction induces a 100-fold increase in conductance of the Au–CNT–Au channel. Ishihara et al.^{73,107} reported the chemiresistive sensing of DMMP using SWCNTs wrapped with metallosupramolecular polymers (see Figure 5b). The polymers are designed to depolymerize upon exposure to DMMP, which

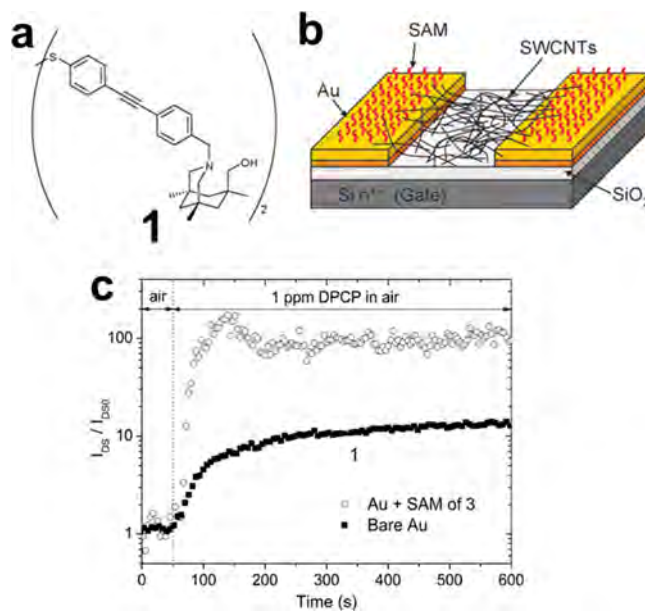


Figure 49. CNT-based sensing of nerve agents. (a) Chemical structure of molecule 1 sensitive toward DPCP under formation of a quaternary ammonium salt. (b) Schematic of CNTFET with gold electrodes functionalized with 1 and (c) response of CNTFET sensor with and without 1-covered Au electrodes upon exposure to DPCP. Reproduced with permission from ref 633. Copyright 2011, American Chemical Society.

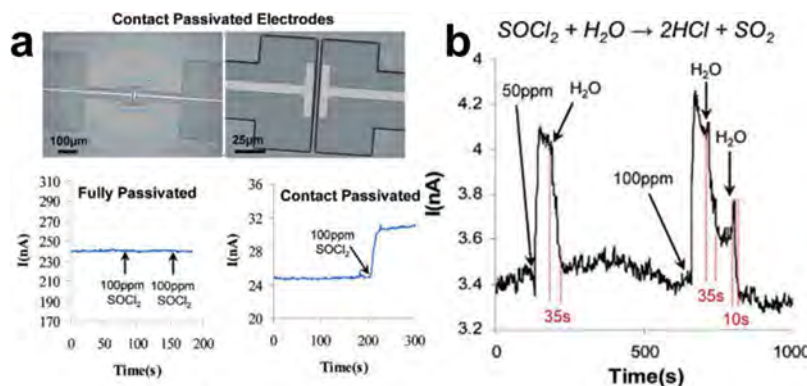


Figure 50. Sensing behavior of a chemiresistive device containing SDS-dispersed CNTs toward thionyl chloride (SOCl₂). (a) Response toward thionyl chloride with and without passivation of the device surface. (Left) Fully passivated devices showed no response toward thionyl chloride. (Right) Contact passivated devices, matching the response of nonpassivated responses toward thionyl chloride. (b) Regeneration of nanotube surface after exposure to thionyl chloride by exposure of the device to humid air. SOCl₂ is hydrolyzed and desorbed from the nanotube surface. Reproduced with permission from ref 43. Copyright 2006, American Chemical Society.

increases the conduction pathways through the nanotube network and the conductance by 5 orders of magnitude. This extraordinarily large effect is caused by a nonlinear disassembly process, wherein SWCNTs are initially isolated from each other by the metallosupramolecular polymer. Disassembly caused the formation of a conductive SWCTN network.

5.1.2. Pulmonary Agents. Pulmonary agents, like chlorine and phosgene, cause lung damage, coughing, dyspnea, and pulmonary edema at high dosage.^{634,635} Chlorine acts by dissociation to give HCl and HOCl that produce other reactive intermediates capable of causing nitration, chlorination, and dimerization of aromatic amino acids.⁶³⁶ Phosgene acts by acylation of nucleophilic moieties in the body (i.e., aminio, hydroxyl, and sulphydryl groups).⁶³⁷ Several groups have developed CNT-based sensors to detect mimics of the pulmonary agents Cl₂, phosgene, and SOCl₂.

Wongwiriyan et al. reported a chemiresistive sensor that comprised pristine CNTs grown between Pt electrodes.⁶³⁸ They reported sensitivity toward oxidizing gases like NO₂ and Cl₂—6% and 50% change in resistance for 50 ppb of NO₂ and Cl₂, respectively—but insensitive toward CO₂, H₂, alkanes, aromatic hydrocarbons, alcohols, ketones, and carboxylic acids. This detection limit is well within the limit of 1 ppm set by OSHA.³¹⁶ Lee et al. reported the chemiresistive sensing of thionyl chloride (SOCl₂) using sodium dodecyl sulfate (SDS)-wrapped CNTs.⁴³ The sensing mechanism toward SOCl₂ was investigated in detail; passivating of the electrode surface did not decrease the response toward SOCl₂ excluding Schottky barrier mechanisms, Figure 50a. Raman spectra before and after exposure indicated that the increase in conductance upon exposure was the result of electron transfer from metallic tubes to SOCl₂. Additionally, the initial conductance of the sensor is restored by hydrolysis of SOCl₂ via exposure of the device to humid air, Figure 50b.

Several groups have reported sensors for pulmonary agents containing selector units that impart selectivity. Li et al. developed sensors that responded selectively to HCl and Cl₂ by functionalizing CNTs with chlorosulfonated polyethylene and hydroxypropyl cellulose, respectively.⁶³⁹ The authors hypothesized that the selectivity of the chlorosulfonated polymer toward Cl₂ can be attributed to the like-dissolves-like principle of solubility. Likewise, the increased polarity of the OH groups in the hydroxypropyl-cellulose-coated CNTs was thought to be responsible for the increased response

toward HCl. Building on these findings, they developed CNT arrays containing 32 sensing channels—containing chlorosulfonated polyethylene and hydroxypropyl cellulose functionalized CNTs—to differentiate between Cl₂, NO₂, HCN, HCl, and a number of VOCs.^{640,641}

Furthermore, CNTs doped with nitrogen, or nitrogen-containing functional groups, have been used to detect Cl₂. Gohier et al. used as-grown, annealed, nitrogen-doped, and polyethylenimine (PEI)-functionalized CNTs to detect Cl₂.⁶⁴² The authors first investigated the influence of structural defects on the CNT sensor. Nitrogen-doped CNTs were fabricated by adding 35 vol % NH₃ to the argon carrier gas during CNT synthesis. For both the as-grown and the annealed CNTs, exposure to Cl₂ induces an increase in the conductance of the CNT network. For nitrogen-doped or PEI-coated CNTs, however, exposure to Cl₂ induces a decrease in the conductance of the CNT network. Overall, the annealed CNTs showed the strongest response toward Cl₂. The authors hypothesized that the difference in response is due to the initial doping level of the CNT material and that the decrease in conductance is indicative of the n-type semiconducting properties of nitrogen-containing sensors. Lee et al. investigated the influence of nitrogen-containing dopants on the semiconducting properties and the resulting sensitivity to SOCl₂.⁶⁴³ In agreement with Gohier et al.,⁶⁴² the authors observed sensing behavior indicative of an n-type semiconductor for PEI-functionalized CNTs.

Apart from these organic selectors, several inorganic materials have found applications in the sensing of pulmonary agents. Multiple groups reported the detection of chlorine using metal NPs/CNT composites, which are based on the catalytic interaction between metal and Cl₂. Popa et al. developed Cl₂ sensors that comprised CNTs blended with hollow Pt–nanocubes, exhibiting a 6-fold increase in sensitivity over pristine CNT sensors.⁶⁴⁴ The increased response upon addition of nanostructured Pt was attributed to the increased surface area and the reductive dissociation of Cl₂ catalyzed by Pt. Similarly, Choi et al. fabricated sensors in which the Pt–nanoparticles were grafted directly on the sidewalls of the CNTs.⁶⁴⁵ Their sensors showed excellent long-term stability with a 10.3% change in resistance for 1 ppm of Cl₂ for newly fabricated sensors that is retained after storing under humid conditions for 6 months. Sharma et al. reported a chemiresistive sensor containing CNT/zinc phthalocyanine

composites that displayed an increase in conductance upon exposure to Cl_2 .⁶⁴⁶ Raman spectroscopic investigations indicated that Cl_2 is bound to the Zn center during exposure. A shift of the Zn core levels toward higher binding energies, as observed from X-ray photoelectron spectra before and during exposure of the selector to Cl_2 , indicates a strong electron transfer to Cl_2 .

5.1.3. Blood Agents. Blood agents act by disrupting the transport of oxygen through the body. Common examples of these agents are carbon monoxide (CO) and cyanide. CO, covered previously in section 2.1.3, binds to the heme groups in hemoglobin, compromising the transport of oxygen from the lungs to the tissue.^{647,648} Cyanide binds to the heme center in the enzyme cytochrome *c* oxidase and thus prevents the utilization of oxygen in the body. Poisoning with cyanide or carbon monoxide causes nausea, dizziness, and headaches, and larger doses can cause loss of consciousness and death.⁶⁴⁹

Only a few examples of CNT-based cyanide sensors have been reported. Srivastava et al. reported the theoretical investigation of HCN binding on pristine CNTs.⁶⁵⁰ In this study, HCN was found to physisorb weakly on the CNT sidewalls with negligible charge transfer. B-Doped CNTs, as investigated by Zhang et al. computationally, demonstrate electron transfer from HCN to the CNTs with a much increased binding energy when compared to pristine CNTs.²⁹⁵ These findings indicate that pristine CNT sensors are unlikely to show significant responses to HCN but that sensors including selectors with electron-withdrawing functionality might impart sensitivity. Yari et al. reported the electrochemical detection of cyanide using MWCNTs filled with AgNO_3 , Figure 51.⁶⁵¹ Cyanide is detected selectively over

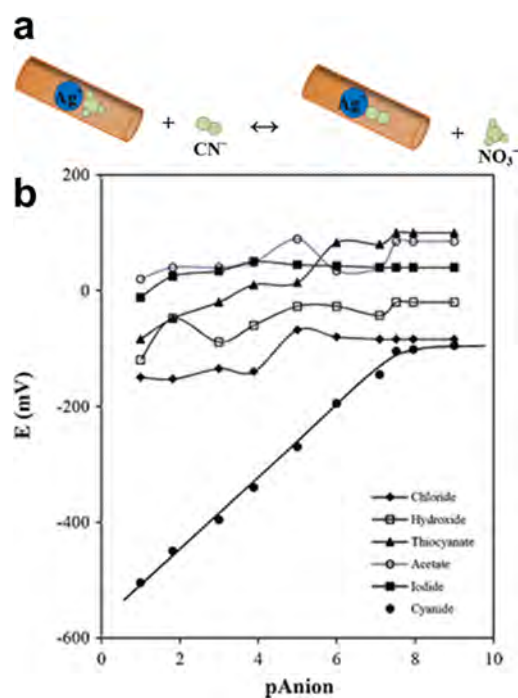


Figure 51. Sensing of blood agent HCN. (a) Schematic representation of the sensing mechanism: nitrate anion in AgNO_3 -filled CNTs (orange) is replaced by cyanide at electrode-solution interface. (b) Potential response of electrochemical sensor toward common anions compared to cyanide (filled circles). Reproduced with permission from ref 651. Copyright 2011, Springer.

thiocyanate, chloride, iodide, hydroxide, and acetate; the authors attributed the selectivity to the capability of Ag(I) ions to form well-known complexes with cyanide as AgCN_2^- and $\text{Ag}[\text{AgCN}_2]$.

5.2. Explosives

Explosive-based weapons are the most common method of carrying out terrorist attacks; they are highly destructive and relatively easy to construct.^{652,653} To prevent terrorist activity, fast and reliable distributed sensing of explosives is of utmost importance. As the detection of high-boiling explosive nitroaromatic compounds like 2,4,6-trinitrotoluene (TNT) in air is complicated by their low vapor pressure, several groups have developed sensors for the precursors or impurities associated with TNT, including nitrotoluene or dinitrotoluene. Additionally, there are nonexplosive markers such as cyclohexanone, which is used to recrystallize the highly explosive RDX as part of its production. Figure 52 shows the chemical structure of the explosive compounds and markers covered in this section.

Pristine CNTs have been demonstrated to be sensitive toward nitroaromatic compounds. Theoretical and experimental investigations confirm that interactions between the electron-accepting nitroaromatics and CNT are dominated by $\pi-\pi$ stacking with minor charge-transfer characteristics.^{654,655} These weaker interactions would seem to indicate that the response of pristine CNT sensors is significantly lower than the response toward the strong electron acceptor, NO_2 . Li et al. compared the chemiresistive detections between nitrotoluene and NO_2 in which the exposure to nitrotoluene induced a semireversible increase in conductance that was 2 orders of magnitude lower than the response of the same sensor toward NO_2 .²⁴⁰ Ruan et al. coated a piezoelectrical microcantilever with pristine CNTs to detect TNT.⁶⁵⁶ During heating of the cantilever, adsorbed nitroaromatic compounds decompose exothermically and this extra heat increases the bending of the microcantilever; this bending can be read out through the piezoelectrical element. Liu et al. reported the chemiresistive sensing of TNT in water in a microfluidic system with a detection limit of 1 ppm.⁶⁵⁷ Chen et al. fabricated flexible pristine CNT sensors which can detect TNT down to 8 ppb.⁶⁵⁸ Kumar et al. used films of pristine CNTs to detect DNT at 0.2–2 ppm chemiresistively. Here the response to DNT is semireversible, and exposure to UV light allows the complete recovery of the sensor.⁶⁵⁹ Although sensitive, these pristine CNT explosive sensors are of limited selectivity.

Biosensors consisting of DNA or peptide-functionalized CNTs show promises in the selective detection of explosives. The ssDNA sensors covered in section 5.1.1, Nerve Agents and Vesicant Agents, have also been used to detect explosives. Different base sequences lead to different responses toward specific explosives, allowing selective detection of specific targets.^{627,628,631} Kim et al. used the tripeptide receptor tryptophan–histidine–tryptophan to selectively detect TNT with CNTs. In this scheme they anchored the tripeptide to a polydiacetylene polymer which was then used to form a lipid layer over a SWCNT device, Figure 53.⁶⁶⁰ The binding of TNT by the receptor induces an increase in the conductance of the active layer, which the authors attribute to the charge-acceptor properties of TNT.

Zhang et al. used carbazolylethynylene oligomer-wrapped CNTs to selectively sense nitroaromatics in a chemiresistive devices, Figure 54.⁶⁶¹ When comparing devices containing

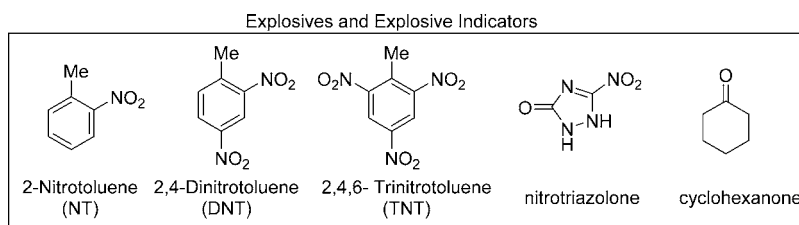


Figure 52. Chemical structures of explosives and secondary explosive indicators.

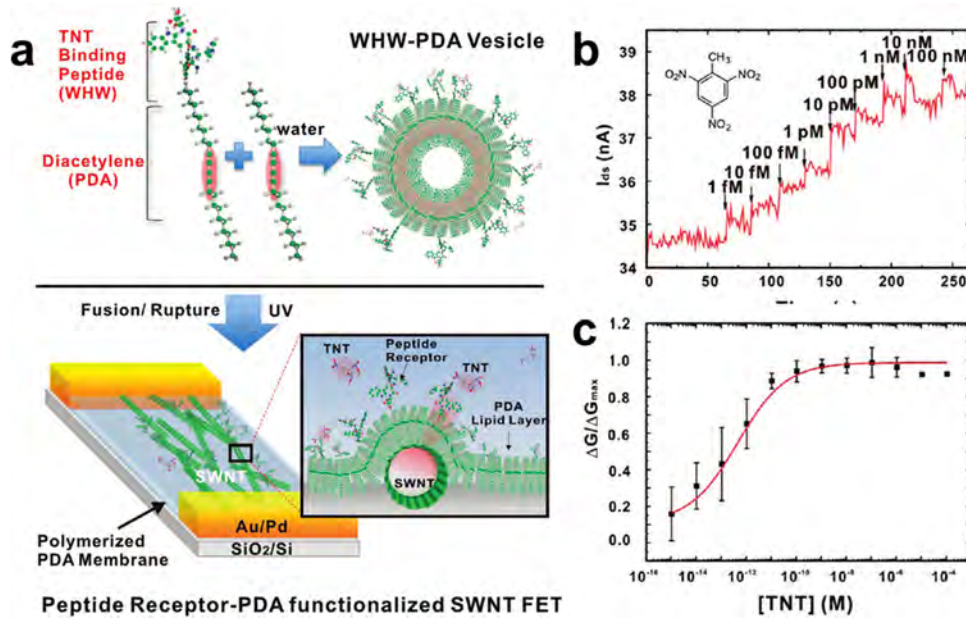


Figure 53. Chemiresistive sensing of 2,4,6-trinitrotoluene (TNT). (a) Schematic of peptide-based TNT sensor. TNT-binding peptide (WHW) conjugated with diacetylene (PDA): after assembly of WHW-PDA nanovesicles in water, the nanovesicle is applied to the SWCNT device. Diacetylene is then polymerized via application of UV light. (b) Real-time change in conductance of WHW-PDA-coated SWCNTs upon injection (arrow) of TNT, and (c) calibration curve of response as a function of TNT concentration. Reproduced with permission from ref 660. Copyright 2011, American Chemical Society.

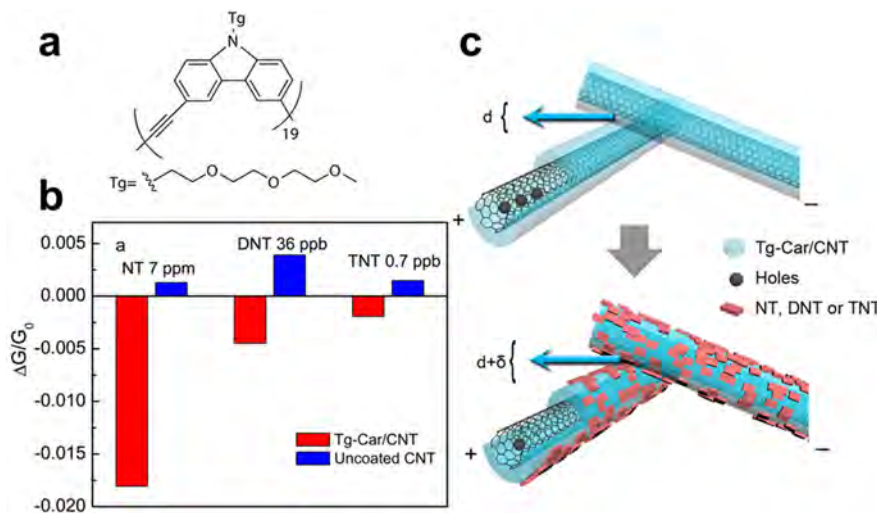


Figure 54. Chemiresistive sensing of nitroaromatics. (a) Molecular structure of Tg-Car oligomer with strong affinity to nitroaromatic explosive compounds. (b) Sensing behavior of wrapped (red) and pristine (blue) CNTs toward 4-nitrotoluene (NT), 2,4-dinitrotoluene (DNT), and 2,4,6-trinitrotoluene (TNT). (c) Schematic of sensing mechanism demonstrating the swelling of oligomer-wrapped CNTs when exposed to nitroaromatics. Reproduced with permission from ref 661. Copyright 2015, American Chemical Society.

pristine CNTs with devices containing wrapped CNTs, the authors observed the opposite responses toward nitro-

aromatics. For devices containing pristine CNTs, an increase in conductance was observed, consistent with the charge-

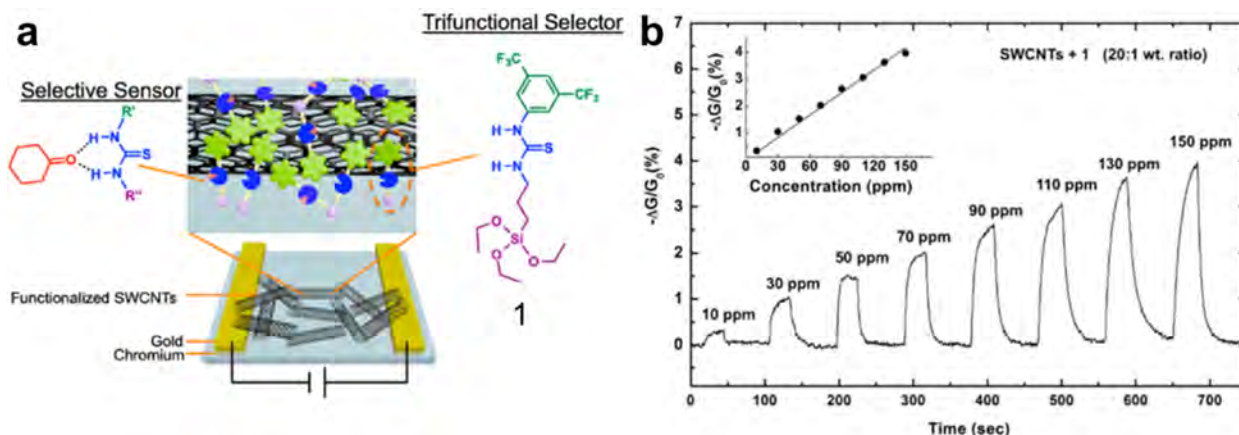


Figure 55. Chemiresistive sensing of cyclohexanone. (a) Schematic sensor containing the chemical structures of trifunctional Selector 1, SWCNT, and sensing device. (b) Sensing traces using a blend of Selector 1 and SWCNTs to detect cyclohexanone at different concentrations. Reproduced with permission from ref 89. Copyright 2013, American Chemical Society.

accepting character of nitroaromatics. For devices containing wrapped CNTs, a decrease in conductance was observed which the authors attributed to swelling of the oligomeric material and the resulting increase in separation between CNTs, Figure 54c. By employing channels of both pristine and wrapped CNTs, the authors were able to separate vapors of TNT, DNT, and NT.

In addition, Hrapovic et al. used Cu nanoparticle/MWCNT composites to detect TNT electrochemically.⁶⁶² Using Cu NP electrodes, TNT exhibits three well-defined redox peaks corresponding to sequential reduction of the three nitro groups to hydroxylamines, permitting the detection of 1 ppb of TNT in Milli-Q water and 50 ppb in complex backgrounds (river water or soil samples). Li et al. used a β -cyclodextrin/MWCNT/graphene oxide composites to detect DNT.⁶⁶³ Similarly, the nitroaromatic can be detected in complex backgrounds including groundwater and soil samples. The cyclic oligosaccharide, β -cyclodextrin, forms hydrophobic pockets in water that can bind DNT and facilitate the detection of TNT at much lower concentrations than is possible with plain carbon electrodes. In addition to electrochemical sensing in water, Wei et al. reported the chemiresistive sensing of nitroaromatics in water using 1-pyrenemethylamine-functionalized CNTs.⁸⁶ The authors report sensitivity for concentrations as low as 10 ppt and good selectivity for TNT over other nitroaromatics.

An alternative approach to sensing the explosive compound or precursors to the explosive compound is the detection of secondary signatures such as solvents that are commonly used in the production of explosive compounds. Cyclohexanone, a recrystallizing agent for RDX and is found in the headspace of plastic explosives, and thereby is a targets for explosives detection.⁶⁶⁴ Frazier and Swager demonstrated the chemiresistive sensing of cyclohexanone using thiourea and/or urea-functionalized SWCNTs.^{89,122} The thiourea motif is known to bind ketones (e.g., cyclohexanone) through a two-point hydrogen bonding. They reported the covalent functionalization of polymer matrix materials that surround the SWCNTs with thiourea derivatives, which increased the response toward cyclohexanone by 100% when compared to pristine CNTs.¹²² They also demonstrated selective and robust sensors using a trifunctional selector (Figure 55a), which can form a cross-linked polymeric network on the surface of the device to

prevent the phase separation of selector and CNT.⁸⁹ Figure 55b shows the response of a sensor containing this trifunctional selector toward 10–150 ppm cyclohexanone; the selector showed a 2-fold increase over pristine CNTs, and polymerization of the triethoxysilane substituents increases the robustness of the selector to heat treatment. The sensors had a highly reproducible response and were sufficiently robust to survive sonication in methanol solution.

6. SUMMARY AND CONCLUDING REMARKS

CNTs are promising active elements of electronic chemical sensors. In this review, we first presented the fundamentals of these sensors: sensing mechanisms, chemical CNT functionalization, device architectures, fabrication methods, performance parameters, and computational models. The reader is then introduced to CNT-based sensors and target analytes for a variety of applications: environmental monitoring, food and agricultural applications, biological sensors, and national security. These discussions are intended to impart a working knowledge of the current state of the field to the reader.

The diversity of sensing schemes that have been reported with CNTs is clearly expansive. There are many examples that are not designed from an intuitive chemical basis or from known solution chemistry and reactivity. This approach is not specific to CNT sensors, and although it is tempting to be dismissive of these empirical methods, some of these schemes may be highly effective in a specific environment. Indeed, in specific applications, there may not be many interferants or a pressing need for precise selectivity. For example, inorganic gases like SO_2 and NO_2 generate a response from almost all CNT-based chemical sensors. In applications, however, where these gases do not occur, their interference becomes a nonissue. Similarly, sensors that respond to NH_3 or biogenic amines will likely have cross reactivity with DMSO, DMF, THF, phosphines, or organic sulfides. If such sensors were designed to ensure the integrity of food packaging, these chemicals are just as problematic as the amines. Thus, preventing reactivity toward these interferants is not always required. However, in general the best and most robust sensors involve well-conceived chemical or biological principles that recognize unique molecular attributes and reactivity of the analytes.

Advances in the sophistication by which CNTs can be functionalized and organized are certain to play a role in evolving this technology. The modularity by which CNTs can be functionalized is allowing for rapid development of sensor methods, and it is clear that we will see a wave of commercial electrical CNT sensors that rival and likely surpass most other chemical sensor types. It is our hope that this review will serve as a guide to developments that can contribute to the adoption of new sensory methods that can protect and improve our environment, safety, and health.

AUTHOR INFORMATION

Corresponding Author

*E-mail: tswager@mit.edu.

ORCID

Vera Schroeder: [0000-0002-6255-4418](https://orcid.org/0000-0002-6255-4418)

Sibo Lin: [0000-0001-5922-6694](https://orcid.org/0000-0001-5922-6694)

Timothy M. Swager: [0000-0002-3577-0510](https://orcid.org/0000-0002-3577-0510)

Notes

The authors declare no competing financial interest.

Biographies

Vera Schroeder received her B.S. degree in Chemistry and her M.S. degree in Materials Chemistry from RWTH Aachen University, where she conducted research with Paul Kögerler in the Department of Inorganic Chemistry and Prof. Ting Xu in the Department of Materials Science & Engineering at the University of California, Berkeley. In 2014, Vera started her Ph.D. studies in Inorganic Chemistry at MIT under the guidance of Timothy M. Swager. Her Ph.D. research focuses on the investigation of carbon nanotube-based chemical sensors and their applications.

Suchol Savagatrup earned his B.S. in Chemical Engineering from the University of California, Berkeley, in 2012, where he conducted research with Rachel Segalman in the Department of Chemical and Biomolecular Engineering and Adam Weber at Lawrence Berkeley National Laboratory. He completed his Ph.D. degree in 2016 at the University of California, San Diego, under the direction of Darren Lipomi, where his work was funded by the NSF Graduate Research Fellowship and the Kaplan Dissertation Year Fellowship. He is currently a postdoctoral fellow in the Swager lab at MIT and a recipient of the Ruth L. Kirschstein Postdoctoral Fellowship.

Maggie He completed her undergraduate studies at the City College of New York and earned her B.S. degree in Chemistry in 2008, where she performed research with Barbara Zajc. She received her M.S. degree in Chemistry in 2010 from the University of Pennsylvania and Ph.D. degree in Chemistry in 2014 from ETH Zürich under the supervision of Jeffrey Bode. She is currently a postdoctoral fellow in the Swager group and a recipient of the Swiss National Science Foundation (SNF) Early Postdoc Mobility Fellowship.

Sibo Lin began his studies at Indiana University, where he conducted computational chemistry research under the guidance of Mu-Hyun Baik and Jennifer C. Green at the University of Oxford, U.K., and earned B.S. degrees in Mathematics and Chemistry in 2008. He then continued studies at the California Institute of Technology with Theodor Agapie in synthetic inorganic chemistry with support from a NSF Graduate Research Fellowship, finishing his Ph.D. degree in 2014. He is currently a postdoctoral researcher at MIT with the Swager group and a recipient of the Ruth L. Kirschstein Postdoctoral Fellowship.

Timothy M. Swager is the John D. MacArthur Professor of Chemistry and the Director, Deshpande Center for Technological Innovation at the Massachusetts Institute of Technology. A native of Montana, he received his B.S. degree from Montana State University in 1983 and Ph.D. degree from the California Institute of Technology in 1988. After a postdoctoral appointment at MIT he was on the chemistry faculty at the University of Pennsylvania and returned to MIT in 1996 as a Professor of Chemistry. His research has been focused at the interface of chemistry and materials science with a particular interest in chemical and biological sensing.

ACKNOWLEDGMENTS

The authors of this article were supported by the KAUST sensor project CRF-2015-SENSORS2719 and the Army Research Office through the Institute for Soldier Nanotechnologies and National Science Foundation (DMR-1410718). S.S. and S.L. were supported by F32 Ruth L. Kirschstein National Research Service Awards. M.H. was supported by NIH Training Grant T32ES007020.

REFERENCES

- (1) De Volder, M. F. L.; Tawfick, S. H.; Baughman, R. H.; Hart, A. J. Carbon Nanotubes: Present and Future Commercial Applications. *Science* **2013**, *339*, 535–539.
- (2) Schnorr, J. M.; Swager, T. M. Emerging Applications of Carbon Nanotubes. *Chem. Mater.* **2011**, *23*, 646–657.
- (3) Hu, L.; Hecht, D. S.; Grüner, G. Carbon Nanotube Thin Films: Fabrication, Properties, and Applications. *Chem. Rev.* **2010**, *110*, 5790–5844.
- (4) Cao, Q.; Rogers, J. a. Ultrathin Films of Single-Walled Carbon Nanotubes for Electronics and Sensors: A Review of Fundamental and Applied Aspects. *Adv. Mater.* **2009**, *21*, 29–53.
- (5) Park, S.; Vosguerichian, M.; Bao, Z. A Review of Fabrication and Applications of Carbon Nanotube Film-Based Flexible Electronics. *Nanoscale* **2013**, *5*, 1727–1752.
- (6) Shulaker, M. M.; Hills, G.; Patil, N.; Wei, H.; Chen, H.-Y. Y.; Wong, H.-S. P. S. P.; Mitra, S. Carbon Nanotube Computer. *Nature* **2013**, *501*, 526–530.
- (7) Hong, G.; Diao, S.; Antaris, A. L.; Dai, H. Carbon Nanomaterials for Biological Imaging and Nanomedicinal Therapy. *Chem. Rev.* **2015**, *115*, 10816–10906.
- (8) Wang, J. Carbon-Nanotube Based Electrochemical Biosensors: A Review. *Electroanalysis* **2005**, *17*, 7–14.
- (9) Meyyappan, M. Carbon Nanotube-Based Chemical Sensors. *Small* **2016**, *12*, 2118–2129.
- (10) Kauffman, D. R.; Star, A. Carbon Nanotube Gas and Vapor Sensors. *Angew. Chem., Int. Ed.* **2008**, *47*, 6550–6570.
- (11) Tasis, D.; Tagmatarchis, N.; Bianco, A.; Prato, M. Chemistry of Carbon Nanotubes. *Chem. Rev.* **2006**, *106*, 1105–1136.
- (12) Ding, L.; Tselev, A.; Wang, J.; Yuan, D.; Chu, H.; McNicholas, T. P.; Li, Y.; Liu, J. Selective Growth of Well-Aligned Semiconducting Single-Walled Carbon Nanotubes. *Nano Lett.* **2009**, *9*, 800–805.
- (13) Harutyunyan, A. R.; Chen, G.; Paronyan, T. M.; Pigos, E. M.; Kuznetsov, O. A.; Hewaparakrama, K.; Kim, S. M.; Zakharov, D.; Stach, E. A.; Sumanasekera, G. U. Preferential Growth of Single-Walled Carbon Nanotubes with Metallic Conductivity. *Science* **2009**, *326*, 116–120.
- (14) Arnold, M. S.; Green, A. A.; Hulvat, J. F.; Stupp, S. I.; Hersam, M. C. Sorting Carbon Nanotubes by Electronic Structure Using Density Differentiation. *Nat. Nanotechnol.* **2006**, *1*, 60–65.
- (15) Lee, H. W.; Yoon, Y.; Park, S.; Oh, J. H.; Hong, S.; Liyanage, L. S.; Wang, H.; Morishita, S.; Patil, N.; Park, Y. J.; et al. Selective Dispersion of High Purity Semiconducting Single-Walled Carbon Nanotubes with Regioregular Poly(3-Alkylthiophene)S. *Nat. Commun.* **2011**, *2*, 541.

(16) Wang, H.; Koleilat, G. I.; Liu, P.; Jimenez-Oses, G.; Lai, Y.; Vosgueritchian, M.; Fang, Y.; Park, S.; Houk, K. N.; Bao, Z. High-Yield Sorting of Small-Diameter Carbon Nanotubes for Solar Cells and Transistors. *ACS Nano* **2014**, *8*, 2609–2617.

(17) Tanaka, T.; Urabe, Y.; Nishide, D.; Kataura, H. Continuous Separation of Metallic and Semiconducting Carbon Nanotubes Using Agarose Gel. *Appl. Phys. Express* **2009**, *2*, 125002.

(18) Yomogida, Y.; Tanaka, T.; Zhang, M.; Yudasaka, M.; Wei, X.; Kataura, H. Industrial-Scale Separation of High-Purity Single-Chirality Single-Wall Carbon Nanotubes for Biological Imaging. *Nat. Commun.* **2016**, *7*, 12056.

(19) Povie, G.; Segawa, Y.; Nishihara, T.; Miyauchi, Y.; Itami, K. Synthesis of a Carbon Nanobelt. *Science* **2017**, *356*, 172–175.

(20) Swager, T. M. The Molecular Wire Approach to Sensory Signal Amplification. *Acc. Chem. Res.* **1998**, *31*, 201–207.

(21) Kong, J.; Franklin, N. R.; Zhou, C.; Chapline, M. G.; Peng, S.; Cho, K.; Dai, H.; Franklin, R. N.; Zhou, C.; Chapline, M. G.; et al. Nanotube Molecular Wires as Chemical Sensors. *Science* **2000**, *287*, 622–625.

(22) Peveler, W. J.; Yazdani, M.; Rotello, V. M. Selectivity and Specificity: Pros and Cons in Sensing. *ACS Sensors* **2016**, *1*, 1282–1285.

(23) Chen, R. J.; Zhang, Y.; Wang, D.; Dai, H. Noncovalent Sidewall Functionalization of Single-Walled Carbon Nanotubes for Protein Immobilization. *J. Am. Chem. Soc.* **2001**, *123*, 3838–3839.

(24) Chen, R. J.; Choi, H. C.; Bangsaruntip, S.; Yenilmez, E.; Tang, X.; Wang, Q.; Chang, Y. L.; Dai, H. An Investigation of the Mechanisms of Electronic Sensing of Protein Adsorption on Carbon Nanotube Devices. *J. Am. Chem. Soc.* **2004**, *126*, 1563–1568.

(25) Zhou, Q.; Swager, T. M. Fluorescent Chemosensors Based on Energy Migration in Conjugated Polymers: The Molecular Wire Approach to Increased Sensitivity. *J. Am. Chem. Soc.* **1995**, *117*, 12593–12602.

(26) Barone, P. W.; Baik, S.; Heller, D. A.; Strano, M. S. Near-Infrared Optical Sensors Based on Single-Walled Carbon Nanotubes. *Nat. Mater.* **2004**, *4*, 86–92.

(27) Boghossian, A. A.; Zhang, J.; Barone, P. W.; Reuel, N. F.; Kim, J. H.; Heller, D. A.; Ahn, J. H.; Hilmer, A. J.; Rwei, A.; Arkalgud, J. R.; et al. Near-Infrared Fluorescent Sensors Based on Single-Walled Carbon Nanotubes for Life Sciences Applications. *ChemSusChem* **2011**, *4*, 848–863.

(28) Yang, W.; Ratinac, K. R.; Ringer, S. R.; Thordarson, P.; Gooding, J. J.; Braet, F. Carbon Nanomaterials in Biosensors: Should You Use Nanotubes or Graphene. *Angew. Chem., Int. Ed.* **2010**, *49*, 2114–2138.

(29) Kauffman, D. R.; Star, A. Graphene versus Carbon Nanotubes for Chemical Sensor and Fuel Cell Applications. *Analyst* **2010**, *135*, 2790–2797.

(30) Wei, N.; Liu, Y.; Xie, H.; Wei, F.; Wang, S.; Peng, L. M. Carbon Nanotube Light Sensors with Linear Dynamic Range of over 120 dB. *Appl. Phys. Lett.* **2014**, *105*, 073107.

(31) Yang, N.; Chen, X.; Ren, T.; Zhang, P.; Yang, D. Carbon Nanotube Based Biosensors. *Sens. Actuators, B* **2015**, *207*, 690–715.

(32) Llobet, E. Gas Sensors Using Carbon Nanomaterials: A Review. *Sens. Actuators, B* **2013**, *179*, 32–45.

(33) Ellis, J. E.; Star, A. Carbon Nanotube Based Gas Sensors toward Breath Analysis. *ChemPlusChem* **2016**, *81*, 1248–1265.

(34) Wang, Y.; Yeow, J. T. W. A Review of Carbon Nanotubes-Based Gas Sensors. *J. Sens.* **2009**, *2009*, 1–24.

(35) Fennell, J. F.; Liu, S. F.; Azzarelli, J. M.; Weis, J. G.; Rochat, S.; Mirica, K. A.; Ravnsbaek, J. B.; Swager, T. M. Nanowire Chemical/Biological Sensors: Status and a Roadmap for the Future. *Angew. Chem., Int. Ed.* **2016**, *55*, 1266–1281.

(36) Bondavalli, P.; Legagneux, P.; Pribat, D. Carbon Nanotubes Based Transistors as Gas Sensors: State of the Art and Critical Review. *Sens. Actuators, B* **2009**, *140*, 304–318.

(37) Boyd, A.; Dube, I.; Fedorov, G.; Paranjape, M.; Barbara, P. Gas Sensing Mechanism of Carbon Nanotubes: From Single Tubes to High-Density Networks. *Carbon* **2014**, *69*, 417–423.

(38) Zhao, J.; Buldum, A.; Han, J.; Lu, J. P. Gas Molecule Adsorption in Carbon Nanotubes and Nanotube Bundles. *Nanotechnology* **2002**, *13*, 195–200.

(39) Collins, P. G.; Bradley, K.; Ishigami, M.; Zettl, A. Extreme Oxygen Sensitivity of Electronic Properties of Carbon Nanotubes. *Science* **2000**, *287*, 1801–1804.

(40) Kang, D.; Park, N.; Ko, J.; Bae, E.; Park, W. Oxygen-Induced p-Type Doping of a Long Individual Single-Walled Carbon Nanotube. *Nanotechnology* **2005**, *16*, 1048–1052.

(41) Novak, J. P.; Snow, E. S.; Houser, E. J.; Park, D.; Stepnowski, J. L.; McGill, R. A. Nerve Agent Detection Using Networks of Single-Walled Carbon Nanotubes. *Appl. Phys. Lett.* **2003**, *83*, 4026–4028.

(42) Peng, G.; Tisch, U.; Haick, H. Detection of Nonpolar Molecules by Means of Carrier Scattering in Random Networks of Carbon Nanotubes: Toward Diagnosis of Diseases via Breath Samples. *Nano Lett.* **2009**, *9*, 1362–1368.

(43) Lee, C. Y.; Baik, S.; Zhang, J.; Masel, R. I.; Strano, M. S. Charge Transfer from Metallic Single-Walled Carbon Nanotube Sensor Arrays. *J. Phys. Chem. B* **2006**, *110*, 11055–11061.

(44) Udomvech, A.; Kerdcharoen, T.; Osotchan, T. First Principles Study of Li and Li+ Adsorbed on Carbon Nanotube: Variation of Tubule Diameter and Length. *Chem. Phys. Lett.* **2005**, *406*, 161–166.

(45) Zanolli, Z.; Leghrif, R.; Felten, A.; Pireaux, J.-J. J.; Llobet, E.; Charlier, J.-C. C. Gas Sensing with Au-Decorated Carbon Nanotubes. *ACS Nano* **2011**, *5*, 4592–4599.

(46) Cao, C.; Kemper, A. F.; Agapito, L.; Zhang, J.-W.; He, Y.; Rinzler, A.; Cheng, H.-P.; Zhang, X.-G.; Rocha, A. R.; Sanvito, S. Nonequilibrium Green's Function Study of Pd4-Cluster-Functionalized Carbon Nanotubes as Hydrogen Sensors. *Phys. Rev. B: Condens. Matter Mater. Phys.* **2009**, *79*, 075127.

(47) Wang, F.; Gu, H.; Swager, T. M. Carbon Nanotube/Polythiophene Chemiresistive Sensors for Chemical Warfare Agents. *J. Am. Chem. Soc.* **2008**, *130*, 5392–5393.

(48) Star, A.; Han, T. R.; Joshi, V.; Gabriel, J. C. P.; Grüner, G. Nanoelectronic Carbon Dioxide Sensors. *Adv. Mater.* **2004**, *16*, 2049–2052.

(49) Star, A.; Joshi, V.; Skarupo, S.; Thomas, D.; Gabriel, J.-C. P. Gas Sensor Array Based on Metal-Decorated Carbon Nanotubes. *J. Phys. Chem. B* **2006**, *110*, 21014–21020.

(50) Zhang, T.; Mubeen, S.; Myung, N. V.; Deshusses, M. A. Recent Progress in Carbon Nanotube-Based Gas Sensors. *Nanotechnology* **2008**, *19*, 332001.

(51) Roberts, M. E.; LeMieux, M. C.; Bao, Z. Sorted and Aligned Single-Walled Carbon Nanotube Networks for Transistor-Based Aqueous Chemical Sensors. *ACS Nano* **2009**, *3*, 3287–3293.

(52) Star, A.; Gabriel, J. C. P.; Bradley, K.; Grüner, G. Electronic Detection of Specific Protein Binding Using Nanotube FET Devices. *Nano Lett.* **2003**, *3*, 459–463.

(53) Heller, I.; Janssens, A. M.; Männik, J.; Minot, E. D.; Lemay, S. G.; Dekker, C.; Mannik, J.; Minot, E. D.; Lemay, S. G.; Dekker, C.; et al. Identifying the Mechanism of Biosensing with Carbon Nanotube Transistors. *Nano Lett.* **2008**, *8*, 591–595.

(54) Rao, A. M.; Eklund, P. C.; Bandow, S.; Thess, A.; Smalley, R. E. Evidence for Charge Transfer in Doped Carbon Nanotube Bundles from Raman Scattering. *Nature* **1997**, *388*, 257–259.

(55) Hatting, B. Optical and Vibrational Properties of Doped Carbon Nanomaterials. Ph.D. Dissertation, Freie Universität Berlin, 2016.

(56) Monteiro, F. H.; Larrude, D. G.; Maia Da Costa, M. E. H.; Freire, F. L. Estimating the Boron Doping Level on Single Wall Carbon Nanotubes Using Raman Spectroscopy. *Mater. Lett.* **2013**, *92*, 224–226.

(57) Panchakarla, L. S.; Govindaraj, A.; Rao, C. N. R. Nitrogen- and Boron-Doped Double-Walled Carbon Nanotubes. *ACS Nano* **2007**, *1*, 494–500.

(58) Lyu, S. C.; Han, J. H.; Shin, K. W.; Sok, J. H. Synthesis of Boron-Doped Double-Walled Carbon Nanotubes by the Catalytic Decomposition of Tetrahydrofuran and Triisopropyl Borate. *Carbon* **2011**, *49*, 1532–1541.

(59) Voggu, R.; Rout, C. S.; Franklin, A. D.; Fisher, T. S.; Rao, C. N. R. Extraordinary Sensitivity of the Electronic Structure and Properties of Single-Walled Carbon Nanotubes to Molecular Charge-Transfer. *J. Phys. Chem. C* **2008**, *112*, 13053–13056.

(60) Shin, H.-J.; Kim, S. M.; Yoon, S.-M.; Benayad, A.; Kim, K. K.; Kim, S. J.; Park, H. K.; Choi, J.-Y.; Lee, Y. H. Tailoring Electronic Structures of Carbon Nanotubes by Solvent with Electron-Donating and -Withdrawing Groups. *J. Am. Chem. Soc.* **2008**, *130*, 2062–2066.

(61) Yim, W.-L.; Gong, X. G.; Liu, Z.-F. Chemisorption of NO₂ on Carbon Nanotubes. *J. Phys. Chem. B* **2003**, *107*, 9363–9369.

(62) Ricca, A.; Bauschlicher, C. W. The Adsorption of NO₂ on (9,0) and (10,0) Carbon Nanotubes. *Chem. Phys.* **2006**, *323*, 511–518.

(63) Zhang, Y.; Suc, C.; Liu, Z.; Li, J. Carbon Nanotubes Functionalized by NO₂: Coexistence of Charge Transfer and Radical Transfer. *J. Phys. Chem. B* **2006**, *110*, 22462–22470.

(64) Soylemez, S.; Yoon, B.; Toppore, L.; Swager, T. M. Quaternized Polymer-Single-Walled Carbon Nanotube Scaffolds for a Chemiresistive Glucose Sensor. *ACS Sensors* **2017**, *2*, 1123–1127.

(65) Li, C.; Thostenson, E. T.; Chou, T. W. Dominant Role of Tunneling Resistance in the Electrical Conductivity of Carbon Nanotube-Based Composites. *Appl. Phys. Lett.* **2007**, *91*, 223114.

(66) Hu, N.; Karube, Y.; Yan, C.; Masuda, Z.; Fukunaga, H. Tunneling Effect in a Polymer/Carbon Nanotube Nanocomposite Strain Sensor. *Acta Mater.* **2008**, *56*, 2929–2936.

(67) Ponnamma, D.; Sadasivuni, K. K.; Strankowski, M.; Guo, Q.; Thomas, S. Synergistic Effect of Multi Walled Carbon Nanotubes and Reduced Graphene Oxides in Natural Rubber for Sensing Application. *Soft Matter* **2013**, *9*, 10343–10353.

(68) Liu, S. F.; Moh, L. C. H.; Swager, T. M. Single-Walled Carbon Nanotube–Metalloporphyrin Chemiresistive Gas Sensor Arrays for Volatile Organic Compounds. *Chem. Mater.* **2015**, *27*, 3560–3563.

(69) Wang, H. C.; Li, Y.; Yang, M. J. Sensors for Organic Vapor Detection Based on Composites of Carbon Nanotubes Functionalized with Polymers. *Sens. Actuators, B* **2007**, *124*, 360–367.

(70) Niu, L.; Luo, Y.; Li, Z. A Highly Selective Chemical Gas Sensor Based on Functionalization of Multi-Walled Carbon Nanotubes with Poly(Ethylene Glycol). *Sens. Actuators, B* **2007**, *126*, 361–367.

(71) Wei, C.; Dai, L.; Roy, A.; Tolle, T. B. Multifunctional Chemical Vapor Sensors of Aligned Carbon Nanotube and Polymer Composites. *J. Am. Chem. Soc.* **2006**, *128*, 1412–1413.

(72) Philip, B.; Abraham, J. K.; Chandrasekhar, A. Carbon Nanotube/PMMA Composite Thin Films for Gas-Sensing Applications. *Smart Mater. Struct.* **2003**, *12*, 935.

(73) Ishihara, S.; O’Kelly, C. J.; Tanaka, T.; Kataura, H.; Labuta, J.; Shingaya, Y.; Nakayama, T.; Ohsawa, T.; Nakanishi, T.; Swager, T. M. Metallic versus Semiconducting SWCNT Chemiresistors: A Case for Separated SWCNTs Wrapped by a Metallosupramolecular Polymer. *ACS Appl. Mater. Interfaces* **2017**, *9*, 38062–38067.

(74) Lobe, J. M.; Swager, T. M. Radiation Detection: Resistivity Responses in Functional Poly(Olefin Sulfone)/Carbon Nanotube Composites. *Angew. Chem., Int. Ed.* **2010**, *49*, 95–98.

(75) Zeininger, L.; He, M.; Hobson, S. T.; Swager, T. M. Resistive and Capacitive γ -Ray Dosimeters Based On Triggered Depolymerization in Carbon Nanotube Composites. *ACS Sensors* **2018**, *3*, 976–983.

(76) Peng, N.; Zhang, Q.; Chow, C. L.; Tan, O. K.; Marzari, N. Sensing Mechanisms for Carbon Nanotube Based NH₃ Gas Detection. *Nano Lett.* **2009**, *9*, 1626.

(77) Bradley, K.; Gabriel, J. C. P.; Star, A.; Grüner, G. Short-Channel Effects in Contact-Passivated Nanotube Chemical Sensors. *Appl. Phys. Lett.* **2003**, *83*, 3821–3823.

(78) Liu, X.; Luo, Z.; Han, S.; Tang, T.; Zhang, D.; Zhou, C. Band Engineering of Carbon Nanotube Field-Effect Transistors via Selected Area Chemical Gating. *Appl. Phys. Lett.* **2005**, *86*, 243501.

(79) Zhang, J.; Boyd, A.; Tselev, A.; Paranjape, M.; Barbara, P. Mechanism of NO₂ Detection in Carbon Nanotube Field Effect Transistor Chemical Sensors. *Appl. Phys. Lett.* **2006**, *88*, 123112.

(80) Salehi-Khojin, A.; Khalili-Araghi, F.; Kuroda, M. A.; Lin, K. Y.; Leburton, J.-P.; Masel, R. I. On the Sensing Mechanism in Carbon Nanotube Chemiresistors. *ACS Nano* **2011**, *5*, 153–158.

(81) Kim, Y.; Lee, S.; Choi, H. H.; Noh, J.-S.; Lee, W. Detection of a Nerve Agent Simulant Using Single-Walled Carbon Nanotube Networks: Dimethyl-Methyl-Phosphonate. *Nanotechnology* **2010**, *21*, 495501.

(82) Maiti, A.; Ricca, A. Metal-Nanotube Interactions - Binding Energies and Wetting Properties. *Chem. Phys. Lett.* **2004**, *395*, 7–11.

(83) Zhu, W.; Kaxiras, E. The Nature of Contact between Pd Leads and Semiconducting Carbon Nanotubes. *Nano Lett.* **2006**, *6*, 1415–1419.

(84) Zhang, M.; Brooks, L. L.; Chartuprayoon, N.; Bosze, W.; Choa, Y. H.; Myung, N. V. Palladium/Single-Walled Carbon Nanotube Back-to-Back Schottky Contact-Based Hydrogen Sensors and Their Sensing Mechanism. *ACS Appl. Mater. Interfaces* **2014**, *6*, 319–326.

(85) Karousis, N.; Tagmatarchis, N.; Tasis, D. Current Progress on the Chemical Modification of Carbon Nanotubes. *Chem. Rev.* **2010**, *110*, 5366–5397.

(86) Wei, L.; Lu, D.; Wang, J.; Wei, H.; Zhao, J.; Geng, H.; Zhang, Y. Highly Sensitive Detection of Trinitrotoluene in Water by Chemiresistive Sensor Based on Noncovalently Amino Functionalized Single-Walled Carbon Nanotube. *Sens. Actuators, B* **2014**, *190*, 529–534.

(87) Zhao, Y.-L.; Hu, L.; Stoddart, J. F.; Gruner, G. Pyrenecyclodextrin-Decorated Single-Walled Carbon Nanotube Field-Effect Transistors as Chemical Sensors. *Adv. Mater.* **2008**, *20*, 1910–1915.

(88) Lerner, M. B.; Kybert, N.; Mendoza, R.; Villechenon, R.; Bonilla Lopez, M. A.; Charlie Johnson, A. T. Scalable, Non-Invasive Glucose Sensor Based on Boronic Acid Functionalized Carbon Nanotube Transistors. *Appl. Phys. Lett.* **2013**, *102*, 183113.

(89) Frazier, K. M.; Swager, T. M. Robust Cyclohexanone Selective Chemiresistors Based on Single-Walled Carbon Nanotubes. *Anal. Chem.* **2013**, *85*, 7154–7158.

(90) Zhu, R.; Azzarelli, J. M.; Swager, T. M. Wireless Hazard Badges to Detect Nerve-Agent Simulants. *Angew. Chem., Int. Ed.* **2016**, *55*, 9662–9666.

(91) Weis, J. G.; Ravnsbæk, J. B.; Mirica, K. A.; Swager, T. M. Employing Halogen Bonding Interactions in Chemiresistive Gas Sensors. *ACS Sensors* **2016**, *1*, 115–119.

(92) Im, J.; Sterner, E.; Swager, T. Integrated Gas Sensing System of SWCNT and Cellulose Polymer Concentrator for Benzene, Toluene, and Xylenes. *Sensors* **2016**, *16*, 183.

(93) Liu, S. F.; Petty, A. R.; Sazama, G. T.; Swager, T. M. Single-Walled Carbon Nanotube/Metalloporphyrin Composites for the Chemiresistive Detection of Amines and Meat Spoilage. *Angew. Chem., Int. Ed.* **2015**, *54*, 6554–6557.

(94) Liu, S. F.; Lin, S.; Swager, T. M. An Organocobalt-Carbon Nanotube Chemiresistive Carbon Monoxide Detector. *ACS Sensors* **2016**, *1*, 354–357.

(95) Lin, S.; Swager, T. M. Carbon Nanotube Formic Acid Sensors Using a Nickel Bis(Ortho -Diiminosemiquinonate) Selector. *ACS Sensors* **2018**, *3*, 569–573.

(96) Esser, B.; Schnorr, J. M.; Swager, T. M. Selective Detection of Ethylene Gas Using Carbon Nanotube-Based Devices: Utility in Determination of Fruit Ripeness. *Angew. Chem., Int. Ed.* **2012**, *51*, 5752–5756.

(97) Wang, F.; Yang, Y.; Swager, T. M. Molecular Recognition for High Selectivity in Carbon Nanotube/Polythiophene Chemiresistors. *Angew. Chem., Int. Ed.* **2008**, *47*, 8394–8396.

(98) Zheng, M.; Jagota, A.; Semke, E. D.; Diner, B. A.; McLean, R. S.; Lustig, S. R.; Richardson, R. E.; Tassi, N. G. DNA-Assisted Dispersion and Separation of Carbon Nanotubes. *Nat. Mater.* **2003**, *2*, 338–342.

(99) Star, A.; Joshi, V.; Han, T. R.; Altoé, M. V. P.; Grüner, G.; Stoddart, J. F. Electronic Detection of the Enzymatic Degradation of Starch. *Org. Lett.* **2004**, *6*, 2089–2092.

(100) Star, A.; Steuerman, D. W.; Heath, J. R.; Stoddart, J. F. Starched Carbon Nanotubes. *Angew. Chem., Int. Ed.* **2002**, *41*, 2508–2512.

(101) Cella, L. N.; Chen, W.; Myung, N. V.; Mulchandani, A. Single-Walled Carbon Nanotube-Based Chemiresistive Affinity Biosensors for Small Molecules: Ultrasensitive Glucose Detection. *J. Am. Chem. Soc.* **2010**, *132*, 5024–5026.

(102) Zhang, M.; Gorski, W. Electrochemical Sensing Platform Based on the Carbon Nanotubes/Redox Mediators-Biopolymer System. *J. Am. Chem. Soc.* **2005**, *127*, 2058–2059.

(103) Star, A.; Liu, Y.; Grant, K.; Ridvan, L.; Stoddart, J. F.; Steuerman, D. W.; Diehl, M. R.; Boukai, A.; Heath, J. R. Noncovalent Side-Wall Functionalization of Single-Walled Carbon Nanotubes. *Macromolecules* **2003**, *36*, 553–560.

(104) Tang, B. Z.; Xu, H. Preparation, Alignment, and Optical Properties of Soluble Poly(Phenylacetylene)-Wrapped Carbon Nanotubes. *Macromolecules* **1999**, *32*, 2569–2576.

(105) Steuerman, D. W.; Star, A.; Narizzano, R.; Choi, H.; Ries, R. S.; Nicolini, C.; Stoddart, J. F.; Heath, J. R. Interactions between Conjugated Polymers and Single-Walled Carbon Nanotubes. *J. Phys. Chem. B* **2002**, *106*, 3124–3130.

(106) Fennell, J.; Hamaguchi, H.; Yoon, B.; Swager, T. Chemiresistor Devices for Chemical Warfare Agent Detection Based on Polymer Wrapped Single-Walled Carbon Nanotubes. *Sensors* **2017**, *17*, 982.

(107) Ishihara, S.; Azzarelli, J. M.; Krikorian, M.; Swager, T. M. Ultratrace Detection of Toxic Chemicals: Triggered Disassembly of Supramolecular Nanotube Wrappers. *J. Am. Chem. Soc.* **2016**, *138*, 8221–8227.

(108) Chen, R. J.; Bangsaruntip, S.; Drouvalakis, K. A.; Wong Shi Kam, N.; Shim, M.; Li, Y.; Kim, W.; Utz, P. J.; Dai, H. Noncovalent Functionalization of Carbon Nanotubes for Highly Specific Electronic Biosensors. *Proc. Natl. Acad. Sci. U. S. A.* **2003**, *100*, 4984–4989.

(109) So, H. M.; Won, K.; Kim, Y. H.; Kim, B. K.; Ryu, B. H.; Na, P. S.; Kim, H.; Lee, J. O. Single-Walled Carbon Nanotube Biosensors Using Aptamers as Molecular Recognition Elements. *J. Am. Chem. Soc.* **2005**, *127*, 11906–11907.

(110) Kong, J.; Chapline, M. G.; Dai, H.; Nanotubes, F. C.; Sensors, M. H. Functionalized Carbon Nanotubes for Molecular Hydrogen Sensors. *Adv. Mater.* **2001**, *13*, 1384–1386.

(111) Sun, Y.; Wang, H. H. High-Performance, Flexible Hydrogen Sensors That Use Carbon Nanotubes Decorated with Palladium Nanoparticles. *Adv. Mater.* **2007**, *19*, 2818–2823.

(112) Mubeen, S.; Zhang, T.; Chartuprayoon, N.; Rheem, Y.; Mulchandani, A.; Myung, N. V.; Deshusses, M. A. Sensitive Detection of H₂S Using Gold Nanoparticle Decorated Single-Walled Carbon Nanotubes. *Anal. Chem.* **2010**, *82*, 250–257.

(113) Lu, G.; Ocola, L. E.; Chen, J. Room-Temperature Gas Sensing Based on Electron Transfer between Discrete Tin Oxide Nanocrystals and Multiwalled Carbon Nanotubes. *Adv. Mater.* **2009**, *21*, 2487–2491.

(114) Mann, J. A.; Rodríguez-López, J.; Abruña, H. D.; Dichtel, W. R. Multivalent Binding Motifs for the Noncovalent Functionalization of Graphene. *J. Am. Chem. Soc.* **2011**, *133*, 17614–17617.

(115) Cao, M.; Fu, A.; Wang, Z.; Liu, J.; Kong, N.; Zong, X.; Liu, H.; Gooding, J. J. Electrochemical and Theoretical Study of Pi-Pi Stacking Interactions between Graphitic Surfaces and Pyrene Derivatives. *J. Phys. Chem. C* **2014**, *118*, 2650–2659.

(116) Huang, J.; Ng, A. L.; Piao, Y.; Chen, C.-F.; Green, A. a.; Sun, C.-F.; Hersam, M. C.; Lee, C. S.; Wang, Y. Covalently Functionalized Double-Walled Carbon Nanotubes Combine High Sensitivity and Selectivity in the Electrical Detection of Small Molecules. *J. Am. Chem. Soc.* **2013**, *135*, 2306–2312.

(117) Wang, F.; Swager, T. M. Diverse Chemiresistors Based upon Covalently Modified Multiwalled Carbon Nanotubes. *J. Am. Chem. Soc.* **2011**, *133*, 11181–11193.

(118) Zhang, W.; Sprafke, J. K.; Ma, M.; Tsui, E. Y.; Sydlik, S. A.; Rutledge, G. C.; Swager, T. M. Modular Functionalization of Carbon Nanotubes and Fullerenes. *J. Am. Chem. Soc.* **2009**, *131*, 8446–8454.

(119) Zhang, W.; Swager, T. M. Functionalization of Single-Walled Carbon Nanotubes and Fullerenes via a Dimethyl Acetylenedicarboxylate-4-Dimethylaminopyridine Zwitterion Approach. *J. Am. Chem. Soc.* **2007**, *129*, 7714–7715.

(120) Weizmann, Y.; Chenoweth, D. M.; Swager, T. M. DNA-CNT Nanowire Networks for DNA Detection. *J. Am. Chem. Soc.* **2011**, *133*, 3238–3241.

(121) Setaro, A.; Adeli, M.; Glaeske, M.; Przyrembel, D.; Bisswanger, T.; Gordeev, G.; Maschietto, F.; Faghani, A.; Paulus, B.; Weinelt, M.; et al. Preserving π -Conjugation in Covalently Functionalized Carbon Nanotubes for Optoelectronic Applications. *Nat. Commun.* **2017**, *8*, 14281.

(122) Schnorr, J. M.; van der Zwaag, D.; Walish, J. J.; Weizmann, Y.; Swager, T. M. Sensory Arrays of Covalently Functionalized Single-Walled Carbon Nanotubes for Explosive Detection. *Adv. Funct. Mater.* **2013**, *23*, 5285–5291.

(123) Gao, C.; He, H.; Zhou, L.; Zheng, X.; Zhang, Y. Scalable Functional Group Engineering of Carbon Nanotubes by Improved One-Step. *Nitrene Chem.* **2009**, *1*, 360–370.

(124) Dionisio, M.; Schnorr, J. M.; Michaelis, V. K.; Griffin, R. G.; Swager, T. M.; Dalcanale, E. Cavitand-Functionalized SWCNTs for N-Methylammonium Detection. *J. Am. Chem. Soc.* **2012**, *134*, 6540–6543.

(125) Paoletti, C.; He, M.; Salvo, P.; Melai, B.; Calisi, N.; Mannini, M.; Cortigiani, B.; Bellagambi, F. G.; Swager, T. M.; Di Francesco, F.; et al. Room Temperature Amine Sensors Enabled by Sidewall Functionalization of Single-Walled Carbon Nanotubes. *RSC Adv.* **2018**, *8*, 5578–5585.

(126) He, M.; Swager, T. M. Covalent Functionalization of Carbon Nanomaterials with Iodonium Salts. *Chem. Mater.* **2016**, *28*, 8542–8549.

(127) Savagatrup, S.; Schroeder, V.; He, X.; Lin, S.; He, M.; Yassine, O.; Salama, K. N.; Zhang, X.-X.; Swager, T. M. Bio-Inspired Carbon Monoxide Sensors with Voltage-Activated Sensitivity. *Angew. Chem., Int. Ed.* **2017**, *S6*, 14066–14070.

(128) Lerner, M. B.; Dailey, J.; Goldsmith, B. R.; Brisson, D.; Charlie Johnson, A. T. Detecting Lyme Disease Using Antibody-Functionalized Single-Walled Carbon Nanotube Transistors. *Biosens. Bioelectron.* **2013**, *45*, 163–167.

(129) Lerner, M. B.; D'Souza, J.; Pazina, T.; Dailey, J.; Goldsmith, B. R.; Robinson, M. K.; Johnson, A. T. C. Hybrids of a Genetically Engineered Antibody and a Carbon Nanotube Transistor for Detection of Prostate Cancer Biomarkers. *ACS Nano* **2012**, *6*, 5143–5149.

(130) Eder, D. Carbon Nanotube - Inorganic Hybrids. *Chem. Rev.* **2010**, *110*, 1348–1385.

(131) Cargnello, M.; Grzelczak, M.; Rodriguez-Gonzalez, B.; Syrgiannis, Z.; Bakhmutsky, K.; La Parola, V.; Liz-Marzán, L. M.; Gorte, R. J.; Prato, M.; Fornasiero, P. Multiwalled Carbon Nanotubes Drive the Activity of Metal@oxide Core-Shell Catalysts in Modular Nanocomposites. *J. Am. Chem. Soc.* **2012**, *134*, 11760–11766.

(132) Liang, Y. X.; Chen, Y. J.; Wang, J. H. Low-Resistance Gas Sensors Fabricated from Multiwalled Carbon Nanotubes Coated with a Thin Tin Oxide Layer. *Appl. Phys. Lett.* **2004**, *85*, 666–668.

(133) Chen, Y.; Zhu, C.; Wang, T. The Enhanced Ethanol Sensing Properties of Multi-Walled Carbon Nanotubes/SnO₂ Core/Shell Nanostructures. *Nanotechnology* **2006**, *17*, 3012–3017.

(134) Vinoth, V.; Wu, J. J.; Asiri, A. M.; Anandan, S. Simultaneous Detection of Dopamine and Ascorbic Acid Using Silicate Network Interlinked Gold Nanoparticles and Multi-Walled Carbon Nanotubes. *Sens. Actuators, B* **2015**, *210*, 731–741.

(135) Ragupathy, D.; Gopalan, A. I.; Lee, K. P. Electrocatalytic Oxidation and Determination of Ascorbic Acid in the Presence of Dopamine at Multiwalled Carbon Nanotube-Silica Network-Gold Nanoparticles Based Nanohybrid Modified Electrode. *Sens. Actuators, B* **2010**, *143*, 696–703.

(136) Ding, M.; Sorescu, D. C.; Star, A. Photoinduced Charge Transfer and Acetone Sensitivity of Single-Walled Carbon Nanotube-Titanium Dioxide Hybrids. *J. Am. Chem. Soc.* **2013**, *135*, 9015–9022.

(137) Ellis, J. E.; Green, U.; Sorescu, D. C.; Zhao, Y.; Star, A. Indium Oxide-Single-Walled Carbon Nanotube Composite for Ethanol Sensing at Room Temperature. *J. Phys. Chem. Lett.* **2015**, *6*, 712–717.

(138) Peng, G.; Wu, S.; Ellis, J. E.; Xu, X.; Xu, G.; Yu, C.; Star, A. Single-Walled Carbon Nanotubes Templatized CuO Networks for Gas Sensing. *J. Mater. Chem. C* **2016**, *4*, 6575–6580.

(139) Zhao, B.; Hu, H.; Haddon, R. C. Synthesis and Properties of a Water-Soluble Single-Walled Carbon Nanotube–Poly(m-Aminobenzene Sulfonic Acid) Graft Copolymer. *Adv. Funct. Mater.* **2004**, *14*, 71–76.

(140) Bekyarova, E.; Davis, M.; Burch, T.; Itkis, M. E.; Zhao, B.; Sunshine, S.; Haddon, R. C. Chemically Functionalized Single-Walled Carbon Nanotubes as Ammonia Sensors. *J. Phys. Chem. B* **2004**, *108*, 19717–19720.

(141) Zhang, T.; Mubeen, S.; Bekyarova, E.; Yoo, B. Y.; Haddon, R. C.; Myung, N. V.; Deshusses, M. A. Poly(m-Aminobenzene Sulfonic Acid) Functionalized Single-Walled Carbon Nanotubes Based Gas Sensor. *Nanotechnology* **2007**, *18*, 165504.

(142) Bekyarova, E.; Kalinina, I.; Sun, X.; Shastry, T.; Worsley, K.; Chi, X.; Itkis, M. E.; Haddon, R. C. Chemically Engineered Single-Walled Carbon Nanotube Materials for the Electronic Detection of Hydrogen Chloride. *Adv. Mater.* **2010**, *22*, 848–852.

(143) Guo, X.; Small, J. P.; Klare, J. E.; Wang, Y.; Purewal, M. S.; Tam, I. W.; Hong, B. H.; Caldwell, R.; Huang, L.; O'Brien, S.; et al. Covalently Bridging Gaps in Single-Walled Carbon Nanotubes with Conducting Molecules. *Science* **2006**, *311*, 356–359.

(144) Guo, X.; Gorodetsky, A. A.; Hone, J.; Barton, J. K.; Nuckolls, C. Conductivity of a Single DNA Duplex Bridging a Carbon Nanotube Gap. *Nat. Nanotechnol.* **2008**, *3*, 163–167.

(145) Weizmann, Y.; Chenoweth, D. M.; Swager, T. M. Addressable Terminaly Linked DNA-CNT Nanowires. *J. Am. Chem. Soc.* **2010**, *132*, 14009–14011.

(146) Weizmann, Y.; Lim, J.; Chenoweth, D. M.; Swager, T. M. Regiospecific Synthesis of Au-Nanorod/SWCNT/Au-Nanorod Heterojunctions. *Nano Lett.* **2010**, *10*, 2466–2469.

(147) Wilson, N. R.; Macpherson, J. V. Carbon Nanotube Tips for Atomic Force Microscopy. *Nat. Nanotechnol.* **2009**, *4*, 483–491.

(148) Dai, H.; Hafner, J. H.; Rinzler, A. G.; Colbert, D. T.; Smalley, R. E. Nanotubes as Nanoprobes in Scanning Probe Microscopy. *Nature* **1996**, *384*, 147–150.

(149) Jariwala, D.; Sangwan, V. K.; Lauhon, L. J.; Marks, T. J.; Hersam, M. C. Carbon Nanomaterials for Electronics, Optoelectronics, Photovoltaics, and Sensing. *Chem. Soc. Rev.* **2013**, *42*, 2824–2860.

(150) Goldsmith, B. R.; Coroneus, J. G.; Kane, A. A.; Weiss, G. A.; Collins, P. G. Monitoring Single-Molecule Reactivity on a Carbon Nanotube. *Nano Lett.* **2008**, *8*, 189–194.

(151) Sorgenfrei, S.; Chiu, C.; Gonzalez, R. L.; Yu, Y.-J.; Kim, P.; Nuckolls, C.; Shepard, K. L. Label-Free Single-Molecule Detection of DNA-Hybridization Kinetics with a Carbon Nanotube Field-Effect Transistor. *Nat. Nanotechnol.* **2011**, *6*, 126–132.

(152) Vernick, S.; Trocchia, S. M.; Warren, S. B.; Young, E. F.; Bouilly, D.; Gonzalez, R. L.; Nuckolls, C.; Shepard, K. L. Electrostatic Melting in a Single-Molecule Field-Effect Transistor with Applications in Genomic Identification. *Nat. Commun.* **2017**, *8*, 15450.

(153) Shim, S.-B.; Imboden, M.; Mohanty, P. Synchronized Oscillation in Coupled Nanomechanical Oscillators. *Science* **2007**, *316*, 95–99.

(154) Chaste, J.; Eichler, A.; Moser, J.; Ceballos, G.; Rurali, R.; Bachtold, A. A Nanomechanical Mass Sensor with Yoctogram Resolution. *Nat. Nanotechnol.* **2012**, *7*, 301–304.

(155) Lee, C. Y.; Choi, W.; Han, J.-H.; Strano, M. S. Coherence Resonance in a Single-Walled Carbon Nanotube Ion Channel. *Science* **2010**, *329*, 1320–1324.

(156) Peng, R.; Tang, X. S.; Li, D. Detection of Individual Molecules and Ions by Carbon Nanotube-Based Differential Resistive Pulse Sensor. *Small* **2018**, *14*, 1800013.

(157) Feldman, A. K.; Steigerwald, M. L.; Guo, X.; Nuckolls, C. Molecular Electronic Devices Based on Single-Walled Carbon Nanotube Electrodes. *Acc. Chem. Res.* **2008**, *41*, 1731–1741.

(158) Gao, X. P. A.; Zheng, G.; Lieber, C. M. Subthreshold Regime Has the Optimal Sensitivity for Nanowire FET Biosensors. *Nano Lett.* **2010**, *10*, 547–552.

(159) Ishikawa, F. N.; Curreli, M.; Olson, C. A.; Liao, H.-I.; Sun, R.; Roberts, R. W.; Cote, R. J.; Thompson, M. E.; Zhou, C. Importance of Controlling Nanotube Density for Highly Sensitive and Reliable Biosensors Functional in Physiological Conditions. *ACS Nano* **2010**, *4*, 6914–6922.

(160) Okuda, S.; Okamoto, S.; Ohno, Y.; Maehashi, K.; Inoue, K.; Matsumoto, K. Horizontally Aligned Carbon Nanotubes on a Quartz Substrate for Chemical and Biological Sensing. *J. Phys. Chem. C* **2012**, *116*, 19490–19495.

(161) Abe, M.; Murata, K.; Ataka, T.; Matsumoto, K. Comparison of Sensitivities of Carbon Nanotube Field-Effect Transistor Biosensors with and without Top Metal Gate. *J. Appl. Phys.* **2008**, *104*, 104304.

(162) Shulaker, M. M.; Hills, G.; Park, R. S.; Howe, R. T.; Saraswat, K.; Wong, H.-S. P.; Mitra, S. Three-Dimensional Integration of Nanotechnologies for Computing and Data Storage on a Single Chip. *Nature* **2017**, *547*, 74–78.

(163) Wu, J.; Antaris, A.; Gong, M.; Dai, H. Top-Down Patterning and Self-Assembly for Regular Arrays of Semiconducting Single-Walled Carbon Nanotubes. *Adv. Mater.* **2014**, *26*, 6151–6156.

(164) Li, X.; Zhang, L.; Wang, X.; Shimoyama, I.; Sun, X.; Seo, W. K.; Dai, H. Langmuir-Blodgett Assembly of Densely Aligned Single-Walled Carbon Nanotubes from Bulk Materials. *J. Am. Chem. Soc.* **2007**, *129*, 4890–4891.

(165) Brady, G. J.; Jenkins, K. R.; Arnold, M. S. Channel Length Scaling Behavior in Transistors Based on Individual versus Dense Arrays of Carbon Nanotubes. *J. Appl. Phys.* **2017**, *122*, 124506.

(166) Lin, C.-T.; Lee, C.-Y.; Chin, T.-S.; Xiang, R.; Ishikawa, K.; Shiomi, J.; Maruyama, S. Anisotropic Electrical Conduction of Vertically-Aligned Single-Walled Carbon Nanotube Films. *Carbon* **2011**, *49*, 1446–1452.

(167) Cao, Q.; Rogers, J. A. Random Networks and Aligned Arrays of Single-Walled Carbon Nanotubes for Electronic Device Applications. *Nano Res.* **2008**, *1*, 259–272.

(168) Li, P.; Xue, W. Selective Deposition and Alignment of Single-Walled Carbon Nanotubes Assisted by Dielectrophoresis: From Thin Films to Individual Nanotubes. *Nanoscale Res. Lett.* **2010**, *5*, 1072–1078.

(169) Biswas, C.; Lee, S. Y.; Ly, T. H.; Ghosh, A.; Dang, Q. N.; Lee, Y. H. Chemically Doped Random Network Carbon Nanotube P–n Junction Diode for Rectifier. *ACS Nano* **2011**, *5*, 9817–9823.

(170) Kong, J.; Soh, H. T.; Cassell, A. M.; Quate, C. F.; Dai, H. Synthesis of Individual Single-Walled Carbon Nanotubes on Patterned Silicon Wafers. *Nature* **1998**, *395*, 878–881.

(171) Silva, G. O.; Michael, Z. P.; Bian, L.; Shurin, G. V.; Mulato, M.; Shurin, M. R.; Star, A. Nanoelectronic Discrimination of Nonmalignant and Malignant Cells Using Nanotube Field-Effect Transistors. *ACS Sensors* **2017**, *2*, 1128–1132.

(172) Abe, M.; Murata, K.; Kojima, A.; Ifuku, Y.; Shimizu, M.; Ataka, T.; Matsumoto, K. Quantitative Detection of Protein Using a Top-Gate Carbon Nanotube Field Effect Transistor. *J. Phys. Chem. C* **2007**, *111*, 8667–8670.

(173) White, H. S.; Kittlesen, G. P.; Wrighton, M. S. Chemical Derivatization of an Array of Three Gold Microelectrodes with Polypyrrole: Fabrication of a Molecule-Based Transistor. *J. Am. Chem. Soc.* **1984**, *106*, 5375–5377.

(174) Yanagi, K.; Kanda, S.; Oshima, Y.; Kitamura, Y.; Kawai, H.; Yamamoto, T.; Takenobu, T.; Nakai, Y.; Maniwa, Y. Tuning of the Thermoelectric Properties of One-Dimensional Material Networks by Electric Double Layer Techniques Using Ionic Liquids. *Nano Lett.* **2014**, *14*, 6437–6442.

(175) Bisri, S. Z.; Shimizu, S.; Nakano, M.; Iwasa, Y. Endeavor of Iontronics: From Fundamentals to Applications of Ion-Controlled Electronics. *Adv. Mater.* **2017**, *29*, 1607054.

(176) Du, H.; Lin, X.; Xu, Z.; Chu, D. Electric Double-Layer Transistors: A Review of Recent Progress. *J. Mater. Sci.* **2015**, *50*, 5641–5673.

(177) Son, B. H.; Park, J.-Y.; Lee, S.; Ahn, Y. H. Suspended Single-Walled Carbon Nanotube Fluidic Sensors. *Nanoscale* **2015**, *7*, 15421–15426.

(178) Rosenblatt, S.; Yaish, Y.; Park, J.; Gore, J.; Sazonova, V.; McEuen, P. L. High Performance Electrolyte Gated Carbon Nanotube Transistors. *Nano Lett.* **2002**, *2*, 869–872.

(179) Lu, C.; Fu, Q.; Huang, S.; Liu, J. Polymer Electrolyte-Gated Carbon Nanotube Field-Effect Transistor. *Nano Lett.* **2004**, *4*, 623–627.

(180) Qi, P.; Javey, A.; Rolandi, M.; Wang, Q.; Yenilmez, E.; Dai, H. Miniature Organic Transistors with Carbon Nanotubes as Quasi-One-Dimensional Electrodes. *J. Am. Chem. Soc.* **2004**, *126*, 11774–11775.

(181) He, Y.; Zhang, J.; Zhao, J. Electron Transport and CO Sensing Characteristics of Fe(II) Porphyrin with Single-Walled Carbon Nanotube Electrodes. *J. Phys. Chem. C* **2014**, *118*, 18325–18333.

(182) Soylemez, S.; Yoon, B.; Toppare, L.; Swager, T. M. Quaternized Polymer–Single-Walled Carbon Nanotube Scaffolds for a Chemiresistive Glucose Sensor. *ACS Sensors* **2017**, *2*, 1123–1127.

(183) Dionisio, M.; Schnorr, J. M.; Michaelis, V. K.; Griffin, R. G.; Swager, T. M.; Dalcanale, E. Cavitand-Functionalized SWCNTs for N-Methylammonium Detection. *J. Am. Chem. Soc.* **2012**, *134*, 6540–6543.

(184) Chen, Y.; Mun, S. C.; Kim, J. A Wide Range Conductometric PH Sensor Made With Titanium Dioxide/Multiwall Carbon Nanotube/Cellulose Hybrid Nanocomposite. *IEEE Sens. J.* **2013**, *13*, 4157–4162.

(185) Kwon, J.-H.; Lee, K.-S.; Lee, Y.-H.; Ju, B.-K. Single-Wall Carbon Nanotube-Based PH Sensor Fabricated by the Spray Method. *Electrochem. Solid-State Lett.* **2006**, *9*, H85.

(186) Tang, R.; Shi, Y.; Hou, Z.; Wei, L. Carbon Nanotube-Based Chemiresistive Sensors. *Sensors* **2017**, *17*, 882.

(187) Mirica, K. A.; Azzarelli, J. M.; Weis, J. G.; Schnorr, J. M.; Swager, T. M. Rapid Prototyping of Carbon-Based Chemiresistive Gas Sensors on Paper. *Proc. Natl. Acad. Sci. U. S. A.* **2013**, *110*, E3265–E3270.

(188) Azzarelli, J. M.; Mirica, K. A.; Ravnsbæk, J. B.; Swager, T. M. Wireless Gas Detection with a Smartphone via RF Communication. *Proc. Natl. Acad. Sci. U. S. A.* **2014**, *111*, 18162–18166.

(189) Zhu, R.; Desroches, M.; Yoon, B.; Swager, T. M. Wireless Oxygen Sensors Enabled by Fe(II)-Polymer Wrapped Carbon Nanotubes. *ACS Sensors* **2017**, *2*, 1044–1050.

(190) Vieira, S. M. C.; Beecher, P.; Haneef, I.; Udrea, F.; Milne, W. I.; Namboothiry, M. A. G.; Carroll, D. L.; Park, J.; Maeng, S. Use of Nanocomposites to Increase Electrical “Gain” in Chemical Sensors. *Appl. Phys. Lett.* **2007**, *91*, 203111.

(191) Wong, Y. M.; Kang, W. P.; Davidson, J. L.; Wisitsora-At, A.; Soh, K. L. A Novel Microelectronic Gas Sensor Utilizing Carbon Nanotubes for Hydrogen Gas Detection. *Sens. Actuators, B* **2003**, *93*, 327–332.

(192) Lim, H.; Song, H. J.; Lee, Y.; Shin, H. J.; Choi, H. C. Carbon Nanotube Schottky Diode via Selective Electrochemical Metal Deposition. *Langmuir* **2010**, *26*, 1464–1467.

(193) Lim, H.; Shin, H. S.; Shin, H. J.; Choi, H. C. Lithium Ions Intercalated into Pyrene-Functionalized Carbon Nanotubes and Their Mass Transport: A Chemical Route to Carbon Nanotube Schottky Diode. *J. Am. Chem. Soc.* **2008**, *130*, 2160–2161.

(194) Zhou, Y.; Gaur, A.; Hur, S. H.; Kocabas, C.; Meitl, M. A.; Shim, M.; Rogers, J. A. P-Channel, n-Channel Thin Film Transistors and p-n Diodes Based on Single Wall Carbon Nanotube Networks. *Nano Lett.* **2004**, *4*, 2031–2035.

(195) Zhou, C.; Kong, J.; Yenilmez, E.; Dai, H. Modulated Chemical Doping of Individual Carbon Nanotubes. *Science* **2000**, *290*, 1552–1555.

(196) Ilani, S.; Donev, L. A. K.; Kindermann, M.; McEuen, P. L. Measurement of the Quantum Capacitance of Interacting Electrons in Carbon Nanotubes. *Nat. Phys.* **2006**, *2*, 687–691.

(197) Liu, Z.; Li, J.; Qiu, Z.-J.; Zhang, Z.-B.; Zheng, L.-R.; Zhang, S.-L. On Gate Capacitance of Nanotube Networks. *IEEE Electron Device Lett.* **2011**, *32*, 641–643.

(198) Kiriya, D.; Chen, K.; Ota, H.; Lin, Y.; Zhao, P.; Yu, Z.; Ha, T.; Javey, A. Design of Surfactant–Substrate Interactions for Roll-to-Roll Assembly of Carbon Nanotubes for Thin-Film Transistors. *J. Am. Chem. Soc.* **2014**, *136*, 11188–11194.

(199) Snow, E. S.; Perkins, F. K.; Houser, E. J.; Badescu, S. C.; Reinecke, T. L. Chemical Detection with a Single-Walled Carbon Nanotube Capacitor. *Science* **2005**, *307*, 1942–1945.

(200) Snow, E. S.; Perkins, F. K.; Robinson, J. A. Chemical Vapor Detection Using Single-Walled Carbon Nanotubes. *Chem. Soc. Rev.* **2006**, *35*, 790–798.

(201) Esen, G.; Fuhrer, M. S.; Ishigami, M.; Williams, E. D. Transmission Line Impedance of Carbon Nanotube Thin Films for Chemical Sensing. *Appl. Phys. Lett.* **2007**, *90*, 123510.

(202) Suehiro, J.; Zhou, G.; Hara, M. Fabrication of a Carbon Nanotube-Based Gas Sensor Using Dielectrophoresis and Its Application for Ammonia Detection by Impedance Spectroscopy. *J. Phys. D: Appl. Phys.* **2003**, *36*, L109–L114.

(203) Varghese, O. K.; Kichambre, P. D.; Gong, D.; Ong, K. G.; Dickey, E. C.; Grimes, C. A. Gas Sensing Characteristics of Multi-Wall Carbon Nanotubes. *Sens. Actuators, B* **2001**, *81*, 32–41.

(204) Zhu, Z. An Overview of Carbon Nanotubes and Graphene for Biosensing Applications. *Nano-Micro Letters*; Springer Berlin Heidelberg, 2017; p 25.

(205) Li, C. A.; Han, K. N.; Pham, X.-H.; Seong, G. H. A Single-Walled Carbon Nanotube Thin Film-Based PH-Sensing Microfluidic Chip. *Analyst* **2014**, *139*, 2011–2015.

(206) Gou, P.; Kraut, N. D.; Feigel, I. M.; Bai, H.; Morgan, G. J.; Chen, Y.; Tang, Y.; Bocan, K.; Stachel, J.; Berger, L.; et al. Carbon Nanotube Chemiresistor for Wireless PH Sensing. *Sci. Rep.* **2015**, *4*, 4468.

(207) Kaempgen, M.; Roth, S. Transparent and Flexible Carbon Nanotube/Polyaniline PH Sensors. *J. Electroanal. Chem.* **2006**, *586*, 72–76.

(208) Hung, S.-C.; Cheng, N.-J.; Yang, C.-F.; Lo, Y.-P. Investigation of Extended-Gate Field-Effect Transistor PH Sensors Based on Different-Temperature-Annealed Bi-Layer MWCNTs-In2O3 Films. *Nanoscale Res. Lett.* **2014**, *9*, 502.

(209) Matsui, Y.; Hoshino, T.; Yoshizawa, M.; Muguruma, H. NADH Sensing Using a Carbon Nanotube Electrode Reinforced with a Plasma-Polymerized Thin Film. *Electrochemistry* **2008**, *76*, 610–613.

(210) Qu, F.; Yang, M.; Jiang, J.; Shen, G.; Yu, R. Amperometric Biosensor for Chlorine Based on Layer-by-Layer Assembled Functionalized Carbon Nanotube and Polyaniline Multilayer Film. *Anal. Biochem.* **2005**, *344*, 108–114.

(211) Wanekaya, A. K. Applications of Nanoscale Carbon-Based Materials in Heavy Metal Sensing and Detection. *Analyst* **2011**, *136*, 4383–4391.

(212) Wang, L.; Wang, X.; Shi, G.; Peng, C.; Ding, Y. Thiocalixarene Covalently Functionalized Multiwalled Carbon Nanotubes as Chemically Modified Electrode Material for Detection of Ultratrace Pb²⁺ Ions. *Anal. Chem.* **2012**, *84*, 10560–10567.

(213) Song, W.; Pang, P.; He, J.; Lindsay, S. Optical and Electrical Detection of Single-Molecule Translocation through Carbon Nanotubes. *ACS Nano* **2013**, *7*, 689–694.

(214) Cao, D.; Pang, P.; Liu, H.; He, J.; Lindsay, S. M. Electronic Sensitivity of a Single-Walled Carbon Nanotube to Internal Electrolyte Composition. *Nanotechnology* **2012**, *23*, 085203.

(215) Chopra, S.; McGuire, K.; Gothard, N.; Rao, A. M.; Pham, A. Selective Gas Detection Using a Carbon Nanotube Sensor. *Appl. Phys. Lett.* **2003**, *83*, 2280–2282.

(216) Picaud, F.; Langlet, R.; Arab, M.; Devel, M.; Girardet, C.; Natarajan, S.; Chopra, S.; Rao, A. M. Gas-Induced Variation in the

Dielectric Properties of Carbon Nanotube Bundles for Selective Sensing. *J. Appl. Phys.* **2005**, *97*, 114316.

(217) Penza, M.; Cassano, G.; Aversa, P.; Antolini, F.; Cusano, A.; Cutolo, A.; Giordano, M.; Nicolais, L. Alcohol Detection Using Carbon Nanotubes Acoustic and Optical Sensors. *Appl. Phys. Lett.* **2004**, *85*, 2379–2381.

(218) Sazonova, V.; Yaish, Y.; Üstünel, H.; Roundy, D.; Arias, T. A.; McEuen, P. L. A Tunable Carbon Nanotube Electromechanical Oscillator. *Nature* **2004**, *431*, 284–287.

(219) Ishihara, S.; Labuta, J.; Nakanishi, T.; Tanaka, T.; Kataura, H. Amperometric Detection of Sub-Ppm Formaldehyde Using Single-Walled Carbon Nanotubes and Hydroxylamines: A Referenced Chemiresistive System. *ACS Sensors* **2017**, *2*, 1405–1409.

(220) Stewart, S.; Ivy, M. A.; Anslyn, E. V. The Use of Principal Component Analysis and Discriminant Analysis in Differential Sensing Routines. *Chem. Soc. Rev.* **2014**, *43*, 70–84.

(221) Collins, P. G.; Arnold, M. S.; Avouris, P. Engineering Carbon Nanotubes and Nanotube Circuits Using Electrical Breakdown. *Science* **2001**, *292*, 706–709.

(222) Seidel, R.; Graham, A. P.; Unger, E.; Duesberg, G. S.; Liebau, M.; Steinhoegl, W.; Kreupl, F.; Hoenlein, W.; Pompe, W. High-Current Nanotube Transistors. *Nano Lett.* **2004**, *4*, 831–834.

(223) Zhang, G.; Qi, P.; Wang, X.; Lu, Y.; Li, X.; Tu, R.; Bangsaruntip, S.; Mann, D.; Zhang, L.; Dai, H. Selective Etching of Metallic Carbon Nanotubes by Gas-Phase Reaction. *Science* **2006**, *314*, 974–977.

(224) Zhao, Q.; Yao, F.; Wang, Z.; Deng, S.; Tong, L.; Liu, K.; Zhang, J. Real-Time Observation of Carbon Nanotube Etching Process Using Polarized Optical Microscope. *Adv. Mater.* **2017**, *29*, 1701959.

(225) Zhang, Y.; Zhang, Y.; Xian, X.; Zhang, J.; Liu, Z. Sorting out Semiconducting Single-Walled Carbon Nanotube Arrays by Preferential Destruction of Metallic Tubes Using Xenon-Lamp Irradiation. *J. Phys. Chem. C* **2008**, *112*, 3849–3856.

(226) Zhou, X.; Boey, F.; Zhang, H. Controlled Growth of Single-Walled Carbon Nanotubes on Patterned Substrates. *Chem. Soc. Rev.* **2011**, *40*, 5221–5231.

(227) Komatsu, N.; Wang, F. A Comprehensive Review on Separation Methods and Techniques for Single-Walled Carbon Nanotubes. *Materials* **2010**, *3*, 3818–3844.

(228) Lei, T.; Pochorovski, I.; Bao, Z. Separation of Semiconducting Carbon Nanotubes for Flexible and Stretchable Electronics Using Polymer Removable Method. *Acc. Chem. Res.* **2017**, *50*, 1096–1104.

(229) Chen, T.; Wei, L.; Zhou, Z.; Shi, D.; Wang, J.; Zhao, J.; Yu, Y.; Wang, Y.; Zhang, Y. Highly Enhanced Gas Sensing in Single-Walled Carbon Nanotube-Based Thin-Film Transistor Sensors by Ultraviolet Light Irradiation. *Nanoscale Res. Lett.* **2012**, *7*, 644.

(230) Tans, S. J.; Verschueren, A. R. M.; Dekker, C. Room-Temperature Transistor Based on a Single Carbon Nanotube. *Nature* **1998**, *393*, 49–52.

(231) Mann, D.; Javey, A.; Kong, J.; Wang, Q.; Dai, H. Ballistic Transport in Metallic Nanotubes with Reliable Pd Ohmic Contacts. *Nano Lett.* **2003**, *3*, 1541–1544.

(232) Frazier, K. M.; Mirica, K. A.; Walish, J. J.; Swager, T. M. Fully-Drawn Carbon-Based Chemical Sensors on Organic and Inorganic Surfaces. *Lab Chip* **2014**, *14*, 4059–4066.

(233) Smith, M. K.; Martin-Peralta, D. G.; Pivak, P. A.; Mirica, K. A. Fabrication of Solid-State Gas Sensors by Drawing: An Undergraduate and High School Introduction to Functional Nanomaterials and Chemical Detection. *J. Chem. Educ.* **2017**, *94*, 1933–1938.

(234) Sekitani, T.; Noguchi, Y.; Hata, K.; Fukushima, T.; Aida, T.; Someya, T. A Rubberlike Stretchable Active Matrix Using Elastic Conductors. *Science* **2008**, *321*, 1468–1472.

(235) Kim, C. B.; Jeong, K. B.; Yang, B. J.; Song, J.-W.; Ku, B.-C.; Lee, S.; Lee, S.-K.; Park, C. Facile Supramolecular Processing of Carbon Nanotubes and Polymers for Electromechanical Sensors. *Angew. Chem., Int. Ed.* **2017**, *56*, 16180–16185.

(236) Schnorr, J. M.; Zentner, C. A.; Petty, A. R.; Swager, T. M. Formulations for Enhanced Chemiresistive Sensing. U.S. Patent 20170212104, July 2016.

(237) Danzer, K.; Currie, L. A. Guidelines for Calibration in Analytical Chemistry. Part I. Fundamentals and Single Component Calibration (IUPAC Recommendations 1998). *Pure Appl. Chem.* **1998**, *70*, 993–1014.

(238) Harris, D. C. *Quantitative Chemical Analysis*; W.H. Freeman and Co.: New York, 2007.

(239) Ammu, S.; Dua, V.; Agnihotra, S. R.; Surwade, S. P.; Phulgirkar, A.; Patel, S.; Manohar, S. K. Flexible, All-Organic Chemiresistor for Detecting Chemically Aggressive Vapors. *J. Am. Chem. Soc.* **2012**, *134*, 4553–4556.

(240) Li, J.; Lu, Y.; Ye, Q.; Cinke, M.; Han, J.; Meyyappan, M. Carbon Nanotube Sensors for Gas and Organic Vapor Detection. *Nano Lett.* **2003**, *3*, 929–933.

(241) Mirica, K. A.; Weis, J. G.; Schnorr, J. M.; Esser, B.; Swager, T. M. Mechanical Drawing of Gas Sensors on Paper. *Angew. Chem., Int. Ed.* **2012**, *51*, 10740–10745.

(242) Torsi, L.; Magliulo, M.; Manoli, K.; Palazzo, G. Organic Field-Effect Transistor Sensors: A Tutorial Review. *Chem. Soc. Rev.* **2013**, *42*, 8612–8628.

(243) Penza, M.; Cassano, G.; Rossi, R.; Rizzo, A.; Signore, M. A.; Alvisi, M.; Lisi, N.; Serra, E.; Giorgi, R. Effect of Growth Catalysts on Gas Sensitivity in Carbon Nanotube Film Based Chemiresistive Sensors. *Appl. Phys. Lett.* **2007**, *90*, 103101.

(244) Wang, S. G.; Zhang, Q.; Yang, D. J.; Sellin, P. J.; Zhong, G. F. Multi-Walled Carbon Nanotube-Based Gas Sensors for NH₃ Detection. *Diamond Relat. Mater.* **2004**, *13*, 1327–1332.

(245) Feng, X.; Irle, S.; Witek, H.; Morokuma, K.; Vidic, R.; Borguet, E. Sensitivity of Ammonia Interaction with Single-Walled Carbon Nanotube Bundles to the Presence of Defect Sites and Functionalities. *J. Am. Chem. Soc.* **2005**, *127*, 10533–10538.

(246) Robinson, J. A.; Snow, E. S.; Bădescu, S. C.; Reinecke, T. L.; Perkins, F. K. Role of Defects in Single-Walled Carbon Nanotube Chemical Sensors. *Nano Lett.* **2006**, *6*, 1747–1751.

(247) Snow, A. W.; Perkins, F. K.; Ancona, M. G.; Robinson, J. T.; Snow, E. S.; Foos, E. E. Disordered Nanomaterials for Chemielectric Vapor Sensing: A Review. *IEEE Sens. J.* **2015**, *15*, 1301–1320.

(248) Fu, D.; Lim, H.; Shi, Y.; Dong, X.; Mhaisalkar, S. G.; Chen, Y.; Moothala, S.; Li, L. Differentiation of Gas Molecules Using Flexible and All-Carbon Nanotube Devices. *J. Phys. Chem. C* **2008**, *112*, 650–653.

(249) Zhao, W.; Fam, D. W. H.; Yin, Z.; Sun, T.; Tan, H. T.; Liu, W.; Tok, A. I. Y.; Boey, Y. C. F.; Zhang, H.; Hng, H. H.; et al. A Carbon Monoxide Gas Sensor Using Oxygen Plasma Modified Carbon Nanotubes. *Nanotechnology* **2012**, *23*, 425502.

(250) Rigoni, F.; Tognolini, S.; Borghetti, P.; Drera, G.; Pagliara, S.; Goldoni, A.; Sangaletti, L. Enhancing the Sensitivity of Chemiresistor Gas Sensors Based on Pristine Carbon Nanotubes to Detect Low-Ppb Ammonia Concentrations in the Environment. *Analyst* **2013**, *138*, 7392–7399.

(251) Quang, N. H.; Van Trinh, M.; Lee, B.-H.; Huh, J.-S. Effect of NH₃ Gas on the Electrical Properties of Single-Walled Carbon Nanotube Bundles. *Sens. Actuators, B* **2006**, *113*, 341–346.

(252) Saito, R.; Fujita, M.; Dresselhaus, G.; Dresselhaus, M. S. Electronic Structure of Chiral Graphene Tubules. *Appl. Phys. Lett.* **1992**, *60*, 2204–2206.

(253) Yang, L.; Han, J. Electronic Structure of Deformed Carbon Nanotubes. *Phys. Rev. Lett.* **2000**, *85*, 154–157.

(254) Berber, S.; Kwon, Y.-K.; Tomanek, D. Unusually High Thermal Conductivity of Carbon Nanotubes. *Phys. Rev. Lett.* **2000**, *84*, 4613–4616.

(255) Lu, J. P. Elastic Properties of Carbon Nanotubes and Nanoropes. *Phys. Rev. Lett.* **1997**, *79*, 1297–1300.

(256) Nardelli, M.; Yakobson, B.; Bernholc, J. Brittle and Ductile Behavior in Carbon Nanotubes. *Phys. Rev. Lett.* **1998**, *81*, 4656–4659.

(257) Yakobson, B. I.; Campbell, M. P.; Brabec, C. J.; Bernholc, J. High Strain Rate Fracture and C-Chain Unraveling in Carbon Nanotubes. *Comput. Mater. Sci.* **1997**, *8*, 341–348.

(258) Iijima, S.; Brabec, C.; Maiti, A.; Bernholc, J. Structural Flexibility of Carbon Nanotubes. *J. Chem. Phys.* **1996**, *104*, 2089–2092.

(259) Overney, G.; Zhong, W.; Tomanek, D. Structural Rigidity and Low-Frequency Vibrational-Modes of Long Carbon Tubules. *Z. Phys. D: At., Mol. Clusters* **1993**, *27*, 93–96.

(260) Bernholc, J.; Brabec, C.; Buongiorno Nardelli, M.; Maiti, a.; Roland, C.; Yakobson, B. I. Theory of Growth and Mechanical Properties of Nanotubes. *Appl. Phys. A: Mater. Sci. Process.* **1998**, *67*, 39–46.

(261) Thostenson, E. T.; Ren, Z.; Chou, T.-W. Advances in the Science and Technology of Carbon Nanotubes and Their Composites: A Review. *Compos. Sci. Technol.* **2001**, *61*, 1899–1912.

(262) Dresselhaus, M. S.; Dresselhaus, G.; Avouris, P. Carbon Nanotubes. *Topics in Applied Physics*; Springer Berlin Heidelberg, 2001; Vol. 80.

(263) Shokrieh, M. M.; Rafiee, R. A Review of the Mechanical Properties of Isolated Carbon Nanotubes and Carbon Nanotube Composites. *Mech. Compos. Mater.* **2010**, *46*, 155–172.

(264) Ruoff, R. S.; Lorents, D. C. Mechanical and Thermal Properties of Carbon Nanotubes. *Carbon* **1995**, *33*, 925–930.

(265) Grimme, S.; Antony, J.; Schwabe, T.; Mück-Lichtenfeld, C. Density Functional Theory with Dispersion Corrections for Supramolecular Structures, Aggregates, and Complexes of (Bio)Organic Molecules. *Org. Biomol. Chem.* **2007**, *5*, 741–758.

(266) Du, A. J.; Smith, S. C. Van Der Waals-Corrected Density Functional Theory: Benchmarking for Hydrogen-Nanotube and Nanotube-Nanotube Interactions. *Nanotechnology* **2005**, *16*, 2118–2123.

(267) Ramirez, J.; Mayo, M. L.; Kilina, S.; Tretiak, S. Electronic Structure and Optical Spectra of Semiconducting Carbon Nanotubes Functionalized by Diazonium Salts. *Chem. Phys.* **2013**, *413*, 89–101.

(268) Demichelis, R.; Noël, Y.; D'Arco, P.; Rérat, M.; Zicovich-Wilson, C. M.; Dovesi, R. Properties of Carbon Nanotubes: An Ab Initio Study Using Large Gaussian Basis Sets and Various DFT Functionals. *J. Phys. Chem. C* **2011**, *115*, 8876–8885.

(269) Peng, S.; Cho, K. Chemical Control of Nanotube Electronics. *Nanotechnology* **2000**, *11*, 57–60.

(270) Santucci, S.; Picozzi, S.; Di Gregorio, F.; Lozzi, L.; Cantalini, C.; Valentini, L.; Kenny, J. M.; Delley, B. NO₂ and CO Gas Adsorption on Carbon Nanotubes: Experiment and Theory. *J. Chem. Phys.* **2003**, *119*, 10904–10910.

(271) Chang, H.; Lee, J. Do; Lee, S. M.; Lee, Y. H. Adsorption of NH₃ and NO₂Molecules on Carbon Nanotubes. *Appl. Phys. Lett.* **2001**, *79*, 3863–3865.

(272) Sivasathya, S.; Thiruvadigal, D. J.; Mathi Jaya, S. Electron Transport through Metallic Single Wall Carbon Nanotubes with Adsorbed NO₂ and NH₃Molecules: A First-Principles Study. *Chem. Phys. Lett.* **2014**, *609*, 76–81.

(273) Sadrzadeh, A.; Farajian, A. A.; Yakobson, B. I. Electron Transport of Nanotube-Based Gas Sensors: An Ab Initio Study. *Appl. Phys. Lett.* **2008**, *92*, 022103.

(274) Seo, K.; Park, K. A.; Kim, C.; Han, S.; Kim, B.; Lee, Y. H. Chirality- and Diameter-Dependent Reactivity of NO₂ on Carbon Nanotube Walls. *J. Am. Chem. Soc.* **2005**, *127*, 15724–15729.

(275) EL-Barbary, A. A.; Eid, Kh. M.; Kamel, M. A.; Osman, H. M.; Ismail, G. H. Effect of Tubular Chiralities and Diameters of Single Carbon Nanotubes on Gas Sensing Behavior : A DFT Analysis. *J. Surf. Eng. Mater. Adv. Technol.* **2014**, *4*, 66–74.

(276) Chen, Z.; Nagase, S.; Hirsch, A.; Haddon, R. C.; Thiel, W.; Schleyer, P. V. R. Side-Wall Opening of Single-Walled Carbon Nanotubes (SWCNTs) by Chemical Modification: A Critical Theoretical Study. *Angew. Chem., Int. Ed.* **2004**, *43*, 1552–1554.

(277) Bettinger, H. F. Effects of Finite Carbon Nanotube Length on Sidewall Addition of Fluorine Atom and Methylene. *Org. Lett.* **2004**, *6*, 731–734.

(278) Baldoni, M.; Sgamellotti, A.; Mercuri, F. Finite-Length Models of Carbon Nanotubes Based on Clar Sextet Theory. *Org. Lett.* **2007**, *9*, 4267–4270.

(279) Clar, E. *Polycyclic Hydrocarbons*; Springer Berlin Heidelberg, 1964; Vol. 2.

(280) Groß, L.; Bahlke, M. P.; Steenbock, T.; Klinke, C.; Herrmann, C. Modeling Adsorbate-Induced Property Changes of Carbon Nanotubes. *J. Comput. Chem.* **2017**, *38*, 861–868.

(281) Matsuo, Y.; Tahara, K.; Nakamura, E. Theoretical Studies on Structures and Aromaticity of Finite-Length Armchair Carbon Nanotubes. *Org. Lett.* **2003**, *5*, 3181–3184.

(282) Ormsby, J. L.; King, B. T. Clar Valence Bond Representation of Pi-Bonding in Carbon Nanotubes. *J. Org. Chem.* **2004**, *69*, 4287–4291.

(283) Baldoni, M.; Selli, D.; Sgamellotti, A.; Mercuri, F. Unraveling the Reactivity of Semiconducting Chiral Carbon Nanotubes through Finite-Length Models Based on Clar Sextet Theory. *J. Phys. Chem. C* **2009**, *113*, 862–866.

(284) Ormsby, J. L.; King, B. T. The Regioselectivity of Addition to Carbon Nanotube Segments. *J. Org. Chem.* **2007**, *72*, 4035–4038.

(285) Mercuri, F.; Sgamellotti, A. First-Principles Investigations on the Functionalization of Chiral and Non-Chiral Carbon Nanotubes by Diels–Alder Cycloaddition Reactions. *Phys. Chem. Chem. Phys.* **2009**, *11*, 563–567.

(286) Adjizian, J. J.; Leghrif, R.; Koos, A. A.; Suarez-Martinez, I.; Crossley, A.; Wagner, P.; Grobert, N.; Llobet, E.; Ewels, C. P. Boron- and Nitrogen-Doped Multi-Wall Carbon Nanotubes for Gas Detection. *Carbon* **2014**, *66*, 662–673.

(287) Hamadanian, M.; Fotooh, F. K. Density Functional Study of Al/N Co-Doped (10,0) Zigzag Single-Walled Carbon Nanotubes as CO Sensor. *Comput. Mater. Sci.* **2014**, *82*, 497–502.

(288) Hizhnyi, Y.; Nedilko, S. G.; Borysiuk, V.; Gubanov, V. A. Computational Studies of Boron- and Nitrogen-Doped Single-Walled Carbon Nanotubes as Potential Sensor Materials of Hydrogen Halide Molecules HX (X = F, Cl, Br). *Int. J. Quantum Chem.* **2015**, *115*, 1475–1482.

(289) Rocha, A. R.; Rossi, M.; Fazzio, A.; da Silva, A. J. R. Designing Real Nanotube-Based Gas Sensors. *Phys. Rev. Lett.* **2008**, *100*, 176803.

(290) Azizi, K.; Karimpanah, M. Computational Study of Al- or P-Doped Single-Walled Carbon Nanotubes as NH₃and NO₂sensors. *Appl. Surf. Sci.* **2013**, *285*, 102–109.

(291) Tavakol, H.; Hassani, F. Adsorption of Molecular Iodine on the Surface of Sulfur-Doped Carbon Nanotubes: Theoretical Study on Their Interactions, Sensor Properties, and Other Applications. *Struct. Chem.* **2015**, *26*, 151–158.

(292) Gowri sankar, P. A.; Udhayakumar, K. Electronic Properties of Boron and Silicon Doped (10, 0) Zigzag Single-Walled Carbon Nanotube upon Gas Molecular Adsorption: A DFT Comparative Study. *J. Nanomater.* **2013**, *2013*, 1–12.

(293) Vikramaditya, T.; Sumithra, K. Effect of Substitutionally Boron-Doped Single-Walled Semiconducting Zigzag Carbon Nanotubes on Ammonia Adsorption. *J. Comput. Chem.* **2014**, *35*, 586–594.

(294) Talla, J. A. First Principles Modeling of Boron-Doped Carbon Nanotube Sensors. *Phys. B* **2012**, *407*, 966–970.

(295) Zhang, Y.; Zhang, D.; Liu, C. Novel Chemical Sensor for Cyanides: Boron-Doped Carbon Nanotubes. *J. Phys. Chem. B* **2006**, *110*, 4671–4674.

(296) Wang, R.; Zhang, D.; Zhang, Y.; Liu, C. Boron-Doped Carbon Nanotubes Serving as a Novel Chemical Sensor for Formaldehyde. *J. Phys. Chem. B* **2006**, *110*, 18267–18271.

(297) Hamadanian, M.; Khoshnevisan, B.; Fotooh, F. K.; Tavangar, Z. Computational Study of Super Cell Al-Substituted Single-Walled Carbon Nanotubes as CO Sensor. *Comput. Mater. Sci.* **2012**, *58*, 45–50.

(298) Zhou, Q.; Wang, C.; Fu, Z.; Zhang, H.; Tang, Y. Adsorption of Formaldehyde Molecule on Al-Doped Vacancy-Defected Single-Walled Carbon Nanotubes: A Theoretical Study. *Comput. Mater. Sci.* **2014**, *82*, 337–344.

(299) Zhang, X.; Dai, Z.; Chen, Q.; Tang, J. A DFT Study of SO₂ and H₂S Gas Adsorption on Au-Doped Single-Walled Carbon Nanotubes. *Phys. Scr.* **2014**, *89*, 065803.

(300) Zhang, X.; Gui, Y.; Xiao, H.; Zhang, Y. Analysis of Adsorption Properties of Typical Partial Discharge Gases on Ni-SWCNTs Using Density Functional Theory. *Appl. Surf. Sci.* **2016**, *379*, 47–54.

(301) Buasaeng, P.; Rakrai, W.; Wanno, B.; Tabtimsai, C. DFT Investigation of NH₃, PH₃, and AsH₃adsorptions on Sc-, Ti-, V-, and Cr-Doped Single-Walled Carbon Nanotubes. *Appl. Surf. Sci.* **2017**, *400*, 506–514.

(302) Zhang, X.; Gong, X. DFT, QTAIM, and NBO Investigations of the Ability of the Fe or Ni Doped CNT to Absorb and Sense CO and NO. *J. Mol. Model.* **2015**, *21*, 225.

(303) Sharafeldin, I. M.; Allam, N. DFT Insights into the Electronic Properties and Adsorption of NO₂ on Metal-Doped Carbon Nanotubes for Gas Sensing Applications. *New J. Chem.* **2017**, *41*, 14936–14944.

(304) Mowbray, D. J.; Garca-Lastra, J. M.; Thygesen, K. S.; Rubio, A.; Jacobsen, K. W. Designing Multifunctional Chemical Sensors Using Ni and Cu Doped Carbon Nanotubes. *Phys. Status Solidi B* **2010**, *247*, 2678–2682.

(305) Cui, S.; Pu, H.; Mattson, E. C.; Lu, G.; Mao, S.; Weinert, M.; Hirschmugl, C. J.; Gajdardziska-Josifovska, M.; Chen, J. Ag Nanocrystal as a Promoter for Carbon Nanotube-Based Room-Temperature Gas Sensors. *Nanoscale* **2012**, *4*, 5887–5894.

(306) Charlier, J.-C.; Arnaud, L.; Avilov, I. V.; Delgado, M.; Demoisson, F.; Espinosa, E. H.; Ewels, C. P.; Felten, A.; Guillot, J.; Ionescu, R.; et al. Carbon Nanotubes Randomly Decorated with Gold Clusters: From Nano 2 Hybrid Atomic Structures to Gas Sensing Prototypes. *Nanotechnology* **2009**, *20*, 375501.

(307) Singh, N. B.; Bhattacharya, B.; Mondal, R.; Sarkar, U. Nickel Cluster Functionalised Carbon Nanotube for CO Molecule Detection: A Theoretical Study. *Mol. Phys.* **2016**, *114*, 671–680.

(308) Singh, N. B.; Bhattacharya, B.; Sarkar, U. Nickel Decorated Single-Wall Carbon Nanotube as CO Sensor. *Soft Nanosci. Lett.* **2013**, *3*, 9–11.

(309) Yoosefian, M.; Raissi, H.; Mola, A. The Hybrid of Pd and SWCNT (Pd Loaded on SWCNT) as an Efficient Sensor for the Formaldehyde Molecule Detection: A DFT Study. *Sens. Actuators, B* **2015**, *212*, 55–62.

(310) Li, L.; Zhang, G.; Chen, L.; Bi, H. M.; Shi, K. Y. Ni(NiO)/Single-Walled Carbon Nanotubes Composite: Synthesis of Electro-Deposition, Gas Sensing Property for NO Gas and Density Functional Theory Calculation. *Mater. Res. Bull.* **2013**, *48*, 504–511.

(311) Liu, S. F.; Lin, S.; Swager, T. M. An Organocobalt–Carbon Nanotube Chemiresistive Carbon Monoxide Detector. *ACS Sensors* **2016**, *1*, 354–357.

(312) Mittal, M.; Kumar, A. Carbon Nanotube (CNT) Gas Sensors for Emissions from Fossil Fuel Burning. *Sens. Actuators, B* **2014**, *203*, 349–362.

(313) Timmer, B.; Olthuis, W.; Van Den Berg, A. Ammonia Sensors and Their Applications - A Review. *Sens. Actuators, B* **2005**, *107*, 666–677.

(314) Michaels, R. A. Emergency Planning and the Acute Toxic Potency of Inhaled Ammonia. *Environ. Health Perspect.* **1999**, *107*, 617–627.

(315) Behera, S. N.; Sharma, M.; Aneja, V. P.; Balasubramanian, R. Ammonia in the Atmosphere: A Review on Emission Sources, Atmospheric Chemistry and Deposition on Terrestrial Bodies. *Environ. Sci. Pollut. Res.* **2013**, *20*, 8092–8131.

(316) *Occupational Safety and Health Standards*; OSHA, 1993; 1910.1000 TABLE Z-1.

(317) *Aquatic Life Ambient Water Quality Criteria for Ammonia–Freshwater* (EPA-822-R-13-001); Environmental Protection Agency, 2013; p 255.

(318) Bradley, K.; Gabriel, J.-C. P.; Briman, M.; Star, A.; Grüner, G. Charge Transfer from Ammonia Physisorbed on Nanotubes. *Phys. Rev. Lett.* **2003**, *91*, 218301.

(319) Jones, F. E.; Talin, A. A.; Léonard, F.; Dentinger, P. M.; Clift, W. M. Effect of Electrode Material on Transport and Chemical Sensing Characteristics of Metal/Carbon Nanotube Contacts. *J. Electron. Mater.* **2006**, *35*, 1641–1646.

(320) Jang, Y. T.; Moon, S. Il; Ahn, J. H.; Lee, Y. H.; Ju, B. K. A Simple Approach in Fabricating Chemical Sensor Using Laterally Grown Multi-Walled Carbon Nanotubes. *Sens. Actuators, B* **2004**, *99*, 118–122.

(321) Jung, H. Y.; Jung, S. M.; Kim, J.; Suh, J. S. Chemical Sensors for Sensing Gas Adsorbed on the Inner Surface of Carbon Nanotube Channels. *Appl. Phys. Lett.* **2007**, *90*, 153114.

(322) Han, J.-W.; Kim, B.; Li, J.; Meyyappan, M. A Carbon Nanotube Based Ammonia Sensor on Cellulose Paper. *RSC Adv.* **2014**, *4*, 549–553.

(323) Goldoni, A.; Larciprete, R.; Petaccia, L.; Lizzit, S. Single-Wall Carbon Nanotube Interaction with Gases: Sample Contaminants and Environmental Monitoring. *J. Am. Chem. Soc.* **2003**, *125*, 11329–11333.

(324) Salehi-Khojin, A.; Khalili-Araghi, F.; Kuroda, M. A.; Lin, K. Y.; Leburton, J.-P.; Masel, R. I. On the Sensing Mechanism in Carbon Nanotube Chemiresistors. *ACS Nano* **2011**, *5*, 153–158.

(325) Cantalini, C.; Valentini, L.; Lozzi, L.; Armentano, I.; Kenny, J. M.; Santucci, S. NO₂ Gas Sensitivity of Carbon Nanotubes Obtained by Plasma Enhanced Chemical Vapor Deposition. *Sens. Actuators, B* **2003**, *93*, 333–337.

(326) Penza, M.; Cassano, G.; Rossi, R.; Alvisi, M.; Rizzo, A.; Signore, M. A.; Dikonomos, T.; Serra, E.; Giorgi, R. Enhancement of Sensitivity in Gas Chemiresistors Based on Carbon Nanotube Surface Functionalized with Noble Metal (Au, Pt) Nanoclusters. *Appl. Phys. Lett.* **2007**, *90*, 173123.

(327) Penza, M.; Rossi, R.; Alvisi, M.; Cassano, G.; Serra, E. Functional Characterization of Carbon Nanotube Networked Films Functionalized with Tuned Loading of Au Nanoclusters for Gas Sensing Applications. *Sens. Actuators, B* **2009**, *140*, 176–184.

(328) Lee, K.; Scardaci, V.; Kim, H.-Y.; Hallam, T.; Nolan, H.; Bolf, B. E.; Maltbie, G. S.; Abbott, J. E.; Duesberg, G. S. Highly Sensitive, Transparent, and Flexible Gas Sensors Based on Gold Nanoparticle Decorated Carbon Nanotubes. *Sens. Actuators, B* **2013**, *188*, 571–575.

(329) Cui, S.; Pu, H.; Lu, G.; Wen, Z.; Mattson, E. C.; Hirschmugl, C.; Gajdardziska-Josifovska, M.; Weinert, M.; Chen, J. Fast and Selective Room-Temperature Ammonia Sensors Using Silver Nanocrystal-Functionalized Carbon Nanotubes. *ACS Appl. Mater. Interfaces* **2012**, *4*, 4898–4904.

(330) Nguyen, L.; Phan, P.; Duong, H.; Nguyen, C.; Nguyen, L. Enhancement of NH₃ Gas Sensitivity at Room Temperature by Carbon Nanotube-Based Sensor Coated with Co Nanoparticles. *Sensors* **2013**, *13*, 1754–1762.

(331) Yoon, B.; Liu, S. F.; Swager, T. M. Surface-Anchored Poly(4-Vinylpyridine)–Single-Walled Carbon Nanotube–Metal Composites for Gas Detection. *Chem. Mater.* **2016**, *28*, 5916–5924.

(332) Duc Hoa, N.; Van Quy, N.; Suk Cho, Y.; Kim, D. Nanocomposite of SWNTs and SnO₂ Fabricated by Soldering Process for Ammonia Gas Sensor Application. *Phys. Status Solidi A* **2007**, *204*, 1820–1824.

(333) Ghaddab, B.; Sanchez, J. B.; Mavon, C.; Paillet, M.; Parret, R.; Zahab, A. A.; Bantignies, J.-L.; Flaud, V.; Beche, E.; Berger, F. Detection of O₃ and NH₃ Using Hybrid Tin Dioxide/Carbon Nanotubes Sensors: Influence of Materials and Processing on Sensor's Sensitivity. *Sens. Actuators, B* **2012**, *170*, 67–74.

(334) Mubeen, S.; Lai, M.; Zhang, T.; Lim, J. H.; Mulchandani, A.; Deshusses, M. A.; Myung, N. V. Hybrid Tin Oxide-SWNT Nanostructures Based Gas Sensor. *Electrochim. Acta* **2013**, *92*, 484–490.

(335) Hoa, N. D.; Van Quy, N.; Kim, D. Nanowire Structured SnO_x-SWNT Composites: High Performance Sensor for NO_x Detection. *Sens. Actuators, B* **2009**, *142*, 253–259.

(336) Rigoni, F.; Drera, G.; Pagliara, S.; Goldoni, A.; Sangaletti, L. High Sensitivity, Moisture Selective, Ammonia Gas Sensors Based on

Single-Walled Carbon Nanotubes Functionalized with Indium Tin Oxide Nanoparticles. *Carbon* **2014**, *80*, 356–363.

(337) Du, N.; Zhang, H.; Chen, B.; Ma, X. Y.; Liu, Z.; Wu, J.; Yang, D. Porous Indium Oxide Nanotubes: Layer-by-Layer Assembly on Carbon-Nanotube Templates and Application for Room-Temperature NH₃ Gas Sensors. *Adv. Mater.* **2007**, *19*, 1641–1645.

(338) Choi, S.-W.; Kim, J.; Byun, Y. T. Highly Sensitive and Selective NO₂ Detection by Pt Nanoparticles-Decorated Single-Walled Carbon Nanotubes and the Underlying Sensing Mechanism. *Sens. Actuators, B* **2017**, *238*, 1032–1042.

(339) Belyarov, E.; Kalinina, I.; Itkis, M. E.; Beer, L.; Cabrera, N.; Haddon, R. C. Mechanism of Ammonia Detection by Chemically Functionalized Single-Walled Carbon Nanotubes: In Situ Electrical and Optical Study of Gas Analyte Detection. *J. Am. Chem. Soc.* **2007**, *129*, 10700–10706.

(340) Zhang, T.; Nix, M. B.; Yoo, B. Y.; Deshusses, M. A.; Myung, N. V. Electrochemically Functionalized Single-Walled Carbon Nanotube Gas Sensor. *Electroanalysis* **2006**, *18*, 1153–1158.

(341) Ding, M.; Tang, Y.; Gou, P.; Reber, M. J.; Star, A. Chemical Sensing with Polyaniline Coated Single-Walled Carbon Nanotubes. *Adv. Mater.* **2011**, *23*, 536–540.

(342) Tian, X.; Wang, Q.; Chen, X.; Yang, W.; Wu, Z.; Xu, X.; Jiang, M.; Zhou, Z. Enhanced Performance of Core-Shell Structured Polyaniline at Helical Carbon Nanotube Hybrids for Ammonia Gas Sensor. *Appl. Phys. Lett.* **2014**, *105*, 203109.

(343) Li, Y.; Wang, H.; Yang, M. N-Type Gas Sensing Characteristics of Chemically Modified Multi-Walled Carbon Nanotubes and PMMA Composite. *Sens. Actuators, B* **2007**, *121*, 496–500.

(344) Datta, K.; Ghosh, P.; More, M. A.; Shirsat, M. D.; Mulchandani, A. Controlled Functionalization of Single-Walled Carbon Nanotubes for Enhanced Ammonia Sensing: A Comparative Study. *J. Phys. D: Appl. Phys.* **2012**, *45*, 355305.

(345) Qi, P.; Vermesh, O.; Grecu, M.; Javey, A.; Wang, Q.; Dai, H.; Peng, S.; Cho, K. J. Toward Large Arrays of Multiplex Functionalized Carbon Nanotube Sensors for Highly Sensitive and Selective Molecular Detection. *Nano Lett.* **2003**, *3*, 347–351.

(346) An, K. H.; Jeong, S. Y.; Hwang, H. R.; Lee, Y. H. Enhanced Sensitivity of a Gas Sensor Incorporating Single-Walled Carbon Nanotube-Polypyrrole Nanocomposites. *Adv. Mater.* **2004**, *16*, 1005–1009.

(347) Liang, X.; Chen, Z.; Wu, H.; Guo, L.; He, C.; Wang, B.; Wu, Y. Enhanced NH₃ -Sensing Behavior of 2,9,16,23-Tetrakis(2,2,3,3-Tetrafluoropropoxy) Metal(II) Phthalocyanine/Multi-Walled Carbon Nanotube Hybrids: An Investigation of the Effects of Central Metals. *Carbon* **2014**, *80*, 268–278.

(348) Kaya, E. N.; Basova, T.; Polyakov, M.; Durmus, M.; Kadem, B.; Hassan, A. Hybrid Materials of Pyrene Substituted Phthalocyanines with Single-Walled Carbon Nanotubes: Structure and Sensing Properties. *RSC Adv.* **2015**, *5*, 91855–91862.

(349) Hübert, T.; Boon-Brett, L.; Black, G.; Banach, U. Hydrogen Sensors - A Review. *Sens. Actuators, B* **2011**, *157*, 329–352.

(350) Dag, S.; Ozturk, Y.; Ciraci, S.; Yildirim, T. Adsorption and Dissociation of Hydrogen Molecules on Bare and Functionalized Carbon Nanotubes. *Phys. Rev. B: Condens. Matter Mater. Phys.* **2005**, *72*, 155404.

(351) Kumar, M. K.; Ramaprabhu, S. Nanostructured Pt Functionlized Multiwalled Carbon Nanotube Based Hydrogen Sensor. *J. Phys. Chem. B* **2006**, *110*, 11291–11298.

(352) Penner, R. M. A Nose for Hydrogen Gas: Fast, Sensitive H₂Sensors Using Electrodeposited Nanomaterials. *Acc. Chem. Res.* **2017**, *50*, 1902–1910.

(353) Su, H. C.; Zhang, M.; Bosze, W.; Lim, J.-H.; Myung, N. V. Metal Nanoparticles and DNA Co-Functionalized Single-Walled Carbon Nanotube Gas Sensors. *Nanotechnology* **2013**, *24*, 505502.

(354) Sayago, I.; Terrado, E.; Lafuente, E.; Horrillo, M. C.; Maser, W. K.; Benito, A. M.; Navarro, R.; Urriolabeitia, E. P.; Martinez, M. T.; Gutierrez, J. Hydrogen Sensors Based on Carbon Nanotubes Thin Films. *Synth. Met.* **2005**, *148*, 15–19.

(355) Sayago, I.; Terrado, E.; Aleixandre, M.; Horrillo, M. C.; Fernández, M. J.; Lozano, J.; Lafuente, E.; Maser, W. K.; Benito, A. M.; Martinez, M. T.; et al. Novel Selective Sensors Based on Carbon Nanotube Films for Hydrogen Detection. *Sens. Actuators, B* **2007**, *122*, 75–80.

(356) Sippel-Oakley, J.; Wang, H.-T.; Kang, B. S.; Wu, Z.; Ren, F.; Rinzler, A. G.; Pearton, S. J. Carbon Nanotube Films for Room Temperature Hydrogen Sensing. *Nanotechnology* **2005**, *16*, 2218–2221.

(357) Mubeen, S.; Zhang, T.; Yoo, B.; Deshusses, M. A.; Myung, N. V. Palladium Nanoparticles Decorated Single-Walled Carbon Nanotube Hydrogen Sensor. *J. Phys. Chem. C* **2007**, *111*, 6321–6327.

(358) Sun, Y.; Wang, H. H. Electrodeposition of Pd Nanoparticles on Single-Walled Carbon Nanotubes for Flexible Hydrogen Sensors. *Appl. Phys. Lett.* **2007**, *90*, 213107.

(359) Khalap, V. R.; Sheps, T.; Kane, A. A.; Collins, P. G. Hydrogen Sensing and Sensitivity of Palladium-Decorated Single-Walled Carbon Nanotubes with Defects. *Nano Lett.* **2010**, *10*, 896–901.

(360) Rumeche, F.; Wang, H. H.; Indacochea, J. E. Development of a Fast-Response/High-Sensitivity Double Wall Carbon Nanotube Nanostructured Hydrogen Sensor. *Sens. Actuators, B* **2012**, *163*, 97–106.

(361) Randeniya, L. K.; Martin, P. J.; Bendavid, A. Detection of Hydrogen Using Multi-Walled Carbon-Nanotube Yarns Coated with Nanocrystalline Pd and Pd/Pt Layered Structures. *Carbon* **2012**, *50*, 1786–1792.

(362) Li, X.; Le Thai, M.; Dutta, R. K.; Qiao, S.; Chandran, G. T.; Penner, R. M. Sub-6 nm Palladium Nanoparticles for Faster, More Sensitive H₂ Detection Using Carbon Nanotube Ropes. *ACS Sensors* **2017**, *2*, 282–289.

(363) Javey, A.; Guo, J.; Wang, Q.; Lundstrom, M.; Dai, H. Ballistic Carbon Nanotube Field-Effect Transistors. *Nature* **2003**, *424*, 654–657.

(364) Choi, B.; Lee, D.; Ahn, J.-H.; Yoon, J.; Lee, J.; Jeon, M.; Kim, D. M.; Kim, D. H.; Park, I.; Choi, Y.-K.; et al. Investigation of Optimal Hydrogen Sensing Performance in Semiconducting Carbon Nanotube Network Transistors with Palladium Electrodes. *Appl. Phys. Lett.* **2015**, *107*, 193108.

(365) Lu, Y.; Li, J.; Han, J.; Ng, H. T.; Binder, C.; Partridge, C.; Meyyappan, M. Room Temperature Methane Detection Using Palladium Loaded Single-Walled Carbon Nanotube Sensors. *Chem. Phys. Lett.* **2004**, *391*, 344–348.

(366) Humayun, M. T.; Divan, R.; Liu, Y.; Gundel, L.; Solomon, P. A.; Paprotny, I. Novel Chemoresistive CH₄ Sensor with 10 Ppm Sensitivity Based on Multiwalled Carbon Nanotubes Functionalized with SnO₂ Nanocrystals. *J. Vac. Sci. Technol., A* **2016**, *34*, 01A131.

(367) Humayun, M. T.; Divan, R.; Stan, L.; Gupta, A.; Rosenmann, D.; Gundel, L.; Solomon, P. A.; Paprotny, I. ZnO Functionalization of Multiwalled Carbon Nanotubes for Methane Sensing at Single Parts per Million Concentration Levels. *J. Vac. Sci. Technol., B: Nanotechnol. Microelectron.: Mater., Process., Meas., Phenom.* **2015**, *33*, 06FF01.

(368) Raub, J. A.; Mathieu-Nolf, M.; Hampson, N. B.; Thom, S. R. Carbon Monoxide Poisoning — a Public Health Perspective. *Toxicology* **2000**, *145*, 1–14.

(369) Carbon Monoxide In Workplace Atmospheres (Direct-Reading Monitor), OSHA Method ID-209; Occupational Safety and Health Administration, 1993.

(370) Thom, S. R. Thom. Hyperbaric-Oxygen Therapy For Acute Carbon Monoxide Poisoning. *N. Engl. J. Med.* **2002**, *347*, 1105–1106.

(371) Thorn, S. R.; Keim, L. W. Carbon Monoxide Poisoning: A Review Epidemiology, Pathophysiology, Clinical Findings, and Treatment Options Including Hyperbaric Oxygen Therapy. *J. Toxicol., Clin. Toxicol.* **1989**, *27*, 141–156.

(372) Swager, T. M. Sensor Technologies Empowered by Materials and Molecular Innovations. *Angew. Chem., Int. Ed.* **2018**, *57*, 4248–4257.

(373) Da Silva, L. B.; Fagan, S. B.; Mota, R. Ab Initio Study of Deformed Carbon Nanotube Sensors for Carbon Monoxide Molecules. *Nano Lett.* **2004**, *4*, 65–67.

(374) Peng, S.; Cho, K. J. Ab Initio Study of Doped Carbon Nanotube Sensors. *Nano Lett.* **2003**, *3*, 513–517.

(375) Wang, R.; Zhang, D.; Sun, W.; Han, Z.; Liu, C. A Novel Aluminum-Doped Carbon Nanotubes Sensor for Carbon Monoxide. *J. Mol. Struct.: THEOCHEM* **2007**, *806*, 93–97.

(376) Bittencourt, C.; Felten, A.; Espinosa, E. H. H.; Ionescu, R.; Llobet, E.; Correig, X.; Pireaux, J.-J. J. WO₃ Films Modified with Functionalised Multi-Wall Carbon Nanotubes: Morphological, Compositional and Gas Response Studies. *Sens. Actuators, B* **2006**, *115*, 33–41.

(377) Hannon, A.; Lu, Y.; Li, J.; Meyyappan, M. Room Temperature Carbon Nanotube Based Sensor for Carbon Monoxide Detection. *J. Sens. Sens. Syst.* **2014**, *3*, 349–354.

(378) Kauffman, D. R.; Sorescu, D. C.; Schofield, D. P.; Allen, B. L.; Jordan, K. D.; Star, A. Understanding the Sensor Response of Metal-Decorated Carbon Nanotubes. *Nano Lett.* **2010**, *10*, 958–963.

(379) Choi, S. W.; Kim, J.; Lee, J. H.; Byun, Y. T. Remarkable Improvement of CO-Sensing Performances in Single-Walled Carbon Nanotubes Due to Modification of the Conducting Channel by Functionalization of Au Nanoparticles. *Sens. Actuators, B* **2016**, *232*, 625–632.

(380) Yoosefian, M.; Barzgari, Z.; Yoosefian, J. Ab Initio Study of Pd-Decorated Single-Walled Carbon Nanotube with C-Vacancy as CO Sensor. *Struct. Chem.* **2014**, *25*, 9–19.

(381) Zhang, Y.; Cui, S.; Chang, J.; Ocola, L. E.; Chen, J. Highly Sensitive Room Temperature Carbon Monoxide Detection Using SnO₂ Nanoparticle-Decorated Semiconducting Single-Walled Carbon Nanotubes. *Nanotechnology* **2013**, *24*, 025503.

(382) Leghrif, R.; Pavelko, R.; Felten, A.; Vasiliev, A.; Cané, C.; Gràcia, I.; Pireaux, J. J.; Llobet, E. Gas Sensors Based on Multiwall Carbon Nanotubes Decorated with Tin Oxide Nanoclusters. *Sens. Actuators, B* **2010**, *145*, 411–416.

(383) Wanna, Y.; Srisukhumbowornchai, N.; Tuantranont, A.; Wisitsoraat, A.; Thavarungkul, N.; Singjai, P. The Effect of Carbon Nanotube Dispersion on CO Gas Sensing Characteristics of Polyaniline Gas Sensor. *J. Nanosci. Nanotechnol.* **2006**, *6*, 3893–3896.

(384) Lin, Y.; Kan, K.; Song, W.; Zhang, G.; Dang, L.; Xie, Y.; Shen, P.; Li, L.; Shi, K. Controllable Synthesis of Co₃O₄/Polyethyleneimine-Carbon Nanotubes Nanocomposites for CO and NH₃ Gas Sensing at Room Temperature. *J. Alloys Compd.* **2015**, *639*, 187–196.

(385) Dong, X.; Fu, D.; Ahmed, M. O.; Shi, Y.; Mhaisalkar, S. G.; Zhang, S.; Moothala, S.; Ho, X.; Rogers, J. A.; Li, L. J. Heme-Enabled Electrical Detection of Carbon Monoxide at Room Temperature Using Networked Carbon Nanotube Field-Effect Transistors. *Chem. Mater.* **2007**, *19*, 6059–6061.

(386) He, Y.; Zhang, J.; Zhao, J. Theoretical Investigation on the Electronic Transport Properties of Iron(II) Porphyrin for CO Sensing with Single-Walled Carbon Nanotubes. *Chem. Lett.* **2014**, *43*, 735–737.

(387) Gabriel, D.; Deshusses, M. a. Retrofitting Existing Chemical Scrubbers to Biotrickling Filters for H₂S Emission Control. *Proc. Natl. Acad. Sci. U. S. A.* **2003**, *100*, 6308–6312.

(388) Hydrogen Sulfide. OSHA Sampling and Analytical Method 1008, Control Number T-1008-FV-01-0609-M.

(389) Yao, F.; Duong, D. L.; Lim, S. C.; Yang, S. B.; Hwang, H. R.; Yu, W. J.; Lee, I. H.; Güneş, F.; Lee, Y. H. Humidity-Assisted Selective Reactivity between NO₂ and SO₂ Gas on Carbon Nanotubes. *J. Mater. Chem.* **2011**, *21*, 4502–4508.

(390) Mäkinen, J.; Mustonen, T.; Halonen, N.; Tóth, G.; Kordás, K.; Vähäkangas, J.; Moilanen, H.; Kukovecz, Á.; Kónya, Z.; Haspel, H.; et al. Inkjet Printed Resistive and Chemical-FET Carbon Nanotube Gas Sensors. *Phys. Status Solidi B* **2008**, *245*, 2335–2338.

(391) Farooqui, M. F.; Karimi, M. A.; Salama, K. N.; Shamim, A. 3D-Printed Disposable Wireless Sensors with Integrated Microelectronics for Large Area Environmental Monitoring. *Adv. Mater. Technol.* **2017**, *2*, 1700051.

(392) Zhang, X.; Yang, B.; Wang, X.; Luo, C. Effect of Plasma Treatment on Multi-Walled Carbon Nanotubes for the Detection of H₂S and SO₂. *Sensors* **2012**, *12*, 9375–9385.

(393) Zhang, X.; Dai, Z.; Wei, L.; Liang, N.; Wu, X. Theoretical Calculation of the Gas-Sensing Properties of Pt-Decorated Carbon Nanotubes. *Sensors* **2013**, *13*, 15159–15171.

(394) Ding, M.; Sorescu, D. C.; Kotchey, G. P.; Star, A. Welding of Gold Nanoparticles on Graphitic Templates for Chemical Sensing. *J. Am. Chem. Soc.* **2012**, *134*, 3472–3479.

(395) Dilonardo, E.; Penza, M.; Alvisi, M.; Di Franco, C.; Rossi, R.; Palmisano, F.; Torsi, L.; Cioffi, N. Electrophoretic Deposition of Au NPs on MWCNT-Based Gas Sensor for Tailored Gas Detection with Enhanced Sensing Properties. *Sens. Actuators, B* **2016**, *223*, 417–428.

(396) Fam, D. W. H.; Tok, A. I. Y.; Palaniappan, A.; Noppawan, P.; Lohani, A.; Mhaisalkar, S. G. Selective Sensing of Hydrogen Sulphide Using Silver Nanoparticle Decorated Carbon Nanotubes. *Sens. Actuators, B* **2009**, *138*, 189–192.

(397) Wu, H.; Chen, Z.; Zhang, J.; Wu, F.; He, C.; Wang, B.; Wu, Y.; Ren, Z. Stably Dispersed Carbon Nanotubes Covalently Bonded to Phthalocyanine Cobalt(II) for Ppb-Level H₂S Sensing at Room Temperature. *J. Mater. Chem. A* **2016**, *4*, 1096–1104.

(398) Mendoza, F.; Hernández, D. M.; Makarov, V.; Febus, E.; Weiner, B. R.; Morell, G. Room Temperature Gas Sensor Based on Tin Dioxide-Carbon Nanotubes Composite Films. *Sens. Actuators, B* **2014**, *190*, 227–233.

(399) Liu, H.; Zhang, W.; Yu, H.; Gao, L.; Song, Z.; Xu, S.; Li, M.; Wang, Y.; Song, H.; Tang, J. Solution-Processed Gas Sensors Employing SnO₂ Quantum Dot/MWCNT Nanocomposites. *ACS Appl. Mater. Interfaces* **2016**, *8*, 840–846.

(400) Dai, H.; Xiao, P.; Lou, Q. Application of SnO₂/MWCNTs Nanocomposite for SF₆ Decomposition Gas Sensor. *Phys. Status Solidi A* **2011**, *208*, 1714–1717.

(401) Asad, M.; Sheikhi, M. H.; Pourfath, M.; Moradi, M. High Sensitive and Selective Flexible H₂S Gas Sensors Based on Cu Nanoparticle Decorated SWCNTs. *Sens. Actuators, B* **2015**, *210*, 1–8.

(402) Asad, M.; Sheikhi, M. H. Highly Sensitive Wireless H₂S Gas Sensors at Room Temperature Based on CuO-SWCNT Hybrid Nanomaterials. *Sens. Actuators, B* **2016**, *231*, 474–483.

(403) Yu, S. Y. S.; Yi, W. Y. W. Single-Walled Carbon Nanotubes as a Chemical Sensor for SO₂ Detection. *IEEE Trans. Nanotechnol.* **2007**, *6*, 545–548.

(404) Suehiro, J.; Zhou, G.; Hara, M. Detection of Partial Discharge in SF₆ Gas Using a Carbon Nanotube-Based Gas Sensor. *Sens. Actuators, B* **2005**, *105*, 164–169.

(405) Li, W.; Ma, J.-J.; Liu, P.; Pan, Z.-L.; He, Q.-Y. First-Principles Study of the Adsorption Sensitivity of Ni-Doped Single-Walled Zigzag (n,0)CNTs (N = 4,5,6) toward SO₂Molecules. *Appl. Surf. Sci.* **2015**, *335*, 17–22.

(406) Edokpolo, B.; Yu, Q. J.; Connell, D. Health Risk Assessment of Ambient Air Concentrations of Benzene, Toluene and Xylene (BTX) in Service Station Environments. *Int. J. Environ. Res. Public Health* **2014**, *11*, 6354–6374.

(407) Saxena, P. A Review of Assessment of Benzene, Toluene, Ethylbenzene and Xylene (BTEX) Concentration in Urban Atmosphere of Delhi. *Int. J. Phys. Sci.* **2012**, *7*, 850–860.

(408) Lim, S. K.; Shin, H. S.; Yoon, K. S.; Kwack, S. J.; Um, Y. M.; Hyeon, J. H.; Kwak, H. M.; Kim, J. Y.; Kim, T. H.; Kim, Y. J.; et al. Risk Assessment of Volatile Organic Compounds Benzene, Toluene, Ethylbenzene, and Xylene (BTEX) in Consumer Products. *J. Toxicol. Environ. Health, Part A* **2014**, *77*, 1502–1521.

(409) Ammonia. OSHA Sampling and Analytical Method 188, Control number T-ID188-FV-02-0201-M.

(410) Pejcic, B.; Crooke, E.; Boyd, L.; Doherty, C. M.; Hill, A. J.; Myers, M.; White, C. Using Plasticizers to Control the Hydrocarbon Selectivity of a Poly(Methyl Methacrylate)-Coated Quartz Crystal Microbalance Sensor. *Anal. Chem.* **2012**, *84*, 8564–8570.

(411) Ju, J. F.; Syu, M. J.; Teng, H. S.; Chou, S. K.; Chang, Y. S. Preparation and Identification of β -Cyclodextrin Polymer Thin Film for Quartz Crystal Microbalance Sensing of Benzene, Toluene, and p-Xylene. *Sens. Actuators, B* **2008**, *132*, 319–326.

(412) Parsons, M. T.; Sydoryk, I.; Lim, A.; McIntyre, T. J.; Tulip, J.; Jäger, W.; McDonald, K. Real-Time Monitoring of Benzene, Toluene,

and p-Xylene in a Photoreaction Chamber with a Tunable Mid-Infrared Laser and Ultraviolet Differential Optical Absorption Spectroscopy. *Appl. Opt.* **2011**, *50*, A90–A99.

(413) Rushi, A. D.; Datta, K. P.; Ghosh, P. S.; Mulchandani, A.; Shirsat, M. D. Selective Discrimination among Benzene, Toluene, and Xylene: Probing Metalloporphyrin-Functionalized Single-Walled Carbon Nanotube-Based Field Effect Transistors. *J. Phys. Chem. C* **2014**, *118*, 24034–24041.

(414) Chatterjee, S.; Castro, M.; Feller, J. F. Tailoring Selectivity of Sprayed Carbon Nanotube Sensors (CNT) towards Volatile Organic Compounds (VOC) with Surfactants. *Sens. Actuators, B* **2015**, *220*, 840–849.

(415) Son, M.; Cho, D. G.; Lim, J. H.; Park, J.; Hong, S.; Ko, H. J.; Park, T. H. Real-Time Monitoring of Geosmin and 2-Methylisoborneol, Representative Odor Compounds in Water Pollution Using Bioelectronic Nose with Human-like Performance. *Biosens. Bioelectron.* **2015**, *74*, 199–206.

(416) Li, P.; Martin, C. M.; Yeung, K. K.; Xue, W. Dielectrophoresis Aligned Single-Walled Carbon Nanotubes as PH Sensors. *Biosensors* **2011**, *1*, 23–35.

(417) Takeda, S.; Nakamura, M.; Ishii, A.; Subagyo, A.; Hosoi, H.; Sueoka, K.; Mukasa, K. A PH Sensor Based on Electric Properties of Nanotubes on a Glass Substrate. *Nanoscale Res. Lett.* **2007**, *2*, 207–212.

(418) Liao, Y.; Zhang, C.; Zhang, Y.; Strong, V.; Tang, J.; Li, X. G.; Kalantar-Zadeh, K.; Hoek, E. M. V.; Wang, K. L.; Kaner, R. B. Carbon Nanotube/Polyaniline Composite Nanofibers: Facile Synthesis and Chemosensors. *Nano Lett.* **2011**, *11*, 954–959.

(419) Ferrer-Anglada, N.; Kaempgen, M.; Roth, S. Transparent and Flexible Carbon Nanotube/Polypyrrole and Carbon Nanotube/Polyaniline PH Sensors. *Phys. Status Solidi B* **2006**, *243*, 3519–3523.

(420) Gumpu, M. B.; Sethuraman, S.; Krishnan, U. M.; Rayappan, J. B. B. A Review on Detection of Heavy Metal Ions in Water - An Electrochemical Approach. *Sens. Actuators, B* **2015**, *213*, 515–533.

(421) Regional Screening Levels (RSLs)-Generic Tables; U.S. Environmental Protection Agency, 2018; <https://www.epa.gov/risk/Regional-screening-levels> (accessed July 31, 2018).

(422) Musameh, M. M.; Hickey, M.; Kyriatzi, I. L. Carbon Nanotube-Based Extraction and Electrochemical Detection of Heavy Metals. *Res. Chem. Intermed.* **2011**, *37*, 675–689.

(423) Li, M.; Gou, H.; Al-Ogaidi, I.; Wu, N. Nanostructured Sensors for Detection of Heavy Metals: A Review. *ACS Sustainable Chem. Eng.* **2013**, *1*, 713–723.

(424) Morton, J.; Havens, N.; Mugweru, A.; Wanekaya, A. K. Detection of Trace Heavy Metal Ions Using Carbon Nanotube Modified Electrodes. *Electroanalysis* **2009**, *21*, 1597–1603.

(425) Zhang, F.; Sun, Y.; Tian, D.; Shin, W. S.; Kim, J. S.; Li, H. Selective Molecular Recognition on Calixarene-Functionalized 3D Surfaces. *Chem. Commun.* **2016**, *52*, 12685–12693.

(426) Kim, T. H.; Lee, J.; Hong, S. Highly Selective Environmental Nanosensors Based on Anomalous Response of Carbon Nanotube Conductance to Mercury Ions. *J. Phys. Chem. C* **2009**, *113*, 19393–19396.

(427) Gou, P.; Kraut, N. D.; Feigel, I. M.; Star, A. Rigid versus Flexible Ligands on Carbon Nanotubes for the Enhanced Sensitivity of Cobalt Ions. *Macromolecules* **2013**, *46*, 1376–1383.

(428) Forzani, E. S.; Li, X.; Zhang, P.; Tao, N.; Zhang, R.; Amlani, I.; Tsui, R.; Nagahara, L. A. Tuning the Chemical Selectivity of SWNT-FETs for Detection of Heavy-Metal Ions. *Small* **2006**, *2*, 1283–1291.

(429) The Future of Food and Agriculture: Trends and Challenges; FAO, 2017; <http://www.Fao.Org/3/a-I6583e.Pdf> (accessed Jan 8, 2018).

(430) Food Losses and Waste in the Context of Sustainable Food Systems. A Report by the High Level Panel of Experts on Food Security and Nutrition of the Committee on World Food Security. *HLPE Rep.* **2014**, *1–6*, 1–116.

(431) Chen, H.; Zuo, X.; Su, S.; Tang, Z.; Wu, A.; Song, S.; Zhang, D.; Fan, C. An Electrochemical Sensor for Pesticide Assays Based on Carbon Nanotube-Enhanced Acetylcholinesterase Activity. *Analyst* **2008**, *133*, 1182–1186.

(432) Burg, S. P.; Burg, E. A. Ethylene Action and the Ripening of Fruits. *Science* **1965**, *148*, 1190–1196.

(433) Lelievre, J.-M.; Latche, A.; Jones, B.; Bouzayen, M.; Pech, J.-C. Ethylene and Fruit Ripening. *Physiol. Plant.* **1997**, *101*, 727–739.

(434) Theologis, A. One Rotten Apple Spoils the Whole Bushel: The Role of Ethylene in Fruit Ripening. *Cell* **1992**, *70*, 181–184.

(435) Leghrif, R.; Llobet, E.; Pavelko, R.; Vasiliev, A. A.; Felten, A.; Pireaux, J. J. Gas Sensing Properties of MWCNTs Decorated with Gold or Tin Oxide Nanoparticles. *Procedia Chem.* **2009**, *1*, 168–171.

(436) Zhang, Z.; Huang, Y.; Ding, W.; Li, G. Multilayer Interparticle Linking Hybrid MOF-199 for Noninvasive Enrichment and Analysis of Plant Hormone Ethylene. *Anal. Chem.* **2014**, *86*, 3533–3540.

(437) Li, Y.; Hodak, M.; Lu, W.; Bernholc, J. Selective Sensing of Ethylene and Glucose Using Carbon-Nanotube-Based Sensors: An Ab Initio Investigation. *Nanoscale* **2017**, *9*, 1687–1698.

(438) Chiu, S.-W.; Tang, K.-T. Towards a Chemiresistive Sensor-Integrated Electronic Nose: A Review. *Sensors* **2013**, *13*, 14214–14247.

(439) Son, M.; Lee, J. Y.; Ko, H. J.; Park, T. H. Bioelectronic Nose: An Emerging Tool for Odor Standardization. *Trends Biotechnol.* **2017**, *35*, 301–307.

(440) Son, M.; Park, T. H. The Bioelectronic Nose and Tongue Using Olfactory and Taste Receptors: Analytical Tools for Food Quality and Safety Assessment. *Biotechnol. Adv.* **2018**, *36*, 371–379.

(441) Wasilewski, T.; Gębicki, J.; Kamysz, W. Advances in Olfaction-Inspired Biomaterials Applied to Bioelectronic Noses. *Sens. Actuators, B* **2018**, *257*, 511–537.

(442) Wasilewski, T.; Gębicki, J.; Kamysz, W. Bioelectronic Nose: Current Status and Perspectives. *Biosens. Bioelectron.* **2017**, *87*, 480–494.

(443) Peris, M.; Escuder-Gilabert, L. A 21st Century Technique for Food Control: Electronic Noses. *Anal. Chim. Acta* **2009**, *638*, 1–15.

(444) Ampuero, S.; Bosset, J. O. The Electronic Nose Applied to Dairy Products: A Review. *Sens. Actuators, B* **2003**, *94*, 1–12.

(445) Wilson, A. D.; Baietto, M. Advances in Electronic-Nose Technologies Developed for Biomedical Applications. *Sensors* **2011**, *11*, 1105–1176.

(446) Jurs, P. C.; Bakken, G. A.; McClelland, H. E. Computational Methods for the Analysis of Chemical Sensor Array Data from Volatile Analytes. *Chem. Rev.* **2000**, *100*, 2649–2678.

(447) Zozulya, S.; Echeverri, F.; Nguyen, T. The Human Olfactory Receptor Repertoire. *Genome Biol.* **2001**, *2*, research0018.1.

(448) Shepherd, G. M. Discrimination of Molecular Signals by the Olfactory Receptor Neuron. *Neuron* **1994**, *13*, 771–790.

(449) Jin, H. J.; Lee, S. H.; Kim, T. H.; Park, J.; Song, H. S.; Park, T. H.; Hong, S. Nanovesicle-Based Bioelectronic Nose Platform Mimicking Human Olfactory Signal Transduction. *Biosens. Bioelectron.* **2012**, *35*, 335–341.

(450) Lim, J. H.; Oh, E. H.; Park, J.; Hong, S.; Park, T. H. Ion-Channel-Coupled Receptor-Based Platform for a Real-Time Measurement of G-Protein-Coupled Receptor Activities. *ACS Nano* **2015**, *9*, 1699–1706.

(451) Kim, T. H.; Lee, S. H.; Lee, J.; Song, H. S.; Oh, E. H.; Park, T. H.; Hong, S. Single-Carbon-Atomic-Resolution Detection of Odorant Molecules Using a Human Olfactory Receptor-Based Bioelectronic Nose. *Adv. Mater.* **2009**, *21*, 91–94.

(452) Song, H. S.; Jin, H. J.; Ahn, S. R.; Kim, D.; Lee, S. H.; Kim, U. K.; Simons, C. T.; Hong, S.; Park, T. H. Bioelectronic Tongue Using Heterodimeric Human Taste Receptor for the Discrimination of Sweeteners with Human-like Performance. *ACS Nano* **2014**, *8*, 9781–9789.

(453) Kim, T. H.; Song, H. S.; Jin, H. J.; Lee, S. H.; Namgung, S.; Kim, U.; Park, T. H.; Hong, S. Bioelectronic Super-Taster Device Based on Taste Receptor-Carbon Nanotube Hybrid Structures. *Lab Chip* **2011**, *11*, 2262–2267.

(454) Son, M.; Kim, D.; Ko, H. J.; Hong, S.; Park, T. H. A Portable and Multiplexed Bioelectronic Sensor Using Human Olfactory and Taste Receptors. *Biosens. Bioelectron.* **2017**, *87*, 901–907.

(455) Song, H. S.; Kwon, O. S.; Lee, S. H.; Park, S. J.; Kim, U. K.; Jang, J.; Park, T. H. Human Taste Receptor-Functionalized Field Effect Transistor as a Human-like Nanobioelectronic Tongue. *Nano Lett.* **2013**, *13*, 172–178.

(456) Lee, S. H.; Jin, H. J.; Song, H. S.; Hong, S.; Park, T. H. Bioelectronic Nose with High Sensitivity and Selectivity Using Chemically Functionalized Carbon Nanotube Combined with Human Olfactory Receptor. *J. Biotechnol.* **2012**, *157*, 467–472.

(457) Lee, S. H.; Kwon, O. S.; Song, H. S.; Park, S. J.; Sung, J. H.; Jang, J.; Park, T. H. Mimicking the Human Smell Sensing Mechanism with an Artificial Nose Platform. *Biomaterials* **2012**, *33*, 1722–1729.

(458) Yoon, H.; Lee, S. H.; Kwon, O. S.; Song, H. S.; Oh, E. H.; Park, T. H.; Jang, J. Polypyrrole Nanotubes Conjugated with Human Olfactory Receptors: High-Performance Transducers for FET-Type Bioelectronic Noses. *Angew. Chem., Int. Ed.* **2009**, *48*, 2755–2758.

(459) Goldsmith, B. R.; Mitala, J. J.; Josue, J.; Castro, A.; Lerner, M. B.; Bayburt, T. H.; Khamis, S. M.; Jones, R. A.; Brand, J. G.; Sligar, S. G.; et al. Biomimetic Chemical Sensors Using Nanoelectronic Readout of Olfactory Receptor Proteins. *ACS Nano* **2011**, *5*, 5408–5416.

(460) Liu, Q.; Zhang, F.; Zhang, D.; Hu, N.; Wang, H.; Jimmy Hsia, K.; Wang, P. Bioelectronic Tongue of Taste Buds on Microelectrode Array for Salt Sensing. *Biosens. Bioelectron.* **2013**, *40*, 115–120.

(461) Qin, Z.; Zhang, B.; Hu, L.; Zhuang, L.; Hu, N.; Wang, P. A Novel Bioelectronic Tongue in Vivo for Highly Sensitive Bitterness Detection with Brain-Machine Interface. *Biosens. Bioelectron.* **2016**, *78*, 374–380.

(462) Zhang, W.; Chen, P.; Zhou, L.; Qin, Z.; Gao, K.; Yao, J.; Li, C.; Wang, P. A Biomimetic Bioelectronic Tongue: A Switch for On-and Off-Response of Acid Sensations. *Biosens. Bioelectron.* **2017**, *92*, 523–528.

(463) Lee, M.; Jung, J. W.; Kim, D.; Ahn, Y. J.; Hong, S.; Kwon, H. W. Discrimination of Umami Tastants Using Floating Electrode-Based Bioelectronic Tongue Mimicking Insect Taste Systems. *ACS Nano* **2015**, *9*, 11728–11736.

(464) Park, J.; Lim, J. H.; Jin, H. J.; Namgung, S.; Lee, S. H.; Park, T. H.; Hong, S. A Bioelectronic Sensor Based on Canine Olfactory Nanovesicle–carbon Nanotube Hybrid Structures for the Fast Assessment of Food Quality. *Analyst* **2012**, *137*, 3249–3254.

(465) Wei, Z.; Zhang, W.; Wang, J. Nickel and Copper Foam Electrodes Modified with Graphene or Carbon Nanotubes for Electrochemical Identification of Chinese Rice Wines. *Microchim. Acta* **2017**, *184*, 3441–3451.

(466) Wang, L. C.; Tang, K. T.; Chiu, S. W.; Yang, S. R.; Kuo, C. T. A Bio-Inspired Two-Layer Multiple-Walled Carbon Nanotube–Polymer Composite Sensor Array and a Bio-Inspired Fast-Adaptive Readout Circuit for a Portable Electronic Nose. *Biosens. Bioelectron.* **2011**, *26*, 4301–4307.

(467) Chiu, S. W.; Wu, H. C.; Chou, T. I.; Chen, H.; Tang, K. T. A Miniature Electronic Nose System Based on an MWNT–Polymer Microsensor Array and a Low-Power Signal-Processing Chip Chemosensors and Chemoreception. *Anal. Bioanal. Chem.* **2014**, *406*, 3985–3994.

(468) Kachoosangi, R. T.; Wildgoose, G. G.; Compton, R. G. Carbon Nanotube-Based Electrochemical Sensors for Quantifying the ‘Heat’ of Chilli Peppers: The Adsorptive Stripping Voltammetric Determination of Capsaicin. *Analyst* **2008**, *133*, 888–895.

(469) *Cost Estimates of Foodborne Illnesses*; United States Department of Agriculture Economic Research Service; <https://www.Ers.Usda.Gov/Data-Products/Cost-Estimates-of-Foodborne-Illnesses/> (accessed July 31, 2018).

(470) Hussain, M.; Dawson, C. Economic Impact of Food Safety Outbreaks on Food Businesses. *Foods* **2013**, *2*, 585–589.

(471) Yam, K. L.; Takhistov, P. T.; Miltz, J. Intelligent Packaging: Concepts and Applications. *J. Food Sci.* **2005**, *70*, R1–10.

(472) Ruiz-Capillas, C.; Jiménez-Colmenero, F. Biogenic Amines in Meat and Meat Products. *Crit. Rev. Food Sci. Nutr.* **2005**, *44*, 489–599.

(473) Naila, A.; Flint, S.; Fletcher, G.; Bremer, P.; Meerink, G. Control of Biogenic Amines in Food—Existing and Emerging Approaches. *J. Food Sci.* **2010**, *75*, R139–R150.

(474) Mehta, R. S.; Bassette, R. Organoleptic, Chemical and Microbiological Changes in Ultra-High-Temperature Sterilized Milk Stored at Room Temperature. *J. Food Prot.* **1978**, *41*, 806–810.

(475) Sinha, R. N.; Tuma, D.; Abramson, D.; Muir, W. E. Fungal Volatiles Associated with Moldy Grain in Ventilated and Non-Ventilated Bin-Stored Wheat. *Mycopathologia* **1988**, *101*, 53–60.

(476) Lee, S. H.; Lim, J. H.; Park, J.; Hong, S.; Park, T. H. Bioelectronic Nose Combined with a Microfluidic System for the Detection of Gaseous Trimethylamine. *Biosens. Bioelectron.* **2015**, *71*, 179–185.

(477) Lee, K. M.; Son, M.; Kang, J. H.; Kim, D.; Hong, S.; Park, T. H.; Chun, H. S.; Choi, S. S. A Triangle Study of Human, Instrument and Bioelectronic Nose for Non-Destructive Sensing of Seafood Freshness. *Sci. Rep.* **2018**, *8*, 547.

(478) Lim, J. H.; Park, J.; Ahn, J. H.; Jin, H. J.; Hong, S.; Park, T. H. A Peptide Receptor-Based Bioelectronic Nose for the Real-Time Determination of Seafood Quality. *Biosens. Bioelectron.* **2013**, *39*, 244–249.

(479) Brody, A. L.; Strupinsky, E. R.; Kline, L. R. *Active Packaging for Food Applications*; CRC Press: Boca Raton, FL, 2001.

(480) Mahajan, R.; Templeton, A.; Harman, A.; Reed, R. A.; Chern, R. T. The Effect of Inert Atmospheric Packaging on Oxidative Degradation in Formulated Granules. *Pharm. Res.* **2005**, *22*, 128–140.

(481) Mills, A. Oxygen Indicators and Intelligent Inks for Packaging. *Chem. Soc. Rev.* **2005**, *34*, 1003–1011.

(482) Ramamoorthy, R.; Dutta, P. K.; Akbar, S. A. Oxygen Sensors: Materials, Methods, Designs and Applications. *J. Mater. Sci.* **2003**, *38*, 4271–4282.

(483) Schwank, J. W.; DiBattista, M. Oxygen Sensors: Materials and Applications. *MRS Bull.* **1999**, *24*, 44–48.

(484) Jouanneau, S.; Recoules, L.; Durand, M. J.; Boukabache, A.; Picot, V.; Primault, Y.; Lakel, A.; Sengelin, M.; Barillon, B.; Thouand, G. Methods for Assessing Biochemical Oxygen Demand (BOD): A Review. *Water Res.* **2014**, *49*, 62–82.

(485) Collins, J.-A.; Rudenski, A.; Gibson, J.; Howard, L.; O’Driscoll, R. Relating Oxygen Partial Pressure, Saturation and Content: The Haemoglobin–oxygen Dissociation Curve. *Breathe* **2015**, *11*, 194–201.

(486) Quaranta, M.; Borisov, S. M.; Klimant, I. Indicators for Optical Oxygen Sensors. *Bioanal. Rev.* **2012**, *4*, 115–157.

(487) Wang, X.; Wolfbeis, O. S. Optical Methods for Sensing and Imaging Oxygen: Materials, Spectroscopies and Applications. *Chem. Soc. Rev.* **2014**, *43*, 3666–3761.

(488) Bradley, K.; Jhi, S. H.; Collins, P. G.; Hone, J.; Cohen, M. L.; Louie, S. G.; Zettl, A. Is the Intrinsic Thermoelectric Power of Carbon Nanotubes Positive? *Phys. Rev. Lett.* **2000**, *85*, 4361–4364.

(489) Rajavel, K.; Lalitha, M.; Radhakrishnan, J. K.; Senthilkumar, L.; Rajendra Kumar, R. T. Multiwalled Carbon Nanotube Oxygen Sensor: Enhanced Oxygen Sensitivity at Room Temperature and Mechanism of Sensing. *ACS Appl. Mater. Interfaces* **2015**, *7*, 23857–23865.

(490) Sumanasekera, G.; Adu, C.; Fang, S.; Eklund, P. Effects of Gas Adsorption and Collisions on Electrical Transport in Single-Walled Carbon Nanotubes. *Phys. Rev. Lett.* **2000**, *85*, 1096–1099.

(491) Tchernatinsky, A.; Desai, S.; Sumanasekera, G. U.; Jayanthi, C. S.; Wu, S. Y.; Nagabhirava, B.; Alphenaar, B. Adsorption of Oxygen Molecules on Individual Single-Wall Carbon Nanotubes. *J. Appl. Phys.* **2006**, *99*, 034306.

(492) Ong, K. G.; Zeng, K.; Grimes, C. A. A Wireless, Passive Carbon Nanotube-Based Gas Sensor. *IEEE Sens. J.* **2002**, *2*, 82–88.

(493) Sorescu, D. C.; Jordan, K. D.; Avouris, P. Theoretical Study of Oxygen Adsorption on Graphite and the (8,0) Single-Walled Carbon Nanotube. *J. Phys. Chem. B* **2001**, *105*, 11227–11232.

(494) Derycke, V.; Martel, R.; Appenzeller, J.; Avouris, P. Controlling Doping and Carrier Injection in Carbon Nanotube Transistors. *Appl. Phys. Lett.* **2002**, *80*, 2773–2775.

(495) Kauffman, D. R.; Shade, C. M.; Uh, H.; Petoud, S.; Star, A. Decorated Carbon Nanotubes with Unique Oxygen Sensitivity. *Nat. Chem.* **2009**, *1*, 500–506.

(496) Liu, Y.; Liu, F.; Pan, X.; Li, J. Protecting the Environment and Public Health from Pesticides. *Environ. Sci. Technol.* **2012**, *46*, S658–S659.

(497) Whitehorn, P. R.; O'Connor, S.; Wackers, F. L.; Goulson, D. Neonicotinoid Pesticide Reduces Bumble Bee Colony Growth and Neonicotinoid Pesticide Reduces Bumble Bee Colony Growth and Queen Production. *Science* **2012**, *336*, 351–352.

(498) Relyea, R. A.; Diecks, N. An Unforeseen Chain of Events: Lethal Effects of Pesticides on Frogs at Sublethal Concentrations. *Ecol. Appl.* **2008**, *18*, 1728–1742.

(499) Bassil, K. L.; Vakil, C.; Sanborn, M.; Cole, D. C.; Kaur, J. S.; Kerr, K. J. Cancer Health Effects of Pesticides. *Can. Fam. Physician* **2007**, *53*, 1704–1711.

(500) Bassil, K. L.; Vakil, C.; Sanborn, M.; Cole, D. C.; Kaur, J. S.; Kerr, K. J.; Sanin, L. H.; Cole, D. C.; Bassil, K. L.; Vakil, C.; et al. Non-Cancer Health Effects of Pesticides. *Can. Fam. Physician* **2007**, *53*, 1712–1720.

(501) Jurewicz, J.; Hanke, W. Prenatal and Childhood Exposure to Pesticides and Neurobehavioral Development: Review of Epidemiological Studies. *Int. J. Occup. Med. Environ. Health* **2008**, *21*, 121–132.

(502) Reddy, D. S.; Colman, E. A Comparative Toxicodrome Analysis of Human Organophosphate and Nerve Agent Poisonings Using Social Media. *Clin. Transl. Sci.* **2017**, *10*, 225–230.

(503) Pimentel, D.; Burgess, M. Environmental and Economic Costs of the Application of Pesticides Primarily in the United States. *Integr. Pest Manag.* **2014**, *3*, 47–71.

(504) Gan, T.; Lv, Z.; Sun, Y.; Shi, Z.; Sun, J.; Zhao, A. Highly Sensitive and Molecular Selective Electrochemical Sensing of 6-Benzylaminopurine with Multiwall Carbon Nanotube@SnS₂-Assisted Signal Amplification. *J. Appl. Electrochem.* **2016**, *46*, 389–401.

(505) Yu, G.; Wu, W.; Zhao, Q.; Wei, X.; Lu, Q. Efficient Immobilization of Acetylcholinesterase onto Amino Functionalized Carbon Nanotubes for the Fabrication of High Sensitive Organophosphorus Pesticides Biosensors. *Biosens. Bioelectron.* **2015**, *68*, 288–294.

(506) Canevari, T. C.; Prado, T. M.; Cincotto, F. H.; Machado, S. A. S. Immobilization of Ruthenium Phthalocyanine on Silica-Coated Multi-Wall Partially Oriented Carbon Nanotubes: Electrochemical Detection of Fenitrothion Pesticide. *Mater. Res. Bull.* **2016**, *76*, 41–47.

(507) Bhatt, V.; Joshi, S.; Becherer, M.; Lugli, P. Flexible, Low-Cost Sensor Based on Electrolyte Gated Carbon Nanotube Field Effect Transistor for Organo-Phosphate Detection. *Sensors* **2017**, *17*, 1147.

(508) Mugadza, T.; Nyokong, T. Electrocatalytic Oxidation of Amitrole and Diuron on Iron(II) Tetraaminophthalocyanine-Single Walled Carbon Nanotube Dendrimer. *Electrochim. Acta* **2010**, *55*, 2606–2613.

(509) Nayak, P.; Anbarasan, B.; Ramaprabhu, S. Fabrication of Organophosphorus Biosensor Using ZnO Nanoparticle-Decorated Carbon Nanotube-Graphene Hybrid Composite Prepared by a Novel Green Technique. *J. Phys. Chem. C* **2013**, *117*, 13202–13209.

(510) Zhang, Y.; Arugula, M. A.; Wales, M.; Wild, J.; Simonian, A. L. A Novel Layer-by-Layer Assembled Multi-Enzyme/CNT Biosensor for Discriminative Detection between Organophosphorus and Non-Organophosphorus Pesticides. *Biosens. Bioelectron.* **2015**, *67*, 287–295.

(511) Wang, J.; Timchalk, C.; Lin, Y. Carbon Nanotube-Based Electrochemical Sensor for Assay of Salivary Cholinesterase Enzyme Activity: An Exposure Biomarker of Organophosphate Pesticides and Nerve Agents. *Environ. Sci. Technol.* **2008**, *42*, 2688–2693.

(512) Wong, A.; Sotomayor, M. D. P. T. Biomimetic Sensor Based on S₁₀15,20-Tetrakis(Pentafluorophenyl)-21H,23H- Porphyrin Iron (III) Chloride and MWCNT for Selective Detection of 2,4-D. *Sens. Actuators, B* **2013**, *181*, 332–339.

(513) Anirudhan, T. S.; Alexander, S. Design and Fabrication of Molecularly Imprinted Polymer-Based Potentiometric Sensor from the Surface Modified Multiwalled Carbon Nanotube for the Determination of Lindane (γ -Hexachlorocyclohexane), an Organochlorine Pesticide. *Biosens. Bioelectron.* **2015**, *64*, 586–593.

(514) Rahemi, V.; Garrido, J. M. P. J.; Borges, F.; Brett, C. M. A.; Garrido, E. M. P. J. Electrochemical Sensor for Simultaneous Determination of Herbicide MCPA and Its Metabolite 4-Chloro-2-Methylphenol. Application to Photodegradation Environmental Monitoring. *Environ. Sci. Pollut. Res.* **2015**, *22*, 4491–4499.

(515) Huang, B.; Zhang, W. De; Chen, C. H.; Yu, Y. X. Electrochemical Determination of Methyl Parathion at a Pd/MWCNTs-Modified Electrode. *Microchim. Acta* **2010**, *171*, 57–62.

(516) Velusamy, V.; Arshak, K.; Korostynska, O.; Oliwa, K.; Adley, C. An Overview of Foodborne Pathogen Detection: In the Perspective of Biosensors. *Biotechnol. Adv.* **2010**, *28*, 232–254.

(517) *Diarrhea: Why Children Are Still Dying and What Can Be Done*; The United Nations Children's Fund (UNICEF)/World Health Organization (WHO), 2009.

(518) *Food Safety and Foodborne Illness*; World Health Organization: Geneva, 2007; Fact sheet no. 237.

(519) Frenzen, P. D.; Drake, A.; Angulo, F. J. Economic Cost of Illness Due to Escherichia Coli O157 Infections in the United States. *J. Food Prot.* **2005**, *68*, 2623–2630.

(520) Mortari, A.; Lorenzelli, L. Recent Sensing Technologies for Pathogen Detection in Milk: A Review. *Biosens. Bioelectron.* **2014**, *60*, 8–21.

(521) Stephen Inbaraj, B.; Chen, B. H. Nanomaterial-Based Sensors for Detection of Foodborne Bacterial Pathogens and Toxins as Well as Pork Adulteration in Meat Products. *J. Food Drug Anal.* **2016**, *24*, 15–28.

(522) Bhardwaj, J.; Devarakonda, S.; Kumar, S.; Jang, J. Development of a Paper-Based Electrochemical Immunosensor Using an Antibody-Single Walled Carbon Nanotubes Bio-Conjugate Modified Electrode for Label-Free Detection of Foodborne Pathogens. *Sens. Actuators, B* **2017**, *253*, 115–123.

(523) Zhao, G.; Zhan, X.; Dou, W. A Disposable Immunosensor for Shigella Flexneri Based on Multiwalled Carbon Nanotube/Sodium Alginate Composite Electrode. *Anal. Biochem.* **2011**, *408*, 53–58.

(524) Viswanathan, S.; Wu, L. C.; Huang, M. R.; Ho, J. A. A. Electrochemical Immunosensor for Cholera Toxin Using Liposomes and Poly(3,4-Ethylenedioxythiophene)-Coated Carbon Nanotubes. *Anal. Chem.* **2006**, *78*, 1115–1121.

(525) Yamada, K.; Kim, C.-T.; Kim, J.-H.; Chung, J.-H.; Lee, H. G.; Jun, S. Single Walled Carbon Nanotube-Based Junction Biosensor for Detection of Escherichia Coli. *PLoS One* **2014**, *9*, e105767.

(526) Yamada, K.; Choi, W.; Lee, I.; Cho, B. K.; Jun, S. Rapid Detection of Multiple Foodborne Pathogens Using a Nanoparticle-Functionalized Multi-Junction Biosensor. *Biosens. Bioelectron.* **2016**, *77*, 137–143.

(527) Balasubramanian, K.; Burghard, M. Biosensors Based on Carbon Nanotubes. *Anal. Bioanal. Chem.* **2006**, *385*, 452–468.

(528) Amann, A.; Costello, B. D. L.; Miekisch, W.; Schubert, J.; Buszewski, B.; Pleil, J.; Ratcliffe, N.; Risby, T. The Human Volatileome: Volatile Organic Compounds (VOCs) in Exhaled Breath, Skin Emanations, Urine, Feces and Saliva. *J. Breath Res.* **2014**, *8*, 034001.

(529) Kim, S. J.; Choi, S. J.; Jang, J. S.; Cho, H. J.; Kim, I. D. Innovative Nanosensor for Disease Diagnosis. *Acc. Chem. Res.* **2017**, *50*, 1587–1596.

(530) Broza, Y. Y.; Haick, H. Nanomaterial-Based Sensors for Detection of Disease by Volatile Organic Compounds. *Nanomedicine* **2013**, *8*, 785–806.

(531) Turner, A. P. F.; Magan, N. Electronic Noses and Disease Diagnostics. *Nat. Rev. Microbiol.* **2004**, *2*, 161–166.

(532) Peng, G.; Hakim, M.; Broza, Y. Y.; Billan, S.; Abdah-Bortnyak, R.; Kuten, A.; Tisch, U.; Haick, H. Detection of Lung, Breast, Colorectal, and Prostate Cancers from Exhaled Breath Using a Single Array of Nanosensors. *Br. J. Cancer* **2010**, *103*, 542–551.

(533) Xu, Z. Q.; Broza, Y. Y.; Ionescu, R.; Tisch, U.; Ding, L.; Liu, H.; Song, Q.; Pan, Y. Y.; Xiong, F. X.; Gu, K. S.; et al. A Nanomaterial-Based Breath Test for Distinguishing Gastric Cancer from Benign Gastric Conditions. *Br. J. Cancer* **2013**, *108*, 941–950.

(534) Amal, H.; Ding, L.; Liu, B. B.; Tisch, U.; Xu, Z. Q.; Shi, D. Y.; Zhao, Y.; Chen, J.; Sun, R. X.; Liu, H.; et al. The Scent Fingerprint of Hepatocarcinoma: In-Vitro Metastasis Prediction with Volatile Organic Compounds (VOCs). *Int. J. Nanomed.* **2012**, *7*, 4135–4146.

(535) Mazzone, P. J.; Hammel, J.; Dweik, R.; Na, J.; Czich, C.; Laskowski, D.; Mekhail, T. Diagnosis of Lung Cancer by the Analysis of Exhaled Breath with a Colorimetric Sensor Array. *Thorax* **2007**, *62*, 565–568.

(536) Hakim, M.; Broza, Y. Y.; Barash, O.; Peled, N.; Phillips, M.; Amann, A.; Haick, H. Volatile Organic Compounds of Lung Cancer and Possible Biochemical Pathways. *Chem. Rev.* **2012**, *112*, 5949–5966.

(537) Tisch, U.; Schlesinger, I.; Ionescu, R.; Nassar, M.; Axelrod, N.; Robertman, D.; Tessler, Y.; Azar, F.; Marmur, A.; Aharon-Peretz, J.; et al. Detection of Alzheimer's and Parkinson's Disease from Exhaled Breath Using Nanomaterial-Based Sensors. *Nanomedicine* **2013**, *8*, 43–56.

(538) Broza, Y. Y.; Har-Shai, L.; Jeries, R.; Cancilla, J. C.; Glass-Marmor, L.; Lejbkowicz, I.; Torrecilla, J. S.; Yao, X.; Feng, X.; Narita, A.; et al. Exhaled Breath Markers for Nonimaging and Noninvasive Measures for Detection of Multiple Sclerosis. *ACS Chem. Neurosci.* **2017**, *8*, 2402–2413.

(539) Novak, B. J.; Blake, D. R.; Meinardi, S.; Rowland, F. S.; Pontello, A.; Cooper, D. M.; Galassetti, P. R. Exhaled Methyl Nitrate as a Noninvasive Marker of Hyperglycemia in Type 1 Diabetes. *Proc. Natl. Acad. Sci. U. S. A.* **2007**, *104*, 15613–15618.

(540) Konvalina, G.; Haick, H. Sensors for Breath Testing: From Nanomaterials to Comprehensive Disease Detection. *Acc. Chem. Res.* **2014**, *47*, 66–76.

(541) Peng, G.; Trock, E.; Haick, H. Detecting Simulated Patterns of Lung Cancer Biomarkers by Random Network of Single-Walled Carbon Nanotubes Coated with Nonpolymeric Organic Materials. *Nano Lett.* **2008**, *8*, 3631–3635.

(542) Nakhleh, M. K.; Amal, H.; Jeries, R.; Broza, Y. Y.; Aboud, M.; Gharra, A.; Igvi, H.; Khatib, S.; Badarneh, S.; Har-Shai, L.; et al. Diagnosis and Classification of 17 Diseases from 1404 Subjects via Pattern Analysis of Exhaled Molecules. *ACS Nano* **2017**, *11*, 112–125.

(543) Owlstone medical; <https://www.owlstonemedical.com/science-technology/breath-biopsy/> (accessed Mar 25, 2018).

(544) Broza, Y. Y.; Mochalski, P.; Ruzsanyi, V.; Amann, A.; Haick, H. Hybrid Volatolomics and Disease Detection. *Angew. Chem., Int. Ed.* **2015**, *54*, 11036–11048.

(545) Amal, H.; Leja, M.; Funka, K.; Skapars, R.; Sivins, A.; Ancans, G.; Liepniene-Karele, I.; Kikuste, I.; Lasina, I.; Haick, H. Detection of Precancerous Gastric Lesions and Gastric Cancer through Exhaled Breath. *Gut* **2016**, *65*, 400–407.

(546) Bajtarevic, A.; Ager, C.; Pienz, M.; Klieber, M.; Schwarz, K.; Ligor, M.; Ligor, T.; Filipiak, W.; Denz, H.; Fiegl, M.; et al. Noninvasive Detection of Lung Cancer by Analysis of Exhaled Breath. *BMC Cancer* **2009**, *9*, 348.

(547) Calenic, B.; Miricescu, D.; Greabu, M.; Kuznetsov, A. V.; Troppmair, J.; Ruzsanyi, V.; Amann, A. Oxidative Stress and Volatile Organic Compounds: Interplay in Pulmonary, Cardio-Vascular, Digestive Tract Systems and Cancer. *Open Chem.* **2015**, *13*, 1020–1030.

(548) Ajibola, O. A.; Smith, D.; Španěl, P.; Ferns, G. A. A. Effects of Dietary Nutrients on Volatile Breath Metabolites. *J. Nutr. Sci.* **2013**, *2*, No. e34, DOI: 10.1017/jns.2013.26.

(549) Shirsat, M. D.; Sarkar, T.; Kakoullis, J.; Myung, N. V.; Konnanath, B.; Spanias, A.; Mulchandani, A. Porphyrin-Functionalized Single-Walled Carbon Nanotube Chemiresistive Sensor Arrays for VOCs. *J. Phys. Chem. C* **2012**, *116*, 3845–3850.

(550) Chatterjee, S.; Castro, M.; Feller, J. F. Tailoring Selectivity of Sprayed Carbon Nanotube Sensors (CNT) towards Volatile Organic Compounds (VOC) with Surfactants. *Sens. Actuators, B* **2015**, *220*, 840–849.

(551) Sarkar, T.; Srinivas, S.; Sarkar, S.; Haddon, R. C.; Mulchandani, A. Single-Walled Carbon Nanotube-Poly(Porphyrin) Hybrid for Volatile Organic Compounds Detection. *J. Phys. Chem. C* **2014**, *118*, 1602–1610.

(552) Wang, X.; Ugur, A.; Goktas, H.; Chen, N.; Wang, M.; Lachman, N.; Kalfon-Cohen, E.; Fang, W.; Wardle, B. L.; Gleason, K. K. Room Temperature Resistive Volatile Organic Compound Sensing Materials Based on a Hybrid Structure of Vertically Aligned Carbon Nanotubes and Conformal OCVD/ICVD Polymer Coatings. *ACS Sensors* **2016**, *1*, 374–383.

(553) Richardson, M.; Moulton, K.; Rabb, D.; Kindopp, S.; Pishe, T.; Yan, C.; Akpinar, I.; Tsoi, B.; Chuck, A. *Capnography for Monitoring End-Tidal CO₂ in Hospital and Pre-Hospital Settings: A Health Technology Assessment*; CADTH: Ottawa, 2016; Vol. 142.

(554) Anderson, C. T.; Breen, P. H. Carbon Dioxide Kinetics and Capnography during Critical Care. *Crit. Care* **2000**, *4*, 207–215.

(555) Bryan, N. S.; Grisham, M. B. Methods to Detect Nitric Oxide and Its Metabolites in Biological Samples. *Free Radical Biol. Med.* **2007**, *43*, 645–657.

(556) Narasimhan, L. R.; Goodman, W.; Patel, C. K. N. Correlation of Breath Ammonia with Blood Urea Nitrogen and Creatinine during Hemodialysis. *Proc. Natl. Acad. Sci. U. S. A.* **2001**, *98*, 4617–4621.

(557) Popa, C.; Dutu, D. C. A.; Cernat, R.; Matei, C.; Bratu, A. M.; Banita, S.; Dumitras, D. C. Ethylene and Ammonia Traces Measurements from the Patients' Breath with Renal Failure via LPAS Method. *Appl. Phys. B: Lasers Opt.* **2011**, *105*, 669–674.

(558) Li, Y.; Li, G.; Wang, X.; Zhu, Z.; Ma, H.; Zhang, T.; Jin, J. Poly(Ionic Liquid)-Wrapped Single-Walled Carbon Nanotubes for Sub-Ppb Detection of CO₂. *Chem. Commun.* **2012**, *48*, 8222–8224.

(559) Olney, D.; Fuller, L.; Santhanam, K. S. V. A Greenhouse Gas Silicon Microchip Sensor Using a Conducting Composite with Single Walled Carbon Nanotubes. *Sens. Actuators, B* **2014**, *191*, 545–552.

(560) Kuzmych, O.; Allen, B. L.; Star, A. Carbon Nanotube Sensors for Exhaled Breath Components. *Nanotechnology* **2007**, *18*, 375502.

(561) Li, G.; Liao, J. M.; Hu, G. Q.; Ma, N. Z.; Wu, P. J. Study of Carbon Nanotube Modified Biosensor for Monitoring Total Cholesterol in Blood. *Biosens. Bioelectron.* **2005**, *20*, 2140–2144.

(562) Yang, J.; Lee, H.; Cho, M.; Nam, J.; Lee, Y. Nonenzymatic Cholesterol Sensor Based on Spontaneous Deposition of Platinum Nanoparticles on Layer-by-Layer Assembled CNT Thin Film. *Sens. Actuators, B* **2012**, *171*–172, 374–379.

(563) Barik, M. A.; Sarma, M. K.; Sarkar, C. R.; Dutta, J. C. Highly Sensitive Potassium-Doped Polypyrrole/Carbon Nanotube-Based Enzyme Field Effect Transistor (ENFET) for Cholesterol Detection. *Appl. Biochem. Biotechnol.* **2014**, *174*, 1104–1114.

(564) Canbay, E.; Akyilmaz, E. Design of a Multiwalled Carbon Nanotube-Nafion-Cysteamine Modified Tyrosinase Biosensor and Its Adaptation of Dopamine Determination. *Anal. Biochem.* **2014**, *444*, 8–15.

(565) Rubianes, M. D.; Rivas, G. A. Enzymatic Biosensors Based on Carbon Nanotubes Paste Electrodes. *Electroanalysis* **2005**, *17*, 73–78.

(566) Kan, X.; Zhou, H.; Li, C.; Zhu, A.; Xing, Z.; Zhao, Z. Imprinted Electrochemical Sensor for Dopamine Recognition and Determination Based on a Carbon Nanotube/Polypyrrole Film. *Electrochim. Acta* **2012**, *63*, 69–75.

(567) Babaei, A.; Taheri, A. R. Nafion/Ni(OH)₂nanoparticles-Carbon Nanotube Composite Modified Glassy Carbon Electrode as a Sensor for Simultaneous Determination of Dopamine and Serotonin in the Presence of Ascorbic Acid. *Sens. Actuators, B* **2013**, *176*, 543–551.

(568) Rand, E.; Periyakaruppan, A.; Tanaka, Z.; Zhang, D. A.; Marsh, M. P.; Andrews, R. J.; Lee, K. H.; Chen, B.; Meyyappan, M.; Koehne, J. E. A Carbon Nanofiber Based Biosensor for Simultaneous Detection of Dopamine and Serotonin in the Presence of Ascorbic Acid. *Biosens. Bioelectron.* **2013**, *42*, 434–438.

(569) Mazloum-Ardakani, M.; Khoshroo, A. High Sensitive Sensor Based on Functionalized Carbon Nanotube/Ionic Liquid Nano-

composite for Simultaneous Determination of Norepinephrine and Serotonin. *J. Electroanal. Chem.* **2014**, *717–718*, 17–23.

(570) Lin, K. C.; Li, Y. S.; Chen, S. M. Electrochemical Determination of Nicotinamide Adenine Dinucleotide and Hydrogen Peroxide Based on Poly(Xanthurenic Acid), Flavin Adenine Dinucleotide and Functionalized Multi-Walled Carbon Nanotubes. *Sens. Actuators, B* **2013**, *184*, 212–219.

(571) Musameh, M.; Wang, J.; Merkoci, A.; Lin, Y. Low-Potential Stable NADH Detection at Carbon-Nanotube-Modified Glassy Carbon Electrodes. *Electrochem. Commun.* **2002**, *4*, 743–746.

(572) Teymourian, H.; Salimi, A.; Hallaj, R. Low Potential Detection of NADH Based on Fe₃O₄nanoparticles/Multiwalled Carbon Nanotubes Composite: Fabrication of Integrated Dehydrogenase-Based Lactate Biosensor. *Biosens. Bioelectron.* **2012**, *33*, 60–68.

(573) Batra, B.; Lata, S.; Rani, S.; Pundir, C. S. Fabrication of a Cytochrome c Biosensor Based on Cytochrome Oxidase/NiO-NPs/CMWCNT/PANI Modified Au Electrode. *J. Biomed. Nanotechnol.* **2013**, *9*, 409–416.

(574) Boussaad, S.; Tao, N. J.; Zhang, R.; Hopson, T.; Nagahara, L. A. In Situ Detection of Cytochrome c Adsorption with Single Walled Carbon Nanotube Device. *Chem. Commun.* **2003**, *13*, 1502.

(575) Lawal, A. T. Synthesis and Utilization of Carbon Nanotubes for Fabrication of Electrochemical Biosensors. *Mater. Res. Bull.* **2016**, *73*, 308–350.

(576) Jacobs, C. B.; Peairs, M. J.; Venton, B. J. Review: Carbon Nanotube Based Electrochemical Sensors for Biomolecules. *Anal. Chim. Acta* **2010**, *662*, 105–127.

(577) Vashist, S. K.; Zheng, D.; Al-Rubeaan, K.; Luong, J. H. T.; Sheu, F. S. Advances in Carbon Nanotube Based Electrochemical Sensors for Bioanalytical Applications. *Biotechnol. Adv.* **2011**, *29*, 169–188.

(578) Tang, H.; Chen, J.; Yao, S.; Nie, L.; Deng, G.; Kuang, Y. Amperometric Glucose Biosensor Based on Adsorption of Glucose Oxidase at Platinum Nanoparticle-Modified Carbon Nanotube Electrode. *Anal. Biochem.* **2004**, *331*, 89–97.

(579) Wang, Y.-T.; Yu, L.; Zhu, Z.-Q.; Zhang, J.; Zhu, J.-Z.; Fan, C. Improved Enzyme Immobilization for Enhanced Bioelectrocatalytic Activity of Glucose Sensor. *Sens. Actuators, B* **2009**, *136*, 332–337.

(580) Chen, K. J.; Lee, C. F.; Rick, J.; Wang, S. H.; Liu, C. C.; Hwang, B. J. Fabrication and Application of Amperometric Glucose Biosensor Based on a Novel PtPd Bimetallic Nanoparticle Decorated Multi-Walled Carbon Nanotube Catalyst. *Biosens. Bioelectron.* **2012**, *33*, 75–81.

(581) Gao, M.; Dai, L.; Wallace, G. G. Biosensors Based on Aligned Carbon Nanotubes Coated with Inherently Conducting Polymers. *Electroanalysis* **2003**, *15*, 1089–1094.

(582) Wang, J.; Musameh, M. Carbon-Nanotubes Doped Poly-pyrrole Glucose Biosensor. *Anal. Chim. Acta* **2005**, *539*, 209–213.

(583) Pilan, L.; Raicopol, M. Highly Selective and Stable Glucose Biosensors Based on Polyaniline/Carbon Nanotubes Composites. *U. P. B. Sci. Bull., Ser. B* **2014**, *76*, 155–166.

(584) Patolsky, F.; Weizmann, Y.; Willner, I. Long-Range Electrical Contacting of Redox Enzymes by SWCNT Connectors. *Angew. Chem., Int. Ed.* **2004**, *43*, 2113–2117.

(585) Tian, K.; Prestgard, M.; Tiwari, A. A Review of Recent Advances in Nonenzymatic Glucose Sensors. *Mater. Sci. Eng., C* **2014**, *41*, 100–118.

(586) Lin, K.-C.; Lin, Y.-C.; Chen, S.-M. A Highly Sensitive Nonenzymatic Glucose Sensor Based on Multi-Walled Carbon Nanotubes Decorated with Nickel and Copper Nanoparticles. *Electrochim. Acta* **2013**, *96*, 164–172.

(587) Gougis, M.; Tabet-Aoul, A.; Ma, D.; Mohamedi, M. Laser Synthesis and Tailor-Design of Nanosized Gold onto Carbon Nanotubes for Non-Enzymatic Electrochemical Glucose Sensor. *Sens. Actuators, B* **2014**, *193*, 363–369.

(588) Baghayeri, M.; Amiri, A.; Farhadi, S. Development of Non-Enzymatic Glucose Sensor Based on Efficient Loading Ag Nanoparticles on Functionalized Carbon Nanotubes. *Sens. Actuators, B* **2016**, *225*, 354–362.

(589) Besteman, K.; Lee, J. O.; Wiertz, F. G. M.; Heering, H. A.; Dekker, C. Enzyme-Coated Carbon Nanotubes as Single-Molecule Biosensors. *Nano Lett.* **2003**, *3*, 727–730.

(590) Lee, D.; Cui, T. Low-Cost, Transparent, and Flexible Single-Walled Carbon Nanotube Nanocomposite Based Ion-Sensitive Field-Effect Transistors for PH/Glucose Sensing. *Biosens. Bioelectron.* **2010**, *25*, 2259–2264.

(591) Wang, J.; Liu, G.; Jan, M. R. Ultrasensitive Electrical Biosensing of Proteins and DNA: Carbon-Nanotube Derived Amplification of the Recognition and Transduction Events. *J. Am. Chem. Soc.* **2004**, *126*, 3010–3011.

(592) Fu, D.; Li, L.-J. Label-Free Electrical Detection of DNA Hybridization Using Carbon Nanotubes and Graphene. *Nano Rev.* **2010**, *1*, 5354.

(593) He, P.; Dai, L. Aligned Carbon Nanotube–DNA Electrochemical Sensors. *Chem. Commun.* **2004**, *3*, 348–349.

(594) Star, A.; Tu, E.; Niemann, J.; Gabriel, J.-C. P.; Joiner, C. S.; Valcke, C. Label-Free Detection of DNA Hybridization Using Carbon Nanotube Network Field-Effect Transistors. *Proc. Natl. Acad. Sci. U. S. A.* **2006**, *103*, 921–926.

(595) Gui, E.-L.; Li, L.-J.; Lee, P. S.; Lohani, A.; Mhaisalkar, S. G.; Cao, Q.; Kang, S. J.; Rogers, J. A.; Tansil, N. C.; Gao, Z. Electrical Detection of Hybridization and Threading Intercalation of Deoxyribonucleic Acid Using Carbon Nanotube Network Field-Effect Transistors. *Appl. Phys. Lett.* **2006**, *89*, 232104.

(596) Dong, X.; Lau, C. M.; Lohani, A.; Mhaisalkar, S. G.; Kasim, J.; Shen, Z.; Ho, X.; Rogers, J. A.; Li, L. J. Electrical Detection of Femtomolar DNA via Gold-Nanoparticle Enhancement in Carbon-Nanotube-Network Field-Effect Transistors. *Adv. Mater.* **2008**, *20*, 2389–2393.

(597) Gui, E. L.; Li, L.-J.; Zhang, K.; Xu, Y.; Dong, X.; Ho, X.; Lee, P. S.; Kasim, J.; Shen, Z. X.; Rogers, J. A.; et al. DNA Sensing by Field-Effect Transistors Based on Networks of Carbon Nanotubes. *J. Am. Chem. Soc.* **2007**, *129*, 14427–14432.

(598) Kelley, S. O.; Barton, J. K. Electron Transfer between Bases in Double Helical DNA. *Science* **1999**, *283*, 375–381.

(599) Fainberg, A. Explosives Detection for Aviation Security. *Science* **1992**, *255*, 1531–1537.

(600) Noort, D.; Benschop, H. P.; Black, R. M. Biomonitoring of Exposure to Chemical Warfare Agents: A Review. *Toxicol. Appl. Pharmacol.* **2002**, *184*, 116–126.

(601) Devi, S. Life after Death—surviving the Attacks on Civilians in Syria. *Lancet* **2018**, *391*, 1009–1011.

(602) Szinicz, L. History of Chemical and Biological Warfare Agents. *Toxicology* **2005**, *214*, 167–181.

(603) Jang, Y. J.; Kim, K.; Tsay, O. G.; Atwood, D. A.; Churchill, D. G. Update 1 of: Destruction and Detection of Chemical Warfare Agents. *Chem. Rev.* **2015**, *115*, PR1–PR76.

(604) Kolakowski, B. M.; Mester, Z. Review of Applications of High-Field Asymmetric Waveform Ion Mobility Spectrometry (FAIMS) and Differential Mobility Spectrometry (DMS). *Analyst* **2007**, *132*, 842–864.

(605) Joo, B. S.; Huh, J. S.; Lee, D. D. Fabrication of Polymer SAW Sensor Array to Classify Chemical Warfare Agents. *Sens. Actuators, B* **2007**, *121*, 47–53.

(606) Liu, G.; Lin, Y. Electrochemical Sensor for Organophosphate Pesticides and Nerve Agents Using Zirconia Nanoparticles as Selective Sorbents. *Anal. Chem.* **2005**, *77*, 5894–5901.

(607) Braue, E. H.; Pannella, M. G. FT-IR Analysis of Chemical Warfare Agents. *Microchim. Acta* **1988**, *94*, 11–16.

(608) Zhou, Q.; Swager, T. M. Methodology for Enhancing the Sensitivity of Fluorescent Chemosensors: Energy Migration in Conjugated Polymers. *J. Am. Chem. Soc.* **1995**, *117*, 7017–7018.

(609) Yang, J. S.; Swager, T. M. Fluorescent Porous Polymer Films as TNT Chemosensors: Electronic and Structural Effects. *J. Am. Chem. Soc.* **1998**, *120*, 11864–11873.

(610) Yang, J.-S.; Swager, T. M. Porous Shape Persistent Fluorescent Polymer Films: An Approach to TNT Sensory Materials. *J. Am. Chem. Soc.* **1998**, *120*, 5321–5322.

(611) Weis, J. G.; Swager, T. M. Thiophene-Fused Tropones as Chemical Warfare Agent-Responsive Building Blocks. *ACS Macro Lett.* **2015**, *4*, 138–142.

(612) Germain, M. E.; Knapp, M. J. Optical Explosives Detection: From Color Changes to Fluorescence Turn-On. *Chem. Soc. Rev.* **2009**, *38*, 2543–2555.

(613) Colovic, M. B.; Krstic, D. Z.; Lazarevic-Pastor, T. D.; Bondzic, A. M.; Vasic, V. M. Acetylcholinesterase Inhibitors: Pharmacology and Toxicology. *Curr. Neuropharmacol.* **2013**, *11*, 315–335.

(614) Wismer, T. *Chemical Warfare Agents and Risks to Animal Health*; Elsevier Inc., 2015.

(615) Wang, Y.; Yang, Z.; Hou, Z.; Xu, D.; Wei, L.; Kong, E. S. W.; Zhang, Y. Flexible Gas Sensors with Assembled Carbon Nanotube Thin Films for DMMP Vapor Detection. *Sens. Actuators, B* **2010**, *150*, 708–714.

(616) Robinson, J. A.; Snow, E. S.; Perkins, F. K. Improved Chemical Detection Using Single-Walled Carbon Nanotube Network Capacitors. *Sens. Actuators, A* **2007**, *135*, 309–314.

(617) Lee, C. Y.; Sharma, R.; Radadia, A. D.; Masel, R. I.; Strano, M. S. On-Chip Micro Gas Chromatograph Enabled by a Noncovalently Functionalized Single-Walled Carbon Nanotube Sensor Array. *Angew. Chem., Int. Ed.* **2008**, *47*, 5018–5021.

(618) Cattanach, K.; Kulkarni, R. D.; Kozlov, M.; Manohar, S. K. Flexible Carbon Nanotube Sensors for Nerve Agent Simulants. *Nanotechnology* **2006**, *17*, 4123–4128.

(619) Chuang, P. K.; Wang, L. C.; Kuo, C. T. Development of a High Performance Integrated Sensor Chip with a Multi-Walled Carbon Nanotube Assisted Sensing Array. *Thin Solid Films* **2013**, *529*, 205–208.

(620) Kumar, D.; Jha, P.; Chouksey, A.; Rawat, J. S. B. S.; Tandon, R. P.; Chaudhury, P. K. 4-(Hexafluoro-2-Hydroxy Isopropyl)Aniline Functionalized Highly Sensitive Flexible SWCNT Sensor for Detection of Nerve Agent Simulant Dimethyl Methylphosphonate. *Mater. Chem. Phys.* **2016**, *181*, 487–494.

(621) Kong, L.; Wang, J.; Fu, X.; Zhong, Y.; Meng, F.; Luo, T.; Liu, J. P-Hexafluoroisopropanol Phenyl Covalently Functionalized Single-Walled Carbon Nanotubes for Detection of Nerve Agents. *Carbon* **2010**, *48*, 1262–1270.

(622) Wei, L.; Shi, D.; Ye, P.; Dai, Z.; Chen, H.; Chen, C.; Wang, J.; Zhang, L.; Xu, D.; Wang, Z.; et al. Hole Doping and Surface Functionalization of Single-Walled Carbon Nanotube Chemiresistive Sensors for Ultrasensitive and Highly Selective Organophosphor Vapor Detection. *Nanotechnology* **2011**, *22*, 425501.

(623) Khan, M. A. K.; Kerman, K.; Petryk, M.; Kraatz, H. B. Noncovalent Modification of Carbon Nanotubes with Ferrocene-Amino Acid Conjugates for Electrochemical Sensing of Chemical Warfare Agent Mimics. *Anal. Chem.* **2008**, *80*, 2574–2582.

(624) Diakowski, P. M.; Xiao, Y.; Petryk, M. W. P.; Kraatz, H.-B. Impedance Based Detection of Chemical Warfare Agent Mimics Using Ferrocene-Lysine Modified Carbon Nanotubes. *Anal. Chem.* **2010**, *82*, 3191–3197.

(625) Xiao, Y.; Petryk, M.; Diakowski, P. M.; Kraatz, H.-B. Covalent Modification of Carbon Nanotubes with Ferrocene-Lysine Derivative for Electrochemical Sensors. In *Proceedings of SPIE - The International Society for Optical Engineering*; Fountain, A. W., III, Gardner, P. J., Eds.; SPIE, 2009; Vol. 7304, p 73040R.

(626) Shankar, A.; Mittal, J.; Jagota, A. Binding between DNA and Carbon Nanotubes Strongly Depends upon Sequence and Chirality. *Langmuir* **2014**, *30*, 3176–3183.

(627) Staii, C.; Johnson, A. T.; Chen, M.; Gelperin, A. DNA-Decorated Carbon Nanotubes for Chemical Sensing. *Nano Lett.* **2005**, *5*, 1774–1778.

(628) Zuniga, C.; Rinaldi, M.; Khamis, S. M.; Johnson, A. T.; Piazza, G. Nanoenabled Microelectromechanical Sensor for Volatile Organic Chemical Detection. *Appl. Phys. Lett.* **2009**, *94*, 223122.

(629) Kybert, N. J.; Lerner, M. B.; Yodh, J. S.; Preti, G.; Johnson, A. T. C. Differentiation of Complex Vapor Mixtures Using Versatile DNA-Carbon Nanotube Chemical Sensor Arrays. *ACS Nano* **2013**, *7*, 2800–2807.

(630) Khamis, S. M.; Jones, R. A.; Johnson, A. T. C.; Preti, G.; Kwak, J.; Gelperin, A. DNA-Decorated Carbon Nanotube-Based FETs as Ultrasensitive Chemical Sensors: Discrimination of Homologues, Structural Isomers, and Optical Isomers. *AIP Adv.* **2012**, *2*, 022110.

(631) Liu, Y.; Chen, C. L.; Zhang, Y.; Sonkusale, S. R.; Wang, M. L.; Dokmeci, M. R. SWNT Based Nanosensors for Wireless Detection of Explosives and Chemical Warfare Agents. *IEEE Sens. J.* **2013**, *13*, 202–210.

(632) Liu, G.; Lin, Y. Biosensor Based on Self-Assembling Acetylcholinesterase on Carbon Nanotubes for Flow Injection/Amperometric Detection of Organophosphate Pesticides and Nerve Agents. *Anal. Chem.* **2006**, *78*, 835–843.

(633) Delalande, M.; Clavaguera, S.; Toure, M.; Carella, A.; Lenfant, S.; Deresmes, D.; Vuillaume, D.; Simonato, J.-P. Chemical Functionalization of Electrodes for Detection of Gaseous Nerve Agents with Carbon Nanotube Field-Effect Transistors. *Chem. Commun.* **2011**, *47*, 6048.

(634) Jaynes, G. D.; Williams, R. M. *Chemical and Biological TERRORISM: Research and Development to Improve Civilian Medical Response*; National Academy Press: Washington, DC, 1999; 20418.

(635) Guo, Y.-L.; Kennedy, T. P.; Michael, J. R.; Sciuto, A. M.; Ghio, A. J.; Adkinson, N. F., Jr.; Gurtner, G. H. Mechanism of Phosgene-Induced Lung Toxicity: Role of Arachidonate Mediators. *J. Appl. Physiol.* **1990**, *69*, 1615–1622.

(636) Evans, R. D. Chlorine : State of the Art. *Lung* **2005**, *183*, 151–167.

(637) Borak, J.; Diller, W. F. Phosgene Exposure: Mechanisms of Injury and Treatment Strategies. *J. Occup. Environ. Med.* **2001**, *43*, 110–119.

(638) Wongwiriyapan, W.; Honda, S.; Konishi, H.; Mizuta, T.; Ikuno, T.; Ito, T.; Maekawa, T.; Suzuki, K.; Ishikawa, H.; Oura, K.; et al. Single-Walled Carbon Nanotube Thin-Film Sensor for Ultrasensitive Gas Detection. *Jpn. J. Appl. Phys.* **2005**, *44*, L482–L484.

(639) Li, J.; Lu, Y.; Meyyappan, M. Nano Chemical Sensors with Polymer-Coated Carbon Nanotubes. *IEEE Sens. J.* **2006**, *6*, 1047–1051.

(640) Lu, Y.; Partridge, C.; Meyyappan, M.; Li, J. A Carbon Nanotube Sensor Array for Sensitive Gas Discrimination Using Principal Component Analysis. *J. Electroanal. Chem.* **2006**, *593*, 105–110.

(641) Lu, Y.; Meyyappan, M.; Li, J. Fabrication of Carbon-Nanotube-Based Sensor Array and Interference Study. *J. Mater. Res.* **2011**, *26*, 2017–2023.

(642) Gohier, A.; Chancalon, J.; Chenevier, P.; Porterat, D.; Mayne-L'Hermite, M.; Reynaud, C. Optimized Network of Multi-Walled Carbon Nanotubes for Chemical Sensing. *Nanotechnology* **2011**, *22*, 105501.

(643) Lee, C. Y.; Strano, M. S. Amine Basicity (p K b) Controls the Analyte Binding Energy on Single Walled Carbon Nanotube Electronic Sensor Arrays. *J. Am. Chem. Soc.* **2008**, *130*, 1766–1773.

(644) Popa, A.; Li, J.; Samia, A. C. S. Hybrid Platinum Nanobox/Carbon Nanotube Composites for Ultrasensitive Gas Sensing. *Small* **2013**, *9*, 3928–3933.

(645) Choi, S. W.; Kim, B. M.; Oh, S. H.; Byun, Y. T. Selective Detection of Chlorine at Room Temperature Utilizing Single-Walled Carbon Nanotubes Functionalized with Platinum Nanoparticles Synthesized via Ultraviolet Irradiation. *Sens. Actuators, B* **2017**, *249*, 414–422.

(646) Sharma, A. K.; Mahajan, A.; Bedi, R. K.; Kumar, S.; Debnath, A. K.; Aswal, D. K. Non-Covalently Anchored Multi-Walled Carbon Nanotubes with Hexa-Decafluorinated Zinc Phthalocyanine as Ppb Level Chemiresistive Chlorine Sensor. *Appl. Surf. Sci.* **2018**, *427*, 202–209.

(647) Thom, S. R. Hyperbaric-Oxygen Therapy For Acute Carbon Monoxide Poisoning. *N. Engl. J. Med.* **2002**, *347*, 1105–1106.

(648) Thorn, S. R.; Keim, L. W. Carbon Monoxide Poisoning: A Review Epidemiology, Pathophysiology, Clinical Findings, and

Treatment Options Including Hyperbaric Oxygen Therapy. *J. Toxicol., Clin. Toxicol.* **1989**, *27*, 141–156.

(649) Baud, F. J. Cyanide: Critical Issues in Diagnosis and Treatment. *Hum. Exp. Toxicol.* **2007**, *26*, 191–201.

(650) Srivastava, A.; Sharma, V.; Kaur, K.; Khan, M. S.; Ahuja, R.; Rao, V. K. Electron Transport Properties of a Single-Walled Carbon Nanotube in the Presence of Hydrogen Cyanide: First-Principles Analysis. *J. Mol. Model.* **2015**, *21*, 173.

(651) Yari, A.; Sepahvand, R. Highly Sensitive Carbon Paste Electrode with Silver-Filled Carbon Nanotubes as a Sensing Element for Determination of Free Cyanide Ion in Aqueous Solutions. *Microchim. Acta* **2011**, *174*, 321–327.

(652) Schlegelmilch, J.; Petkova, E. P.; Martinez, S.; Redlener, I. E. Acts of Terrorism and Mass Violence Targeting Schools: Analysis and Implications for Preparedness in the USA. *J. Bus. Contin. Emer. Plan.* **2017**, *10*, 280–289.

(653) Shvetsov, A.; Shvetsova, S.; Kozyrev, V. A.; Spharov, V. A.; Sheremet, N. M. The “Car-Bomb” as a Terrorist Tool at Metro Stations, Railway Terminals and Airports. *J. Transp. Secur.* **2017**, *10*, 31–43.

(654) Woods, L. M.; Bădescu, Ș. C.; Reinecke, T. L.; Bădescu, Ș. C.; Reinecke, T. L. Adsorption of Simple Benzene Derivatives on Carbon Nanotubes. *Phys. Rev. B: Condens. Matter Mater. Phys.* **2007**, *75*, 155415.

(655) Star, A.; Han, T.-R.; Gabriel, J.-C. P.; Bradley, K.; Grüner, G. Interaction of Aromatic Compounds with Carbon Nanotubes: Correlation to the Hammett Parameter of the Substituent and Measured Carbon Nanotube FET Response. *Nano Lett.* **2003**, *3*, 1421–1423.

(656) Ruan, W.; Li, Y.; Tan, Z.; Liu, L.; Jiang, K.; Wang, Z. In Situ Synthesized Carbon Nanotube Networks on a Microcantilever for Sensitive Detection of Explosive Vapors. *Sens. Actuators, B* **2013**, *176*, 141–148.

(657) Liu, Y.; Li, X.; Dokmeci, M. R.; Wang, M. L. Carbon Nanotube Sensors Integrated inside a Microfluidic Channel for Water Quality Monitoring. *Proceedings of SPIE 7981 Sensors and Smart Structures Technologies for Civil, Mechanical, and Aerospace Systems*; SPIE, 2011; p 79811I.

(658) Chen, P.-C.; Sukcharoenchoke, S.; Ryu, K.; Gomez de Arco, L.; Badmaev, A.; Wang, C.; Zhou, C. 2,4,6-Trinitrotoluene (TNT) Chemical Sensing Based on Aligned Single-Walled Carbon Nanotubes and ZnO Nanowires. *Adv. Mater.* **2010**, *22*, 1900–1904.

(659) Kumar, D.; Jha, P.; Chouksey, A.; Tandon, R. P.; Chaudhury, P. K.; Rawat, J. S. Flexible Single Walled Nanotube Based Chemical Sensor for 2,4-Dinitrotoluene Sensing. *J. Mater. Sci.: Mater. Electron.* **2018**, *29*, 6200–6205.

(660) Kim, T. H.; Lee, B. Y.; Jaworski, J.; Yokoyama, K.; Chung, W. J.; Wang, E.; Hong, S.; Majumdar, A.; Lee, S. W. Selective and Sensitive TNT Sensors Using Biomimetic Polydiacetylene-Coated CNT-FETs. *ACS Nano* **2011**, *5*, 2824–2830.

(661) Zhang, Y.; Xu, M.; Bunes, B. R.; Wu, N.; Gross, D. E.; Moore, J. S.; Zang, L. Oligomer-Coated Carbon Nanotube Chemiresistive Sensors for Selective Detection of Nitroaromatic Explosives. *ACS Appl. Mater. Interfaces* **2015**, *7*, 7471–7475.

(662) Hrapovic, S.; Majid, E.; Liu, Y.; Male, K.; Luong, J. H. T. Metallic Nanoparticle-Carbon Nanotube Composites for Electrochemical Determination of Explosive Nitroaromatic Compounds. *Anal. Chem.* **2006**, *78*, 5504–5512.

(663) Li, J.; Feng, H.; Feng, Y.; Liu, J.; Liu, Y.; Jiang, J.; Qian, D. A Glassy Carbon Electrode Modified with β -Cyclodextrin, Multiwalled Carbon Nanotubes and Graphene Oxide for Sensitive Determination of 1,3-Dinitrobenzene. *Microchim. Acta* **2014**, *181*, 1369–1377.

(664) Lai, H.; Leung, A.; Magee, M.; Almirall, J. R. Identification of Volatile Chemical Signatures from Plastic Explosives by SPME-GC/MS and Detection by Ion Mobility Spectrometry. *Anal. Bioanal. Chem.* **2010**, *396*, 2997–3007.